Microbial methylated amine metabolism in marine surface waters

Ian Lidbury

A thesis submitted to the School of Life Sciences in fulfilment of the requirements for the degree of Doctor of Philosophy

December 2014

University of Warwick
Coventry, UK

Table of Contents

List of Figures

List of Tables

Declaration

I declare that the work presented in this thesis was conducted by me under the direct supervision of Dr. Yin Chen and Professor J. Colin Murrell, with the exception of those instances where as follows: 1) Chapter 4, construction of the mutant *ΔtmoR::Gm* was conducted by Dr. Zhidong Zhang, under my supervision 2) Chapter 4, DMS oxidation characteristics of the mutant, *ΔtmoR::Gm*, was performed by Eileen Muhs. 3) Chapter 7, a number of the cloning steps conducted during construction of the *bet* mutants strains were performed by George Kimberley under my supervision. 4) Construction of the mutant, *Δtmm::Gm*, was carried out by Dr. Yin Chen prior to me undertaking the project. None of the work presented has been previously submitted for any other degree. Some of the data presented in Chapters 3, 4 and 5, have been published as part of manuscripts (Lidbury, I. *et al*. (2014) Trimethylamine *N*—oxide metabolism by abundant marine heterotrophic bacteria. *PNAS*. **111** (7): 2710-2715, and Lidbury I. *et al*. (2014) Trimethylamine and trimethylamine N-oxide are supplementary energy sources for a marine heterotrophic bacterium: implications for marine carbon and nitrogen cycling. *ISME J*. Published ahead of print. doi:10.1038/ismej.2014.149).

Ian Lidbury

Acknowledgments

I would like to acknowledge the guidance, both technical and academic, and generous support of my primary supervisor, Dr. Yin Chen, as well as the time he has dedicated towards thought provoking discussions. I would like to pay special thanks to my second supervisor, Prof. Colin Murrell (University of East Anglia) for his expert guidance and critical review of the work conducted during this project. I would also like to thank him for his invaluable expertise in writing and reviewing scientific reports. To all the members, both present and past, of the Chen Lab, Murrell Lab and Schäfer Lab and departmental support staff for their support throughout the project. A special mention to Julie Scanlan is warranted for her expertise and often generous attention to dealing with technical issues that arose during the project. I would like to pay tribute to Prof. David Scanlan and Dr. Hendrik Schäfer for their advice and useful discussions. Lastly, I would like to mention my colleague, Dr. Jack Lee, a dear friend who is partly responsible for stimulating my passion in microbiology and research.

Abbreviations

ABC	ATP-binding cassette
AmpR	ampicillin (resistance)
ADP	adenosine diphosphate
ATP	adenosine triphosphate
asRNA	antisense RNA
BCCT	betaine-carnitine-choline transporter
BetA	choline dehydrogenase
BetB	betaine aldehyde dehydrogenase
BetC	choline sulfatase
BetI	regulator of *betAB*
BetT	BCCT-type choline transporter
BetX	SBP with affinity for GBT
BHMT	betaine homocycsteine methyltransferase
BIS	*N*,*N*'-methylenebisacrylamide
BIS TRIS	2-[Bis-(2-hydroxyethyl)-amino]-2-hydroxymethyl-propane-1,3-diol
BLAST	basic local alignment search tool
bp	base pairs
BSA	bovine serum albumin
C	carbon
ChoX	SBP with affinity for choline
CO_2	carbon dioxide
Da	Dalton
DCPIP	2,6-dichlorophenolindophenol
DH	dehydrogenase
DMA	dimethylamine
DMF	dimethylformamide
DMG	dimethylglycine
DMGDH	dimethylglycine dehydrogenase
DMS	dimethylsulfide
DMSO	dimethylsulfoxide
DMSP	dimethylosulfonioproprionate
DNA	deoxyribonucleic acid
DNase	deoxyribonuclease
DON	dissolved organic nitrogen
dH_2O	distilled water
dNTP	deoxynucleotide triphosphate
DTT	dithiothreitol
dw	dry weight
EDTA	ethylendiaminetetraacetic acid
Fae	formaldehyde activating enyzme
FDH	formate dehydrogenase
Fhs	formyl-H_4F synthetase
FID	flame ionisation detector
FAD	flavin-adenine dinucleotide
g	gram / acceleration due to gravity
GBT	glycine betaine
GC	gas chromatography

GMA	γ-glutamylmethylamide
GMA/NMG	glutamate-mediated pathway for MMA catabolism
GmaS	GMA synthetase
Gm^R	gentamicin (resistance)
GSH	glutathione
h	hour
H_4F	tetrahydrofolate
H4MPT	tetrahydromethanopterin
HEPES	4-(2-hydroxyethyl)-1-piperazineethanesulfonic acid
IMG	Integrated microbial genomes
JGI	Joint genome institute
Kan^R	kanamycin (resistance)
l	litre
LacZ	β-galactosidase
M	molar
MCS	multiple cloning site
MAMS	marine ammonium mineral salts
MDH	methanol dehydrogenase
MIC	minimum inhibitory concentration
mg	milligram
min	minute
MK	myokinase
ml	millilitre
mM	millimolar
mol	mole
MRC	marine *Roseobacter* clade
mRNA	messenger RNA
MA	methylated amine
MMA	monomethylamine
MMADH	MMA dehydrogenase
NAD+	nicotinamide adenine dinucleotide (oxidised form)
NADH	nicotinamide adenine dinucleotide (reduced form)
NADP+	nicotinamide adenine dinucleotide phosphate (oxidised form)
NADPH	nicotinamide adenine dinucleotide phosphate (reduced form)
NCBI	National Centre for Biotechnology Information
ng	nanogram
NmgS	N-methylglutmate synthase
MgdABCD	N-methylglutmate dehydrogenase
NH_4^+	ammonium
NH_4Cl	ammonium chloride
NTC	no-template control
OD_{440}	optical density at 440 nm
OD_{540}	optical density at 540 nm
OD_{600}	optical density at 600 nm
ORF	open reading frame
ori	origin of replication
oriT	origin of transfer
P	phosphorus
PAGE	polyacrylamide gel electrophoresis
PCR	polymerase chain reaction
PIPES	1,4-piperazinediethanesulfonic acid
QA	quaternary amine
RBS	ribosomal binding site

RNA	ribonucleic acid
RNase	ribonuclease
rRNA	ribosomal ribonucleic acid
RT-PCR	reverse transcriptase PCR
RubisCO	ribulose 1,5-bisphosphate carboxylase-oxygenase
RuMP	ribulose monophosphate
s	seconds
SBP	substrate binding protein
SD	Shine-Dalgarno
SDS	sodium dodecyl sulphate
TBE	tris borate EDTA
TCA	trichloroacetic acid / tricarboxylic acid
TE	tris EDTA
TMA	trimethylamine
TMADH	TMA dehydrogenase
TMAO	trimethylamine *N*-oxide
Tdm	TMAO demethylase
Tmm	TMA monooxygenase
TmoR	Lys-R-type repressible regulator of Tmm
TmoV	Transmembrane region of the TMAO transporter
TmoW	Transmembrane region of the TMAO transporter
TmoX	SBP with affinity for TMAO
TmoXWV	TMAO ABC-type transporter
Tris	tris (hydroxymethyl) aminomethane
v/v	volume to volume
w/v	weight to volume
X-gal	5-bromo-4-chloro-3-indoyl-β-D-galactoside
YTSS	yeast extract, tryptone, seasalts
YPSS	yeast extract, peptone, seasalts

Abstract

Methylated amines, such as trimethylamine (TMA) and trimethylamine *N*-oxide, are nitrogenous compounds that are thought to be ubiquitous in the marine environment. TMA is a product of the anaerobic degradation of quaternary amines, such as glycine betaine and choline. Through a set of complex chemical and biological interactions, methylated amines play a role in regulating the planet's climate. Microbial degradation of methylated amines is thought to be a sink for these compounds in the marine environment, however some of the key genes and enzymes responsible for the degradation of methylated amines are unknown. Using *Ruegeria pomeroyi* DSS-3 as the model organism, the key enzymes for the uptake and catabolism of trimethylamine *N*-oxide were identified and it was discovered that these genes and enzymes are highly expressed in the seawater, as revealed by the re-analysis of a number of recent metatranscriptomic and metaproteomic datasets. Again using *R. pomeroyi* as the model organism, it was shown that trimethylamine and trimethylamine *N*-oxide can be oxidised to CO_2 to generate reducing equivalents and ATP. The generation of this reducing power results in a number of physiological benefits which are further discussed in detail. It was determined that bacteria possessing trimethylamine monooxygenase, the key enzyme required for the oxidation of TMA could also oxidise the reduced sulfur compound, dimethylsulfide, when supplemented with methylated amines. The ecology of methylated amine-utilising bacteria was investigated using a newly designed primer set targeting the trimethylamine *N*-oxide demethylase. The results are presented in detail within. The key genes and enzymes essential for the catabolism of the quaternary amine, choline were also discovered, again using *R. pomeroyi* as the model organism. The occurrence of genes required for the catabolism of choline are widespread among certain groups of marine bacteria known to interaction with eukaryotic biota, suggesting that this compound may be an essential nutrient for these organisms.

Chapter 1

Introduction

1.1. A brief introduction into microbial oceanography

Marine phytoplankton are predominantly microscopic eukaryotic and bacterial cells that grow by fixing atmospheric carbon dioxide (CO_2) into organic carbon (C) and they have been shaping the planets' biogeochemical cycles for over 3 billion years (Falkowski et al., 1998). The evolution of oxygenic photosynthesis by the phytoplankton led to the production of atmospheric oxygen (~2.2 billion year ago) where its concentration slowly increased until there was sharp rise (in geological terms) around 540 million years ago as all major O_2 sinks became saturated (Holland et al., 1986; Riding, 1992). Oceanic primary production (the fixation of inorganic C, usually CO_2, into organic matter) is performed by a range of phytoplankton including eukaryotic organisms, such diatoms, dinoflagellates and prymnesiophytes, for example *Emiliania huxleyi*. The cumulative primary production in the oceans is equivalent to approximately half the global total, therefore every second breath that we breathe is derived from marine microorganisms (Field et al., 1998). A significant proportion of oceanic primary production is also performed by prokaryotic microbes, named cyanobacteria (*Synechococcus* and *Prochlorococcus*) (Falkowski et al., 1998). In stark contrast to land plants, which have a total biomass of ~600 Pg C (1 Pg = 10^{15} g), the biomass of marine phytoplankton totals 2 Pg C (Giovannoni and Vergin, 2012). In addition, the turnover times for marine phytoplankton are as little as 6 days compared to an average of 15 years for land plants (Giovannoni and Vergin, 2012). Therefore, as we alter our planets' atmosphere, through the burning of fossil fuels and related activities, marine phytoplankton are likely to respond quicker than their terrestrial counterparts. Thanks to advances in molecular techniques, which have taken the emphasis away from traditional cultivation methods, it is now understood that the

majority of secondary production within the oceans is carried about by the heterotrophic bacterioplankton and mediated by bacteriophage-like viruses (Azam et al., 1983; Rusch et al., 2007; Suttle, 2007). This advancement in our understanding of microbial communities has led researchers to re-think the way that we view the cycling of nutrients within the oceans, which ultimately effects ecosystem functioning (Azam et al., 1983).

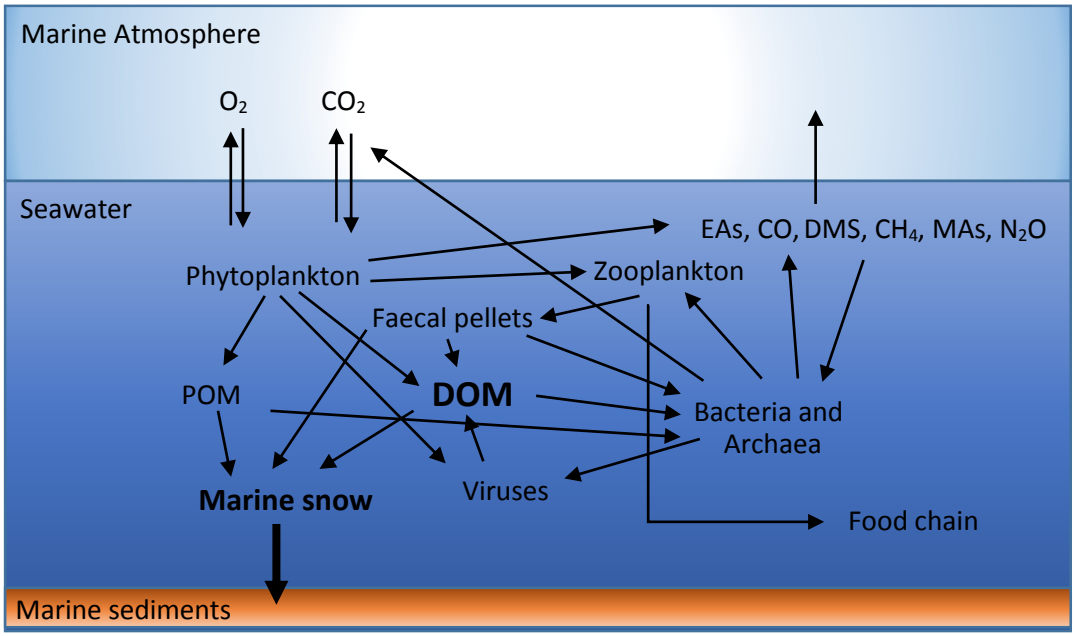

Figure 1.1. The flow of matter and energy within the surface seawater mediated by the interactions between different marine microorganisms. A small proportion of the inorganic carbon fixed into biological material escapes remineralisation and is sequestered in the deep ocean and marine sediments. Adapted from Suttle (2007), Azam et al. (1983) and Azam and Malfatti (2007). Abbreviations: DOM, dissolved organic matter; POM, particulate organic matter; EAs, ethylamines; MAs, methylamines; CO, carbon monoxide; CH_4, methane; N_2O, nitrous oxide; DMS, dimethylsulfide, CO_2, carbon dioxide, O_2, oxygen.

Collectively, the microorganisms that inhabit the marine environment constitute up to 90% of the biomass within the planets' oceans and their interaction drives biogeochemical cycles (Azam et al., 1983; Suttle, 2007). The majority of C that is fixed into biomass by the phytoplankton is ultimately respired back as remineralised CO_2 by heterotrophic bacteria (Giovannoni and Vergin, 2012). Therefore, marine microorganisms are essentially the lungs of the oceans, controlling the amount of

CO_2 that is either taken up from or released back into the atmosphere (Giovannoni and Vergin, 2012). The biological C pump refers to a process in which fixed organic C escapes microbial remineralisation back into CO_2 and is sequestered in the deep ocean and marine sediments (Falkowski et al., 1998). The strength of the biological C pump (C remineralised versus C sequestered) is controlled by a number of variables which are not fully understood. However, one factor known to control the strength of the pump is the interaction between the C cycle and a number of other nutrient cycles, for example nitrogen (N) and phosphorus (P) (Falkowski et al., 1998).

1.2. The microbial ecology of the marine heterotrophic bacteria within the surface seawater.

The abiotic composition of the surface seawater (photic zone, <250 m in depth) of the worlds' oceans is diverse over both space and time, regions can therefore have very different spatiotemporal microbial community structure. For example, the North and South Atlantic Tropical gyres, as well as regions in the Pacific Ocean, are typified by having a chronic shortage of nutrients and prolonged periods of low primary productivity (Polovina et al., 2008; Giovannoni and Vergin, 2012). On the other hand, temperate coastal waters tend to be richer in nutrients and show strong seasonal patterns of productivity (Falkowski et al., 1998). Microorganisms that live in the open ocean gyres, although phylogenetically divergent, are well adapted to living in these conditions (oligotrophy) and share a number of phenotypic characteristics. These low-nutrient regions are dominated by the autotrophic cyanobacterium, *Prochlorococcus* and heterotrophic bacteria related to the SAR11 clade (Campbell et al., 1997; DuRand et al., 2001; Morris et al., 2002). These microorganisms have a high surface area: volume ratio and possess a suite of high

affinity transporters that make them very effective at scavenging nutrients (Partensky et al., 1999; Giovannoni et al., 2005). They also have small genomes which contain less regulatory genes and have a low GC content, which potentially reduces their requirement of N and P (Rocap et al., 2003; Giovannoni et al., 2005; Giovannoni et al., 2014). Both the Bermuda Atlantic Time-series Study (BATS) and the Hawaiian Ocean Time-series Study (HOT) have monitored the bacterial communities present at sites in the Sargasso Sea (Atlantic Ocean) and Pacific Ocean, respectively. Both BATS and HOT are considered oligotrophic systems and during the summer months, the bacterial community in the surface waters is dominated by members of the SAR11 clade (*Pelagibacteraceae*, subsclade 1) *Puniceispirillum* (*Alphaproteobacteria*) and SAR86 (*Gammaproteobacteria*), whilst the deep cholorphyll maximum (DCM) is dominated by *Prochlorococcus*. The Sargasso Sea (BATS) has a stronger pattern of seasonality than that observed at HOT, due to more seasonality in abiotic factors such as temperature, day light hours and depth of the mixed layer (Giovannoni and Vergin, 2012). During the spring time at BATS, there is a greater spike in the level of primary production which is driven by the increase in abundance of larger eukaryotic microalgal species. The heterotrophic community at BATS responds accordingly. Marine *Actinobacteria* and a different subclade of the SAR11 clade (subclade 1b) become one of the abundant bacterial groups (Giovannoni and Vergin, 2012). In addition to these springtime events, anti-cyclonic eddies are a common feature within the Sargasso Sea and result in the transient increase in periods of primary production (Bibby et al., 2008). These anti-cyclonic events result in the mixing of nutrient-rich deeper waters with the warmer surface waters, triggering a burst in diatom growth which can last up to several months, having implications for the biological C pump

(increased vertical C export) (Bibby et al., 2008). Again, changes in primary production are quickly followed with changes to the heterotrophic community and a rise in the number of *Roseobacter* cells within the eddy core has been observed (Nelson et al., 2014). Even in the Sargasso Sea, which has repetitive patterns of community structure, many rare bacterial taxa still have patterns of seasonality like their more abundant counterparts, however, some rare bacterial taxa show much more complex and transient peaks in abundance for which the reasons are still unknown (Vergin et al., 2013). Furthermore, the link between metabolic activity and the numerical abundance of cells is often inversely related, making predictions about the role certain microbial groups play in nutrient cycling challenging (Hunt et al., 2013).

Another well-studied marine survey site is station L4, of the coast of Plymouth, UK. Station L4 is situated in the English Channel and is near the mouth of the Tamar River whose outflow leads to a fairly consistent supply of nutrients to the site (http://www.westernchannelobservatory.org.uk/index.php). Station L4 is also typified by strong seasonal dynamics where a phytoplankton spring bloom occurs annually. A six-year deep sequencing study at this site revealed the repetitive nature of the bacterial community which displayed a rhythmical annual pattern over the course of the study period (Gilbert et al., 2012). During the winter months at station L4, when primary production is low, the SAR11 clade are the dominant bacterial group in the seawater (Gilbert et al., 2012). However, during the spring and summer time, the marine Roseobacter clade (MRC) (see section 1.10.) becomes the dominant bacterial group, responding to influxes of organic C, driven by primary production (Gilbert et al., 2012; Taylor et al., 2014) (Figure 1.2). This site is one of many examples which illustrates that the MRC is associated with high periods of

primary production often generated by eukaryotic microalgae (Hahnke et al. 2013; González et al., 2000; Nelson et al., 2014). The North Sea and coastal waters off of the Southeast of the United States also witness a greater number of MRC cells during the summer than during the winter, when primary production is elevated (Buchan et al., 2005).

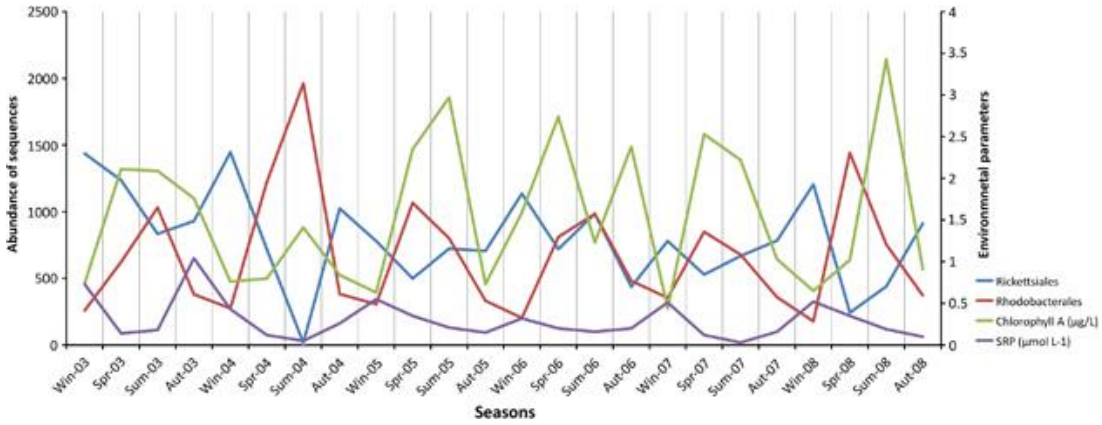

Figure 1.2. Seasonal dynamics of the bacterial Orders, *Rickettsiales* (predominantly SAR11) and *Rhodobacterales* (predominantly MRC), and environmental parameters, chlorophyll a and soluble reactive phosphorus (SRP) in the L4 6-year time series. Frequency is recorded based on abundances (abundance of sequences per taxa) within a resampled abundance of 4505 sequences per sample. Taken from Gilbert et al. (2012).

1.3. Nitrogen and methylated amines in the marine environment

Along with P, N is considered one of the primary limiting nutrients to the oceanic primary productivity (Zehr and Kudela, 2011). Indeed, several experiments have shown that primary productivity is enhanced when seawater is supplemented with N or N and P together (Thomas, 1970; Ryther and Dunstan, 1971; Elser et al., 2000). The vast majority of N is in the form of di-nitrogen gas (N_2) for which only a small subset of marine microorganisms can 'fix' N_2 into biologically available ammonium (NH_4^+) (Capone and Carpenter, 1982). The atmosphere is ~80% N_2, therefore the supply of N into the oceans is theoretically unlimited, however N fixation, which is mediated through nitrogenase metalloproteins, is often limited by

the availability of iron which is required as a cofactor (Kustka et al., 2003; Zehr and Kudela, 2011). Dissolved organic N (DON) is the second largest pool of N after N_2 (standing stock concentration, 5-50 mM) as inorganic forms of N, such as NH_4^+ and nitrate, are rapidly taken up by microorganisms (Capone et al, 2008). Methylated amines (MAs) form part of the DON pool and are thought to be ubiquitous in the marine environment as their precursors, trimethylamine (TMAO), glycine betaine (GBT), choline and carnitine are osmolytes and abundant within eukaryotic cells (Ikawa and Taylor, 1973; Treberg et al., 2006).

1.4. The environmental significance of methylamines

The most abundant amine compounds found in the atmosphere are trimethylamine (TMA), dimethylamine (DMA), monomethylamine (MMA), trimethylamine (TEA), diethylamine (DEA) and monomethylamine (MEA), as well as 1-propanamine and 1-butanamine (Ge et al., 2011). These compounds are emitted from a variety of sources including the oceans, sewage, automobiles, fish processing, chemical manufacturing, vegetation and animal husbandry, to name a few (Ge et al., 2011). Both abiotic and biotic processes result in the release of amines into the atmosphere (Figure 1.3) and this annual flux is estimated at 285±78 Gg yr^{-1} for which the oceans are predicted to produce ~80 Gg yr^{-1} (Ge et al., 2011). However, as large uncertainties remain about the cycling of MAs, especially DMA, these figures will surely be revised when analytical methods for the detection of MAs improve.

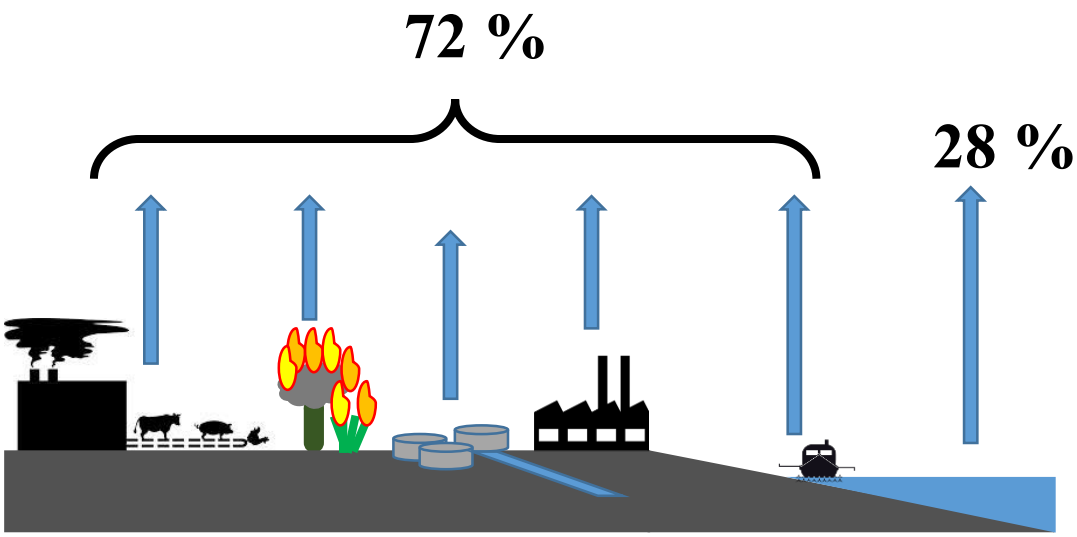

Figure 1.3. The annual flux of methylamines into the atmosphere from a range of sources, including animal husbandry, the oceans, fossil fuel combustion, textile production and the fish industry to name a few. The figure was produced using data presented in (Ge et al., 2011).

MAs form part of a mix of trace gases that are emitted from the oceans and collectively, these trace gases have major implications for the climate, largely through the production of particulate marine aerosols (Carpenter et al., 2012). A number of studies have detected MAs in the atmosphere above marine surface waters; for example, one study showed that MAs constitute up to 20% of the gaseous basic compounds over the Arabian Sea (Gibb et al., 1999). MAs were also detected in the atmosphere above marine waters in Tampa Bay, Florida (Calderón et al., 2007). Apart from methanesulfonic acid (MSA), DMA and DEA salts were the most abundant secondary organic aerosols (SOAs) detected in fine marine particles at sites located in the North and Tropical Atlantic Ocean (Facchini et al., 2008). The production of both DMA and DEA in the surface seawater is thought to be driven through biotic processes and their subsequent emission from the surface seawater is the likely source of these compounds found in fine marine particles (Facchini et al., 2008; Müller et al., 2009). Interestingly, the concentrations

of MMA, DMA and DEA in fine marine particles over Cape Verde reached much higher levels during an unexpected winter algal bloom, than during the classic spring/summer bloom (Müller et al., 2009). This study highlights the needs for a better understanding of the processes governing the sources and sinks of these compounds. For example, one explanation for the increased concentrations of these SOAs in this region may be due to a less active bacterial community during the winter resulting in less microbial degradation of these compounds before they flux into the atmosphere.

The flux of MAs into the atmosphere is of great importance as they can undergo a number of different reactions resulting in a complex set of effects to the climate. For example, they can influence the absorption and scattering of UV radiation and the formation of cloud condensation nuclei (CCN) (Ge et al., 2011). Off the coast of California, during times of increased chlorophyll *a* in the surface seawater, a rise in CCN activity has been linked to changes in the composition of SOAs, including the increase in amine-derived compounds (Sorooshian et al., 2009). MAs can also undergo reactions that result in the formation of carcinogenic compounds which can have direct effects on human health through the contamination of drinking water (Mitch et al., 2003). Under anoxic conditions, MAs are growth substrates for methanogens and the growth of these microorganisms results in the production of methane as a metabolic by-product (King, 1984). In fact, between 35-90% of methane production from saltmarsh sediments or slurries is generated using TMA as the primary substrate (Oremland and Polcin, 1982; King et al., 1983). Methane has a strong radiative forcing, 25 times greater than that of CO_2, therefore making it a potent greenhouse gas. MAs can also be beneficial, from an anthropogenic perspective, as these basic compounds can neutralise the acidity of the atmosphere

by reacting with compounds such as sulfuric acid and nitric acid (Place Jr et al., 2010). Therefore, understanding the sources of atmospheric MAs and sinks in the marine environment is vital for helping to predict regional and global future climate models as well as determine the impacts MAs may have on human health.

1.5. Concentrations of methylamines in the marine environment

MAs form part of the DON pool and are thought to be ubiquitous in the marine environment as their precursors, TMAO, GBT, choline and carnitine are abundant within eukaryotic cells (Ikawa and Taylor, 1973; Rebouche, 1992; Treberg et al., 2006). Historically, the *in situ* quantification of MAs in the marine environment has proven very challenging and the number of studies reporting standing stock concentrations are limited (Carpenter et al., 2012). In the Arabian Sea and Mediterranean Sea, MMA, DMA and TMA were correlated with diatoms and mesozookplankton grazing, suggesting phytoplankton with a higher nitrogen requirements may be a source of MAs (Gibb et al., 1999). In this study, MMA was the most abundant MA species (10-25 nM) whilst TMA was the least abundant (up to 1.5 nM). In contrast to the Arabian Sea and Mediterranean Sea, seawater of the coast of Hawaii and Massachusetts had higher concentrations of MA species (MMA, Massachusetts, 200 nM), but DMA (Massachusetts, 9 nM) was the least abundant species in the seawater, not TMA (Massachusetts, 40 nM (Van Neste et al., 1987). The concentration of MAs in marine sediments is at least one order of magnitude higher than that of MAs in the water column, with TMA being the most abundant MA species (4.7 μM) (King, 1984). This is in line with the notion that the major route for the production of MAs is predicted to be the anaerobic degradation of quaternary amine (QAs), producing TMA (King, 1984; Fitzsimons et al., 2001). In surface seawater from the Arctic Ocean, MAs, along with TMAO and methylated

sulfur compounds were quantified along a depth profile and throughout a seasonal cycle (Gibb and Hatton, 2004). In this region, the mean concentration of TMA = 1.6 ± 1.8 nM whilst TMAO = 15.2 ± 16.6 nM (Gibb and Hatton, 2004). In the same seawater samples, DMSO was also more abundant than DMS, suggesting that the oxidation of TMA and DMS is actively taking place in the surface seawater (Gibb and Hatton, 2004).

1.6 Microbial degradation of methylated amines

1.6.1. Microbial degradation of monomethylamine

The degradation of MAs such as TMA, DMA and MMA, is carried out by two different pathways. The first involves a number of dehydrogenases that can sequentially demethylate each MA species, producing formaldehyde at each step as a product (Chistoserdova, 2011). Formaldehyde is toxic and is often conjugated to a suitable cofactor where it undergoes further metabolism (see section1.8). This pathway does not produce TMAO as an intermediate. The most studied dehydrogenase in this pathway is the tryptophan tryptophylquinone (TTQ)-dependent MMA dehydrogenase (MMADH) that is encoded by *mauA* and *mauB* in the *mauBEDAGLMN* cluster (Davidson, 2004). This gene cluster occurs in a small number of methylotrophic bacteria of the *Alphaproteobacteria* and *Gammaproteobacteria* however its distribution in the environment is patchy (Chistoserdova et al., 2009; Chistoserdova, 2011). Recently, it was discovered that another indirect route for microbial MMA degradation exists which involves the transfer of the methyl group to glutamate followed by subsequent release of both NH_4^+ and formaldehyde presumably in the form of methylene-H_4F (Chen et al., 2010b; Latypova et al., 2010). This process involves three enzymes, γ-glutamylmethylamide (GMA) synthase (GmaS), *N*-methylglutamate (NMG)

synthase (MgsABC) and NMG dehydrogenase (MgdABCD) (Latypova et al., 2010). GmaS and MgsABC, which consists of three subunits encoded by *mgsABC*, are almost always located in a single operon. MgdABCD, which consists of four subunits encoded by four separate genes (*mgdABCD*), is invariably located in a separate region on the genome, but often within the proximal genetic neighbourhood (Chen et al., 2010b; Latypova et al., 2010).

The *mgdABCD* is homologous to the four-gene cluster, *soxABCD*, which encodes a multimeric sarcosine (mono-methylglycine) oxidase that is involved in the final step of GBT demethylation (see section 1.6.7) (Chlumsky et al., 1995; Latypova et al., 2010). Within the marine environment, there are very few examples of bacteria possessing genes for MMADH whilst the genes required for the GMA/NMG pathway of MMA oxidation are present in a number of ecologically important marine heterotrophs, including members of the SAR11 clade and MRC (Figure 1.4). It has been shown that these genes are functional in non-methylotrophic bacteria of the MRC (Chen et al., 2010b; Chen et al., 2011).

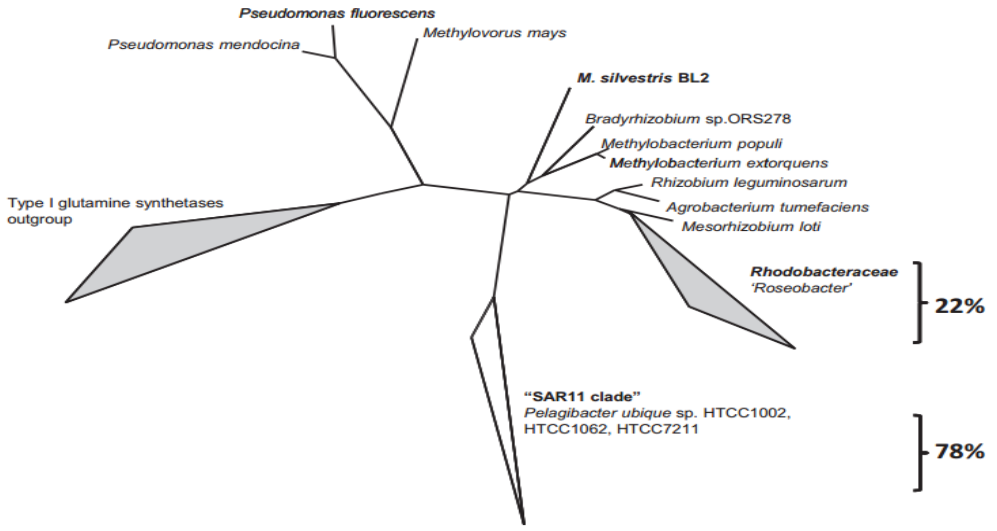

Figure 1.4. An unrooted tree showing GmaS homologs retrieved from sequenced bacterial genomes and the Global Ocean Sampling expedition data set. The neighbour-joining tree was constructed using sequences retrieved from sequenced bacterial genomes (~400 amino acids). Environmental sequences were added by parsimony. Percentages represent the relative abundance of sequences retrieved from the global ocean survey (GOS) (Reisch et al., 2007). Taken from (Chen et al., 2011).

1.6.2. Microbial degradation of trimethylamine

Unlike the TMA dehydrogenase (TMADH) that does not produce TMAO, TMA monooxygenase (Tmm) oxidises TMA to TMAO using NADPH as an electron donor and oxygen as the oxidising agent (Chen et al., 2011). Tmm belongs to a class of flavin-containing monooxygenases (FMOs) which were originally characterised from mammalian liver cells (Williams et al., 1985). Interest in these FMOs grew due to their ability to oxidise a wide range of N and sulfur related compounds as well as xenobiotics, including pharmaceutical drugs (Krueger and Williams, 2005). FMOs are typified by the presence of a conserved sequence motif (similar to Baeyer-Villiger monooxygenases) which represents the site where flavin adenine dinucleotide (FAD) binds (Fraaije et al. 2002). Introducing mutations in human FMO can results in the accumulation of TMA which can be detected in the person's breath or urine, ultimately resulting in the condition, trimethylaminuria (fish odour syndrome), caused by an inability to oxidise TMA into its non-odourous metabolite TMAO (Mitchell and Smith, 2001).

Recently, it has also been shown that bacterial FMOs can also oxidise TMA to TMAO using NADPH as the electron donor and it was discovered that the gene encoding Tmm (*tmm*) is highly prevalent within marine metagenomes, where it is found in approximately 20% of bacterial cells inhabiting the surface seawater of the oceans (Chen et al., 2011). The reason for the widespread occurrence of *tmm* is due to its presence in both the MRC and SAR11 clade (Figure 1.5), which collectively dominate coastal and open ocean surface seawaters (González et al., 2000; Morris et al., 2002; Buchan et al., 2005; Alonso and Pernthaler, 2006).

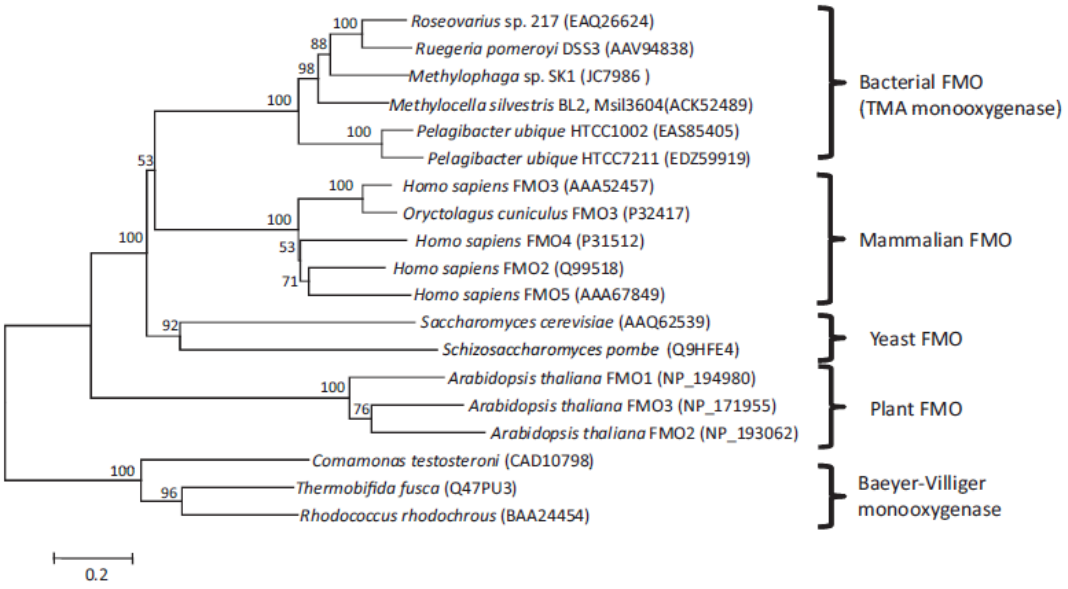

Figure 1.5. A neighbour-joining phylogenetic tree showing the relationship of Tmm to other FMOs. The tree was drawn using the MEGA4 (50) based on an alignment of ~450 amino acids of FMOs. Baeyer–Villiger monooxygenases were used as an outgroup. Bootstrap values of 100 replicates are shown. Taken from Chen et al. (2011).

The *tmm* gene was identified in the soil bacterium *Methylocella silvestris* BL2 where mutagenesis of ORF Msil3604, led to the eradication of growth on TMA, but not downstream metabolites (Chen et al., 2011). Again using *M. silvestris* as the model organism, Chen et al. (2011) showed that the two ORFs either side of *tmm* (ORF, Msil3604) were upregulated at both the transcriptional and translational levels in MMA- and TMA-grown cultures, and it was predicted these may be involved in MA metabolism (Figure 1.6). Tmm from both the MRC and SAR11 clade has a high affinity for the volatile organosulfur compound, DMS, as well as its cognate substrate TMA (Table 1.1). However, Tmm from these bacteria did not have a strong affinity for dimethylsulfoxide (DMSO), a similar property to that of mammalian FMOs (Krueger and Williams, 2005; Chen et al., 2011).

A

Annotation	Glycine cleavage T protein	Bacterial flavin-containing monooxygenase	Glycine cleavage T protein
Polypeptide abundance in			
TMA	0.72%	1.60%	4.16%
MMA	1.35%	3.88%	6.20%
MeOH	Not detectable	Not detectable	Not detectable
Transcription in			
TMA	+	+	+
MeOH	-	-	-

B

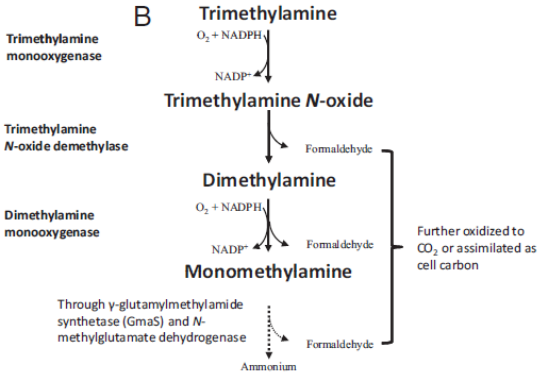

Figure 1.6. (A) A summary of comparative proteomics and transcriptional analyses of the three-gene cluster containing a bacterial FMO in *M. silvestris*. The function was based on the annotation from the genome sequence using BLASTP search; the abundance of each of the polypeptides is shown in percentages of the total soluble proteome in each condition, and the presence (+) or absence (−) of transcription of each gene was confirmed by RT-PCR. MeOH, methanol; MMA, monomethylamine; TMA, trimethylamine. (B) The proposed pathway for TMA oxidation involving Tmm. Taken from Chen et al. (2011).

Table 1.1. Steady-state kinetics enzyme assays on purified recombinant Tmm cloned from marine bacteria or *Methylocella silvestris* BL2 and expressed heterologously in *E. coli*. Taken from Chen et al. (2011).

	Substrate	K_m, μM	V_{max}, nmol·min^{-1}·mg^{-1}
Methylocella silvestris BL2	TMA	9.4 ± 2.1	29.4 ± 3.2
	DMA	89.7 ± 13.2	6.9 ± 0.1
	DMS	10.3 ± 0.7	34.6 ± 0.2
	DMSO	3,575 ± 151	4.8 ± 1.5
Ruegeria pomeroyi DSS-3	TMA	20.8 ± 2.9	267.7 ± 52.2
	DMA	1,119.7 ± 55.3	83.7 ± 4.0
	DMS	97.3 ± 8.8	374.5 ± 83.2
	DMSO	16,424.5 ± 1,033.2	70.4 ± 10.5
Roseovarius sp. 217	TMA	21.6 ± 1.9	1,133.6 ± 58.6
	DMA	864.2 ± 35.3	358.0 ± 12.3
	DMS	25.7 ± 4.1	577.4 ± 75.7
	DMSO	16,340.8 ± 1155.2	179.4 ± 41.2
Pelagibacter ubique HTCC7211	TMA	28.5 ± 4.4	67.3 ± 3.2
	DMA	306.1 ± 51.3	41.4 ± 2.7
	DMS	26.4 ± 7.2	97.2 ± 6.9
	DMSO	7,456.0 ± 907.8	41.3 ± 4.7
Pelagibacter ubique HTCC1002	TMA	27.5 ± 4.2	70.8 ± 7.7
	DMA	1,237.7 ± 98.5	41.2 ± 5.6
	DMS	33.2 ± 5.6	50.8 ± 5.0
	DMSO	19,334.3 ± 1,870.4	29.9 ± 8.9

DMA, dimethylamine; DMS, dimethylsulfide; DMSO, dimethyl sulfoxide; TMA, trimethylamine.

Chen et al. (2012) screened a number of genome-sequenced MRC isolates for the presence of the gene (*tmm*) encoding Tmm as well as other genes involved in MA metabolism, such as *gmaS*, *mgsABC* and *mgdABCD*. It was discovered that 15/40 isolates contained *tmm* whilst slightly more (19/40) contain the genes involved in MMA catabolism. All MRC isolates that contained *tmm* and MA-related genes could grow on either TMA or MMA as a sole N source. Isolates related to the genus, *Roseovarius*, could also grow on TMA or MMA as a sole C and energy source (methylotrophy) (Chen, 2012). Bacterioplankton in the Sargasso Sea, typically dominated by members of the SAR11 clade (Wu et al., 2000; Morris et al., 2002), can oxidise TMA to CO_2 (Sun et al., 2011) (Figure 1.7). C*andidatus* Pelagibacter ubique HTCC1062, a member of the SAR11 clade, can also catabolise TMAO and MMA and other related methylated compounds to generate intracellular ATP during periods of C starvation (Sun et al., 2011) (Figure 1.7b).

(A)

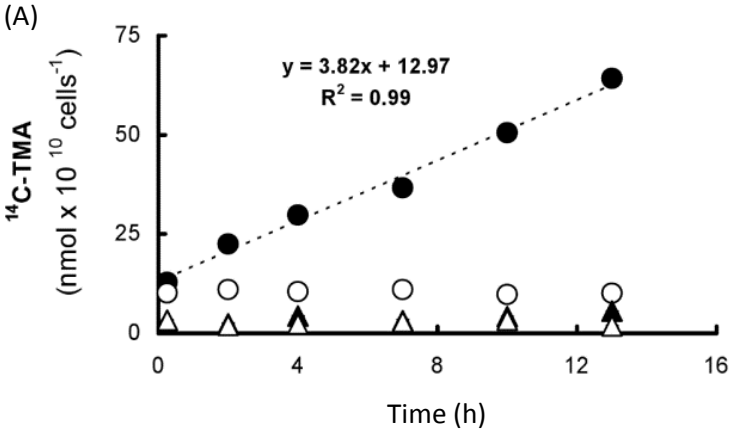

▲ Oxidation ($^{14}CO_2$) of live cells

△ Oxidation ($^{14}CO_2$) of dead cells (-ve control)

● Incorporation of live cells

○ Incorporation of dead cells (-ve control)

(B)

Test compounds[b]	samples	Cellular ATP content (Mean ± SD; zeptogram cell^{-1})
formate	T	32±3
	N	29±8
	P	221±4
* methanol	T	48±0
	N	16±3
	P	160±8
* formaldehyde	T	33±6
	N	14±1
	P	77±5
* DMSP	T	23±3
	N	16±1
	P	163±7
* methylamine	T	27±1
	N	18±0
	P	145±10
* glycine betaine	T	41±1
	N	23±3
	P	132±3
* TMAO	T	63±5
	N	26±2
	P	148±10

Figure 1.7. (A) ^{14}C-labeled compound utilization by *Candidatus* P. ubique HTCC1062 in culture. HTCC1062 Cells from log phase were collected and resuspended in artificial seawater media (ASW). Radioisotope assays were conducted at room temperature (22 ºC) in ASW amended with 5 µM ^{14}C-TMA **(B)** Quantification of intracellular ATP of starved ubique HTCC1062 cells after 2 h incubations with C1 and methylated compounds. b. Asterisk indicates statistical significance (p-value <0.01) between ‘‘no compound added’’ and ‘‘test compound’’ treatments. Abbreviations: T, test compound added; N, no substrate control; P, pyruvate added (positive control). Taken from Sun et al. (2011).

1.6.3. TMAO and DMA degradation

TMAO can serve as a substrate for both aerobic and anaerobic bacterial growth where in the latter it serves as a terminal electron acceptor during respiration, generating TMA as a product (Arata et al., 1992; Gon et al., 2001). TMAO reductase is the enzyme responsible for this anaerobic process and was originally characterised in *Escherichia coli* (Gon et al., 2001) and later identified in *Roseobacter denitrificans*, a member of the MRC (Arata et al., 1992; Gon et al., 2001). There are two forms of TMAO reductase that both have broad substrate specificity, including an affinity for DMSO (Silvestro et al., 1989). It is now known that the bacterial reduction of TMAO to TMA is responsible for the fouling smell associated with rotting fish (Barrett and Kwan, 1985).

Unlike the genes involved in TMA and MMA catabolism, the genes for the aerobic catabolism of TMAO and DMA are unknown. A eukaryotic TMAO demethylase (Tdm) is known to exist in nature (Parkin and Hultin, 1986; Kimura et al., 2000; Fu et al., 2006) and research focused on characterising this enzyme as one of the products of TMAO demethylation is formaldehyde, which is toxic to humans and therefore has implications for the fish food industry. Tdm has been purified from teleost fish species, including redhake (Parkin and Hultin, 1986) and Alaskan Pollock (Kimura et al., 2000) as well as molluscs, such as the Humboldt squid (Fu et al., 2006). Bacterial Tdm has been purified and characterised, first from *Bacillus* sp. PM6 (Myers and Zatman, 1971) and shortly after in *Aminobacter aminovorans* AM1 (formerly known as *Pseudomonas aminovorans*) (Large, 1971). Bacterial Tdm has a lower K_m (2-4 mM) than eukaryotic Tdm (26 – 30 mM) and also a higher molecular weight (*Bacillus* sp. PM6 36 – 47 kDa; eukaryotic Tdm - 17.5- 25 kDa). Unlike Tdm purified from *Bacillus*, the partially-purified Tdm from *A.*

aminovorans was not inhibited by the addition of TMA and it also had a different optimal pH (*Bacillus*, pH 7.5; *A*. *aminovorans*, pH 6) (Large, 1971). In all cases, the product of *in vitro* non-oxidative demethylation was formaldehyde.

Again using *A*. *aminovorans* as the model bacterium, DMA monooxygenase (Dmm) was purified from MA-grown cells and was shown to be an NADPH-dependent enzyme that produces MMA and formaldehyde (Alberta and Dawson, 1987). Dmm has a native molecular weight of ~210 kDa and consists of three subunits, 42,000, 36,000 and 24,000 kDa in size, each of which are essential for *in vitro* activity (Alberta and Dawson, 1987). Dmm is predicted to be an iron-containing monooxygenase which is distinct from that of cytochrome P-450, another well-studied type of iron-containing monooxygenase (Alberta and Dawson, 1987).

1.6.4. Quaternary amines and their degradation

QAs consisting of carnitine, choline and GBT are thought to be linked with a wide variety of eukaryotic and prokaryotic organisms where they have a number of structural, signaling and osmoregulatory roles (Ikawa and Taylor, 1973; Landfald and Strøm, 1986; Graham and Wilkinson, 1992). Choline and GBT are ecologically important compounds as they can be degraded anaerobically, producing MAs, which affect climate regulation (see section 1.3). Choline and GBT consist of a tertiary amine group with a two-C side chain (acetate) which is cleaved off during their catabolism, resulting in the production of TMA (King, 1984). Recently it was discovered that carnitine can be transformed to TMA under oxic conditions through aerobic cleavage of the C4 side group (Zhu et al., 2014). This study provided the first piece of evidence that the production of TMA from QAs can also occur in non-

anoxic environments. Below is a detailed breakdown of the current knowledge regarding the catabolism of choline and GBT.

1.6.5. Choline and its role in eukaryotic cells

Choline is an essential constituent of eukaryotic cells where it can either be incorporated into the polar head group of the phospholipid, phosphatidylcholine, or sphingolipids. Choline plays an essential role in the transfer of methyl groups between cellular compounds and can be transformed into the neurotransmitter, acetylcholine (Ikawa and Taylor, 1973). In the marine environment, concentrations of choline are in the low nM range and one of the major sources is thought to be marine microalgae (Ikawa and Taylor, 1973; Roulier et al., 1990). Choline can also be found in another two forms, choline O-sulfate and choline O-phosphate, which are present in a wide variety of eukaryotic organisms (Ikawa and Taylor, 1973). Choline O-phosphate, usually found in phospholipids and sphingolipids, can be found in its non-lipoidal form within the cell. It has been suggested that due to its high solubility in organic solvents, as well as its high abundance in plant saps, choline can act as a carrier molecule for the transport of phosphate across plant cell membranes (Maizel et al., 1956). Choline O-sulfate has been shown to accumulate in a number of plant species that are typified by their ability to undergo periods of salt stress, usually through the influx of sea water (Ikawa and Taylor, 1973). Therefore it is assumed that choline O-sulfate acts as a compatible solute for organisms, helping stabilise cell osmolarity. Specifically, choline O-sulfate is accumulated in higher plants (Hanson et al., 1991), marine algae and marine fungi (Catalfomo et al., 1973; Blunden and Gordon, 1986). It has also been shown to confer osmoregulatory properties in bacteria, namely, *E. coli* and *Salmonella*

typhimurium, when grown under conditions of high salt concentration (Hanson et al., 1991).

1.6.6. Bacterial uptake and metabolism of choline

Although it has been reported in a few instances, bacterial cells do not commonly use choline as part of a moiety in the lipid bilayer. However, there are examples of bacteria that are capable of utilising choline as a component of the lipid bilayer. For example, the uptake of choline into the plant pathogen, *Agrobacterium tumefaciens* is partially required for the synthesis of phosphatidylcholine, a constituent of this bacterium's cell membrane (Aktas et al., 2011). In this bacterium, phosphatidylcholine is required for virulence, motility, biofilm formation and responding to environmental stressors (Wessel et al., 2006; Aktas et al., 2011). A similar role for choline also takes place in the human pathogen, *Streptococcus pneumoniae*, where choline is incorporated into either the cell wall or membrane, influencing cell morphology and surface attachment to host cells (Vollmer and Tomasz, 2001).

There are multiple pathways involved in the degradation of choline, but in aerobic environments, the most common pathway involves the two-step oxidation of choline to GBT via the intermediate, betaine aldehyde, using the enzymes choline dehydrogenase (BetA) and betaine aldehyde dehydrogenase (BetB) (Andresen et al., 1988) (Figure 1.8).

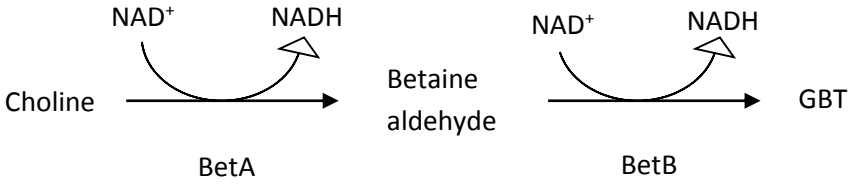

Figure 1.8. Oxidation of choline to GBT is a two-step process via the intermediate, betaine aldehyde. Each oxidation reaction generates the reducing equivalent, NADH. Abbreviations: BetA, choline dehydrogenase; BetB, betaine aldehyde dehydrogenase.

The gene operon *betIAB* was identified in *E. coli* and shown to be essential for the conversion of choline to GBT (Andresen et al., 1988). A repressor molecule, BetI, has been shown to regulate *betAB* in a choline-dependent manner and the three genes encoding for these proteins are often found within a single operon, *betIAB* (Lamark et al., 1991; Lamark et al., 1996). In *E. coli*, the *betIAB* operon also responds to osmotic stress (Lamark et al., 1996). Choline also provides a source of C, N and energy for bacteria, such as *Sinorhizobium meliloti* (Smith et al., 1988). In addition, this compound also been implicated in the regulation of virulence factors associated with the opportunistic pathogen, *Pseudomonas aeruginosa* (Wargo et al., 2008). For example, choline catabolites, namely GBT and dimethylglycine (DMG), lead to the upregulation of phospholipase C (PlcH) and phosphorylcholine phosphatase (PchP) (Wargo et al., 2009). Choline, through its conversion to GBT, also serves as a potent osmoprotectant for bacteria, such as *E. coli*, when challenged with increasing salt concentrations, however, choline itself has no osmoprotectant properties (Landfald and Strøm, 1986; Styrvold et al., 1986; Graham and Wilkinson, 1992; Boch et al., 1994). GBT fulfils its role as an osmolyte by helping proteins and protein assemblies maintain proper conformation and therefore biological function in the face of changing osmotic conditions (Landfald

and Strøm, 1986; Styrvold et al., 1986; Graham and Wilkinson, 1992; Boch et al., 1994).

There are two main types transporters involved in the uptake of choline into the cell. The first is a proton-coupled betaine-carnitine-choline-transporter (BCCT), which is encoded by a single gene (*betT*) that was originally identified and characterised in *E. coli* (Lamark et al., 1991). Another BetT homolog was also identified in *Pseudomonas syringae* DC3000 (Chen and Beattie, 2008). The two BetT-type transporters have different kinetics. The BetT from *E. coli* is a high affinity (8 μM) but low velocity (5 nmol min^{-1}mg.$protein^{-1}$) transporter, whilst the BetT from *P. syringae* is a low affinity (877 μM) but high velocity (80 nmol min^{-1} mg.$protein^{-1}$) transporter (Lamark et al., 1991; Chen and Beattie, 2008). BCCT-type transporters are ubiquitous in microorganisms where they function in the uptake of compatible solutes, including dimethylsulfoniopropionate (DMSP) (Ziegler et al., 2010; Sun et al., 2012). The BCCT-type transporter responsible for DMSP uptake is different from other BCCT-type transporters in that it has a wider substrate specificity and can also transport GBT and choline (Sun et al., 2012). The second type of choline transporter is an ATP-binding cassette (ABC)-type transporter. ABC transporters form one of the largest gene superfamilies found within many bacterial genomes (Young and Holland, 1999) and their expression is frequently detected in the marine environment (Sowell et al., 2008; Ottesen et al., 2011; Sowell et al., 2011). ABC transporters are essential for bacteria because they are responsible for the uptake of a wide range of compounds, such as sugars, amino acids, metals, and vitamins, at the expense of ATP (Davidson and Chen, 2004). They usually consist of three subunits: a transmembrane domain, which is bound to an inner membrane-bound ATP-binding domain and a periplasmic substrate-

binding protein (SBP), which binds a given ligand. SBPs confer substrate specificity and can bind their ligands with very high affinity (Albers et al., 1999; Chen et al., 2010a). One group of ABC transporters specialises in the uptake of compatible osmolytes and structurally related compounds, such as GBT, choline, carnitine, and proline betaine (Berntsson et al., 2010; Chen et al., 2010a; Thomas, 2010). In *S*. *meliloti*, three distinct SBPs, ChoX, CaiX, BetX, bind their given ligands, choline, carnitine or GBT, respectively, and use a single transmembrane permease/ATP-binding domain to transport the osmolyte across the cell membrane (Figure 1.9). Interestingly, CaiX and BetX were specific only for their primary ligands whereas ChoX could also transport GBT as well as choline (Chen et al., 2010a). In estuarine waters, choline is rapidly taken up by bacterial cells and used as either a growth substrate or as an osmolyte (after conversion to GBT). The ratio of GBT oxidation versus accumulation is dependent on the salinity of the external environment (Kiene, 1998).

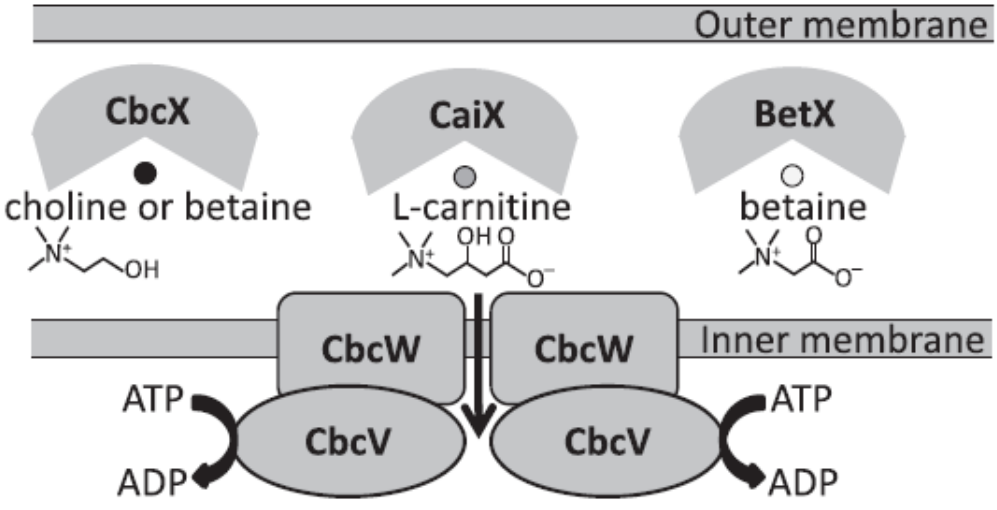

Figure 1.9. Model of the interacting components comprising the choline ABC transporter of *P*. *aeruginosa* and *P*. *syringae*. Taken from Chen et al (2010). Abbreviations, CbcX, the substrate binding protein specific for choline, referred to as ChoX in the text; CaiX is the substrate binding protein specific for carnitine; BetX is the substrate binding protein specific for GBT; CbcW is the transmembrane permease of the ABC transporter; CbcV is the ATP-binding domain of the ABC transporter.

1.6.7. Microbial degradation of GBT and it metabolites

In bacteria, two distinct types of enzymes are known to be involved in the aerobic catabolism of GBT to dimethylglycine (DMG). One is GBT demethylase (GbcAB) encoded by *gbcAB* in *Pseudomonas aeruginosa* (Wargo et al., 2008) and the other is GBT homocysteine methyltransferase (BHMT) found in *S*. *meliloti* (Barra et al., 2006). BHMT is involved in methionine synthesis where the methyl group from GBT is transferred to homocysteine producing methionine. BHMT has a domain similar to that of methionine synthase (MetH) in *E*. *coli* which synthesises methionine from homocysteine, this time using methylene-H_4F as the donor and liberating H_4F (Barra et al., 2006). GbcAB is an oxygen-dependent demethylase (Figure 1.10) which is predicted to produce formaldehyde and DMG and therefore has a different mechanism to BHMT (Wargo et al., 2008).

Figure 1.10. The two pathways/mechanisms for GBT catabolism known to exist in aerobic bacteria. On the left is GBT homocysteine methyltransferase (BHMT) which transfers the methyl group onto a suitable acceptor, in this case homocysteine. This enzyme is essential in the soil bacterium *S*. *meliloti* (Barra et al., 2006). On the right is the oxygen-dependent GBT demethylase (GbcAB) that is essential for growth on GBT in the human pathogen, *Pseudomonas aeruginosa* (Wargo et al., 2008).

In the same study, a unique DMG demethylase, similar to the characterised, *N*-methylproline demethylase that produces sarcosine as a product, was also identified. The authors also showed that the major enzyme involved in sarcosine

demethylation to glycine (the final demethylation step of GBT) is the multi-subunit enzyme, sarcosine oxidase, encoded by the gene cluster, *soxABDG*, which was originally characterised in *Corynebacterium* spp. (Chlumsky et al., 1995). An alternative pathway for DMG degradation also exists for bacteria. For example, the gram-positive bacterium, *Arthrobacter globiformis* uses a DMG oxidase, which is similar to that of the mammalian DMG dehydrogenase (Steenkamp and Husain, 1982; Otto et al., 1996), containing a tetrahydrofolate (H_4F)-binding domain (Meskys et al., 2001). No DMG dehydrogenase has been characterised in gram-negative bacteria, although recent comparative genomic analysis has identified potential homologs to mammalian DMG dehydrogenases (Steenkamp and Husain, 1982; Otto et al., 1996) in the genomes of *Phaeobacter gallaeciensis* and SAR11 bacteria (Sun et al., 2011; Thole et al., 2012).

1.7. One carbon compound utilisation – a brief introduction

One C (C1) metabolism refers to the metabolism of compounds that do not contain C-C bonds. The most common examples include, methane, methanol, TMA, TMAO and MMA. Microorganisms that are capable of growth on C1 compounds as their sole C and energy source, are classified as methylotrophs. A small subset of these microorganisms can also utilise methane, are named methanotrophs. In all cases the methyl groups associated with these C1 compounds are converted to formaldehyde which is then either conjugated to the carrier molecules H_4F, glutathione (GSH) or tetrahydromethanopterin (H_4MPT) (Chistoserdova et al., 2009). In a limited number of instances, a more simple system for the direct utilisation of formaldehyde, via a formaldehyde dehydrogenase, is adopted (Tanaka et al., 2003). However, in the vast majority of methylotrophs, the cofactor-conjugated C1 unit is either dissimilated to CO_2 to generate reducing power and

ATP or assimilated into biomass. Methylotrophs can be broadly categorised into two different groups based on their chosen mechanism of C1 assimilation. Type 1 methylotrophs, typically obligate methylotrophs, use the ribulose monophosphate (RuMP) pathway for C1 assimilation where formaldehyde serves as the entry point (Anthony, 1982). Type II methylotrophs, generally facultative methylotrophs, assimilate the C1 units through the serine cycle where methylene-H_4F serves as the entry point (Anthony, 1982). The majority of methylotrophs use H_4MPT as the primary carrier molecule for C1 oxidation. In this pathway, formate is produced and it is at this branch point that in Type II methylotrophs, the C1 unit is either fully oxidised to CO_2, or fed through the H_4F-linked pathway (reductive direction) ultimately producing methylene-H_4F which enters the serine cycle, mediated by the enzyme, serine hydroxymethyltransferase (Anthony, 1982). In a recent review, the various steps of methylotrophy were broken down into various modules which have distinct metabolic goals: 1) The oxidation (usually demethylation) of a methylated compounds, releasing a C1 unit, 2) The oxidation of the C1 unit, and 3) The assimilation of the C1 unit, either via formaldehyde (RuMP cycle) or methylene-H_4F (serine). CO_2 that is produced during the oxidation of the C1 unit can also be assimilated through either the Serine cycle or the Calvin-Benson-Bassham (CBB) cycle or both (Chistoserdova, 2011). An overview illustrating the various pathways in methylotrohy is shown in Figure 1.11)

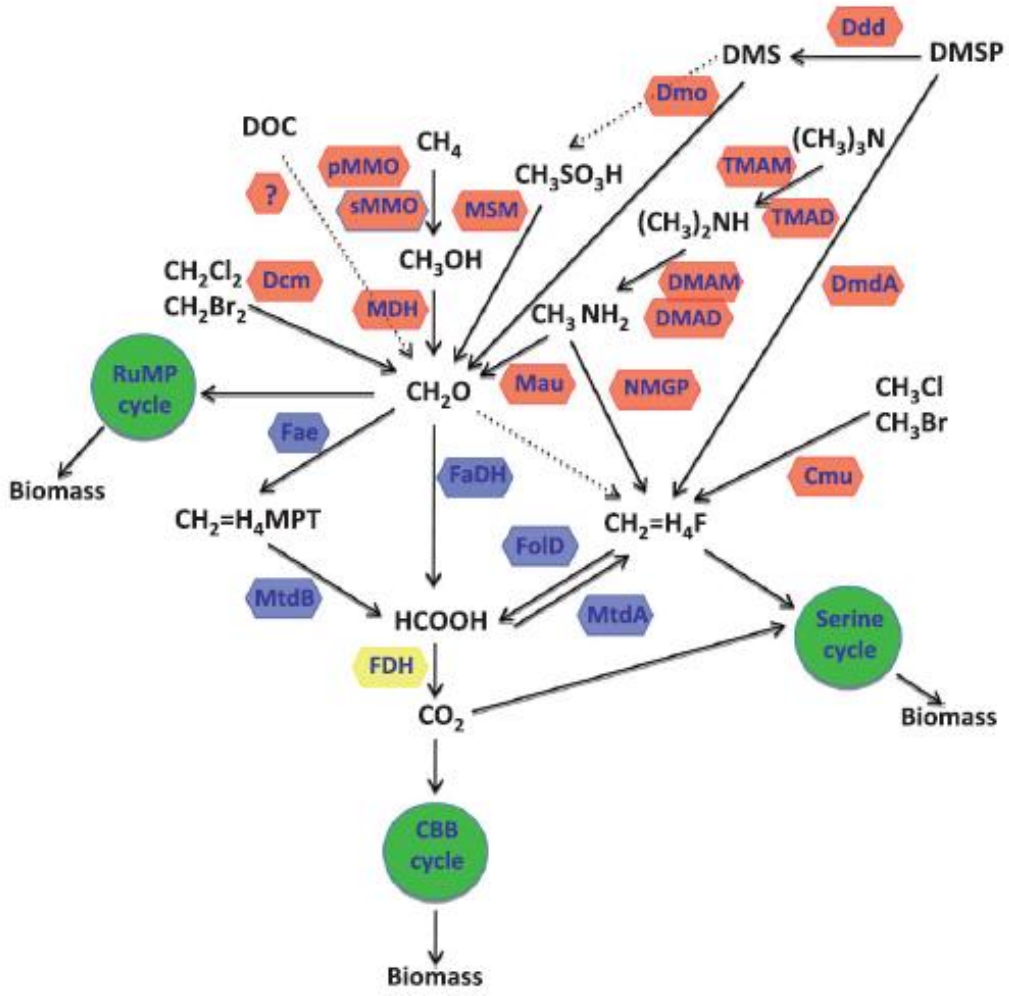

Figure 1.11. A simplified diagram depicting major substrates and intermediates and major methylotrophy metabolic modules. Primary oxidation (demethylation, dehalogenation) modules are shown in red, formaldehyde (methyl-H_4F) handling modules are shown in blue, formate dehydrogenase module is shown in yellow and assimilation modules are shown in green. Dashed lines depict non-enzymatic reactions, or lack of biochemical knowledge, or both. Abbreviations for enzymes as follows; Ddd, DMSP lyases; Dmo, DMS monooxygenase; MSM, MSA monooxygenase; TMAM, TMA monooxygenase; TMAD, TMA dehydrogenase; DMAM, DMA monooxygenase; DMAD, DMA dehydrogenase; Mau, MMA dehydrogenase; NMGP, GMA/NMG pathway (see section 1.6.1); DmdA, DMSP demthylase; Cmu, monohalogenated methyltransferases; pMMO, particulate methane monooxygenase; sMMO, soluble methane monooxygenase; MDH, methanol dehydrogenase; Dcm, dihalogenated dehalogenase/glutathione S-transferase; Fae, formaldehyde activating enzyme; FaDH, formaldehyde dehydrogenase; FolD, 5,10-methylene-H_4F dehydrogenase/ methenyl-H_4F Cyclohydrolase; MtdA, 5,10-methylene-H_4F dehydrogenase; MtdB, 5, 10-methylene-H_4MPT; FDH, formate dehydrogenase. Abbreviations for compounds; DOC, dissolved organic carbon; CO_2, carbon dioxide; HCOOH, formate, CH_2O, formaldehyde; $CH_2{=}H_4F$, methylene-H_4F; CH_3OH, methanol; CH_4, methane; CH_2Cl_2, di-chloromethane; CH_2Br_2, di-bromomethane; DMS, dimethylsulfide; DMSP, dimethylsulfoniopropionate; CH_3S0_3H, methanesulfonate $(CH_3)_3N$, trimethylamine, $(CH_3)_2N$, Dimethylamine; $(CH_3)N$, monomethylamine. Taken from (Chistoserdova, 2011).

1.8. C1 oxidation pathways in marine bacteria

Recently it was discovered, primarily through comparative genomic analysis, that a number of marine bacterial strains have the genes necessary for the oxidation of methylated compounds (Moran et al., 2004; Giovannoni et al., 2005). In the marine environment, the majority of bacteria possessing these genes are heterotrophic bacteria that can grow on organic C substrates with differing length C-C bonds (Sun et al., 2011; Chen, 2012). Unlike the more traditional obligate methylotrophs, such as *Methylophaga*, marine heterotrophs, including members of the MRC and SAR11 clade, do not have the genes required for the conjugation of formaldehyde with the carrier-molecule, H_4MPT, however they do possess the genes required for H_4F-linked C1 oxidation (Boden et al., 2011b; Sun et al., 2011; Chen, 2012; Halsey et al., 2012). In the H_4F-linked C1 oxidation pathway, the bifunctional enzyme, 5, 10-methylene-H_4F dehydrogenase/ methenyl-H_4F cyclohydrolase (FolD) first converts methylene-H_4F to methenyl-H_4F and then oxidises this to produce formyl-H_4F (Figure 1.11). 10-formyl-H_4F synthetase (Fhs) then converts formyl-H_4F to formate.

In Type II methylotrophs, Fhs has a primary role in C1 assimilation where it works in reverse, generating formyl-H_4F from formate, consuming ATP in the process (Marx et al., 2003b). From here two alternatives to FolD, MtdA and Fch, which have methylene-H_4F dehydrogenase and methenyl-H_4F cyclohydrolase activities, respectively, work in reverse generating methylene-H_4F which then serves as the entry point for C1 assimilation via the serine cycle (see Chistoserdova (2011) and references within). Although a *folD* mutant could be complemented with *mtdA*, an *mtdA* mutant could not be complemented with *folD*, thus illustrating that FolD is unidirectional and only has a role in C1 dissimilation (Studer et al., 2002; Marx and

Lidstrom, 2004). *mtdA* and *fchA* are not present in the genomes of either the SAR11 clade or MRC, strengthening the hypothesis that the H_4F pathway is primarily a route for C1 oxidation. In addition to Fhs, some MRC isolates possess another enzyme, formyl-H_4F demformylase (PurU), which can also carry out the oxidation of formyl-H_4F to formate (Nagy et al., 1995) (Figure 1.12). Formate dehydrogenase (Fdh) carries out the final step and completes full oxidation to CO_2 coupling this with the reduction of NAD^+ to NADH.

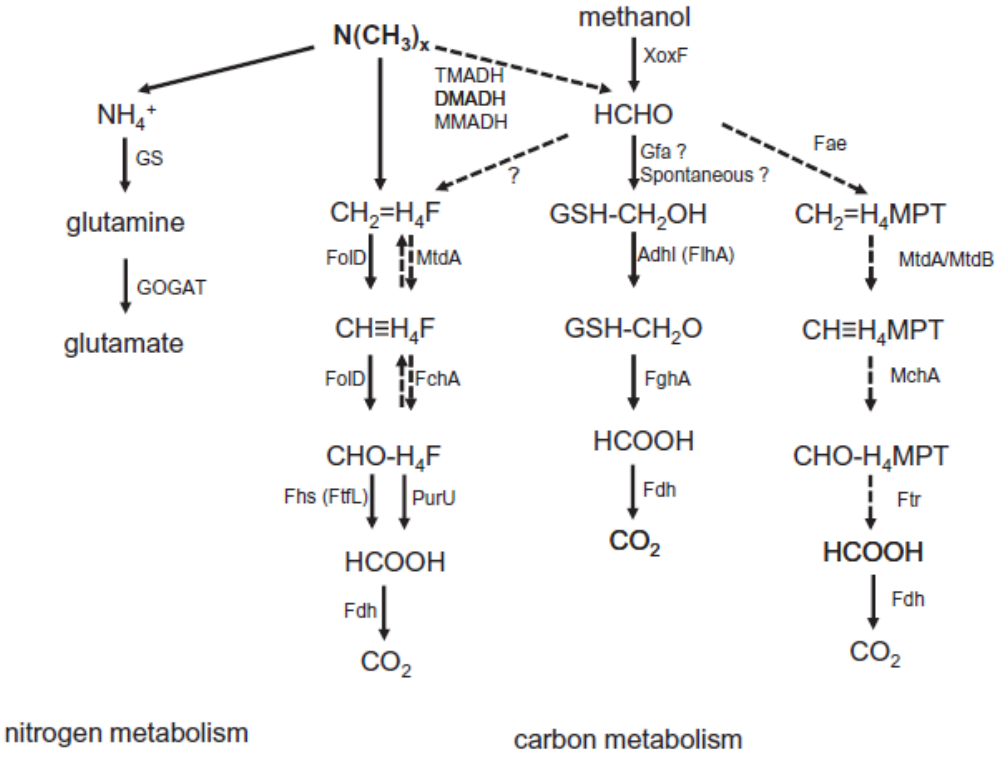

Figure 1.12. Proposed C1 oxidation pathways and N assimilation pathways in MA metabolism by the MRC isolates. The *Roseobacter* genomes lack genes (indicated by dashed lines) encoding the H_4MPT-linked C1 oxidation pathway, genes encoding MADH, DMADH and MMADH, as well as genes encoding the conversion of 5,10-methylene tetrahydrofolate (CH_2 = H_4F) to 10-formyl tetrahydrofolate (CH ≡ H_4F). Abbreviations: H_4F, tetrahydrofolate; H_4MPT, tetrahydromethanopterin; GSH, glutathione; GS, glutamine synthetase; GOGAT, glutamate synthase (glutamine:2-oxoglutarate aminotransferase); TMADH, trimethylamine dehydrogenase; DMADH, dimethylamine dehydrogenase; MMADH, monomethylamine dehydrogenase.

1.9. The marine *Roseobacter* clade (MRC)

The MRC is a monophyletic group (~87% identity in 16S rRNA genes) of bacteria within the family *Rhodobacteraceae* (Buchan et al., 2005). The MRC are an ecologically significant clade, sometimes representing up to 20% of the bacterial cells in marine coastal waters (Buchan et al., 2005; Giebel et al., 2011). The use of both 'omics' and physiological experimentation has revealed that MRC bacteria harbour an extraordinary ability to metabolise a wide range of substrates to support their growth (Moran et al., 2004; Buchan et al., 2005; Newton et al., 2010). This clade is frequently detected during eukaryotic phytoplankton blooms or found in close associations with eukaryotic biota and a number of strains have been isolated from a wide range of environmental niches, including arctic sea ice, the phytosphere, epiphytic plants, coral mucus and larvae, turbot larva rearings, seahorse mucus and a number of different molluscs (Hahnke et al. 2013; González et al., 2000; Hjelm et al., 2004; Buchan et al., 2005; Porsby et al., 2008; Wagner-Dobler et al., 2009; Lema et al., 2014; Nelson et al., 2014). Due to their high level of metabolic diversity, and high *in situ* metabolic activity (Alonso and Pernthaler, 2006), the MRC plays a major role in C, sulfur and N cycling within dynamic coastal surface waters (González et al., 1999; González et al., 2000; Buchan et al., 2005; Moran and Miller, 2007; Chen, 2012). Efforts to construct a phylogenetic comparison of sequenced isolated from this clade has proven be challenging using conventional single-locus analysis due to the high level of horizontal gene transfer observed within this clade (Biers et al., 2008). To overcome this problem, Newton et al. (2010) adopted a multi-locus comparison method of phylogeny and revealed the presence of 5 major sub-groups within the MRC. Voget et al. (2014) later incorporated *Planktomarina temperata* (Figure 1.13), an isolate related to the

Roseobacter clade affiliated (RCA) group, frequently the major group detected in temperate and polar waters, but absent in tropical and subtropical waters (Selje et al., 2004; Giebel et al., 2009; Giebel et al., 2011; Voget et al., 2014). A number of MRC isolates are amenable to conventional cultivation and genetic manipulation methods and are therefore ideal candidates for the study of bacterial metabolism and physiology (Buchan et al., 2005; Sorokin et al., 2005; Prado et al., 2009; Boden et al., 2011c; Cunliffe, 2011).

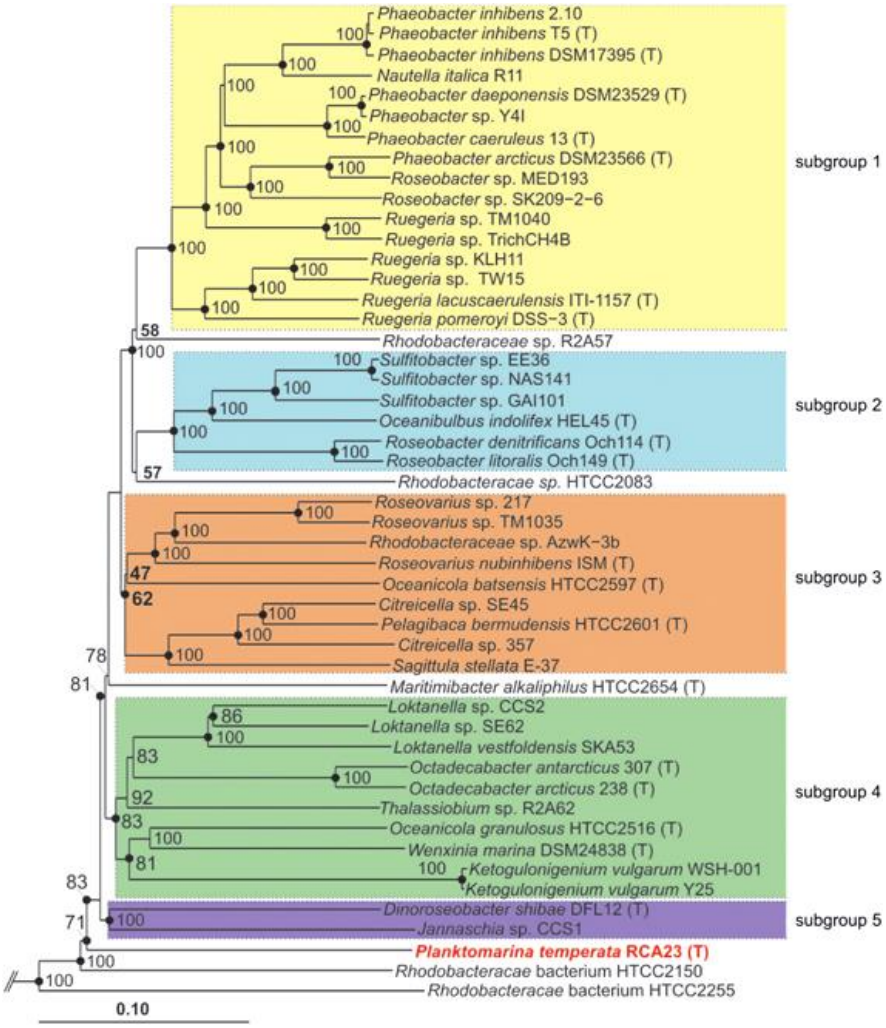

Figure 1.13. Neighbour-joining tree based on multilocus sequence analysis (MLSA) of genome sequenced organisms of the MRC. The tree was constructed using ARB v5.1 and is based on a similar tree of Newton *et al*. (2010) but includes additional genomes sequences and an extended gene set. Filled circles indicate nodes also recovered reproducibility with maximum-likelihood calculation. Subclades of the MRC are marked by different colours. *Escherichia coli* MG1655 was used as an outgroup. Abbreviations: T, type strains.

The MRC have been heavily implicated the cycling of reduced sulfur compounds, such as the osmolyte, dimethylsulfoniopropionate (DMSP), that is produced by the phytoplankton (González et al., 1999; Vila et al., 2004; Howard et al., 2008). *Roseobacter* cells have been shown to be the major players responsible for taking up DMSP during phytoplankton blooms (Vila et al., 2004). Interest in the cycling of DMSP has been driven by the notion that one of its metabolites, DMS can lead to the formation of CCN, therefore increasing cloud albedo and theoretically helping to reflect UV radiation back into space (Charlson et al., 1987). The link between increased sunlight, temperature, phytoplankton production and ultimately increased DMS, is predicted to help self-regulate the planets' climate in a negative feedback manner and this process was named the CLAW hypothesis (Charlson et al., 1987). A number of DMSP lyases, which can cleave DMSP into DMS have been identified using isolates from the MRC and it is now evident that the MRC is a producer of oceanic DMS (Kirkwood et al., 2010; Curson et al., 2011; Todd et al., 2012).

1.10. *Ruegeria pomeroyi* DSS3 – an introduction

Ruegeria pomeroyi DSS-3 is a member of the MRC that was isolated off the coast of Georgia, USA, during a phytoplankton bloom, using DMSP as the sole C source (González et al., 2003). *R. pomeroyi* was one of the first fully sequenced bacterial genomes and this research identified that this bacterium has a variety of mechanisms for the acquisition of both C, N, sulfur and energy (Moran et al., 2004). For example, Moran and colleagues (2004) have identified the genes involved in the oxidation of both carbon monoxide (CO) and thiosulfate, two processes which help generate reducing power and ATP (Friedrich et al., 2001; Sorokin et al., 2005; Cunliffe, 2011). *R. pomeroyi* is a classic heterotrophic bacterium capable of

utilising a range of organic C substrates, including differing length polysaccharides, as a sole C and energy source (González et al., 2003). Unlike a number of other MRC isolates, *R*. *pomeroyi* does not contain any photopigments, such as bacteriochlorophyll, to enable the light-stimulated production of reducing power (Newton et al., 2010). Recent work has shown that *R*. *pomeroyi* can grow on TMA or MMA as a sole N source, but has an incomplete set of genes required for the incorporation of C1 units, via the serine cycle, released during the catabolism of methylated compounds. Accordingly, *R*. *pomeroyi* cannot grow on TMA or MMA as a sole C and energy source and is not a true methylotroph. Due to the ease of cultivating this bacterium, *R*. *pomeroyi* has fast become a model marine bacterium to study bacterial metabolism. (Chen et al., 2011; Sebastian and Ammerman, 2011; Cunliffe, 2012; Todd et al., 2012). For example, genes involved in DMSP cleavage and phosphate acquisition were experimentally confirmed using this bacterium (Sebastian and Ammerman, 2009; Sebastian and Ammerman, 2011; Todd et al., 2012)

1.11. Project aims

The aims of this project were as follows:

1. To identify the key genes and enzymes responsible for the metabolism of TMAO in marine bacteria using *R*. *pomeroyi* as the model organism;
2. To investigate the regulatory mechanisms controlling expression of Tmm in *R*. *pomeroyi* and whether or not DMS oxidation in *R*. *pomeroyi* can be stimulated;
3. To investigate whether the oxidation of TMA or TMAO has any beneficially effect on the physiology of *R*. *pomeroyi*;

4. To determine if the H4F-linked pathway for C1 oxidation is essential for the turnover of MAs in *R. pomeroyi*;
5. To develop functional primers that allow for the environmental screening of Tdm in the marine environment;
6. To identify the genes and enzymes involved in choline metabolism in marine bacteria using *R. pomeroyi* as the model organism.

Chapter 2

Materials and Methods

2.1. Cultivation of marine bacterial strains

All reagents were made using Milli-Q H_2O and sterilised by autoclaving at 121°C for 15 min. All ingredients that were sensitive to autoclaving were filtered-sterilised through a 0.2 µm membrane (Millipore, Darmstadt, Germany). The adjustment of pH was performed when necessary with the careful addition of NaOH or HCl. The vitamins solution was passed through a sterivex 0.2 µm membrane under pressure through a peristaltic pump.

2.1.1. Maintenance of marine *Roseobacter* strains

All strains listed in Table 2.1 were stored at -80°C in Diffco 2216 Marine broth containing 10% glycerol. For all experiments, cells were revived on marine broth agar plates (1.5%) and incubated at room temperature (~20°C) prior to short term storage at 4°C.

2.1.2. Antibiotics used for *Ruegeria pomeroyi*

All antibiotics were prepared by the in-house media preparation team. The following concentrations required to isolate and maintain *Ruegeria pomeroyi* mutant strains were as follows: kanamycin (80 µg ml^{-1}), gentamicin (10 µg ml^{-1}) spectinomycin (150 µg ml^{-1}).

2.1.3. Physiological experimentation with marine *Roseobacter* strains

Two minimal medium recipes were used throughout the course of study. A range of C sources and nitrogen sources were used depending on the specific experiment being conducted. A minimal sea salt medium adapted from (Chen 2012) was used. Briefly, the ingredients were: Seasalts (Sigma-Aldrich, Gillingham, UK) 30g l^{-1}, 10mM 4-(2-hydroxyethyl)piperazine-1-ethanesulfonic acid sodium (HEPES) pH 8 (Sigma-Aldrich, UK), 1mM $NaPO_4$ solution, 50µM $FeCl_2$, Vitamins solution (1 ml

l^{-1}) (Kanagawa et al., 1982). All ingredients were added to seasalts (2-4 % w/ v) after autoclaving. The second minimal medium used was the marine ammonium mineral salt medium (MAMS) adapted from (Schäfer, 2007). Vitamins solution was added the same as for the seasalts medium.

2.1.4. Preparation and transformation of electrocompetent *R. pomeroyi* cells

Electrocompetent cells were prepared by modifying the protocol developed by Sebastian et al. (2009). Briefly, *R. pomeroyi* was grown in a MAMS with glucose (10 mM) as the C source and NH_4^+ (7.5 mM) as the N source. Cells (50 mL) were incubated at 30 °C until the cultures reached an OD_{540} of ~0.4. Cells were washed four times with ice-cold, sterile 10% (v/v) glycerol to remove salts and then resuspended in a final volume of 2 mL 10% glycerol. 50-µL aliquots were rapidly frozen in dry ice/ethanol and stored at −80°C for a maximum for 4 months.

For transformation, cells were thawed on ice for 5 min prior to mixing with 50-200 ng of DNA. Cell suspensions were placed into a 1mm gap "Electroporation Cuvette Plus" (BTX, Harvard Apparatus Inc., MA, USA). The settings used were as follows: 2.5 kV/mm, 200 A resistance, and 25 Ω capacitance. The time constant varied between 3.9 and 4.5 ms.

2.1.5. Cultivation of *Methylomonas methanica* MC09

Methylomonas methanica MC09 was maintained on MAMS agar with methane (5% v/v in the head space) as the sole C source. For all experiments *M. marina* was grown in MAMS as described above with methanol (1 mM) added as the sole C source. All *M. methanica* cultures were incubated at 25ºC and liquid cultures agitated in an orbital shaker (150 rpm).

2.1.6. Co-culture of *R. pomeroyi* and *Methylomonas methanica* MC09 (Chapter 4)

R. pomeroyi wild-type and the mutant, *Δtmm::Gm*, were grown using either TMA or TMAO (0.5 mM) as the sole N source, respectively (OD_{540} ~0.3). Cells were resuspended in fresh medium containing 1 mM methanol. For each strain, triplicate cultures were set up using either TMA (1 mM) or NH_4^+ (1 mM) as the sole N source. *M. methanica* was grown using methanol as the C source (2mM) and $NH4^+$ (0.5mM) as the limiting nutrient until the onset of stationary phase. To determine *M. methanica* cell counts, serial dilutions were generated (n=3) and 10 µl were spotted (n=3) on MAMS plates with methane as the sole C source and incubated at 25 ^oC. 5% (v/v) inocula of *M. methanica* (~10^7 cells) were added to each *R. pomeroyi* culture. Co-cultures were incubated at 25 ^oC on a rotary shaker (150 r.p.m.).

2.1.7. Calibration of optical density against biomass (mg dry weight l^{-1}) for *R. pomeroyi*

R. pomeroyi cultures (500 ml) were grown on glucose and NH_4^+ with or without TMA (3 mM) to an OD_{540} ~1.4. Cells were diluted to 0, 25, 50, 75 % (n=3) in MAMS and the OD_{540} was recorded prior to filtration onto 0.22 µm nitrocellulose filters (Millipore, UK). Cells trapped on the filter pads were washed twice with 15 ml sterile dH_2O to remove salts and other debris before being placed in a drying oven at 60^oC. Filters were repeatedly weighed until a constant weight was achieved. A standard curve was plotted for OD_{540} against dry weight (Chapter 5, section 5.3.2). For all conversions of optical density at 540 nm (OD_{540}) to dry weight, a constant of 1 OD unit at OD_{540} = 254 mg dry weight l^{-1} was applied.

2.1.10. Viable cell counts of *R. pomeroyi* during carbon/energy starvation (Chapter 4)

R. pomeroyi was grown in MAMS with TMA (3 mM) or TMAO (3 mM) as the sole N source to a final OD_{540} ~0.5. Cells were re-suspended in MAMS with no exogenous C and then aliquoted (20 ml) into 125 ml serum vials (n=3) with either no exogenous C (control), or TMA (1 mM) or TMAO (1 mM). For cell counts, serial dilutions were generated (n=3) and 10 µl were spotted (n=3) on ½ YPSS (per l; 2 g yeast extract, 1.25 g peptone, 20 g seasalts from Sigma-Aldrich) plates and incubated at 30°C. TMA and TMAO were quantified by ion-exchange chromatography as described in section 2.5.3.

2.2. *Escherichia coli*

All *Escherichia coli* strains were cultivated on Luria-Bertani (LB) medium (Sambrook et al., 2001). For growth on agar plates, Bacto agar (Difco) was added to a final volume (1.5% w/v). Stock cultures were frozen in LB with the addition of 10% (v/v) glycerol and stored at -80°C. Liquid cultures were incubated at 30-37°C on an orbital shaker (150 rpm).

2.2.1. Antibiotics used for *Escherichia coli*

The antibiotics used and their appropriate concentrations were as follows: kanamycin (25-50 µg ml^{-1}), gentamicin (10 µg ml^{-1}), spectinomycin (25 µg ml^{-1}), tetracycline (10 µg ml^{-1}), ampicillin (100 µg ml^{-1})

2.2.2. Transformation of chemically competent *E. coli* cells

Escherichia coli JM109 high competency cells (Promega, Fitchburg, WI, USA) were used for all routine cloning steps performed during this project. Cells were thawed on ice for 5 min, prior to the addition of 1-2 µl of nucleic acid and the

resulting suspension was put back on ice for a further 18 min. Cells were placed in to a hot H_2O bath at 42°C for 45-50 s and returned to ice for 2 min. 500-750 µl of SOC medium (Sambrook et al., 2001) was added and the cell suspension was placed in a shaking incubator (150 rpm) at 37°C for 1-1.5 h. Cells were plated onto LB agar plates containing the appropriate antibiotic(s).

2.2.3. Preparation and transformation of electrocompetent *E. coli* cells

Escherichia coli S17-1 was grown (250 ml) to mid-exponential phase (OD_{600} ~0.4-0.5) and immediately placed on ice for 20 min using sterile flat bottom plastic centrifuge tubes (500 ml). Cells were washed three times in sterile ice cold 10% (v/v) glycerol (first wash 200 ml; second wash 150 ml, third wash 100 ml). Centrifugation steps were performed at 8,000 x g. Cells were concentrated in 2 ml ice cold 10% (v/v) glycerol and divided into 50 µl aliquots. Aliquots were subjected to rapid freezing using liquid nitrogen and stored at -80°C.

2.2.4. Bi-parental mating of *E. coli* 217-1 and *R. pomeroyi*

5 ml of overnight-grown *E. coli* 217-1 and 20 ml of overnight-grown *R. pomeoroyi* cells were pelleted (1,800 x g for 5 mins) and resuspended in 300 µl MAMS medium by gentle agitation via pipetting up and down. The cell suspensions were mixed and placed on a filter pad (0.22 µm, Millipore) laid on top of ½ YPSS agar. After 18-24 hours incubation, cells were removed from the filter and plated out onto Sea salts minimal medium plates containing the appropriate antibiotic using succinate as a sole carbon and energy source (8 mM) and MMA as a nitrogen source (3 mM) to select against *E. coli*. Colinies were restreaked onto plates using the appropriate antibiotic and a kanamycin plate to select for kanamycin sensitive mutants that had lost the pk18*mobsacB* plasmid through a double homologous recombination event.

2.3. Extraction of nucleic acids

2.3.1. Extraction of DNA from marine bacteria

All DNA extractions were performed using the FastDNA™ SPIN Kit for Soil (MP Biomedicals, LLC, CA, USA) according to the manufacturer's instructions. For cultivated bacterial isolates, 1 -10 ml of liquid culture was centrifuged (8, 000 x g for 5 min) to generate a cell pellet. For isolation of DNA from seawater samples, between 250-750 ml was passed through a 145 μm filter (Millipore, Darmstadt, Germany) and then passed through a 0.22 μm filter (Millipore, Darmstadt, Germany) to collect biomass. Filters were placed in the lysis tubes and the subsequent extraction steps were performed according to the manufacturer's instructions.

2.3.2. RNA extraction from *R. pomeroyi*

For RNA work, all glassware, water and solutions were treated with diethylpyrocarbonate (DEPC) (or prepared with DEPC-treated water where appropriate) by shaking overnight at 37 °C in a 0.1% v/v solution prior to autoclaving (Preparation of DEPC-treated solutions was performed by Dr. Jason Stephenson). All plasticware, tips etc was RNase-free. Total RNA was isolated from *R. pomeroyi* using the hot acid-phenol method of Gilbert et al. (2000). The quality of the RNA was checked by running a small volume on a 1% (w/v) TBE-agarose gel. DNA was removed by one treatment using RNase-free DNase (Promega) and followed by purification using an RNeasy spin column (Qiagen, Crawley, UK) following the manufacturer's instructions (RNA-clean up protocol). Removal of all traces of DNA was confirmed by the absence of a 16S rRNA PCR product, using the primer set 341F/518R (Table 2.2), in reactions using 1 μl or 4 μl

(150-200 ng of RNA equivalent) of RNA template undergoing 30 cycles of PCR. In addition, minus (-) reverse transcriptase (RT) controls were performed in parallel to cDNA library preparation to ensure no DNA contamination was affecting the results from RT-PCR (see section 2.4.9).

2.3.3. Small-scale plasmid extraction from *E. coli* (mini-prep)

Small scale plasmid preparations were carried out using 1.5-5 ml overnight *E. coli* cultures using the Qiaprep Miniprep Kit (Qiagen) or GeneJET kit (Fermentas) according to the manufacturer's instructions.

2.3.4. Extraction of low copy-number plasmid DNA from *E. coli* (midi-prep)

To increase the yield of DNA retrieved from *E. coli* carrying a low-copy number plasmid, the Qiapep Midiprep Kit (Qiagen) was used according to the manufacturer's instructions.

2.4. Nucleic acid manipulation techniques

2.4.1. Quantification of DNA/RNA

Nucleic acids were quantified by using the ND-1000 spectrophotometer (NanoDrop Technologies Inc.,Wilmington, DE, USA). Integrity and purity of DNA was checked on a 1% w/v agarose gel made with TBE buffer.

2.4.2. Polymerase chain reaction (PCR)

PCRs were performed in either 25 µl or 50 µl reaction volume depending on the downstream application. Typically, when DNA was needed for further processing, a larger 50 µl reaction was used. Reactions were performed using the T-100 thermocycler (Bio-rad Laboratories Inc., Hercules, CA, USA) using either Dreamtaq (Fermentas), KAPATaq (KAPA biosystems, Willimgton, MA, USA) or

Pfu polymerase (Promega). Routine 50 µl reactions contained the following: 1 x Buffer, $MgCl_2$ (1.5 mM) usually incorporated in the buffer, 0.8 mM dNTPs (0.2 mM each nucleotide), 0.4 µM of the appropriate forward and reverse primer and *Taq* DNA polymerase (2.5 units). For some environmental work, the quantity of *Taq* was doubled to improve the yield of the PCR product. The reaction was made up to volume with nuclease-free sterile dH_2O. For the direct amplification of DNA from cells (colony PCR), DMSO (4%, v/v) and BSA (0.04%, w/v) were added to the reaction to help stabilise enzymes and permeabilise cell membranes. A typical reaction consisted of 3 min (increased to 5 min for colony PCR) denaturatation step at 95ºC, followed by 30 cycles of, 95ºC for 1 min, an annealing step (45-60ºC dependent on primers) of 30 s, an elongation step at 72ºC for an appropriate length of time (30 s for every 500 bp), followed by a final elongation step at 72ºC for 5 min. If reactions were run overnight, products were held at 8ºC in the T-100 thermocycler (Bio-rad). No template controls (no added DNA) were always run in parallel to check for contamination.

2.4.3. DNA restriction digests

Restriction digestion of DNA was carried out with enzymes from Promega or Fermentas according to the manufacturer's recommendations. Routine restriction digest reactions to check for plasmid integrity were performed using 500 ng of DNA. For restriction digest reactions where further downstream processing of DNA was required, roughly 3 µg of DNA was used. For reactions containing high quantities of DNA, the length of digestion was extended to 20-30 min to allow complete digestion.

2.4.4. DNA purification

DNA fragments were routinely excised from TBE agarose gels and the DNA was further purified using QIAquick (Qiagen) or Nucleospin (Macherey-Nagel, Düren, Germany) Gel Extraction Kits according to the manufacturers' instructions. PCR products of well-defined size were purified using the same protocol but without excision from gels. To increase the concentration of nucleic acids for downstream applications, 15 µl of elution buffer was used as the final volume for elution.

2.4.5. DNA ligations

Ligations were routinely carried out in 10 µl reactions using varying amounts of DNA and varying ratios of vector: insert. Typically the ratio of vector: insert was at least 1: 2. T4 DNA ligase (Promega, or Fermentas) was used according to the manufacturer's instructions. Apart from TA overhang cloning into pGEM-T vectors, where reactions were incubated at room temperature for 1 h, a ligation reactions were usually incubated overnight at 16^{o}C.

2.4.6. Cloning of PCR products

PCR products were cloned into pGEM-T Easy (Promega) according to the manufacturer's instructions. Where *Pfu* polymerase was used for high fidelity PCR amplification, the purified PCR product was incubated for a further 20 min (20 µl total volume) at 72^{o}C with dATP (0.2 mM), *Taq* polymerase (KAPA) (2.5 units) and 1 x KAPA*Taq* buffer to add an adenosine overhang at the 3' end of each strand.

2.4.7. Clone library construction

PCR products targeting the *tmm* and *tdm* genes were cloned as described in section 2.4.6. Direct amplification of DNA from colonies was performed using the primers M13F/M13R (Viera and Messing, 1982) targeting regions external to the targeted

PCR products. Amplification of DNA was confirmed by gel electrophoresis and desired products were purified as described in section 2.4.4.

2.4.8. Sequencing of DNA

PCR products (80-100 ng) or purified plasmids (500 ng) were combined with 5 pmol of the appropriate primer and made up to a total volume of 10 µl and submitted for Sanger sequencing (GATC, Germany). Sequence data were analysed in SeqMan Pro, part of the Lasergene software suite (DNASTAR, Madison, WA, USA), to check for DNA integrity and fidelity. Often, when dealing with sequences greater than 500 bp, primers targeting both ends of the sequence were used to generate a contiguous sequence.

2.4.9. Reverse transcriptase PCR (RT-PCR)

Reverse transcription was performed using SuperScript II (Invitrogen), according to the manufacturer's guidelines. Gene specific primers (2 µM) were used to target different transcripts. Between 100 and 200 ng of total RNA was used as a template for cDNA synthesis. For each reaction, a negative control (minus (-) RT) was also set where reverse transcriptase was substituted with H_2O. Prior to cDNA synthesis, contamination with DNA was checked for by PCR using either the 16S rRNA gene or *tmm* as the target.

2.4.10. Agarose gel electrophoresis

DNA fragments were separated in 0.5 – 2 % (w/v) agarose gels in 1 × TBE. 1kb plus DNA ladder (Fermentas) was used to estimate the sizes of DNA fragments. Ethidium bromide (0.5 µg ml^{-1}) was added to gels prior to casting. Gels were visualised on a Gene Genius transilluminator (Syngene, Cambridge, UK).

2.5. Analytical Methods

2.5.1. Quantification of Glucose

Prior to analysis, cells were removed from the culture medium by centrifugation at 12, 000 x *g* for 5 min. Quantification of glucose in the culture medium was achieved using the glucose (HK) assay kit (Sigma-Aldrich) according to the manufacturer's instructions. To conserve assay reagents, the assay was reduced to 100 µl reagent and 20 µl sample. This increased the number of assays from 20 to 200 per kit. A standard curve was generated using known quantities of glucose and verified against the standards provided by the manufacturer. For glucose concentrations above 5 mM the culture was diluted 1 in 2 to maintain a linear regression between absorbance (340 nm) and glucose concentration.

2.5.2. Quantification of intracellular ATP concentrations

R. pomeroyi wild-type and mutant strains were grown using either TMA or TMAO as the sole N source and cells were harvested by centrifugation (10 min; 8,000 g) at late exponential phase (1×10^9 cells ml^{-1}) and washed twice with fresh MAMS medium to remove exogenous C. Cells were re-suspended in MAMS medium minus glucose, given TMA (1 mM), TMAO (1 mM) or no exogenous energy source and then aliquoted (500 µl) into 2 mL microcentrifuge tubes (n=3). Cells were left for 16 h before adding a further 500 µL of each test compound. After 1 h, 100 µl of cell suspension was mixed with 100 µl of BacTiter Glo cell viability kit (Promega) and incubated for 5 min before recording luciferase activity on a Luminoskan^{TM} Ascent microplate luminometer (Thermo Scientific). A standard curve was generated using ATP standards (100 µM, 10 µM, 1 µM 100 nM 10 nM, 1 nM) generated from a 1mM stock solution of ATP (Abcam, Cambridge, UK).

2.6.2. Quantification of protein

Total protein concentration was determined using the Bio-Rad Protein Assay (Bio-Rad) according to the manufacturer's instructions. A standard curve was generated using bovine serum albumin (BSA, 0.25, 0.5, 0.75, 1 mg ml^{-1}).

2.5.3. Quantification of MAs, QAs and NH_4^+ by cation exchange ion chromatography

Quantification of MAs, QAs and NH_4^+ was achieved by cation-exchange ion chromatograph equipped with a Metrosep C4/250-mm separation column and a conductivity detector (Metrohm). The eluent used for separation was as follows (10x stock solution): ddH_2O up to 1 L, nitric acid (1.4 M), 500 ml acetone, 350 ml 2, 4-pyridinedicarboxylic acid monohydrate (PDCA). Eluent stock solution was stored at 4°C and diluted with ddH_2O prior to use.

2.5.4. Quantification of dimethylsulfide (DMS) by gas chromatography

R. pomeroyi cultures incubated with DMS were grown in 125 ml serum vials and sealed with rubber stoppers. Quantification of DMS in headspace gas was measured by injecting 100 µl of a headspace gas sample into a Shimadzu GC-2010 Plus gas chromatograph (Shimadzu Corporation, Columbia, U.S.A.) fitted with a 1 mm by 30 µm capillary dimethylpolysiloxane column (Shimadzu Corporation, Columbia, U.S.A.). Helium was used as the carrier gas (flow rate, 25 ml min-1) and the column temperature was 250°C. A flame ionization detector (FID) was used to detect DMS and methanethiol (MeSH). DMS concentrations were calculated by regression analysis based on a five-point calibration with standard DMS solutions in MAMS (Muhs, unpublished data).

2.6. Protein methods

2.6.1. Physical lysis of cells

Cells were broken for enzyme assays by passing three times through a French Press unit (American Instrument) at 110 megapascals at 4°C. Cell debris was removed by centrifugation at 17,000 x *g* for 20 min at 4°C. Cell-free extracts were placed on ice until further analysis.

2.6.3. Sodium dodecyl sulphate (SDS)-PAGE analysis

For routine analyses of purified protein purification or protein expression of IPTG-induced recombinant proteins, Mini-PROTEAN TGX precast polyacrylaminde gels (Bio-rad, USA) were used in conjunction with a Mini-PROTEAN tetra cell kit (Bio-rad, USA). Electrophoresis was conducted at 160-200 V during separation, using running buffer containing glycine (72 g l^{-1}), Tris base (15 g l^{-1}) and SDS (5 g l^{-1}). PageRuler Plus prestained protein ladder (Fermentas) was used as molecular mass markers.

2.6.3. His-tag purification

Recombinant protein with an N-terminus His-tag was purified using the His-Tag purification kit (Novagen, Merck Millipore, Germany) according to the manufacturer's instructions. Recombinant proteins were eluted using an elution buffer, containing 1 M imidazole, 0.5 M NaCl and 20 mM Tris-HCl (pH 7.9). A slight modification to collection of the eluted protein was made whereby purified protein was collected in 200 µl aliquots.

2.7. Enzyme assays

2.7.1. Detection of NADPH-dependent monooxygenase activity

Activity assays were performed as previously described by Chen (2012). Briefly, all enzyme assays were performed in triplicate using fresh cell-free crude extracts in 10 mM 1,4-piperazinediethanesulfonic acid (PIPES) buffer (pH 7.6) at room temperature (~21°C). TMA monooxygenase activities were assayed by quantifying the decrease in absorbance at 340 nm of substrate-dependent oxidation of NADPH (Melford Laboratories) according to the protocol of Chandler (1983). A final concentration of 1 mM TMA was used in the reactions. Negative controls were set up replacing TMA with H_2O to determine the endogenous rate of NADPH depletion in the cell-free extracts. Between 1-2 mg of protein were used for each reaction. All enzyme assays were performed in 1 ml cuvettes using a final volume of 1 ml. An extinction coefficient of 6.22 mM-1 cm^{-1} was used to calculate the specific activity (Chen, 2012).

2.7.2. Quantification of β-galactosidase activity (Miller assay)

Solutions used:

Z-buffer stock solution; 4.27 g Na_2HPO_4, 2.75 g $NaH_2PO_4 \bullet H_2O$, 0.375 g KCl,0.125 g, $MgSO_4 \bullet 7H_2O$ were made up to a final volume of 500 ml with the addition H_2O and adjusted to pH 7.0. Solution was stored at 4°C. Prior to daily use, 50 ml was mixed with 0.14 ml ß-mercaptoethanol. Fresh O-nitrophenyl-ß-D-galactoside (ONPG) (4 mg ml^{-1}) was prepared daily. 1 M Na_2CO_3 was prepared and stored at 4ºC.

Transconjugants, carrying the appropriate *lacfusion* plasmid, were stored on marine broth agar plates containing spectinomycin (175 µg ml^{-1}). Fresh cells were prepared

by re-streaking onto new agar within a week prior to the enzyme assays. Colonies were picked and placed into ½ YTSS containing spectinomycin (175 μg ml^{-1}) and grown overnight and this culture was used as an inoculum (2.5 %, v/v). Cells were grown overnight in MAMS with succinate (8 mM) as the C source containing the appropriate test compounds at a final concentration 0.5-1 mM. 10 ml of cells were harvested (centrifugation 8,000 x g for 10 min) and washed with Z Buffer (5 ml) prior to resuspension in 1 ml Z buffer. The protocol for determining β-galactosidase activity was adapted from Miller et al. (1972). Briefly, concentrated cells were diluted (1 in10) in Z buffer and the OD_{600} was recorded. 1 ml was transferred into 2 ml microcentrifuge tubes into which 2 drops chloroform and 1 drop SDS (0.1%, v/v) were added prior to vortexing to permeabilise the cell membranes. Lysed cells were pre-incubated at 30ºC for 2 min prior to the addition of 200 μl of the chromogenic substrate, ONPG. The reaction mixture was vortexed and incubated on a rotary shaker (150 r.p.m) at 30ºC. The enzymatic production of O-nitrophenol (ONP) resulted in the yellowing of the mixture. As soon as this yellowing occurred, the reaction was stopped using Na_2CO_3 (500 μl), which raises the pH of the mixture to pH 11, denaturing the enzyme. The time of the first incubation before the reaction was stopped was recorded. The reaction mixture was incubated for a further 5 min at 30ºC on a rotary shaker (150 r.p.m) to allow for complete colour development (Figure 2.1). To remove cell debris, reaction mixtures were centrifuged at 15,000 x *g* for 5 min. The production of ONP was quantified by recording the absorbance at 420 nm. The following equation was used to convert recording into Miller Units:

$$\text{Activity} = \frac{OD_{420}}{OD_{650} \times \text{time} \times \text{vol}} \times 1000$$

Time = time of reaction (min)
Vol = volume of cells used (ml)

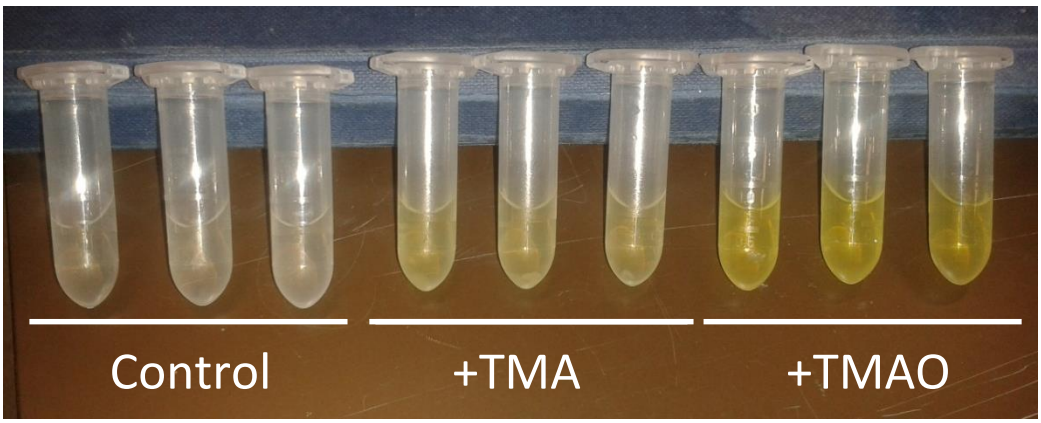

Figure 2.1. An example of the β-galactosidase activity assay. Microcentrifuge tubes shown were used to generate the results in Chapter 3, using the *Δtmm::Gm* mutant of *R. pomeroyi*.

Table 2.1. A complete list of strains and plasmids used throughout the course of this study

Plasmids/ strains	Description/use	Reference
Escherichia coli BLR(DE3) pLysS	Host for heterologously protein expression	(Sambrook et al., 2001)
E. coli S17.1	Electrocompetent cells used for mating	(Simon et al. 1983)
E. coli JM109	Routine host for cloning	(Sambrook et al., 2001)
Roseovarius sp. 217	Isolated from station L4 using methyl halide as the C and energy source	(Schäfer et al., 2005)
Roseovarius sp. TM1035	Isolated from a dinoflagellate culture	(Miller and Belas, 2004)
Roseobacter litoralis Och149	Isolated from seaweed	(Shiba, 1991)
Roseobacter sp. SK209-2-6	Isolated from Australian coastal amrine sediments	(Shiba, 1991)
Citreicella sp. SE45	Isolated from a US salt marsh	(Gifford et al., 2013)
R. pomeroyi	Wild type	(González et al., 2003)
R. pomeroyi Δtmm::Gm	Wild type with disrupted *tmm*	Thesis
R. pomeroyi Δtmm::Gm+tmm:DSS-3	*Tmm* mutant complemented with pBIL103	Thesis
R. pomeroyi Δtmm::Gm+tmm:217	*Tmm* mutant complemented with pBIL104	Thesis
R. pomeroyi Δtdm::Gm	Wild type with disrupted *tdm*	Thesis
R. pomeroyi Δtdm+DSS-3	*tdm* mutant complemented with pBIL001	Thesis
R. pomeroyi Δtdm+HIMB59	*tdm* mutant complemented with pBIL002	Thesis
R. pomeroyi ΔtmoXW::Gm	Wild type with disrupted *tmoXW*	Thesis
R. pomeroyi ΔtmoX::Gm	Wild type with disrupted *tmoX*	Thesis
R. pomeroyi ΔtmoX+tmoX:DSS-3	*tmoX* mutant complemented with pBIL101	Thesis
R. pomeroyi ΔtmoX+tmoX:HIMB59	*tmoX* mutant complemented with pBIL102	Thesis

Plasmids/ strains	Description/ use	Reference
R. pomeroyi Δfhs-1::Gm	Wild-type with disrupted *fhs-1*	Thesis
R. pomeroyi ΔtmoR::Gm	Wild-type with disrupted *tmoR*	Thesis
R. pomeroyi Δfhs-1::Gm Δfhs-2::Spc	Wild-type with both copies disrupted	Thesis
R. pomeroyi Δ+fhs:DSS-3	*Fhs-1fhs-2* mutant complemented pIL105	Thesis
Ruegeria pomeroyi DSS-3 *Δ1552::Gm*	Wild-type with disrupted SPO1552	Thesis
R. pomeroyi ΔtmoX::Gm Δ1552::Spc	Wild-type with disrupted *tmoX* and SPO1552	Thesis
R. pomeroyi ΔbetA::Gm	Wild-type with disrupted *betA*	Thesis
R. pomeroyi ΔbetB::Gm	Wild-type with disrupted *betB*	Thesis
R. pomeroyi ΔbetC::Gm	Wild-type with disrupted *betC*	Thesis
R. pomeroyi ΔbetT::Gm	Wild-type with disrupted *betT*	Thesis
R. pomeroyi Δ1578::Gm	Wild-type with disrupted SPO1578	Thesis
R. pomeroyi ΔbetA::Gm	Wild-type with disrupted *betA*	Thesis
R. pomeroyi ΔbetB::Gm	Wild-type with disrupted *betB*	Thesis
R. pomeroyi ΔbetC::Gm	Wild-type with disrupted *betC*	Thesis
R. pomeroyi ΔbetT::Gm	Wild-type with disrupted *betT*	Thesis
R. pomeroyi Δfhs1::Gm Δfhs2::Spc	Wild-type with both copies of *fhs* disrupted (*fhs* null mutant)	Thesis
R. pomeroyi Δfhs + fhs:DSS3	*fhs* null mutant complemented with native *fhs*	Thesis

Plasmids/ strains	Description/ use	Reference
R. pomeroyi ΔSPO1552::Gm	Wild-type with disrupted SPO1552	Thesis
p34S-Gm	Source of the gentamicin cassette	(Dennis and Zylstra., 1998)
pk18mobsacB	Suicide vector for *R. pomeroyi*, KanR	(Schäfer et al. 1994)
pBBR1MCS-km	Broad-host-range plasmid, KanR	(Kovach ME et al.. 1995)
pBIO1878	SpcR derivative of pMP220 with LacZ reporter gene	(Todd et al., 2012)
pBIL001	*tdm* of *R. pomeroyi* and the promoter of SPO1562 cloned into pBBR1MCS-km	Thesis
pBIL002	*tdm* of *Pelagibacter* strain HIMB59 and the promoter of SPO1562 cloned into pBBR1MCS-km	Thesis
pBIL101	SPO1548 (*tmoX*) and its promoter cloned into pBBR1MCS-km	Thesis
pBIL102	*tmoX* from strain HIMB59 and the promoter of SPO1548 cloned into pBBR1MCS-km	Thesis
pBIL103	SPO1551 (*tmm*) and its promoter cloned into pBBR1MCS-km	Thesis
pBIL104	*Tmm* from *Roseovarius* sp. 217 and the promoter of SPO1551 cloned in pBBR1MCS-km	Thesis
pBIL105	SPO1557 (*fhs-1*) and the promoter for its operon cloned into pBBR1MCS-km	Thesis
pKIL101	Internal fragment of SPO1562 (*tdm*) and the Gm^R cassette cloned into pK18mobsacB	Thesis
pKIL201	Internal fragment of SPO1548 (*tmoX*) and SPO1549 (*tmoXV*) and the Gm^R cassette cloned into pK18mobsacB	Thesis

Plasmids/ strains	Description/ use	Reference
pKIL202	Internal fragment of SPO1548 (*tmoX*) and the Gm^R cassette cloned into pK18mobsacB	Thesis
pBIOIL101	SPO1548 (*tmoX*) promoter cloned into pBIO1878	Thesis
pBIOIL102	SPO1551 (*tmm*) promoter cloned into pBIO1878	Thesis
pKIL301	Mutated *betA* and the Gm^R cassette cloned into pK18mobsacB	Thesis
pKIL302	Mutated *betB* and the Gm^R cassette cloned into pK18mobsacB	Thesis
pKIL303	Mutated *betC* and the Gm^R cassette cloned into pK18mobsacB	Thesis
pKIL304	Mutated *betT* and the Gm^R cassette cloned into pK18mobsacB	Thesis
pKIL305	Mutated *fhs1* and the Gm^R cassette cloned into pK18mobsacB	Thesis
pKIL306	Mutated *fhs2* and the Spc^R cassette cloned into pK18mobsacB	Thesis
pBIL301	Native *fhs* and the promoter upstream of the H_4F-linked C1 oxidation operon cloned into the vector pBBR1MCS-km	Thesis
pKIL401	Mutated SPO1552 and the Gm^R cassette cloned into pk18mobsacB	Thesis

Table 2.2. A list of primers used throughout the course of study

Primer	Sequence	Used for
Tdm_AF1_EcoRI	ATCAGGAATTCACCGTGTGAGATCGTCTGTG	Cloning region A of SPO1562 (*tdm*)
Tdm_AR1_XbaI	AATGCTCTAGAACACTGGAAATCGGTGCATT	Cloning region A of SPO1562 (*tdm*)
Tdm_BF1_XbaI	AATGCTCTAGAGTCTATACCGCCATGTGCT	Cloning region B of SPO1562 (*tdm*)
Tdm_BR1_PstI	CAATGCTGCAGTAGCCGGCAAAGATCAACC	Cloning region B of SPO1562 (*tdm*)
Tdm_CONF_F1	GAACGGAACGCTATGTGGTT	Confirmation of *Δtdm:Gm*
Tdm_CONF_F2	TCTCCATCCGGTCGTAAAAG	Confirmation of *Δtdm:Gm*
TmoX_AF_HindIII	CAATAAGCTTTCGCTCTGCTTTGACATGAG	Cloning region A of SPO1548 (*tmoX*)
TmoX_AR_XbaI	CAATTCTAGAAAAGGCCCCTTCCCACAC	Cloning region A of SPO1548 (*tmoX*)
TmoX_BF_XbaI	CAATTCTAGAACTTTGCCGAAGCGGTCT	Cloning region B of SPO1548 (*tmoX*)

Primer	Sequence 5' to 3'	Reference
TmoX_BR_PstI	CAATCTGCAGGCGCGAATATCGTCGAAC	Cloning region B of SPO1548 (*tmoX*)
TmoX_CONF_F1	ATCTGCGCGAGGAACATAAC	Confirmation of *ΔtmoX:Gm*
TmoX_CONF_R1	AAAGGACTGGAACACCATGC	Confirmation of *ΔtmoX:Gm*
TmoXW_AF_HindIII	CAATAAGCTTGAAATCGCTGCAAATGATCC	Cloning region A of SPO1548 (*tmoX*)
TmoXW_AR_XbaI	CAATTCTAGAACCGGACCATCCAGATAGC	Cloning region A of SPO1548 (*tmoX*)
TmoXW_BF_XbaI	CAATTCTAGAGGGCGCGAGGATTATTTC	Cloning region B of SPO1549 (*tmoW*)
TmoXW_BR_PstI	CAATCTGCAGGCTTGCCTTCAACAGGATGT	Cloning region B of SPO1549 (*tmoW*)
TmoXW_CONF_F1	CCGTTCGATTTGGTCGTATT	Confirmation of *ΔtmoXW:Gm*
TmoXW_CONF_R1	ATGTCCCATTGTCCGATCAT	Confirmation of *ΔtmoXW:Gm*
Tdm_DSS-3_F1_NdeI	CAATCATATGATGCTGGATACCAAATATCCCGAGAT	Cloning SPO1562 (*tdm*)

Primer	Sequence 5’ to 3’	Reference
Tdm_DSS-3_R1_EcoRI	CAATGAATTCTCAAGAGCGGGGTCTGGTTTTCTGCG	Cloning SPO1562 (*tdm*)
Tdm_prom_F1_XbaI	CAATCATATGGTTGCCACTCCGGTCATTTG	Cloning the promoter of SPO1562 (*tdm*)
Tdm_prom_R1_NdeI	CAATTCTAGAAACCCCAGCCCGGTCGCCAG	Cloning the promoter of SPO1562 (*tdm*)
TmoX_Prom_F_KpnI	CAATGGTCCAATTCAAAATCAACGCGCAAT	Cloning the TmoXWV promoter *lac* fusion
TmoX_Prom_R_PstI	CAATCTGCAGGCCGCCGAACCTGGAGAGAGTG	Cloning the TmoXWV promoter for *lac* fusion
TmoX_F1_BamHI	CAGAGGATCCGTGCGATTGTTTCGAGAAATCGC	Cloning SPO1548 (*tmoX*)
TmoX_R1_XbaI	CAATTCTAGAGATTAGCCGTCCAGCCAGGGGCG	Cloning SPO1548 (*tmoX*)
TmoX_Prom_F2_HindIII	CAATAAGCTTATTCAAAATCAACGCGCAAT	Cloning the promoter of SPO1548 (*tmoX*)
TmoX_Prom_R2_BamHI	CAATGGATCCGCCGCCGAACCTGGAGAGAGTG	Cloning the promoter of SPO1548 (*tmoX*)
Tmm_screen_F1	TCTGGAATTCGCCGACTATT	Confirmation of *Δtmm::Gm*

Primer	Sequence 5’ to 3’	Reference
Tmm_screen_R1	AGATACGCCTCCATGCTGTC	Confirmation of *Δtmm::Gm*
Spo1552_AF_PstI	CAATCTGCAGTCCCTGCTTGGTTGGATCAA	Thesis
Spo1552_AR_BamHI	CAATGGATCCCCTTGTTGGCCGTCAGAAAG	Thesis
Spo1552_BF_BamHI	CAATGGATCCCTGCACGCTGGACAATTACC	Thesis
Spo1552_BR_XbaI	CAATTCTAGACTAGTCCACCAGATCGCGG	Thesis
Spo1552_CF	TGTTGCTTTTCACGGACCAG	Thesis
Spo1552_CR	GATCACCAAGCTGCATCTGG	Thesis
Spo1088_AF_HindIII	CAATAAGCTTGGCAGCAAGGAAAGACAGAC	Cloning 5’ end (region A) of *betA*
Spo1088_AR_BamHI	CAATGGATCCGCTTCTCGCCGTTATAGTCG	Cloning 5’ end (region A) of *betA*
Spo1088_BF_BamHI	CAATGGATCCAATGGCTGTTCACCAAGACC	Cloning 3’ end (region B) of *betA*
Spo1088_BR_XbaI	CAATTCTAGAATTGGTGATCTGCGGAAAGA	Cloning 3’ end (region B) of *betA*
Spo1087_Cho_perm_AF_PstI	CAATCTGCAGGATGTCCCGAATGCGTTT	Cloning 5’ end (region A) of *betT*

Primer	Sequence 5’ to 3’	Reference
Spo1087_Cho_perm_AR_XbaI	CAATTCTAGATTGTTGACCAGCTTCACC AG	Cloning 5’ end (region A) of *betT*
Spo1087_Cho_perm_BF_XbaI	CAATTCTAGACCTTGGCGATCTGGTTCTC	Cloning 3’ end (region B) of *betT*
Spo1087_Cho_perm_BR_Hind III	CAATAAGCTTACGATGACAAAATCCGCT TC	Cloning 3’ end (region B) of *betT*
Spo0084_AF_PstI	CAATCTGCAGATTTTCAACTCTGCCCGTTT	Cloning 5’ end (region A) of *betB*
Spo0084_AR_XbaI	CAATTCTAGAACGGACGGTATAGGCGAAAT	Cloning 5’ end (region A) of *betB*
Spo0084_BF_XbaI	CAATTCTAGAATATGTCGACAAGGGCAAGG	Cloning 3’ end (region B) of *betB*
Spo0084_BR_HindIII	CAATAAGCTTATTCCGGCTTCTTTCTGGTT	Cloning 3’ end (region B) of *betB*
Spo1083 _AF_PstI	CAATCTGCAGTCCTGATCCTGATGGTGGAT	Cloning 5’ end (region A) of *betC*
Spo1083_ AR_BamHI	CAATGGATCCGATCGTAAAGCTTGGCCTTG	Cloning 5’ end (region A) of *betC*
Spo1083_BF_BamHI	CAATGGATCCACACGCCGGTTTCTACCAT	Cloning 3’ end (region B) of *betC*

Primer	Sequence 5’ to 3’	Reference
Spo1083_BR_XbaI	CAATTCTAGACCTCTGGCTTTCCTCCAGAT	Cloning 3’ end (region B) of *betC*
Spo1557_AF_XbaI:	TCTAGAGTCACCTATCCCTCGCTCAG	Cloning upstream of 5’ end (region A) of *fhs1*
Spo1557_AR_SalI	ATGCTGTCGACTACGCCATCTGATGATTTCC	Cloning upstream of 5’ end (region A) of *fhs1*
Spo1557_BF_SalI	ATGCTGTCGACGATCGAGGGCTTGTTCTGAG	Cloning downstream of 3’ end (region B) of *fhs1*
Spo1557_BR_HindIII	AAGCTTTTCAGCTCTGCCACATGTTC	Cloning downstream of 3’ end (region B) of *fhs1*
Spo3103_AF_XbaI	CAATTCTAGAATTTCCATGCGATCACCAGC	Cloning 5’ end (region A) of *fhs2*
Spo3103_AR_BamHI	CCAATGGATCCACGTAATCGGCCACTTTCA	Cloning 5’ end (region A) of *fhs2*
Spo3103_BF_BamHI	CAATGGATCCGGCGATCAACCATTTCGTTCA	Cloning 3’ end (region B) of *fhs2*
Spo3103_BR_HindIII	CCAATAAGCTTCATTCAACCGGATGGTCTCT	Cloning 3’ end (region B) of *fhs2*
Spo1088_CON_F1	CTATATCGCGGGCAATGTCG	Confirmation of *ΔbetA::Gm*

Primer	Sequence 5' to 3'	Reference
Spo1088_CON_R1	GACAGGGATCAAATCGGGTG	Confirmation of *ΔbetA::Gm*
Spo1087_CON_F1	CATGCAGGATCGACAACAGG	Confirmation of *ΔbetT::Gm*
Spo1087_CON_R1	GTTGTTCAGATGCGGTTCGG	Confirmation of *ΔbetT::Gm*
Spo0084_CON_F1	GATACCGGTCGAAGGGAGAG	Confirmation of *ΔbetB::Gm*
Spo0084_CON_R1	GGCAGGACAATCTTTCACGG	Confirmation of *ΔbetB::Gm*
Spo1083_CON_F1	CTGATCGACGGGCTCTACAT	Confirmation of *ΔbetC::Gm*
Spo1083_CON_R1	GCCATCACGTAGGTTTCGAC	Confirmation of *ΔbetC::Gm*
Spo1557_CON_F1	GAGATGAAGCGCAACATGAA	Confirmation of *Δfhs1::Gm*
Spo1557_CON_R1	TACCCAGAAGACCCACGTTC	Confirmation of *Δfhs1::Gm*
Spo3103_CON_F1	GACCATCGACATGGAAAACC	Confirmation of *Δfhs2::Spc in Δfhs1::Gm*
Spo3103_CON_R1	TTCAGCTCTGCCACATGTTC	Confirmation of *Δfhs2::Spc in Δfhs1::Gm*
Fhs_promF1_KpnI	CAATGGTACCTCTTGTGGGCCAA	Cloning the promoter for the H_4F-linked oxidation pathway
Fhs_promR1_SalI	CAATGTCGACCCGTCAACACCTC	Cloning the promoter for the H_4F-linked oxidation pathway

Primer	Sequence 5’ to 3’	Reference
Fhs-1_F1_SalI	CAATGTCGACATGGCGTACAAGA	Cloning the *fhs* in *R. pomeroyi*
Fhs_1_R1_BamHI	CAATGGATCCTCAGAACAAGCCCTCGATCTG	Cloning the *fhs* in *R. pomeroyi*
16SrRNA_27F	AGAGTTTGATCCTGGCTCAG	(Weisburg et al., 1991)
16S rRNA_1492R	GGTTACCTTGTTACGACTT	(Weisburg et al., 1991)
tmm_Roseo_F	ATGTAYCGYTAYCTVTGGTC	(Chen, 2012)
tmm_Roseo_R	GTGAACCACTGRTCCTGCAT	(Chen, 2012)
gmaS_Roseo_F	CCNGCBCAYCCSGAYATGCT	(Chen, 2012)
gmaS_Roseo_R	GTGCGGTTRTTGCCVGHCCA	(Chen, 2012)
tdm_screen_1581F	GTCGTYTAYWCNGCNATGTG	Thesis
tdm_screen_1631F	AAYTTYMGNTGGATHKGYGG	Thesis
tdm_screen_2082R	CCDAYNCCNGCYTCRAANGGRTC	Thesis
tmm_RTPCR_F	CCGGCTACAAGCATTTCTTC	Thesis
tmm_RTPCR_R	GATGTCTTCGCCCTTGTGTT	Thesis
Fhs_RTPCR_F	GTCTCTAGGGCCGACAT	Thesis
Fhs_RTPCR_R	AGCGAGCAGGTGATCTCG	Thesis
16S_341F	CCTACGGGAGGCAGCAG	(Muyzer et al., 1993)

Primer	Sequence 5’ to 3’	Reference
16S_518R	ATTACCGCGGCTGCTGG	(Muyzer et al., 1993)
Astmm1_F1	ATTCCAGACCTTCCTTGGGG	Thesis
Astmm1_R1	GAATTACACCTGGCGCACC	Thesis
Astmm1_R2	CAATTGCGCGCCTTTCAATC	Thesis
Astmm2_F1	CATGAGGTGATCGACTTGGC	Thesis
Astmm2_F2	CAGTTGTCGGGCCATTTGAA	Thesis
Astmm2_F3	CGGTGTTCTTGTCGACCTTG	Thesis
Astmm2_F4	TCGGGCAGGAAGTTGAAGAA	Thesis
Astmm2_R1	AATTCGCGGGCAAGGACATT	Thesis
Astmm2_R2	CCTCGGGCCATTTCTCGA	Thesis
Astmm2_R3	AGGAAGGTCTGGAATTCGCC	Thesis
Spect_F1	ACTACATTTCGCYCATCGCC	(Chen et al., 2011)

Chapter 3

TMAO metabolism in marine bacteria

3.1. Introduction

TMAO has been detected in the oceans' surface waters and is found at concentrations (4 -74 nM) comparable to reduced sulfur compounds, such as DMS and DMSO (Gibb and Hatton, 2004). Metabolism of TMAO by marine bacteria from different phylogenetic groups has been recently documented (Sun et al., 2011; Halsey et al., 2012), however the genes and enzymes responsible for this process are unknown. TMAO demethylase (Tdm) has been partially purified from *Aminobacter aminovorans* AM1 and has been shown to produce DMA and formaldehyde from TMAO (Large, 1971). Chen et al. (2011) identified several peptides that were enriched in TMA- and MMA-grown cultures of *Methylocella silvestris*. This work has provided an avenue for further research on the metabolism of TMAO. Transporters involved in the uptake of structurally-related QAs, such as GBT, choline and carnitine have been extensively researched. It is known that a number of different ABC-type or BCCT-type transport systems are in place to help facilitate the uptake of these potential nutrients (Nau-Wagner et al., 1999; Horn et al., 2006; Chen et al., 2010a). Again using *A. aminovorans* as the model organism, a bacterial TMAO transporter, related to the ABC-type family of transporters, has been shown to exist in nature (Raymond and Plopper, 2002). However, no genes responsible for encoding this transporter have been identified.

R. pomeroyi, a member of the MRC, has frequently been used to gain a better understanding of the ecophysiology of marine bacteria as it is easy to cultivate using standard laboratory techniques. A number of studies have used *R. pomeroyi* to identify key genes and enzymes involved in certain metabolic pathways using classical mutagenesis techniques, e.g. the identification of the *ddd* genes involved

in the cleavage of DMS or the genes involved in the uptake of phosphate (Sebastian and Ammerman, 2009; Green et al., 2013).

The aim of the work presented in this Chapter was to identify the genes involved in the transport and catabolism of TMAO using *R*. *pomeroyi* as the model system. A marker exchange mutagenesis method was developed to construct *R*. *pomeroyi* 'knock-out' mutants. Using this approach, the key genes responsible for the transport and catabolism of TMAO were identified.

3.2. Results

3.2.1. Identification and characterisation of TMAO demethylase in marine bacteria

3.2.1.1. Identification of an ORF in *R*. *pomeroyi* predicted to encode Tdm

Chen et al. (2011) identified a number of peptides that were upregulated when *M*. *silvestris* was grown in the presence of MAs. One of these peptides was designated, Msil3603, a 2,350 bp (780 aa) ORF that included two domains. Towards the N-terminus is a domain of unknown function (DUF) 1989. Near the C-terminus of Msil3603 is a H_4F-binding domain, predicted to be involved in the conjugation of free formaldehyde (produced during the demethylation of TMAO) with H_4F, forming methylene-H_4F. It is predicted that methylene-H_4F is the entry point for the oxidation of the C1 groups, mediated by the H_4F-linked pathway (Chen, 2012). Therefore, the working hypothesis is that Msil3603 is involved in the demethylation of TMAO to DMA. Using the National Centre for Biotechnology Information (NCBI) protein database a BLASTP search was conducted against the genome of

R. *pomeroyi* using Msil3603 as the query sequence. An ORF, SPO1562 (NCBI accession, YP_166803.2), was identified in *R*. *pomeroyi*, which is annotated as a gene encoding a glycine cleavage T protein (GcvT). SPO1562 contains a H_4F-binding domain towards C-terminus and the DUF1989 domain towards the N-terminus, similar to Msil3603 towards.

3.2.1.2. Heterologous expression of the putative Tdm from *R. pomeroyi* and *Pelagibacteraceae* strain HIMB59

To confirm this gene encodes Tdm, SPO1562 was cloned into the IPTG-inducible expression vector, pET28a (Novagen, UK) and the resultant plasmid was transformed into the expression host, *Escherichia coli* BLR (DE3). A homolog from *Pelagibacteraceae* strain HIMB59 (strain HIMB59), a member of the abundant SAR11 clade (Grote et al., 2012), was chemically synthesised (GenScript Corporation, Piscataway Township, NJ, USA) and cloned into the same expression system. Both of these two *E*. *coli* strains were grown (37^{o}C) separately in LB medium and after 2-3 h growth (OD_{600} = 0.5-0.6), 0.2 mM IPTG was added to the cultures to induce expression of the putative Tdm homologs. As *E*. *coli* can take up and subsequently utilise TMAO as a terminal electron acceptor (Buc et al., 1999), TMAO (1 mM) was added to the cultures upon addition of IPTG. Cultures were incubated overnight at 25^{o}C and TMAO and DMA in the culture medium was quantified by cation exchange ion chromatography (Chapter 2, section 2.5.3). An empty vector control (pET28a only) was also transformed into *E*. *coli* and cultures were grown under identical growth conditions. *E*. *coli* cells containing the expressed (IPTG-induced) Tdm homolog from *R*. *pomeroyi* produced 931 ± 45 μM DMA, whilst the no IPTG control culture only produced 143 ± 49 μM DMA (Figure 3.1). IPTG-induced cultures containing the Tdm homolog from strain HIMB59

produced 171 ± 34 μM DMA and no-IPTG control cultures did not produce any DMA. The empty vector cultures did not produce any DMA in either the IPTG or no IPTG added controls, confirming that DMA production is a result of Tdm-dependent TMAO demethylation. It is interesting to note that the TMAO from all cultures was consumed even in cultures where either small amounts or no DMA was produced. In cultures where little Tdm-dependent demethylation occurred, TMAO was reduced to TMA by TMAO reductase (TorA) under aerobic or micro-aerophilic conditions. As TMAO was still depleted in the empty vector controls, TorA of *E. coli* may have been in competition with the recombinant Tdm from strain HIMB59 and therefore the amount of DMA produced may be lower than expected based on enzyme kinetics alone. Consequently, although the difference in the DMA production between the two different Tdm is quite large, the actual difference in activity may be less.

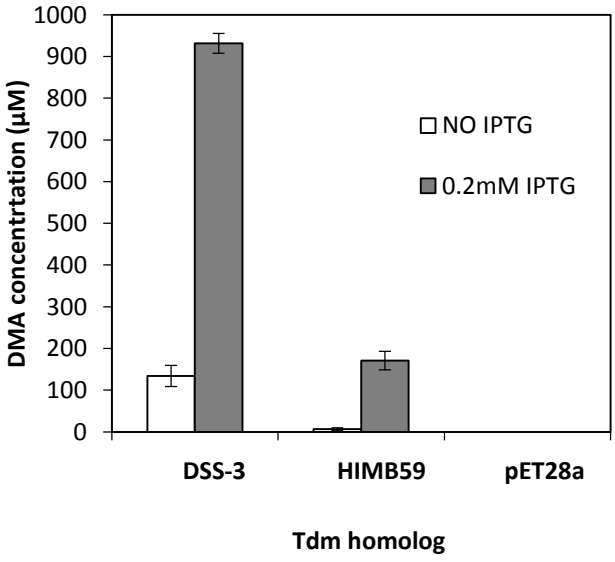

Figure 3.1. Production of DMA from TMAO demethylation by recombinant Tdm of *R. pomeroyi* and *Pelagibacteraceae* strain HIMB59. pET28a represents the control empty vector with no insert. Error bars denote SDs of triplicate measurements. Abbreviations: IPTG, isopropyl β-D-1-thiogalactopyranoside.

3.2.1.3. Marker exchange mutagenesis of the putative tdm *in* R. *pomeroyi*

To confirm that Tdm is essential for TMAO catabolism in *R*. *pomeroyi*, SPO1562 and its 5' intergenic region (containing DUF1989) were targeted for marker exchange mutagenesis using gentamicin as the resistance marker (Gm^R). To ensure no polar effect of transcription occurred, the orientation of the gentamicin cassette was checked to confirm that Gm^R was inserted in the same orientation as *tdm* (Figure 3.2a). Details for the construction of the *Δtdm::Gm* mutant are outlined in Figure 3.3. To allow for homologous recombination to take place, the plasmid containing the mutated *tdm* was mobilised into *R*. *pomeroyi* via conjugation with *E*. *coli* S17.1 Confirmation of a double crossover mutant was carried out by PCR and sequencing (Figure 3.2b).

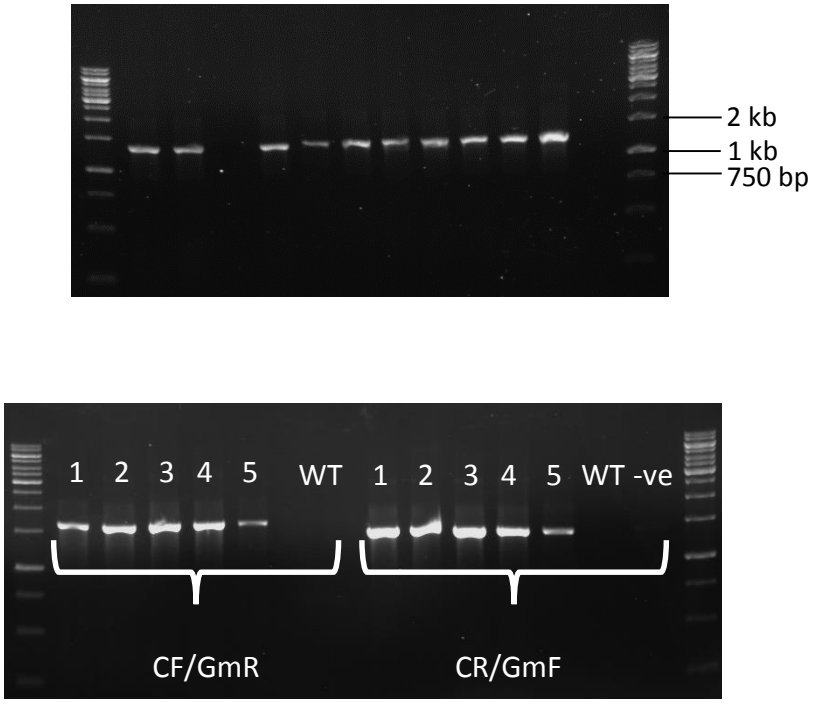

Figure 3.2. **(A)** The orientation of the gentamicin cassette was checked in multiple clones using the primer Tdm-AF and Gent_F1 (Table 2.2). **(B)** Double crossover transconjugants were selected for by their sensitivity to kanamycin and confirmed by PCR using the primers Tdm-CF and Gent_R (lanes 1-5) and the primers Gent_R1 and Tdm-CR lanes (8-12). No product was amplified from wild-type cells using either primer set (lanes 6, 13).

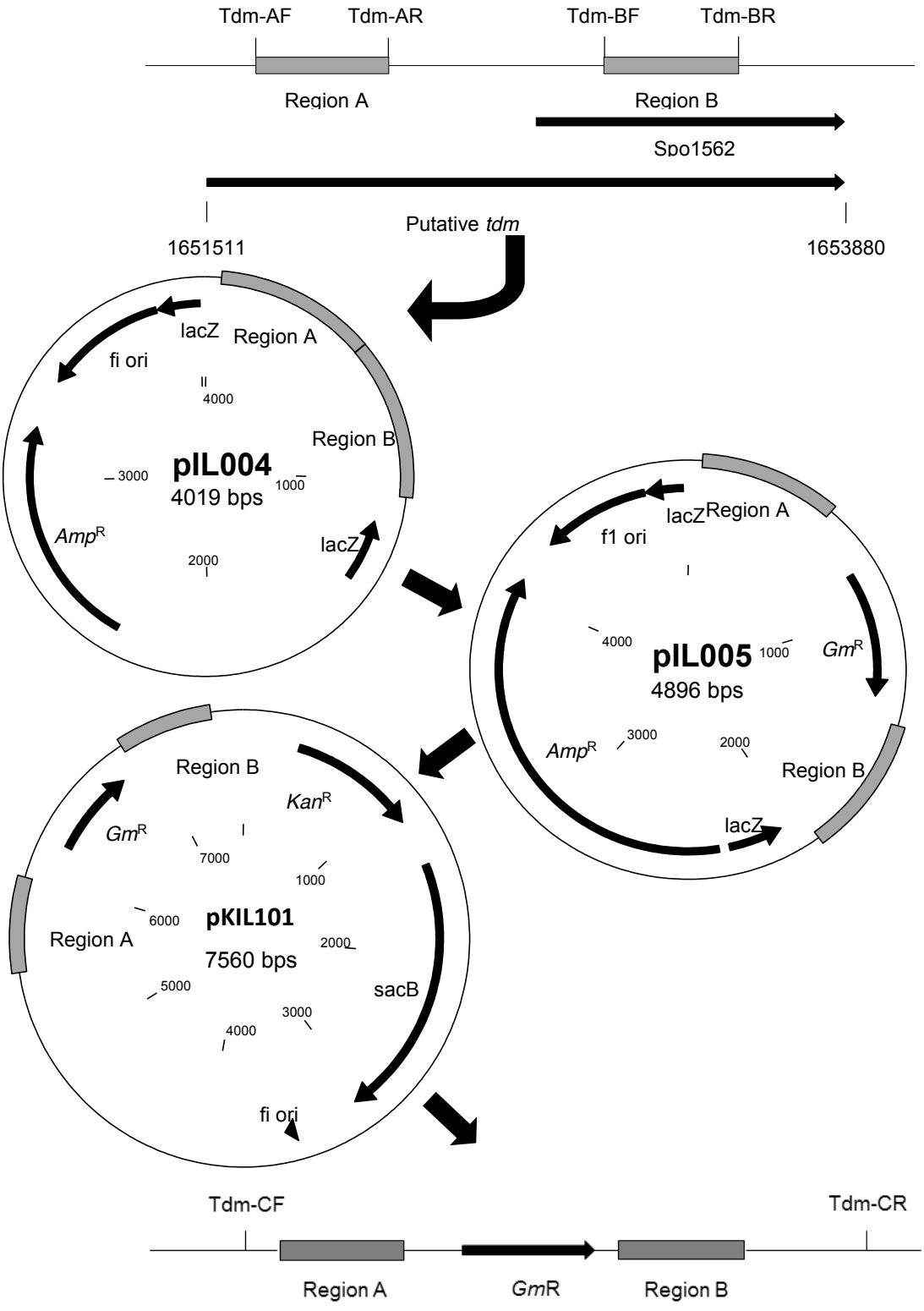

Figure 3.3. Construction of the *Δtdm::Gm* mutant. Two regions within the putative Tdm were amplified from wild-type *R. pomeroyi*. Both regions were ligated together using an *Xba*I site and cloned into pGEM-T (Promega, UK). The gentamicin cassette was inserted between the two regions at the *Xba*I site (pIL005). The engineered construct was cloned into the suicide vector, pk18mob*sacB*, generating the plasmid, pKIL101.

The wild-type and mutant strains were grown in a seasalts medium (Chapter 2, section 2.1.5) with succinate (10 mM) as the sole C source and either TMA (500 μM) or TMAO (500 μM) as a sole N source. The wild-type grew well on TMA and TMAO as a sole N source whilst *Δtdm::Gm* failed to grow on either substrate (Figure 3.4b). Consequently, TMA or TMAO consumption occurred in wild-type cultures, whilst in the mutant cultures, no TMAO was consumed. Small amounts of TMA were consumed in the mutant cultures due to oxidation by the Tmm (Chen et al., 2011) leading to the detection of trace levels of TMAO in the medium during these conditions (data not shown).

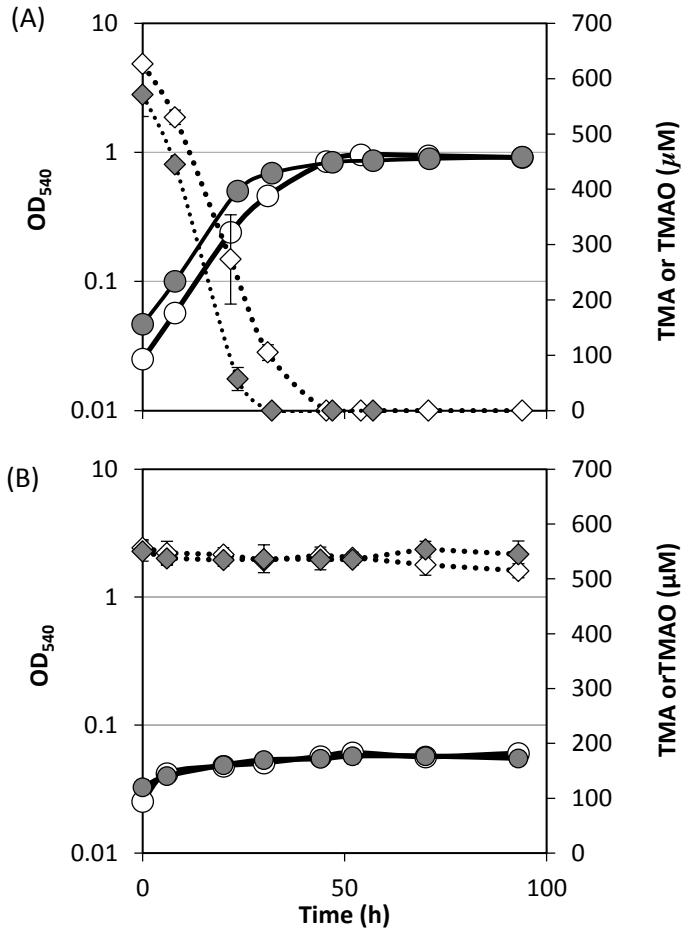

Figure 3.4. Growth of *R. pomeroyi* wild-type (A) and the *Δtdm::Gm* mutant (B) using TMA (grey circles) or TMAO (white circles) as a sole N source (0.5 mM). TMA (grey diamonds) and TMAO (white diamonds) were quantified by ion chromotography. Cultures were grown in triplicate and error bars denote SD.

3.2.1.4. Complementation of the *Δtdm::Gm* with the native tdm

The 250 bp upstream region of *tdm*, predicted to contain the promoter (section 3.2.2.7), was cloned into the expression vector, pET28a, containing either *tdm* from *R*. *pomeroyi* or strain HIMB59, using the restriction sites, *Nde*I and *Xba*I, immediately upstream of the *tdm* homologs. Each *tdm* and the promoter from *R*. *pomeroyi* were then digested out of the pET28a plasmid and separately cloned into pBBR1MCS-km (Kovach et al., 1995). The resultant plasmids were each mobilised into the *Δtdm::Gm* mutant via conjugation and transconjugants were selected for on kanamycin plates, generating the strain *Δtdm+tdm:DSS-3* and *Δtdm+tdm:HIMB59*. *Δtdm+tdm:DSS-3* had a phenotype similar to that of the wild-type for growth on both TMA and TMAO as a sole N source (Figure 3.5a). For Δ*tdm+tdm:HIMB59*, restoration of growth on TMA and TMAO was also achieved, however the growth rate was slower than that of either the wild-type or *Δtdm+tdm:DSS-3* (Figure 3.5b). Insertion of the empty plasmid, pBBR1MCS-km, did not result in the restoration of growth in the mutant, *Δtdm::Gm*.

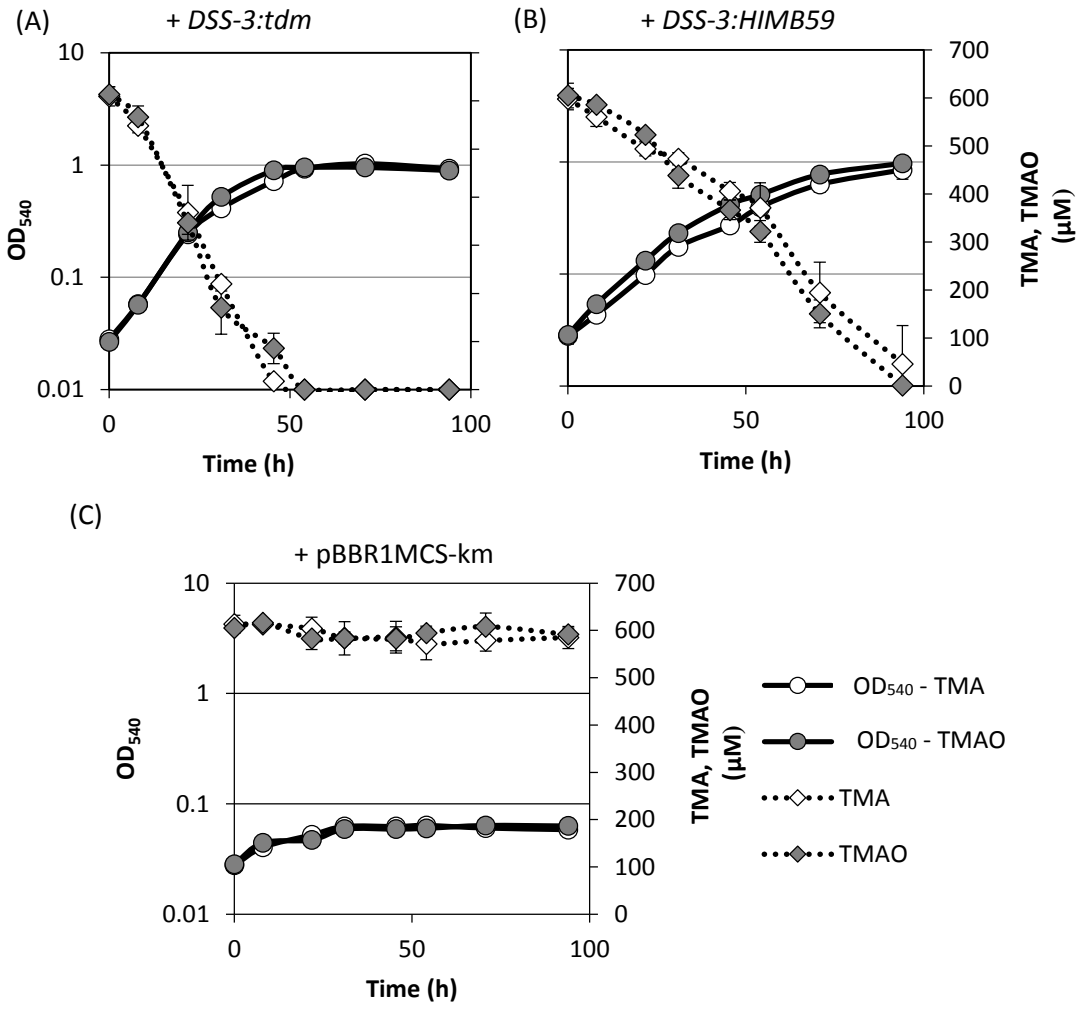

Figure 3.5. Growth of the *Δtdm::Gm* mutant complemented with its native *tdm* from *R. pomeroyi* (A) or the *tdm* from strain HIMB59 (B) on TMA (grey) or TMAO (white) as a sole N source (0.5 mM). Complementation with the empty vector, pBBR1MCS-km did not restore growth (C). Cultures were grown in triplicate and error bars denote SD.

3.2.1.5. Screening the MRC for the presence of *tdm*

Within the MRC, 19/ 42 isolates investigated had the genes required for growth on TMAO (Table 3.1). A number of isolates related to the MRC were screened for their ability to grow on TMAO as a sole N source. Growth on TMAO was correlated to the presence of *tdm* in their genomes, confirming that this gene is essential in the catabolism of TMAO. Interestingly, three of the sequenced isolates, *Roseibium* sp. TrichSDK4, *Ruegeria* sp. TW15, and *Roseobacter* sp. SK209-2-6 had the gene

required for growth on TMAO (*tdm*), but did not have the gene required for growth on its precursor, TMA (*tmm*). When one of these isolates, *Roseobacter* sp. SK209-2-6, was tested, it grew on TMAO, but not TMA (Table 3.1). This strengthens the hypothesis that marine bacteria can utilise TMAO through direct uptake from the seawater.

Table 3.1 Comparative genomic analysis of MA-utilising genes in genome-sequenced MRC bacteria and their subsequent growth on MAs.

Strain	***tmm***	***tdm***	**TMA**	**TMAO**
Citreicella sp. E45	+	+	+	+
Citreicella sp. 357	+	+	NT	NT
Dinoroseobacter shibae DFL12	-	-	-	-
Jannashia sp. CCS1	-	-	NT	NT
Labrenzia aggregata IAM 12614	-	-	NT	NT
Loktanella sp. CCS2	-	-	NT	NT
Maritimibacter alkaliphilus HTCC2654	-	-	NT	NT
Nautella italic R11	-	-	NT	NT
Oceanibulbus indolifex HEL-45	-	-	NT	NT
Oceanicola batsensis HTCC2597	-	-	-	-
Oceanicola granulosus HTCC2516	-	-	NT	NT
Octadecabacter antarcticus 238	+	+	NT	NT
Octadecabacter antarcticus 307	-	-	NT	NT
Pelagibaca bermudensis HTCC2601	+	+	NT	NT
Phaeobacter gallaeciensis 2.10	-	-	NT	NT
Phaeobacter gallaeciensis BS107	-	-	-	-
Roseibium sp. TrichSKD4	-	+	NT	NT
Roseobacter denitrificans OCh 114	+	+	+	+
Roseobacter litoralis Och 149	+	+	+	+
Roseobacter sp. AzwK-3b	+	+	NT	NT
Roseobacter sp. MED193	-	-	-	-
Roseobacter sp. SK209-2-6	-	+	-	+
Roseovarius nubinhibens ISM	+	+	+	+
Roseovarius sp. 217	+	+	+	+
Roseovarius sp. TM1035	+	+	+	+
Ruegeria lacuscaerulensis ITI-1157	-	-	NT	NT
Ruegeria pomeroyi DSS-3	+	+	+	+
Ruegeria sp. TW15	-	+	NT	NT

Strain	*tmm*	*tdm*	TMA	TMAO
Sagittula stellata E-37	-	-	-	-
Sulfitobacter sp. EE-36	-	-	-	-
Sulfitobacter sp. NAS-14.1	-	-	NT	NT
Thalassobium sp. R2A62	+	+	NT	NT
Rhodobacterales bacterium HTCC2083	+	+	NT	NT
Rhodobacterales bacterium HTCC2150	+	+	NT	NT
Rhodobacterales bacterium Y4I	+	+	NT	NT
Rhodobacteraceae bacterium KLH11	-	-	NT	NT
Rhodobacterales sp. HTCC2255	+	+	NT	NT

Abbreviations and symbols; -, no growth; + growth; NT, not tested.

3.2.1.6. Phylogeny of Tdm in the marine environment

Using Tdm from *R. pomeroyi* as the query, the Integrated Microbial Genomes database at the Joint Genome Institute (IMG/ JGI) was scrutinised to generate a BLASTp database. A number of Tdm sequences were retrieved from a range of phylogenetically divergent marine bacterial groups including members of the MRC and SAR11 clade of the *Alphaproteobacteria* (Figure 3.6). Approximately half of the isolates related to the MRC contain the genes for MA metabolism, including *tdm* (see Table 3.1). *tdm* homologs were also present in members of the *Gammaproteobacteria* and *Deltaproteobacteria*, despite the fact that these genomes were retrieved via single cell genomics for which the genome completeness index is typically ~40-60% (Swan et al., 2013). All the genomes of SAR11 isolates containing *tdm* also had *tmm*. No SAR11 isolates had *tdm* and not the genes necessary for MMA catabolism suggesting that, providing they can convert DMA to MMA, they should be capable of growth on these compounds as a sole N source. The *tdm* was also found in a number of *Roseobacter* strains identified through single cell genomics (Swan et al., 2013). These strains are predicted to have streamlined genomes and to have lost a number of non-essential

genes, possibly to aid in reducing the N and phosphorus quota of the cells (Swan et al., 2013; Giovannoni et al., 2014). Interestingly, a *tmm* homolog was also identified in the cyanobacterium, *Trichodesmium erythraeum* IMS101, but none of the other genes involved in the catabolism of the downstream metabolites were present in its genome. Interestingly, a number of MRC isolates and a representative of the SAR116 clade have a Tdm-like homolog which forms an outgroup with the *bona fide* Tdm homologs (Figure 3.7).

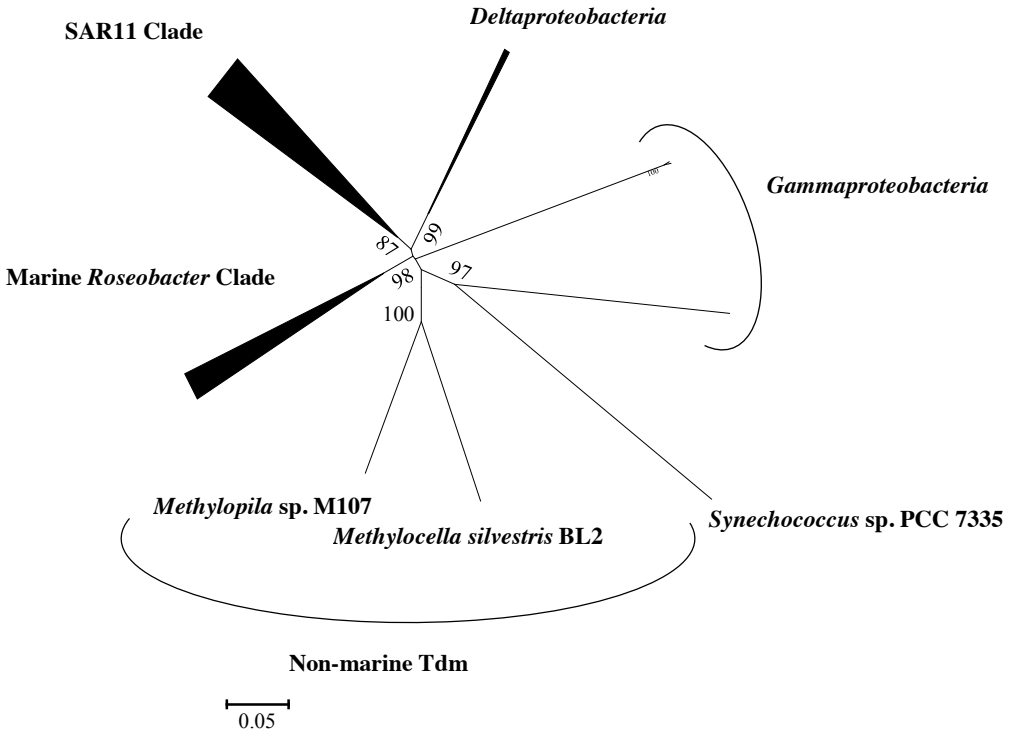

Figure 3.6. Neighbour-joining phylogenetic analysis of Tdm retrieved from the genomes of sequenced marine bacteria. The evolutionary distance was compouted using the p-distance method. Bootstrap values (500 replicates) greater than 60% are shown. The scale bar denotes the number of amino acid differences per site. The analysis involved 49 Tdm sequences. There were a total of 468 amino acid residues in the alignment. Phylogenetic analyses were conducted in MEGA5.1.

3.2.1.7. Retrieval of Tdm homlogs from the Global Ocean Survey (GOS) database

To further identify the abundance of the Tdm in the marine environment, another BLASTP database was generated using the GOS peptide dataset (Rusch et al., 2007) and the same query sequence from *R. pomeroyi*. For each sampling site, the number of sequence hits retrieved were normalised to generate the number of hits per 100,000 total reads. Hits were retrieved from both open ocean and coastal ocean sites with the abundance of Tdm at each site following a similar trend to the abundance of Tmm (Figure 3.7). To estimate the number of Tdm-containing bacteria in the GOS dataset, the number of Tdm hits were normalised against the average number of six housekeeping genes (*recA, rpoB, gyrB, atpB, sp70, tufA*) number of housekeeping genes as previously described (Howard et al., 2008, Chen et al., 2011) It was estimated that 21% of bacterial cells in the surface waters, represented in the GOS, contain Tdm which is comparable to Tmm (20%) and GmaS (22%) (Chen et al., 2011). The similarity between Tdm and Tmm abundance throughout the GOS is due to the presence of these two homologs in the ubiquitous SAR11 clade which dominates many of the sampling sites used for this dataset (Morris et al., 2002).

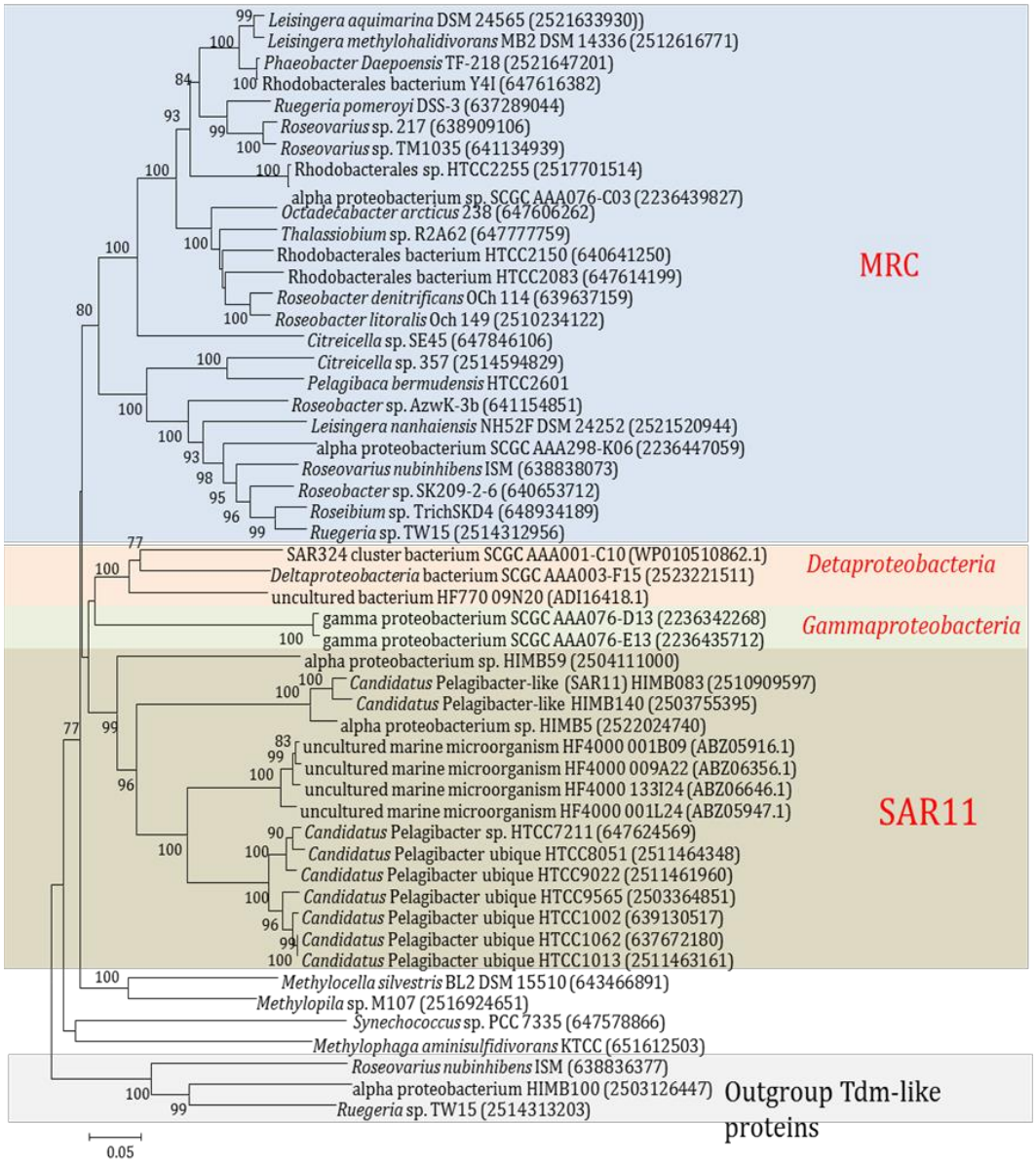

Figure 3.7. Detailed analysis of the phylogenetic distribution of Tdm gene among marine bacteria. Nodes at some of the major branched with high bootstrap values (500 replicates) are indicated. The tree was constructed using the neighbour-joining method using the software package, MEGA (Tamura et al., 2011).

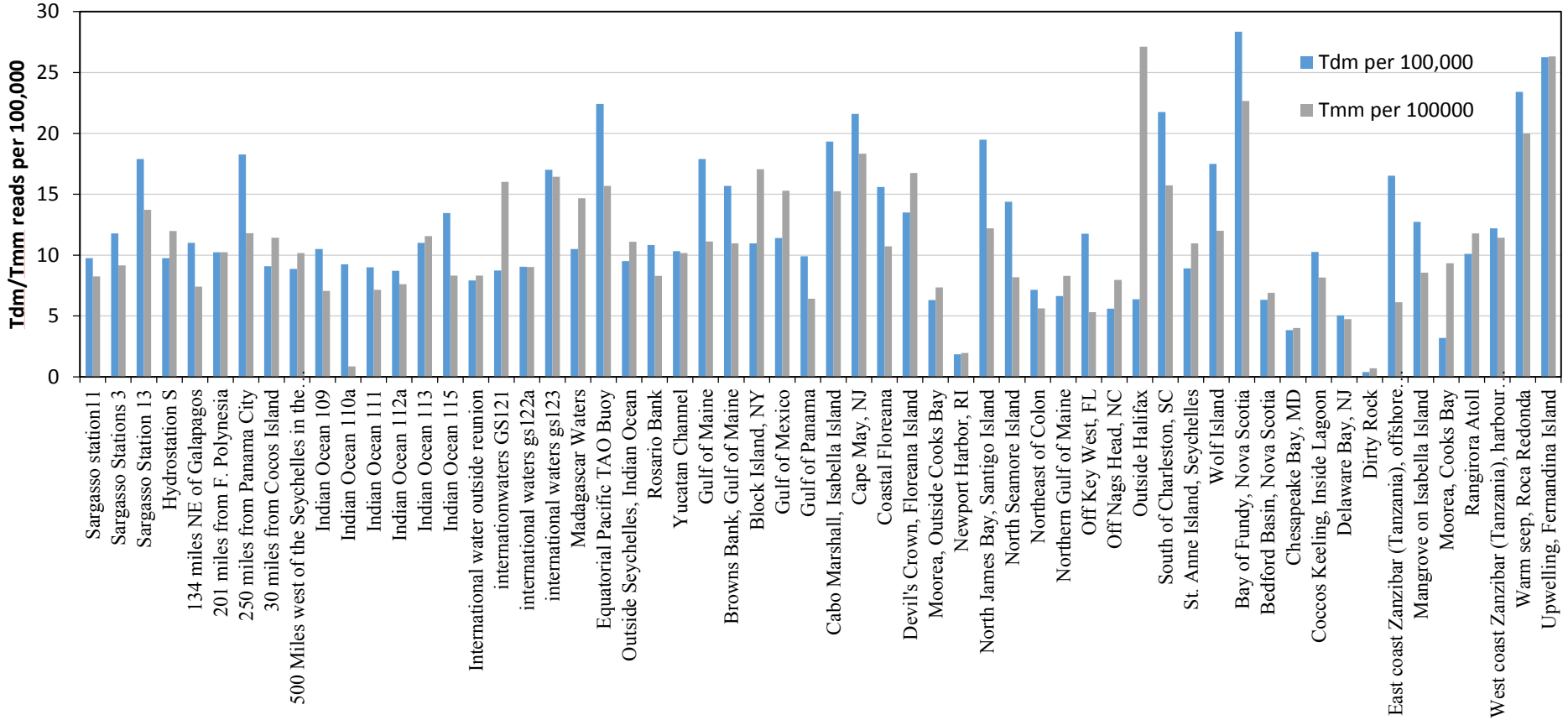

Figure 3.8. Abundance of Tmm and Tdm at sites throughout the Global Ocean Survey. Tmm and Tdm abundances are given per 100,000 reads. The length of Tdm and Tmm were normalised to the length of RecA. Percentage of bacteria containing Tmm or Tdm was calculated by divding the number of hits (Tdm or Tmm) by average number of housekeeping genes detected at each site.

3.2.2. Identification of a novel TMAO-specific ABC transporter

3.2.2.1. Genomic analysis of the Tdm neighbourhood from marine bacteria

To identify any specific transporters that may be involved in the uptake of either TMAO or other MAs, the genetic neighbourhoods surrounding *tdm* from a range of phylogenetically diverse marine bacteria that possess *tdm* were analysed. In all bacteria possessing *tdm*, there was a three ORF cluster (SPO1548-SPO1550, in *R*. *pomeroyi*) annotated as genes encoding the three subunits of glycine/ proline betaine ABC transporter. The first gene in the cluster was annotated as a gene encoding the SBP (hereafter termed, TmoX), the second the inner membrane ATP-binding domain (hereafter termed, TmoW) and the larger third, the transmembrane permease (hereafter termed, TmoV). In *R*. *pomeroyi*, these genes were situated downstream and on the opposite strand to *tmm* (Figure 3.8). This gene configuration was also found in a number of other marine bacteria including isolates from the SAR11 clade. In members of the genus, *Roseovarius*, the three genes were located next two three ORFs annotated as the genes, *torRTS*, which encode for the regulator of the TMAO reductase (TorA) (Buc et al., 1999) (Figure 3.8). In *E*. *coli*, the Tor operon is involved in the reduction of TMAO to TMA during periods of anaerobic respiration (Buc et al., 1999). However, in members of the genus, *Roseovarius*, the gene encoding the TorA is absent and therefore it is predicted that *torRTS* may have a role in regulating the uptake of TMAO primarily for the catabolism of this compound. Interestingly, the isolates from the MRC that contain *tdm* but not *tmm*, for example, *Roseobacter* sp. SK209-2-6 and *Roseibium* sp. TrichSDK4, the genes encoding the TMAO transporter are found in a potential operon with *tdm* suggesting that they may be co-transcribed (Figure 3.8). The same pattern is seen for members

of the *Gammaproteobacteria* and *Deltaproteobacteria*, as well as *Pelagibacteraceae* strain HIMB59 where the four genes are in an apparent operon. All bacteria possessing the genes encoding for the putative TMAO transporter, *tmoXWV*, contain *tdm*. Taken together, these data suggest that this transporter, encoded by *tmoXWV*, is involved in the rapid uptake of TMAO in the marine environment.

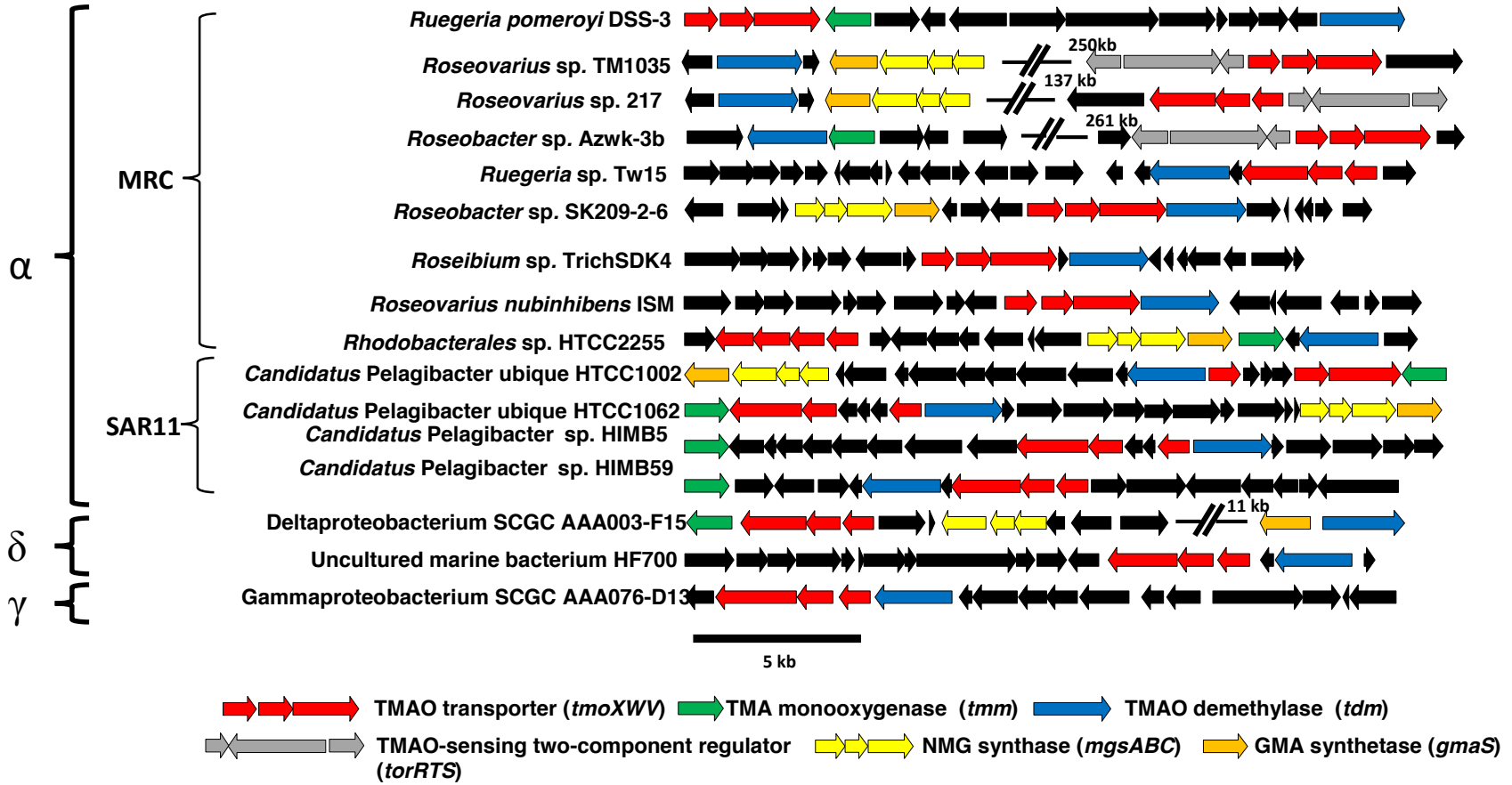

Figure 3.9. Gene neighbourhoods of the genes (*tmoXWV*) that encode the TMAO transporter (red) among representative genome-sequenced marine bacteria. All genes coloured black have no confirmed functional relationship with TMAO metabolism. α, *Alphaproteobacteria*; δ, *Deltaproteobacteria*; γ, *Gammaproteobacteria*; GMA, γ-glutamylmethylamide; NMG, N-methylglutamate.

3.2.2.2. Phylogenetic analysis of the putative TmoX from *R. pomeroyi* and *Pelagibacteraceae* strain HIMB59

Berntsson et al. (2010) constructed a comprehensive phylogeny of all SBPs based on structural classification and concluded that these proteins can be grouped into seven major clusters (A-G). Within this phylogeny, all osmolyte transporters grouped into subgroup III of cluster F. All the putative TmoX homologs found in marine bacteria, *R. pomeroyi*, *Roseovarius* sp. 217 and strain HIMB59, were aligned with a number of characterised osmolyte SBPs that fell into subcluster III (Figure 3.9 & 3.10). All TmoX homologs formed a distinct branch within subcluster III for which two smaller groups were evident, those from MRC isolates and those from the SAR11 clade, as well as TmoX homologs from uncultured marine *Gammaproteobacteria* and *Deltaproteobacteria* (Figures 3.9 & 3.10). The evidence from this analysis supports the notion that the putative TmoX is a distinct SBP that is similar to other osmolyte SBPs. During this analysis, it became apparent that a distinct ChoX branch formed which included a SBP from *Roseovarius* sp. 217. This suggests that some marine bacteria may have the ChoXWV operon to facilitate the rapid uptake of choline from the environment (see Chapter 7).

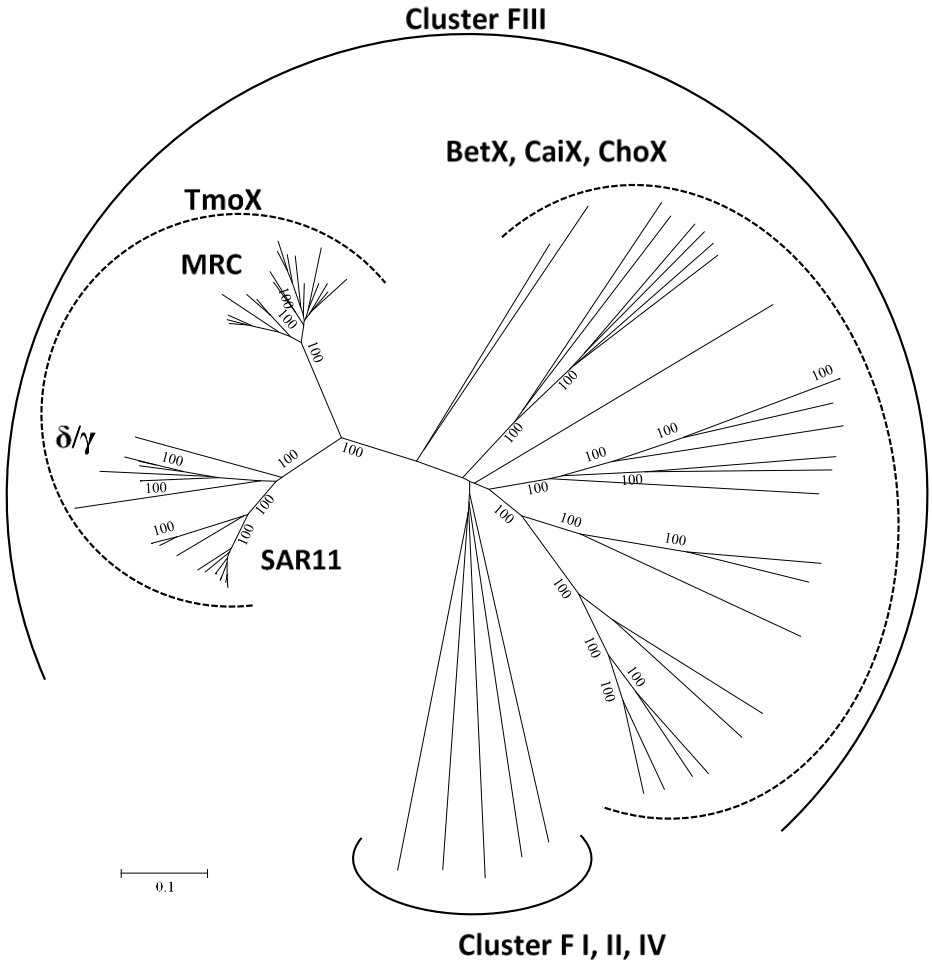

Figure 3.10. Phylogenetic analysis of the SBP, TmoX, of the TMAO-specific transporter in relation to other characterised SBPs. Current known SBPs specific for osmolytes, such as choline, glycine betaine, and carnitine, fall into the cluster F of the ABC superfamily (Berntsson et al., 2010). The evolutionary history was inferred using the neighbour-joining method. Bootstrap values (500 replicates) greater than 99% are shown. The scale bar represents the number of amino acid differences per site. The analysis involved 69 SBP sequences. There were a total of 296 amino acids positions in the alignment. Evolutionary analyses were conducted in MEGA. δ, *Deltaproteobacteria*; *Gammaproteobacteria*; BetX, glycine betaine/ proline betaine SBP; CaiX, carnitine SBP; ChoX, choline SBP.

The TmoX homologs related to the *Deltaproteobacteria* and *Gammaproteobacteria* are most similar to the SAR11 TmoX homologs, which is surprising considering that both the MRC and SAR11 clade belong to the *Alphaproteobacteria* (Figure 3.10). Horizontal gene transfer between phylogenetically distant bacterial taxa is the likely explanation for this and suggests that this trait may provide a key adaptive

ability to free-living cells inhabiting the water column. All the TmoX homologs related to the *Deltaproteobacteria* and *Gammaproteobacteria* are found in the genomes of uncultivated bacteria whose DNA was obtained through single-cell genomics (Swan et al., 2013). It should be noted that not all bacteria that possess *tdm* in their genomes have a glycine/ proline betaine-type ABC transporter. For example, *M*. *silvestris* has a putative TMAO permease (*tmoP*) and this gene is also found adjacent to *tdm* in a number of *Paracoccus* spp. (data not shown). Also, *Methylophaga aminisulfidivorans* AM1 does not have *tmoXWV* in its genome despite possessing *tdm*.

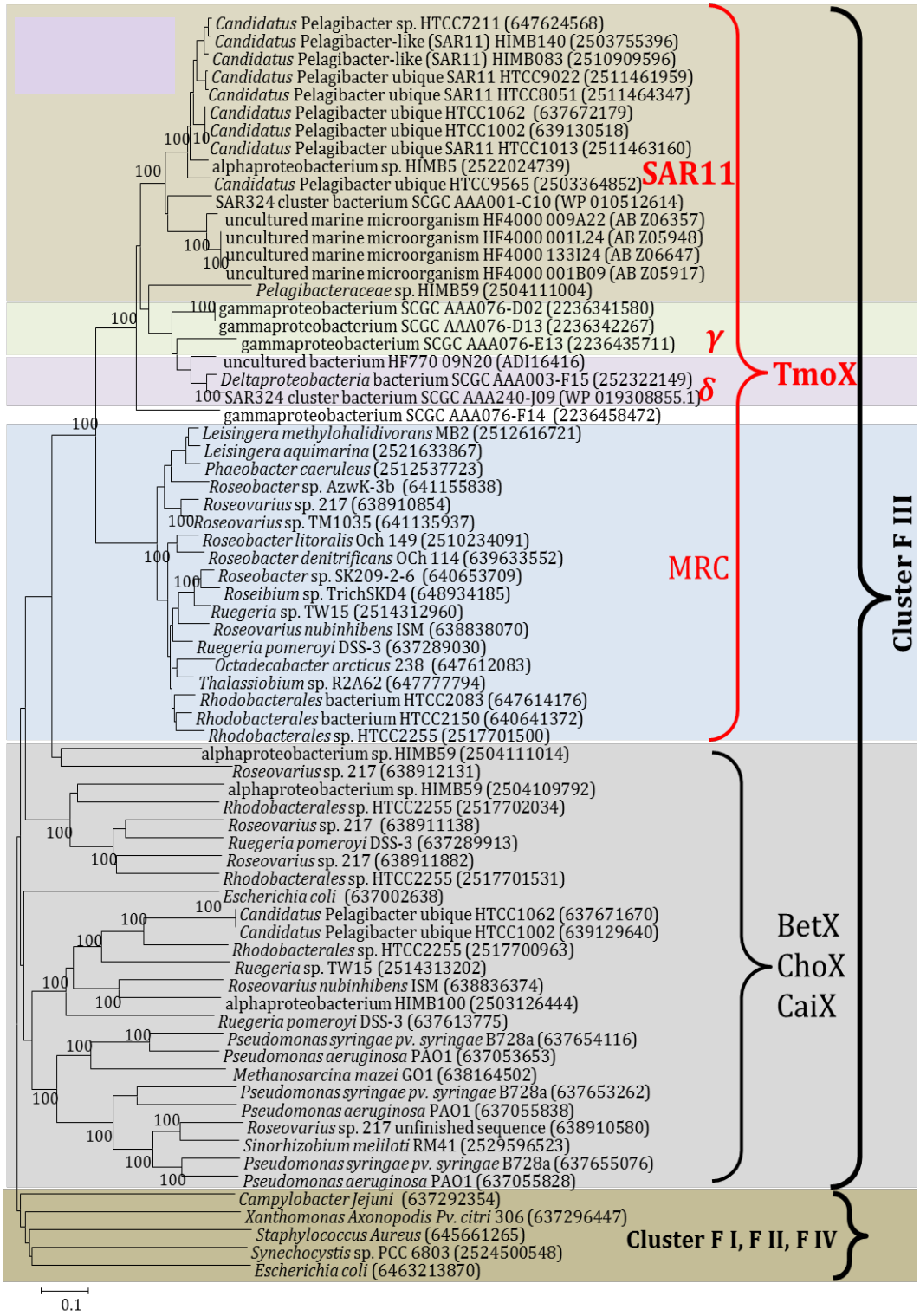

Figure 3.11. Neighbour-joining phylogenetic tree showing the distribution of TmoX among marine bacteria. High bootstrap values (500 replicates) at some of the major nodes are shown. Integrated Microbial Genomes (IMG) gene numbers are given in brackets. Where no IMG gene number is possible, accession numbers referring to the National Center for Biotechnology Information (NCBI) database were used.

3.2.2.3. Marker exchange mutagenesis of the putative TMAO ABC transporter in *R. pomeroyi*

To determine if this ABC-type transporter does indeed facilitate TMAO uptake in *R. pomeroyi*, two mutants were constructed. The first targeted *tmoX* and *tmoW* to disrupt both the putative SBP and the inner membrane component of the TMAO transporter, respectively, generating the mutant *ΔtmoXW::Gm* (Figure 3.11a). The second targeted only *tmoX*, generating the mutant, *ΔtmoX::Gm* (Figure 3.11b). The second mutant was constructed to test the hypothesis that TmoX is essential for the rapid uptake of TMAO and other SBPs would not interact with the transmembrane permease region (TmoV) of the transporter. This mutant would also enable the complementation with a single gene (*tmoX*) instead of inserting two or possibly three of the genes (*tmoXWV*) into the expression plasmid, pBBR1MCS-km. Double crossover events during the construction of both mutants were again selected for by their sensitivity to kanamycin and subsequently confirmed by PCR and sequencing (Figure 3.12a, b).

(A)

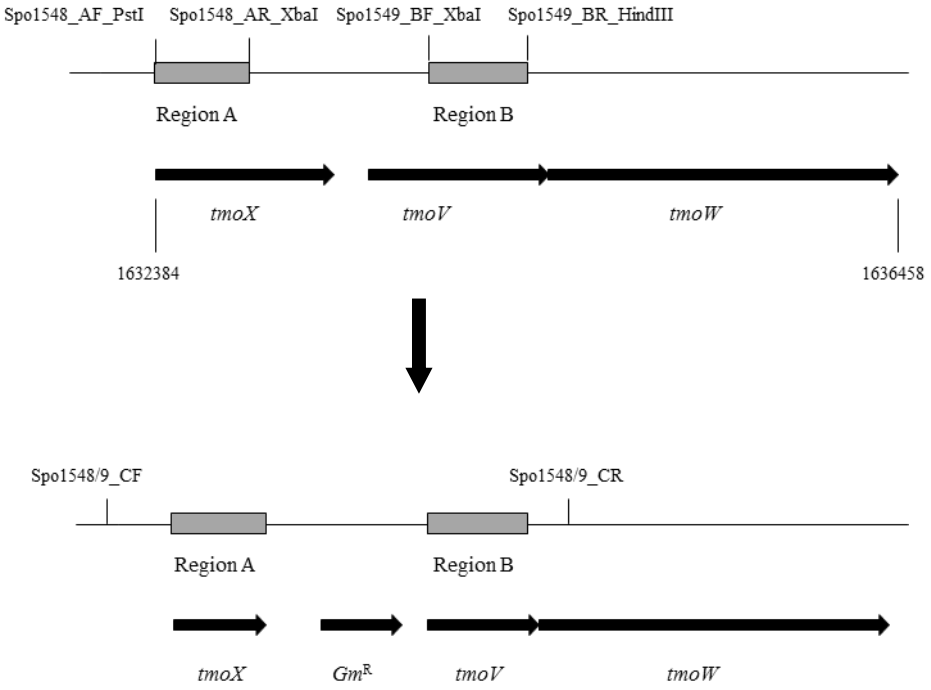

(B)

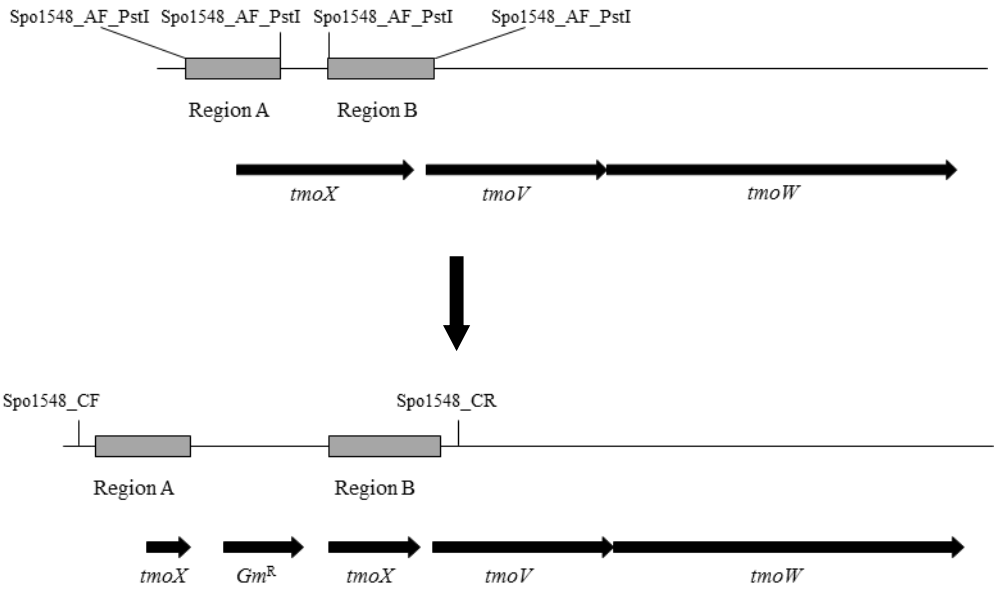

Figure 3.12. Genetic map of the *tmoXWV* gene cluster. PCR primers used for the amplification of regions used for marker exchange mutagenesis enabling the construction of the mutant *tmoXW::Gm* **(A)** and *tmoX::Gm* mutant **(B)**. Primers used for confirmation of marker exchange mutagenesis where the gentamicin resistance gene was inserted are shown.

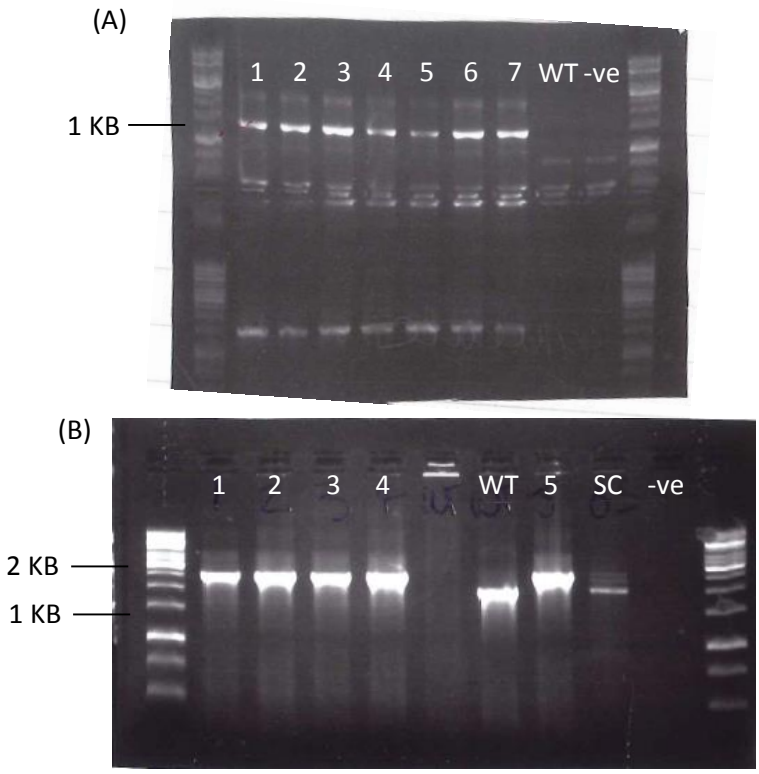

Figure 3.13. Confirmation by PCR that a double crossover homologous recombination event occurred, generating the mutants, *ΔtmoXW::Gm* **(A)** using the primers Gent_F1/Spo1548-9_CR (top row) and Gent_R1/Spo1548-9_CF (bottom row) and the *ΔtmoX::Gm* **(B)** using the primers Spo1548_CF/CR. The size of the region is greater for the mutant compared to wild-type. Numbers represent PCR assays with different potential double crossover transconjugants.

3.2.2.4. Growth characteristics of the two TMAO transporter mutants of *R. pomeroyi*

The two mutants were tested for their ability to grow on TMA or TMAO as a sole N source. For either *ΔtmoXV::Gm* or *ΔtmoX::Gm*, growth on TMA was unaffected suggesting that this transporter does not have a role in uptake of TMA. However, both mutants displayed a significant reduction in their ability to grow on TMAO as a sole N source which could be explained by a lower rate of TMAO depletion from the culture medium (Figure 3.13). Unlike the *Δtdm::Gm* mutant, the two transporter mutants were still able to grow slowly on TMAO as a sole N source and unlike the catabolic mutant, still slowly depleted TMAO from the medium. Therefore, TMAO

may be able to enter the cell through another transport system which probably has a low affinity for this substrate but can facilitate transport at the unnaturally high concentrations used in this experiment.

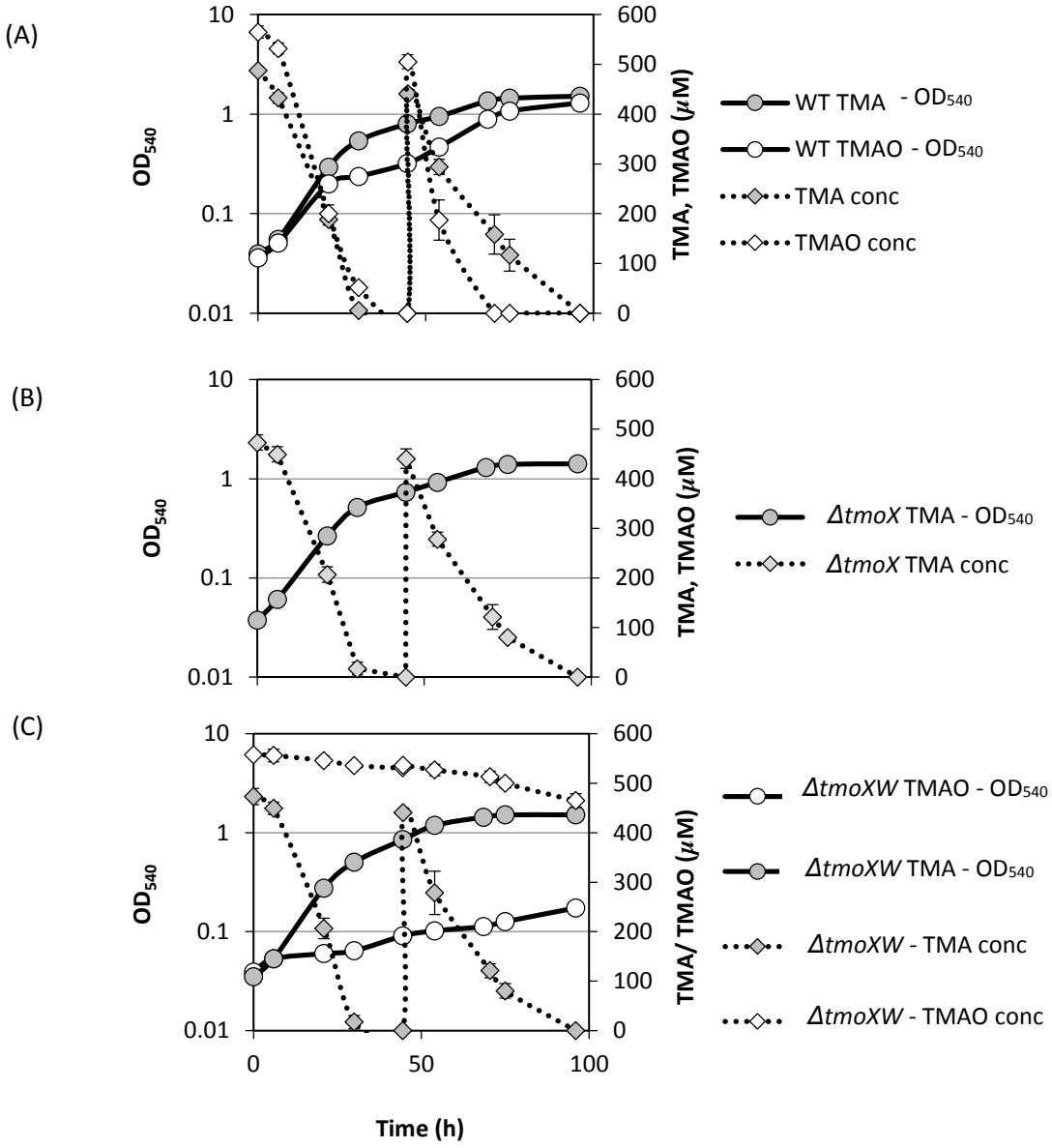

Figure 3.14. Growth of *R. pomeroyi* DSS-3 and the TMAO transporter mutants on TMA and TMAO as a sole N source. **(A)** *R. pomeroyi* wild type was grown on either TMA (grey circles) or TMAO (white circles) and concentrations of TMA (grey diamonds) and TMAO (white diamonds) were quantified during growth. **(B)** *R. pomeroyi* mutant *ΔtmoX::Gm* was grown on TMA (grey circles) and the concentration of TMA (grey diamonds) was quantified throughout growth. **(C)** The mutant, *ΔtmoXW::Gm*, was grown on TMA (grey circles) or TMAO (white circles) as a sole N source. The concentrations of TMA (grey diamonds) or TMAO (white diamonds) was quantified throughout during growth. Once TMA/TMAO was depleted in the medium, a second dose (final concentration 0.5 mM) was added at 48 h. All cultures were grown in triplicate and error bars denote SD.

3.2.2.5. Complementation of the mutant, *ΔtmoX::Gm*, with its native *tmoX*

To confirm that *tmoX* is essential for the rapid uptake of TMAO, the native *tmoX* from *R*. *pomeroyi* along with its promoter were cloned into the broad-host range vector, pBBR1MSC-km (Kovach et al., 1995) and mobilised into the *ΔtmoX::Gm* mutant. Unfortunately, this gene appeared to be toxic to *E*. *coli*, therefore the cloning was complicated. Originally, the gene and its promoter were amplified and cloned into pGEM-T, but no colonies appeared that had the correct insert. To overcome this, *tmoX* alone was amplified and cloned into pGEM-T. Only when IPTG (drives expression of the gene) was not added to the plates, did any colonies grow that had the correct insert (*tmoX*). The gene was successfully cloned into the expression vector pBBR1MCS-km, but when the promoter was added, again no colonies that contained the full sequence (*tmoX* + promoter) were obtained. The three colonies that grew all had point mutations, confirming that this gene was probably toxic to *E*. *coli* and that any intact genes being expressed caused a toxic effect through overproduction of TmoX. In order to achieve complementation, a larger ligation reaction (100 µl) was set up and purified using an on-column purification kit (Chapter 2, section 2.4.4). The resulting plasmid DNA (pBIL101) was mobilised into the *tmoX::Gm* mutant via electroporation, generating the strain *ΔtmoX+tmoX:DSS3*. Two Kan^R *R*. *pomeroyi* transformants were screened for possession of the plasmid and insertion of the promoter was checked via digestion using the appropriate enzymes. *Bam*HI and *Xba*I released a fragment approximately 1 kb in length corresponding to the *tmoX*. A restriction digest with *Hind*III and *Xba*I released a construct approximately 260 bp longer which corresponded to the *tmoX* plus its promoter, confirming that the promoter had been incorporated into the cut plasmid, generating the plasmid, pBIL101 (Figure 3.14a). pBIL101.

Complementation of the mutant with its native *tmoX* restored the ability of the mutant to grow on TMAO as a sole N source as a rate comparable to the wild-type strain (Figure 3.14b). This confirmed that TmoX is essential for the rapid uptake of TMAO.

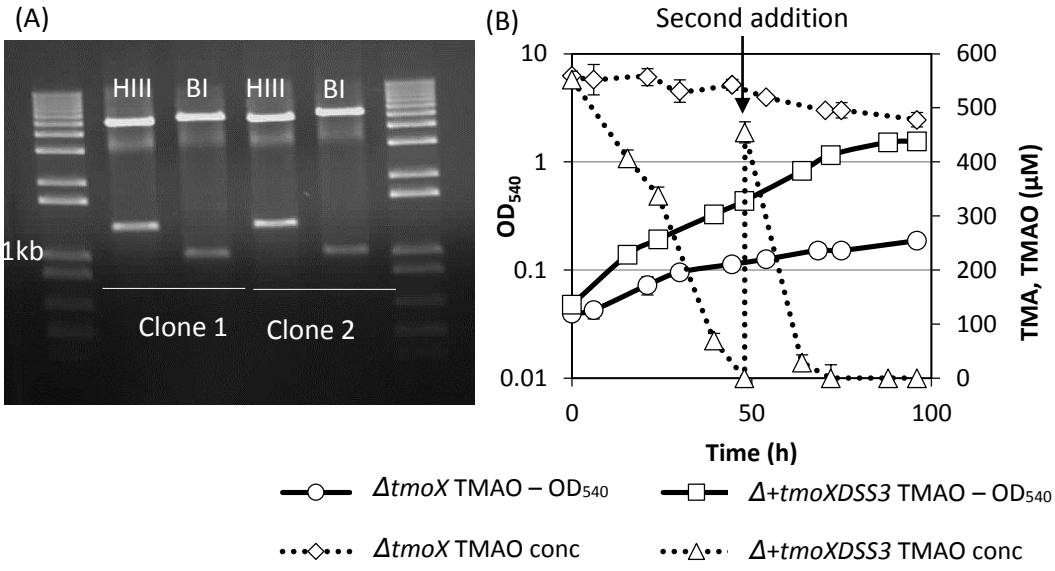

Figure 3.15. (Left panel) Restriction digest of the plasmid purified from the transconjugants resistant to kanamycin. Lanes 1 and 3 have been digested with *Hind*III and *Xba*I. Lanes 2 and 4 have been digested with *Bam*HI and *Xba*I. **(Right panel)** Growth on the mutant, *ΔtmoX::Gm*, and *ΔtmoX +tmoX:DSS3*, on TMAO as a sole N source. Cultures were grown in triplicate and error bars denote SD.

3.2.2.6. Complementation of the mutant, *ΔtmoX::Gm*, with the *tmoX* from *Pelagibacteraceae* strain HIMB59

To determine if the TmoX homolog from SAR11 strains also facilitates the uptake of TMAO, the putative TmoX homolog from *Pelagibacteraceae* strain HIMB59 was synthesised (GenScript Incorporation) and the gene was codon optimised for *R. pomeroyi*. As described in section 3.2.2.4., this gene was toxic when expressed in *E. coli*, therefore the same cloning steps outlined in section 3.2.2.4 were repeated, generating the complemented mutant strain *ΔtmoX +tmoX:HIMB59*. Incorporation of the plasmid, pIL102, was confirmed by PCR (Figure 3.15a). The complemented strain, *ΔtmoX +tmoX:HIMB59* and a complemented strain with the empty plasmid,

pBBR1MCS-km (*ΔtmoX* +pBBR1MCS-km), set up as a control, were grown on TMAO as the sole N source. After almost 200 h, *ΔtmoX +tmoX:HIMB59* had degraded all the TMAO added (~500 µM) to the medium whilst there was ~345 µM TMAO left in the medium containing *ΔtmoX* +pBBR1MCS-km. *ΔtmoX +tmoX:HIMB59* depleted a further 765 µM TMAO that was supplemented after 200 h and reached a final OD_{540} ~ 1.25. In contrast, *ΔtmoX* +pBBR1MCS-km only reached a final OD_{540} ~ 0.194 and did not show any growth after 183 h.

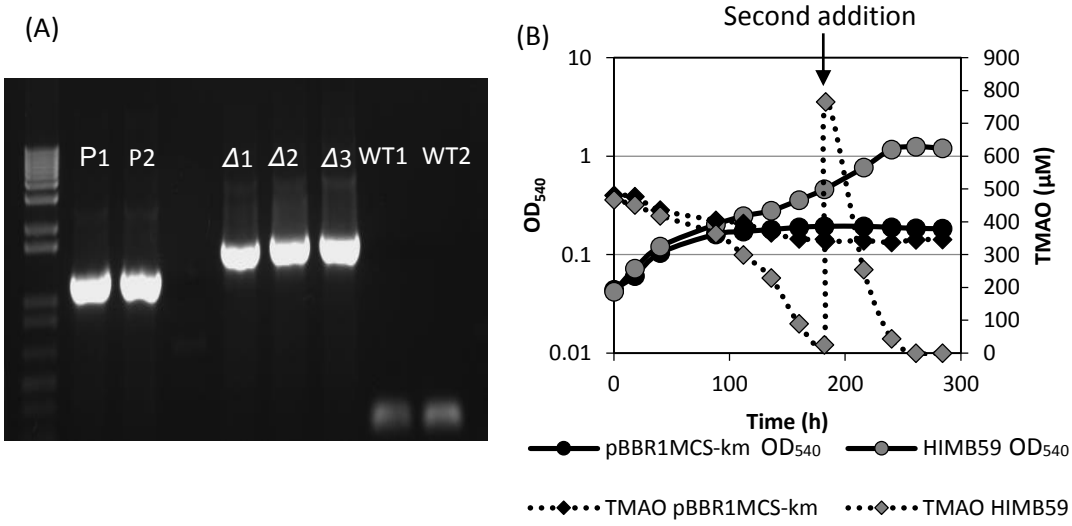

Figure 3.16. (Left panel) Confirmation by PCR using the primers, M13F/M13R (Viera and Messing, 1982), that the mutant, *ΔtmoX::Gm*, was transformed with the plasmid, pBIL102 (see Table 2.1). Lanes 1 and 2 amplified a PCR product from pBBR1MCS-km containing *tmoX* prior to insertion of the promoter of *tmoX*. **(Right panel)** Growth of the mutant complemented with plasmid, pBIL102 or the empty vector, pBBR1MCS-km on TMAO as a sole N source. TMAO was quantified throughout the experiment (diamonds). Results are the mean of triplicate cultures and error bars denote SD. Ladder is the same as in figure 3.14.

3.2.2.7. Characterisation of the *ΔtmoXW::Gm* and *ΔtmoX::Gm* mutants on other methylated amine compounds

To determine whether or not TmoXWV also has a primary role in transporting other structurally related compounds, the two mutants, *ΔtmoXW::Gm* and *ΔtmoX::Gm* were grown on carnitine, choline, GBT, TMA. As MMA and DMA were used to select for mutant *R. pomeroyi* transconjugants after conjugations during marker exchange mutagenesis, these two compounds were not tested further. Growth rates

were then calculated for TMAO and the other remaining MAs and QAs. Wild-type *R*. *pomeroyi* had a growth rate of 0.049± 0.03 h^{-1} when grown on TMAO (Figure 3.16), whilst the *ΔtmoXW::Gm* and *ΔtmoX::Gm* mutants growth rates were significantly lower (t-Test = $p<0.05$) at 0.011±0.02 h^{-1} and 0.012±0.03 h^{-1}, respectively. For carnitine, choline, GBT and TMA, there was no significant difference (t-test, $p>0.05$) between the growth rates. Growth on TMA was approximately 0.063 h^{-1}, whilst choline and GBT had the highest growth rates at ~0.086 h^{-1} and ~0.087 h^{-1}, respectively.

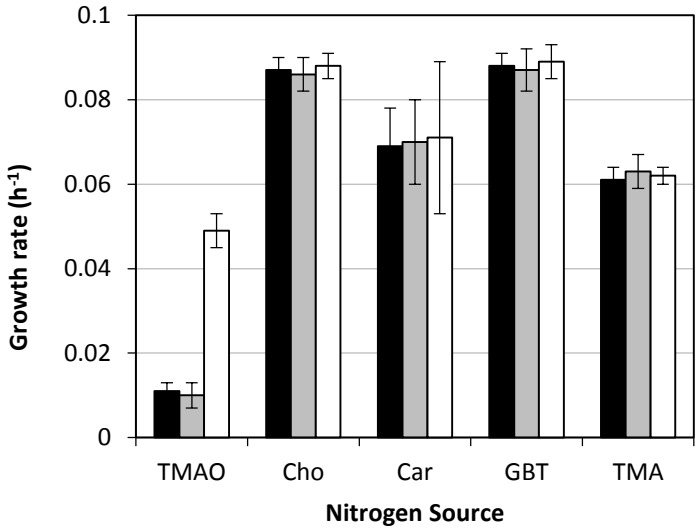

Figure 3.17. Effects of different compatible osmolytes on the growth of the *R*. *pomeroyi* mutants, *ΔtmoXW:Gm* and *ΔtmoX::Gm*. The growth rates of *R*. *pomeroyi* wild-type (white bars) and the two transporter mutants, *ΔtmoX::Gm* (gray bars) and *ΔtmoXW::Gm* (black bars), were determined for each osmolyte and TMA as a sole N source. Cultures were grown in triplicate and error bars denote SD.

3.2.2.8. Sensitivity of the promoter of *tmoXWV* to different structurally related compounds

As the genome of *R*. *pomeroyi* has a number of putative transporters of similar function throughout its genome, it cannot be ruled out that other transporters may be able to take up these other compounds, thereby masking the effect TmoXWV has on the uptake of QAs and TMA. Screening the activity of the promoter of

tmoXWV, at the transcriptional level, against the other methylated compounds will help to better understand the role of this transporter in the ocean. Using the online software program, Neural Network Promoter Prediction (Berkeley Drosophila Genome Project, BDGP; http://www.fruitfly.org/seq_tools/promoter.html) (Reese, 2001), a promoter was predicted in the 5' upstream region (Figure 3.17). The 250 bp region upstream of *tmoX* was cloned into the broad host-range promoter-probe vector, pBIO1878 (Todd et al., 2012), upstream of the *lacZ* reporter gene, generating the plasmid, pBIOL101. pBIOIL101 (pBIO1878 + the promoter of *tmoXWV*) was mobilised into wild-type *R. pomeroyi* via conjugation and transconjugants were selected on spectinomycin plates.

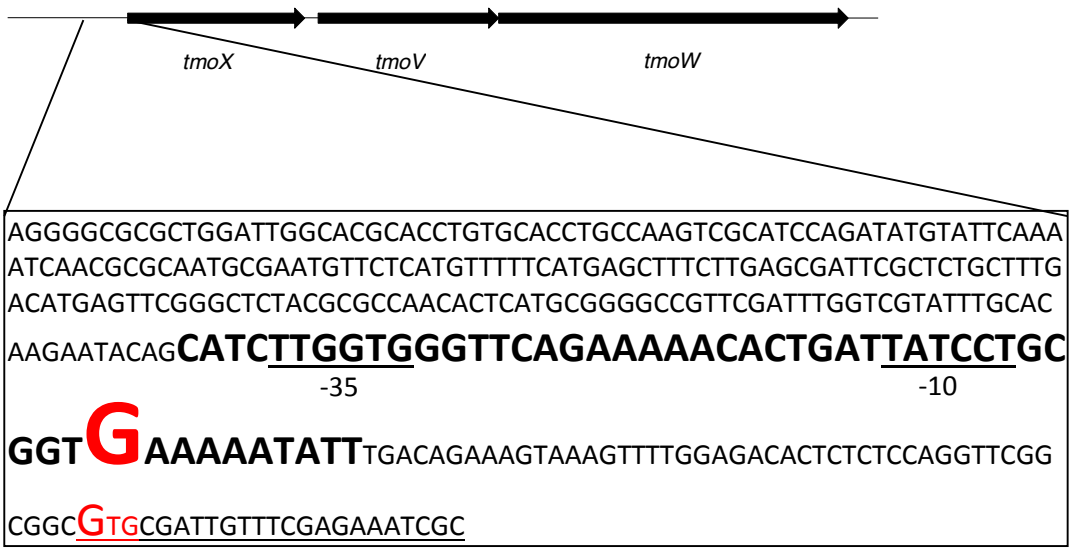

Figure 3.18. The promoter region of the *tmoXWV* predicted using the prediction software, Neural Network Promoter Prediction. The large red character indicated a potential transcriptional start site. The red GTG indicates the start codon for *tmoX*. The Shine Dalgarno sequence (-10) and the -35 consensus sequence are shown.

A transconjugant was grown overnight in MAMS containing succinate and NH_4^+ +/- TMA, TMAO, GBT, choline or carnitine (1mM) prior to assaying for β-galactosidase (LacZ) activity (Chapter 2, section 2.7.2). Whilst, no induction of the *tmoXWV* was observed for GBT, choline and carnitine, there was 6-fold induction

when cells were exposed to TMAO (870 ± 34), compared to that of the control (130 ± 7). This result together with the growth analysis (section 3.2.2.6) suggests that the primary role of this transporter is for the rapid uptake of TMAO only.

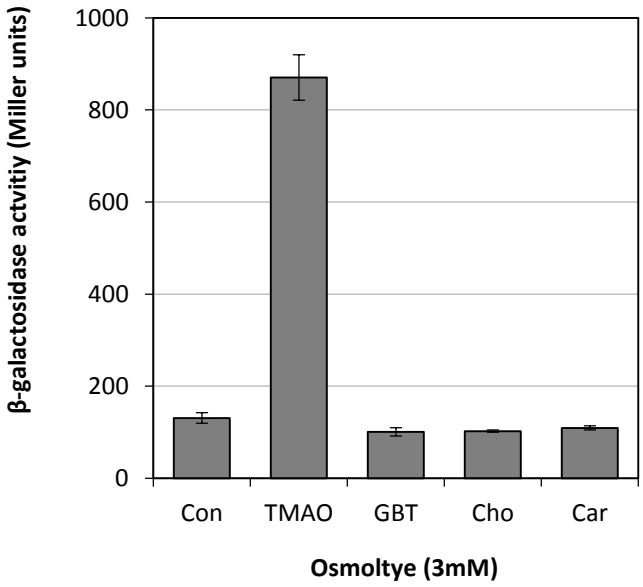

Figure 3.19. Cultures of *R*. *pomeroyi* DSS-3 containing the *tmoX–lacZ* fusion plasmid, pBIL101, were grown in the presence of each compatible osmolyte (3 mM). Cultures were grown and assayed for β-galactosidase activity in triplicate and error bars denote SDs. Abbreviations: Car, carnitine; Cho, choline; Con, control, GBT, glycine betaine, TMAO, trimethylamine *N*-oxide.

The sensitivity of the promoter of *tmoXWV* against TMA was also investigated. For wild-type *R*. *pomeroyi* containing, pBIOL101, TMA led to the induction of the promoter, albeit it at a lower level compared to TMAO (Figure 3.19a). When the cells were grown only on TMA or TMAO as the sole N source the level of induction of the promoter of *tmoXWV* was greater than when the cells were grown on TMA or TMAO in the presence of NH_4^+. This suggests that in *R*. *pomeroyi*, induction of *tmoXWV* may be regulated in part by the availability of NH_4^+. As TMAO is an intracellular metabolite of TMA, the promoter-probe vector, pBIL101, was mobilised into the mutant, *Δtmm::Gm*, which has lost the ability to oxidise TMA to TMAO (Chapter 4, section 4.2.1). When this new transconjugant, *Δtmm::Gm*

+pBIL101, was grown in the presence of TMA or TMAO, there was a marked decrease in the level of transcription of *tmoXWV* in cells exposed to TMA (Figure 3.19b). However, there was still strong transcription of the promoter of *tmoXWV* when *Δtmm::Gm* +pBIL101 was grown in the presence of TMAO. Together, these data strongly suggest that the primary function of TmoXWV is to facilitate the rapid uptake of TMAO from the seawater.

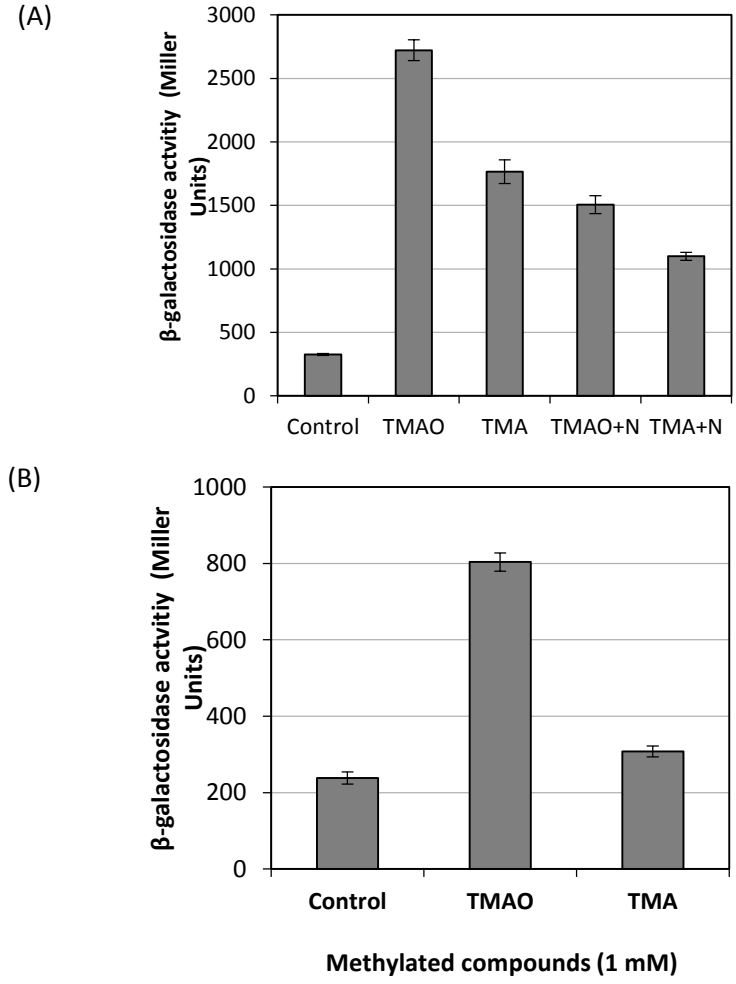

Figure 3.20. (A) Wild-type *R. pomeroyi* DSS-3 containing the *tmoX–lacZ* fusion plasmid pBIL101 were grown in MAMS medium in the presence of TMA (1 mM) or TMAO (1 mM) with succinate (8 mM) as the C source, or in the presence of TMA (0.5 mM) or TMAO (0.5 mM) with additional NH_4^+ (4 mM) (TMA+N and TMAO+N, respectively) and succinate (8 mM). B-galactosidase activity was assayed in triplicate and error bars denote SDs. **(B)** The *R. pomeroyi* mutant, *Δtmm::Gm*, containing pBIL101 was grown for 16 h in the presence of additional TMA (0.5 mM) or TMAO (0.5 mM) and β-galactosidase activities were assayed in triplicate. Growth was performed in a defined medium with succinate (8 mM) as the C source and ammonium as the N source (4 mM). Error bars denote SDs.

3.3. Discussion

The results presented above have built on the work by Chen et al. (2011) which discovered that the genes required for the turnover of TMA are abundant in the marine environment. It has also confirmed the hypothesis that a gene encoding an enzyme with a H_4F-binding domain is responsible for the demethylation of TMAO to DMA. This agrees with the prediction that the H_4F-linked C1 oxidation pathway is the main route for the oxidation of the methyl groups released during the catabolism of MAs (Chen, 2012). Tdm appears to be even more abundant in marine bacteria than Tmm and a number of different bacteria that are capable of catabolising only TMAO but not TMA were also identified. This metabolic trait was confirmed using *Roseobacter* sp. SK209-2-6 which does not possess *tmm* but does have *tdm* and could only grow on TMAO, but not TMA as a sole N source. *Roseibium* sp. TrichSKD4, another member of the marine *Roseobacter* clade isolated from a *Trichodesmium* bloom (IMG/ JGI database, Project ID: Gp0004194), is also lacking *tmm*, but does have the genes necessary for complete TMAO catabolism. Interestingly, a *bona fide tmm* homolog (identity, 53.6% to *R*. *pomeroyi*; 76.65% to *C*. Pelagibacter ubique HTCC1062) was located within the genome of *Trichodesmium erythraeum*. However, no other genes that are required for the catabolism of MAs were identified within the genome of *T*. *erythraeum* and it can therefore be hypothesised that these two organisms may have a mutualistic interaction.

A *tdm* homolog and *tmoX* homolog were also found in the genome of a SAR324 cluster bacterium, which is predominantly found in the deep ocean "twilight zone" where photosynthesis does not occur (Swan et al., 2011; Sheik et al., 2013). TMAO

metabolism by SAR324 bacteria may help facilitate their chemoautotrophic lifestyle, supplementing energy predominantly derived from the oxidation of reduced S compounds (Swan et al., 2011). Genes required for the H_4F-linked oxidation of the methyl groups were indeed expressed among the SAR324 cluster bacteria inhabiting deep-sea marine plumes (Sheik et al., 2013). The ability of SAR324 bacteria to use TMAO is in line with the recent discovery that they are capable of using a range of electron donors and acceptors, which may help explain their prevalence in the dark ocean (Sheik et al., 2013).

The TMAO transporter, TmoXWV, in *R*. *pomeroyi* appears to be specific for TMAO although we cannot rule out the possibility that this transporter can also transport other structurally-related compounds. TmoX in *R*. *pomeroyi* has a number of homologs (SPO1131, SPO2441, SPOA0231, identity, 21-34%), as well as a number of BCCT-type transporters in its genome. It is therefore reasonable to assume that a number of different transporters are responsible for the high affinity uptake of each individual compound tested in section 3.2.2.7, although they may also have low affinities for other structurally related compounds. A BCCT-type transporter found within the genomes of various MRC isolates was expressed heterologously in a mutant strain of *E*. *coli* that can no longer uptake DMSP, GBT or choline (Sun et al., 2012). Overexpression of this transporter in this mutant resulted in the uptake of not only DMSP, but also GBT and choline, suggesting that this transporter has a broad substrate specificity for these structurally-related methylated compounds (Sun et al., 2012). In *S*. *meliloti* a number of SBPs, CaiX, BetX, ChoX, all have high affinities for their respective cognate substrates, but also have low affinity for these other compounds (Chen, et al , 2010). The same trait was observed for ChoX of *Brucella aborta* where, based on fluorescence binding

affinity assays, the affinity (K_D) for choline was 7 ± 2 nM whilst its affinity for GBT was 350 ± 30 μM (Herrmann et al., 2013). In the marine environment, TmoX is likely to bind its cognate ligand, TMAO, as the *in situ* concentration for MAs (King, 1984; Gibb and Hatton, 2004) and QAs (King, 1984; Kiene, 1998) is close to the expected K_D values for of their given SBPs. In addition, as TmoXWV expression is not regulated, at the transcriptional level, by other structurally-related compounds, it is very unlikely that this transport is required for the rapid uptake of TMAO.

The fact that some bacteria lack Tmm, coupled with the existence of a TMAO-specific transporter, suggests that bacteria take up TMAO directly from the seawater. The conversion of TMA to TMAO requires an extra enzyme (Tmm) and NADPH as a reducing equivalent (Chen et al., 2011), therefore marine bacteria capable of taking up TMAO directly from seawater may benefit energetically by bypassing the requirement for TMA oxidation by Tmm. Although studies on the *in situ* concentrations of TMAO in seawater are limited, there is evidence that TMAO is more abundant than TMA in the surface seawater (Gibb and Hatton, 2004). There are several reasons that could explain this: 1) The direct release of TMAO into the marine environment from a variety of marine organisms may result in a greater input of TMAO into marine surface waters. 2) Production of TMA relies on the reduction of QAs and/or TMAO, which may be a limiting step on TMA production in oxygenated surface waters. 3) Differences in enzyme kinetics between Tmm and Tdm, where Tmm may have a greater affinity for TMA than Tdm has for TMAO (Myers and Zatman, 1971; Parkin and Hultin, 1986; Chen et al., 2011). This final explanation may result in the faster removal of TMA from the water column compared to TMAO.

Reanalysis of a number of recently published metatranscriptomic and metaproteomics studies revealed that the TmoX is highly expressed *in situ* in members of the MRC and SAR11 clade (Sowell et al., 2008; Ottesen et al., 2011; Williams et al., 2012; Gifford et al., 2013; Ottesen et al., 2013). For example, analysis of metatranscriptomic data of bacterioplankton from the Monterey Bay of California showed that the TMAO transporter is one of the most highly expressed transporters in the MRC representative, *Rhodobacterales* sp. HTCC2255 (ZP_01447069), an abundant member of the microbial community at this study site (Ottesen et al., 2011). Off the coast of northern California, *tmoX* from SAR11 bacteria (Cluster 686, YP_266709) is among the 10 most highly expressed genes in the SAR11 metatranscriptome (Ottesen et al., 2013). Metaproteomic data collected from the Sargasso Sea also revealed that a polypeptide identified as TmoX, closely related to TmoX of the SAR11 isolate, *C*. Pelagibacter sp. 7211 (PB7211_687), was among the 10 most highly expressed transporter proteins (Sowell et al., 2008). Also, during the summer and winter months in Antarctic surface seawater, a TmoX closely related to the TmoX of *C*. Pelagibacter ubique HTCC1002 (PU1002_06741) was also highly expressed (Williams et al., 2012). Not only has expression of the TMAO transporter been frequently observed in natural seawater by metatranscriptomic and metaproteomic studies, but Tdm expression (Cluster 435, YP_266710) has also been seen in bacterioplankton assemblages inhabiting the surface seawater (Ottesen et al., 2013). The high level of *tmoX* and *tdm* expression in SAR11 and MRC bacteria from natural bacterioplankton communities suggests that TMAO may serve as an important substrate for energy generation (Sun et al., 2011), and it may also be an important source of N for these heterotrophs in the marine environment (Chen, 2012).

Chapter 4

Regulation of Tmm in *R. pomeroyi*

4.1. Introduction

Chen et al. (2011) previously showed that Tmm has a similar affinity for the reduced sulfur compound, DMS, as it does for its cognate substrate, TMA. In this study it was revealed that Tmm has a K_m ~20 μM for both TMA and DMS. *R. pomeroyi* was shown to oxidise low concentrations of DMS when supplemented with either glucose or a complex medium, such as ½ YTSS (González et al., 1999). However, several attempts to replicate these results have proven unsuccessful (Schaefer, Todd and Johnston, personal communications). *R. pomeroyi*, along with other members of the MRC, can grow on DMSP as a sole C, sulfur and energy source and they have been shown to be a source of DMS during periods of increased primary production (González et al., 2000; González et al., 2003; Malmstrom et al., 2004; Buchan et al., 2005; Hatton et al., 2012; Nelson et al., 2014). As Tmm is highly abundant in marine surface seawater and has the ability to efficiently transform DMS to DMSO (Chen et al., 2011), this enzyme may have significant implications for the cycling of reduced sulfur compounds. Understanding the transcriptional regulation governing the activity of Tmm is therefore of great importance.

To gain a better understanding of the role that Tmm may play in the cycling of DMS, *R. pomeroyi* was used as a model organism to investigate the regulation of this enzyme, using a suite of molecular techniques. To determine if DMS oxidation could be stimulated in *R. pomeroyi*, a putative transcriptional repressor was identified and targeted for mutagenesis. The results presented in this Chapter reveal that in *R. pomeroyi*, the expression of Tmm is controlled at different regulatory checkpoints.

4.2. Results

4.2.1. Mutagenesis of *tmm* of *R. pomeroyi*

The mutant, *Δtmm::Gm*, was briefly introduced in Chapter 3 (section 3.2.2.7) when assessing the specificity of the TMAO transporter. Mutagenesis of the *tmm* confirmed that this gene is essential for growth on TMA as a sole N source and growth on other downstream metabolites was not affected (Figure 4.1A). The mutant, *Δtmm::Gm*, was complemented with either its native *tmm* or with *tmm* from *Roseovarius* sp. 217. To achieve this, the native promoter (5' upstream region of *tmm*) was used to drive expression of either *tmm* (Chapter 3). Complementation of the mutant was confirmed by PCR using the primers, tmmscreen_F1 and tmmscreen_R1 (Figure 4.2). As expected, complementation with either *tmm* homolog resulted in the restoration of growth on TMA as a sole N source due to a restoration in the catabolism of TMA (Figure 4.1B).

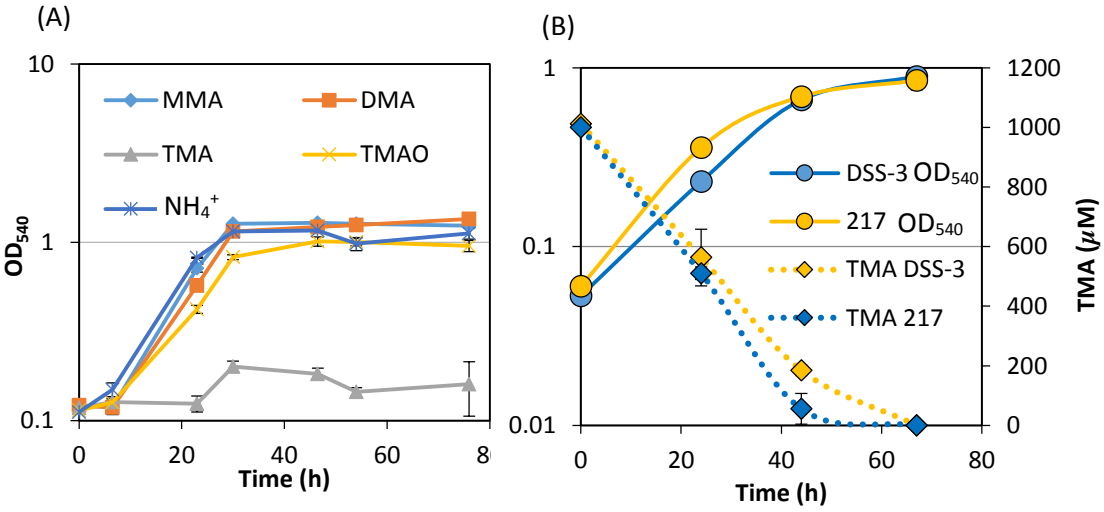

Figure 4.1. (A) Growth of the mutant, *Δtmm::Gm*, on different MAs and NH_4^+ (positive control) as a sole N source and succinate as the sole C source. (B) Growth of *Δtmm::Gm+tmm:DDS3* (Blue) and *Δtmm::Gm+tmm:217* (yellow) on TMA as a sole N source. All cultures were grown in triplicate. Error bars denote SD.

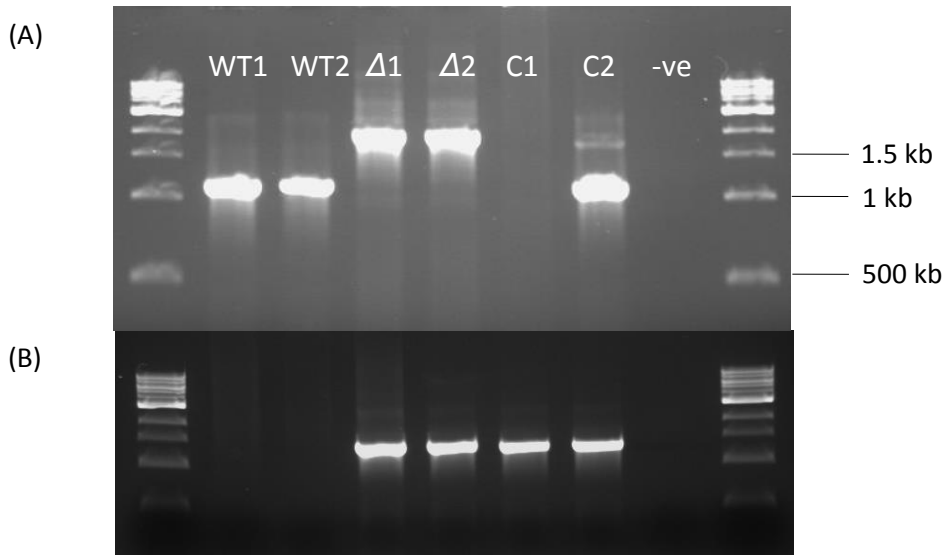

Figure 4.2. PCR assays confirming complementation of the mutant, *Δtmm::Gm*, with the native *tmm* from *R*. *pomeroyi*. **(A)** The primers, Tmm_CF and Tmm_CR, targeting the *tmm* were used. The mutant *Δtmm::Gm* (lanes 3-4), with *tmm* containing the gentamicin insert generated a larger product (~2 kb), whilst the wild-type (WT) and complemented mutant (C1, C2, lanes 5 and 6) have a smaller product (~1 kb), due to the presence of a functional Tmm. **(B)** The primers Tmm_CR and Gent_R were used to confirm that the positive result from the previous PCR came from mutant cells. Unlike the mutant or complemented mutant, no product could be amplified from wild-type, which lacks the gentamicin resistance cassette.

4.2.2. Screening the sensitivity of the promoter of *tmm* to different methylated compounds

To better understand the sensitivity of the promoter of *tmm* to different methylated compounds, the 5' upstream region of the *tmm* was cloned into the promoter-probe vector pBIO1878 (Todd et al., 2012), generating the plasmid, pBIOL102, as previously described in Chapter 3. A *R*. *pomeroyi* transconjugant was grown overnight with glucose and NH_4^+ as the C and N sources, respectively, and MMA, DMA, TMA, TMAO, DMS and DMSO (all 0.5 mM) were added individually to the culture medium. Results from the LacZ assay show that the promoter of *tmm* was not sensitive to either TMAO or DMSO, for which purified recombinant Tmm has a very low affinity (Chen et al 2011). The promoter of *tmm* was sensitive to both MMA and DMA, with DMA leading to a 2.3-fold induction in LacZ activity

(Figure 4.3). TMA resulted in a 3-fold induction in LacZ activity, whilst DMS resulted in the greatest induction (7-fold), suggesting that the promoter of *tmm* is more sensitive to DMS than TMA. This is noteworthy since purified recombinant Tmm from different marine bacteria, including, *R. pomeroyi*, has a high affinity for DMS as well as TMA (Chen et al. 2011)

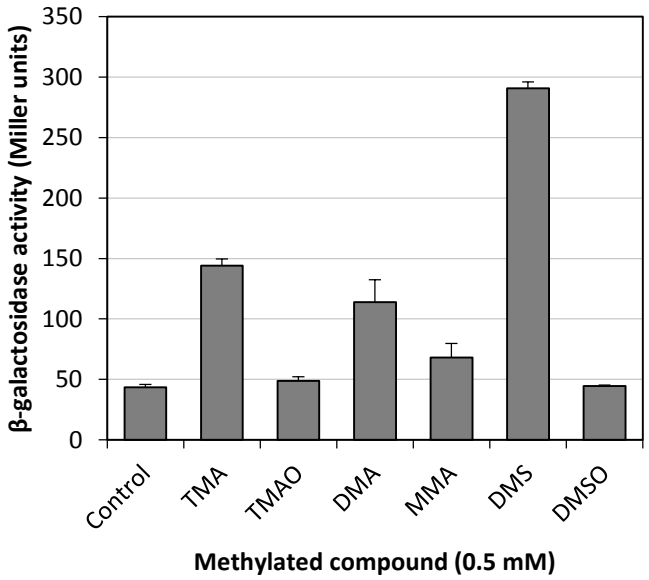

Figure 4.3. Cultures of *R. pomeroyi* DSS-3 wild-type containing the *tmm–lacZ* fusion plasmid, pBIOL102, were grown in the presence of each methylated compound (0.5 mM). Cultures were grown and assayed in triplicate for *β*-galactosidase activity and error bars denote SD. Abbreviations; TMA, trimethylamine; TMAO, trimethylamine *N*-oxide; DMA, dimethylamine; MMA, monomethylamine; DMS, dimethylsulfide; DMSO, dimethylsulfoxide.

4.2.3. Detection of Tmm activity from cell-free extracts of *R. pomeroyi*

To determine if Tmm is expressed at the protein level during growth in the presence of various methylated compounds, *R. pomeroyi* was grown on glucose as a C source and NH_4^+ as a N source in the presence of either TMA (1mM) or DMS (1mM). Cells were harvested during mid-exponential phase (OD_{540} ~0.6) and concentrated in PIPES buffer prior to cell lysis. Depletion of NADPH over time was determined by measuring the absorbance at 340 nm (Chapter 2, section 2.7.1) using cell-free

extracts containing TMA (test) or water (control). Cell-free extracts grown in the presence of TMA depleted NADPH at a faster rate than the water controls (Figure 4.4A). The specific activity for TMA-grown cell-free extracts was determined to be 1.9 ± 0.5 nmol min^{-1} mg^{-1} protein (Figure 4.4B). Cell-free extracts grown in the presence of DMS, did not have any detectable enzyme activity. *R. pomeroyi* was then grown using TMAO as a sole N source plus or minus DMS (1mM) prior to assaying for Tmm activity. No Tmm activity was detected in TMAO-grown cell-free extracts (Figure 4.4B), however TMAO plus DMS-grown cell free extracts had detectable Tmm activity (1.21 ± 0.3 nmol min^{-1} mg^{-1} protein).

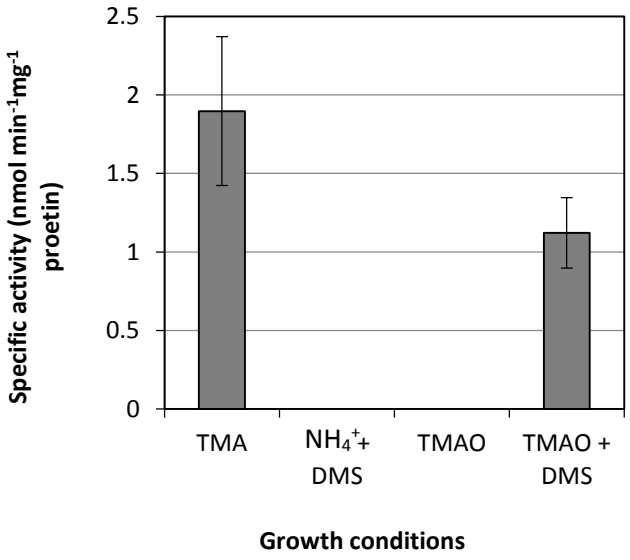

Figure 4.4. Calculated specific activities for *R. pomeroyi* cell-free extracts grown under different conditions. Results presents are the mean of triplicate enzyme assays. Error bars denote SD.

4.2.4. Transcriptional analysis of *tmm* by RT-PCR

To confirm the results obtained from the LacZ reporter assays, RNA was extracted from exponential phase *R. pomeroyi* cells (OD_{540} ~0.5) grown under similar growth

conditions as those stated in section 4.2.1. RNA extracted from *R*. *pomeroyi* cultures was free from any excessive degradation as all three expected bands representing intact ribosomal RNA were present (Figure 4.5). After DNA-digestion, RNA was subject to cDNA library preparation using a gene specific reverse primer initially targeting the 16S rRNA gene and then one targeting *tmm* (see M and M, Table 2.2). cDNA libraries were subjected to 30 cycles of PCR using the conditions outlined in the Chapter 2, section 2.4.2.

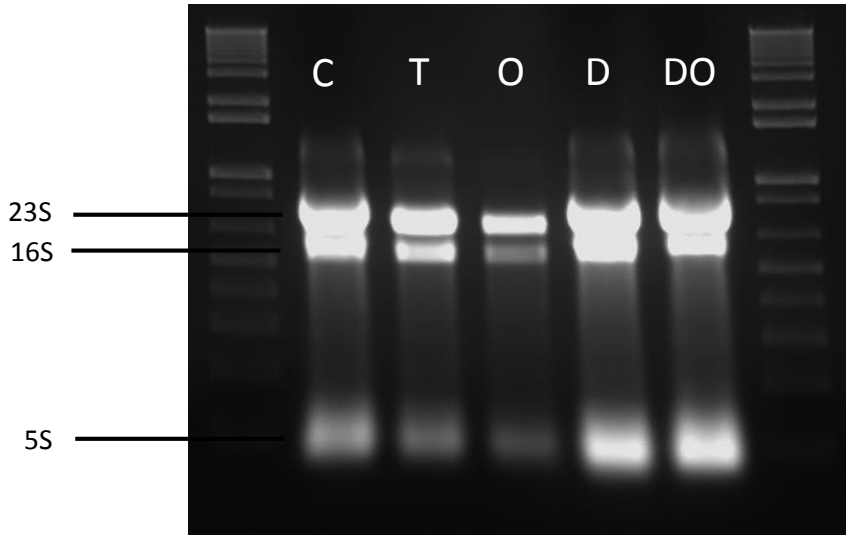

Figure 4.5. RNA extracted from *R*. *pomeroyi* grown under differing growth conditions containing the three major ribosomal RNA bands, 23S, 16S, 5S. Abbreviations; C, control (glucose + NH_4^+); T, TMA; O, TMAO; D, control + DMS; DO, TMAO + DMS.

Although the results from RT-PCR should be treated with caution, no obvious differences between the levels of 16S rRNA gene transcription (housekeeping gene) from either culture was evident (Figure 4.6A). Conversely, there did appear to be a clear upregulation of *tmm* when grown in the presence of TMA when compared with the control (Figure 4.6B). Controls with no reverse transcriptase added were

also performed in parallel to ensure that products obtained were a direct result of the amplification of cDNA and not DNA contamination. For cells grown on glucose and NH_4^+ (control), a faint product was detected which was stronger than the very faint band detected in the minus (-) RT control suggesting that *tmm* may have a basal level of transcription. Ideally, the analysis would have been repeated with 2 rounds of DNase treatment to make sure there was no background signal detection in the (-) RT controls, however due to time constraints this was not possible. Although there is a very low signal detected in some of the – RT controls as well as the no template control for 16S rRNA, there is a very strong signal detected from the samples treated with RT indicating that this strong signal is driven by the presence of cDNA. For TMAO-, DMS- and TMAO + DMS-grown cells, a product was amplified by PCR indicating that upregulation of *tmm* occurs in these growth conditions. The only disparity between the LacZ assay and the RT-PCR came from the TMAO-grown cells, however, in the RT-PCR analysis, TMAO was the sole N source whereas in the LacZ assay, NH_4^+ was also in the medium. Therefore it cannot be ruled out that some effect of N-dependent regulation may also regulate Tmm. This is in agreement with the results obtained in Chapter 3 which showed that *tmoX* has a greater level of induction in cultures grown without NH_4^+ (section 3.2.2.7). Evidence that DMS also effects the transcription of *tmm* was confirmed (Figure 4.6B). Taken together with the Tmm enzyme activity results, these data from RT-PCR suggest that in *R. pomeroyi* there might be an unknown mechanism of post-transcriptional regulation controlling the expression of Tmm.

(A)

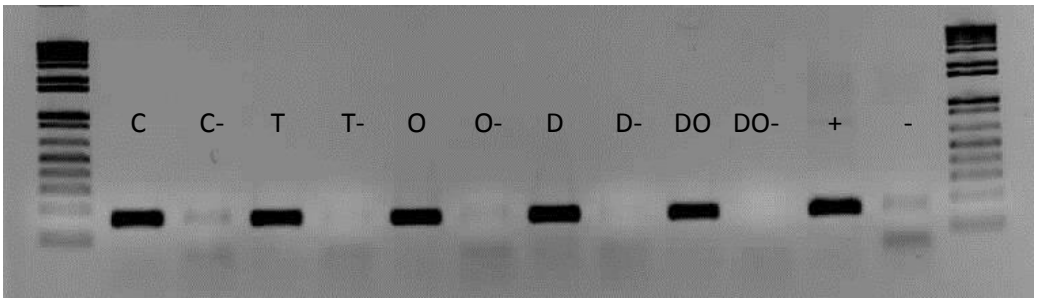

(B)

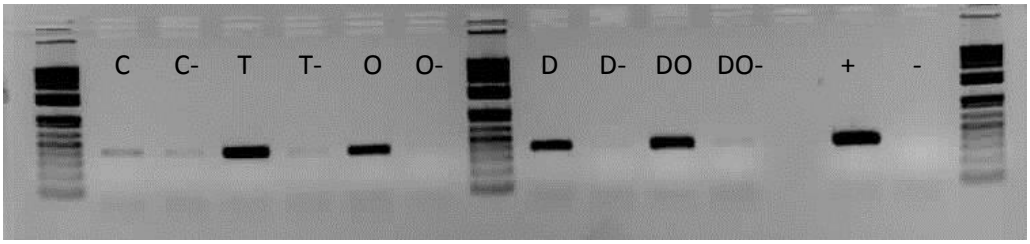

Figure 4.6. RT-PCR targeting the 16S rRNA gene **(A)** and *tmm* **(B)** in *R*. *pomeroyi* when grown on different N sources. Abbreviations; C, NH_4^+-grown; T, TMA-grown; O, TMAO-grown; D, NH_4^+ + DMS; DO, TMAO + DMS. – symbol denotes minus (–) RT controls. A positive control with *R*. *pomeroyi* DNA was also performed as well as negative (no template) control.

4.2.5. DMS oxidation by *R. pomeroyi*

R. *pomeroyi* was originally shown to oxidise DMS when DMS was supplied at low concentrations (<50 μM) and this process was enhanced when supplemented with glucose or a complex medium (González et al., 1999). As purified Tmm from marine bacteria can oxidise DMS (Chen et al., 2011) and Tmm activity can be induced by TMA as well as a TMAO + DMS (section 4.2.3), the ability of *R*. *pomeroyi* to oxidise DMS when grown on MAs was tested. To do this, *R*. *pomeroyi* wild-type or the mutant, *Δtmm::Gm*, were grown on glucose (10 mM) as a sole C source and either 0.5 mM NH_4^+, MMA, DMA, TMAO or TMA as a sole N source with the addition of DMS (1 mM). *Δtmm::Gm* was not grown on glucose and TMA as this would result in no growth (see section 4.2.1). Under all other conditions,

both the mutant and wild-type grew to an OD_{540} 0.5-0.7 (Figure 4.7a). Cells were N-limited, meaning that a C and energy source was still available during the onset of stationary phase. This should help maintain the cell viability of *R. pomeroyi* during the stationary phase of growth and therefore not inhibit DMS oxidation. NH_4^+- and MMA-grown cells did not oxidise any DMS during growth on glucose (Figure 4.7b). For NH_4^+, this is in line with the fact DMS alone does not induce Tmm activity (Figure 4.3b). After an initial lag, wild-type cells grown on TMA and TMAO oxidised all the DMS after 89 h, with the majority of DMS oxidation taking place between 45 and 89 h (Figure 4.7b). DMA-grown wild-type cells had a slower, but still significant rate of DMS oxidation (~50% of DMS after 260 h). Although growth was unaffected in the mutant, *Δtmm::Gm*, none of the conditions resulted in any DMS oxidation, confirming that in *R. pomeroyi* DMS oxidation is dependent on a functional Tmm. Both complemented mutant strains (outlined in section 4.2.1.) had the ability to oxidise DMS when grown in the presence of TMA restored (data not shown).

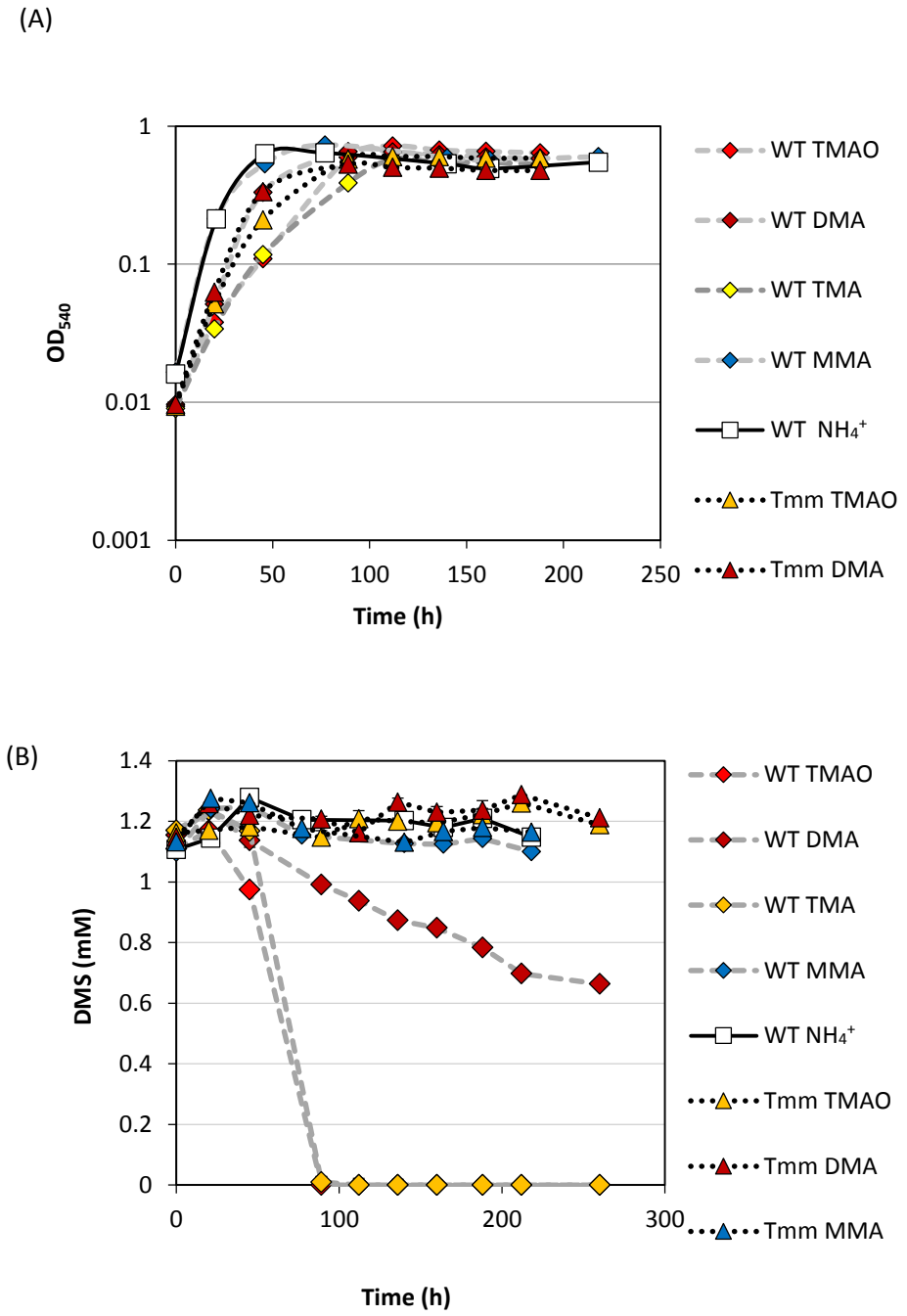

Figure 4.7. (A) Growth of *R. pomeroyi* wild-type (WT) or mutant, *Δtmm::Gm* (Tmm) on different amines as a sole N source supplemented with DMS (1mM). **(B)** DMS was quantified throughout the experiment. Cultures were grown in triplicate and error bars denote SD.

4.2.6. Mutation of the lysR-type repressor, *tmoR*, of *R. pomeroyi*

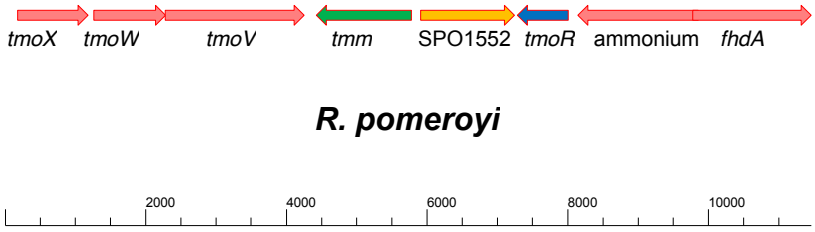

Figure 4.8. Gene neighbourhood of *tmm* in *R. pomeroyi*. Scale bar denotes number of base pairs. Abbreviations: *tmm*, TMA monooxygenase; *tmoXWV*, TMAO transporter, *tmoR*, regulator of *tmm*; ammonium, unknown ammonium-type transporters; *fhdA*, alpha subunit of formate dehydrogenase SPO1552 is a putative amino acid substrate binding protein form the HAAT family..

In *R. pomeroyi*, *tmm* is adjacent to a substrate binding protein (SBP) (SPO1552) from the hydrophobic amino acid uptake transporter (HAAT) family. SPO1552 is on the opposite strand to *tmm* (Figure 4.8). Upstream of the SPO1552 and on the same strand as *tmm* is a lysR-type repressor (SPO1553), hereafter designated *tmoR*. This ORF is also found in other MRC isolates that contain *tmm*. Therefore, the hypothesis is that this regulator is involved in regulation of *tmm*. To determine if this is a repressible regulator, the same *tmm:lacZ* promoter-probe, pBIOL102, (section 4.2.2) was transformed into the newly constructed mutant, *ΔtmoR::Gm*, and a transconjugant was grown in the presence of either TMA, TMAO or DMS (0.5 mM). A control culture with no methylated compound added was also grown overnight. Unlike the wild-type *tmm:lacZ* transconjugant, all four growth conditions resulted in the strong induction of LacZ activity, indicating that mutagenesis of *tmoR* results in constitutive expression of *tmm* (Figure 4.9). Mutant cell-free extracts grown without the addition of any methylated compounds had greater levels of LacZ activity (398 ± 16 Miller units) compared to wild-type cells

(43 ± 2 Miller units). Unlike the wild-type, for *ΔtmoR::Gm*, there was no clear induction of *tmm* in the presence of DMS (Figure 4.9). For *ΔtmoR::Gm,* TMA only resulted in a slight induction (< 2-fold) and not the 3-fold induction that was observed for the wild-type.

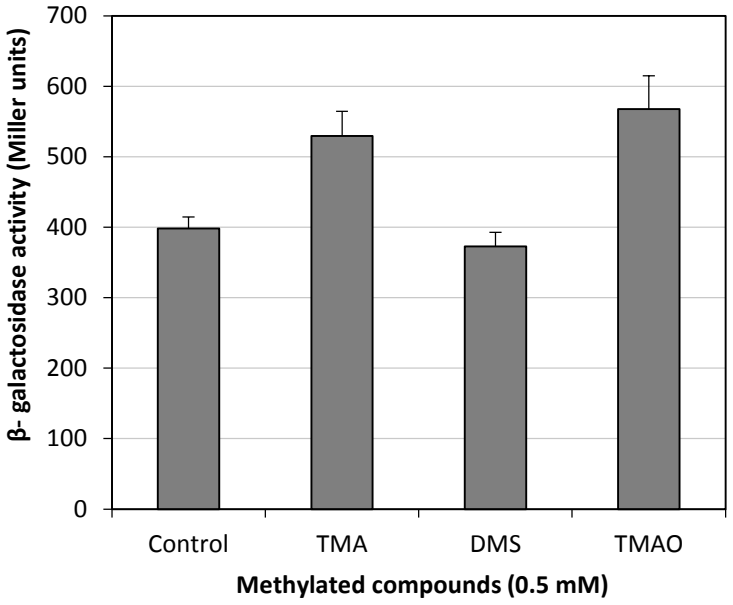

Figure 4.9. Mutant, *ΔtmoR::Gm*, containing the *tmm–lacZ* fusion plasmid, pBIIOL102, was grown on glucose and NH_4^+ in the presence of different methylated compounds (0.5 mM). Cultures were assayed for β-galactosidase activity in triplicate and error bars denote SD.

To confirm that *tmm* is constitutively expressed when TmoR is nonfunctional, RNA was isolated from cultures grown on glucose and NH_4^+ plus or minus TMA. Again, 30 cycles of PCR were performed using primers targeting *tmm*. Duplicate cultures for both plus or minus TMA-grown *R. pomeroyi* were screened and results from RT-PCR confirmed that there appeared to be no significant different in level of transcription of *tmm* (Figure 4.10). This confirms that *tmm* is transcribed in the absence of TMA due to a non-functional repressor. Again, –RT controls did not result in the amplification of any PCR product for any growth condition.

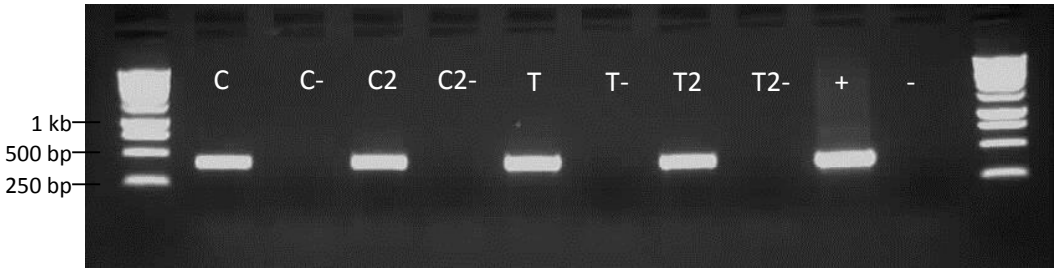

Figure 4.10. RT-PCR targeting *tmm*. Abbreviations: C, *ΔtmoR::Gm* grown on glucose and NH_4; T, *ΔtmoR::Gm* grown on glucose and TMA; – symbol denotes minus (–) RT controls. A positive control with *R. pomeroyi* DNA was also performed as well as negative (no template) control.

4.2.7. DMS oxidation by the *ΔtmoR::Gm* mutant

As DMS leads to the transcription of *tmm*, but does not result in the induction of *tmm* activity (and therefore no DMS oxidation), a similar DMS oxidation profile to that of the wild-type should be observed for the mutant, *ΔtmoR::Gm*. *ΔtmoR::Gm* was grown under the same conditions as the wild-type (section 4.2.5), however the concentration of N source was doubled to 1 mM. As expected, DMS oxidation only took place in the presence of downstream metabolites further indicating that some level of post-transcriptional regulation is taking place that allows for the translation of a functional Tmm (Figure 4.11). The only difference between the wild-type and the *ΔtmoR::Gm* mutant was that MMA appeared to stimulate DMS oxidation in the mutant where as it did not in the wild-type. Although DMS oxidation appeared to be faster in the *ΔtmoR::Gm* mutant, the number of cells in the cultures during the experiment was greater. For example, during the first 50 h, wild type cultures grown on DMA, TMA or TMAO reached an OD_{540} ~0.1-0.25, whereas the mutant cultures had reached an OD_{540} ~1.5 (Figure 4.11). A combination of a greater starting inocula coupled with a higher concentration of MAs used was the likely cause for this observed effect. However, according to the LacZ assays, a stronger transcription of *tmm* in the mutant occurred and this may have resulted in a greater

amount of Tmm activity. Nevertheless, there was no DMS oxidation in the *ΔtmoR::Gm* cultures incubated with NH_4^+ alone, highlighting the fact that full expression of Tmm requires the presence of MAs.

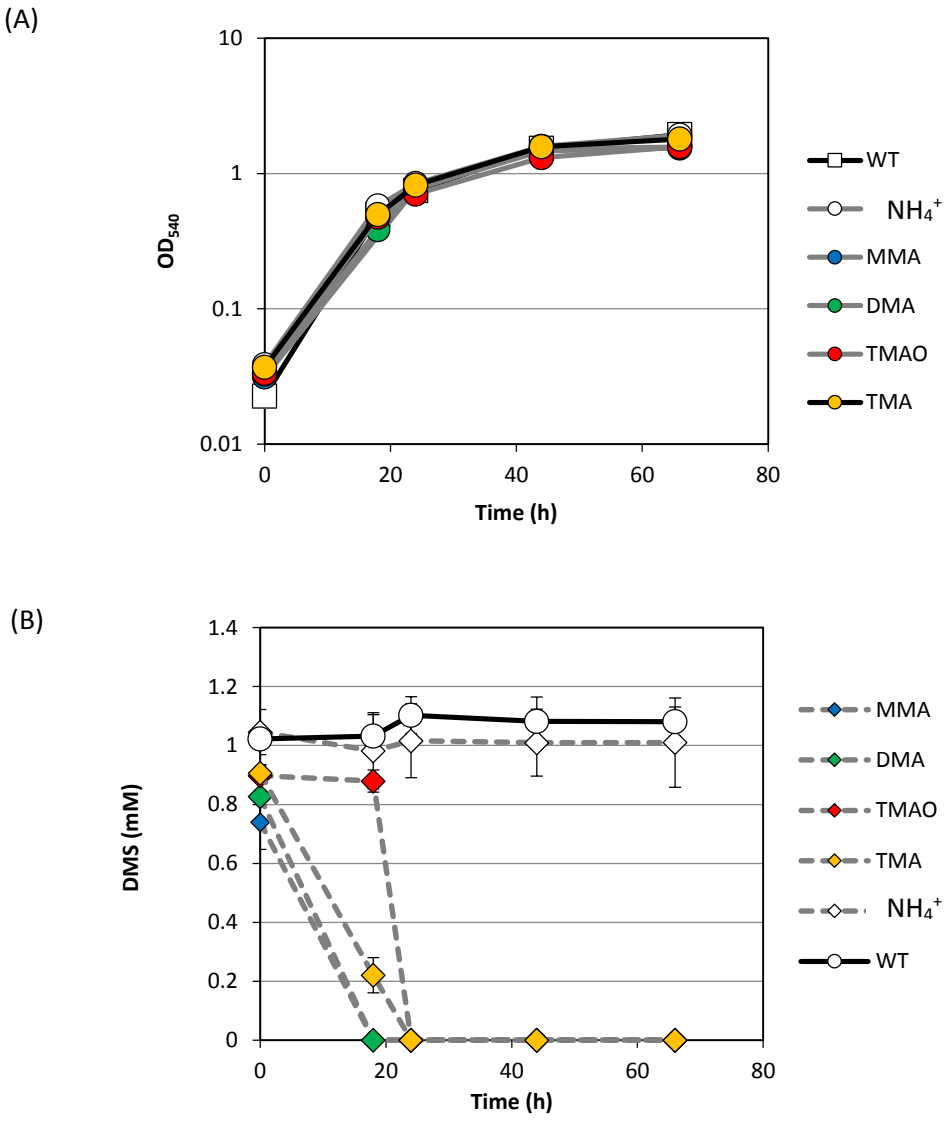

Figure 4.11. (A) Growth of the mutant, *ΔtmoR::Gm*, on different amines as a sole N source supplemented with DMS (1mM). **(B)** DMS was quantified throughout the experiment. Cultures were grown in triplicate and error bars denote SD. WT represents wild-type cultures grown on NH_4^+ as a nitrogen source.

4.2.8. Involvement of antisense RNA in post-transcriptionally regulating *tmm*

One possible mechanism for the post-transcriptional regulation of *tmm* in *R. pomeroyi* could involve *cis*-acting antisense RNA (asRNA). AsRNA is transcribed from the complementary strand of a gene, either within or partially within the coding region and can regulate gene expression by a variety of mechanisms (Thomason and Storz, 2010; Georg and Hess, 2011; Sesto et al., 2013). The anti-sense sequence of *tmm* was screened for the presence of any putative promoters that could signify the start of transcription on this strand. Using the same promoter prediction software as described in section 3.2.2.7, two putative promoter regions were detected (Figure 4.12). One was situated towards the 5' end of the sense strand (as*tmm*1) and another was situated in the middle of *tmm* (as*tmm*2). Primers were designed to target regions just upstream (5') of these putative promoters (on the antisense strand) to screen for the presence of any RNA transcripts when *R. pomeroyi* was grown under the conditions outlined in section 4.2.4.

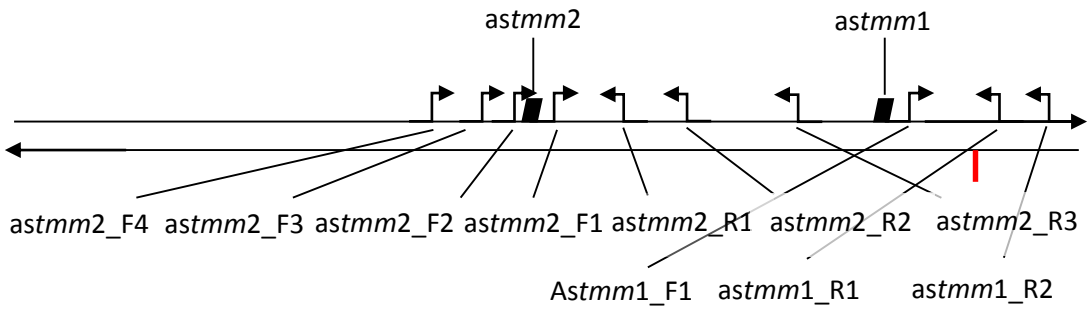

Figure 4.12. Region of DNA spanning *tmm* (complement strand on the bottom) showing the start codon in red. The putative promoter regions identified using the neural network software (see Chapter 3.2.2.7) are labeled as *astmm*1 and *astmm*2. Arrows denote primers designed to target the putative asRNA molecules located on the strand opposite to the sense strand of *tmm*.

RNA from *R. pomeroyi* cultures that were grown on glucose and NH_4^+ or glucose and NH_4^+ plus TMA were screened for the presence of any asRNA using the primers sets outlines in Figure 4.11. An initial screen showed that in the presence of TMA, there appeared to be an upregulation of asRNA. The product generated from cDNA generated using the reverse primer, *astmm2*_R2, targeting as*tmm2* showed the greatest level of upregulation, whilst there was less of an upregulation of as*tmm1* (Figure 4.13). There was no apparent difference in the transcription of the 16S rRNA gene between cultures. A low level of DNA Contamination was evident in all samples with higher levels detected for *tmm* assays, therefore new reagents were used for subsequent profiling of the asRNA molecules. Preliminary evidence suggested that *astmm*2 was upregulated, however as there was a low level of DNA contamination, these PCR assays were repeated, focusing on this putative RNA molecule. In all subsequent steps, to ensure that PCR products were obtained form cDNA alone, minus (-) reverse transcriptase (RT) controls were displayed on gels for a direct comparison.

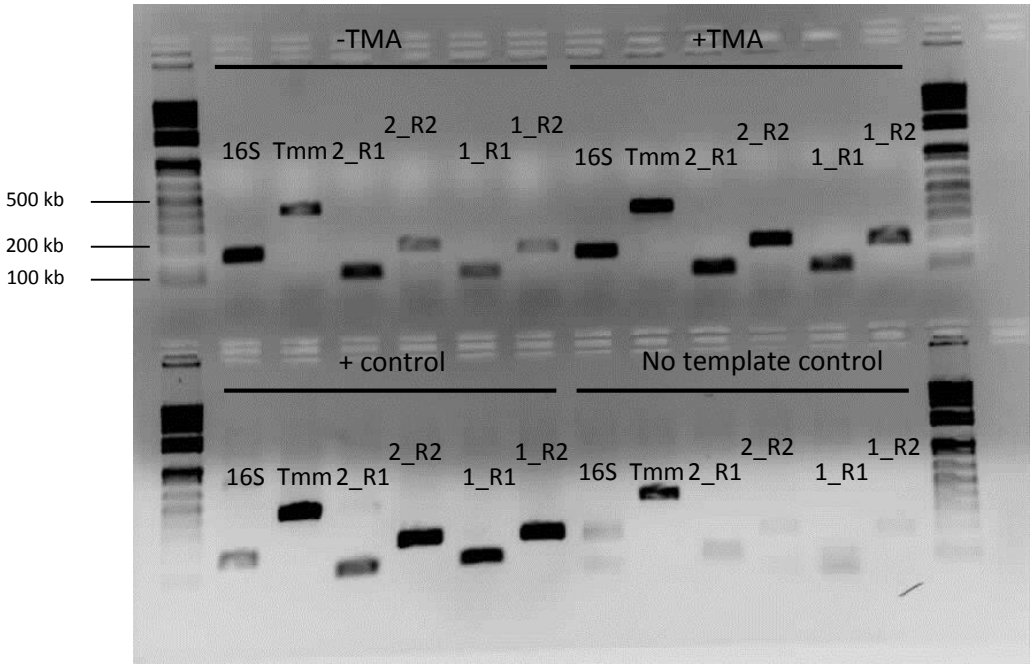

Figure 4.13. RT-PCR of the two asRNA molecules, *astmm1* and *astmm2* complementary to the sense strand of *tmm* of *R*. *pomeroyi*. *R*. *pomeroyi* was on grown glucose and NH_4^+ +/- TMA. 2_R1 represents *astmm2* amplified using the primers *astmm2*_F1/ R1. 2_R2 represents *astmm2* amplified using the primers *astmm2*_F1/R2. 1_R1 represents *astmm1* amplified using the primers, *astmm2*_F1/R1. 1_R2 represents *astmm1* amplified using the primers, *astmm1*_F1/R2.

The primer sets targeting as*tmm2* were used for further asRNA profiling using RNA extracted from duplicate cultures. Again, a clear upregulation of *astmm2* was observed for cultures grown in the presence of TMA (Figure 4.14A). To gain a better estimation of where the 3' end of the asRNA molecule was located, a different reverse primer, *astmm2*_R3, targeting a region 250 bp downstream on the anti-sense strand, was used to generate a cDNA library. The forward primer, *astmm2*_F1 was used for PCR. No product was amplified from cDNA libraries generated from RNA isolated from any growth conditions (Figure 4.14B). However, the DNA positive control did amplify a PCR product of the correct size (~450 bp). It can therefore be concluded that the 3'end of the asRNA lies somewhere between the reverse primers, *astmm*_R2 and *astmm*_R3.

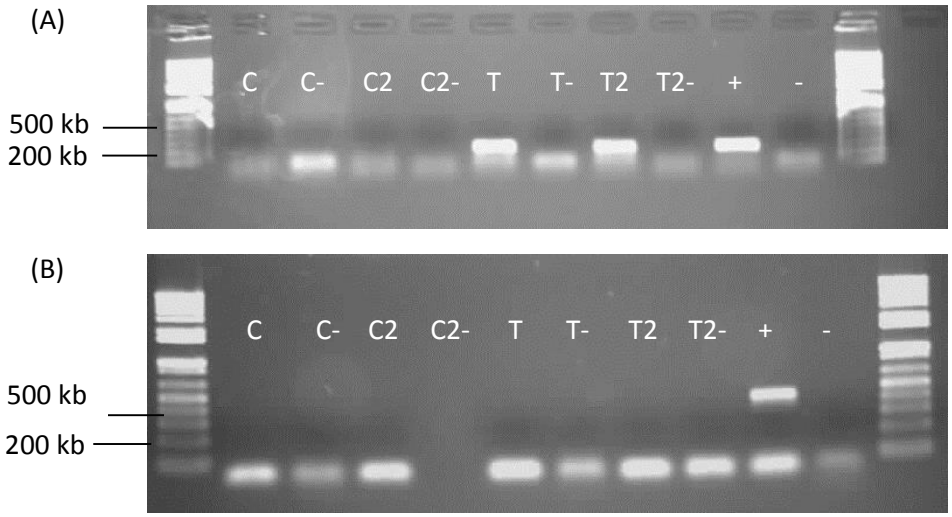

Figure 4.14. RT-PCR of the a*stmm*686. Amplification from cDNA libraries generated using the reverse primer, *astmm*_R2 **(A)**. Amplification from cDNA libraries generated using the reverse primer, *astmm*_R3 **(B)**. Abbreviations: C, control; T, +TMA. Lane 9, positive control using template DNA. Lane 10, negative no template control; (-) symbol denotes minus (-) reverse transcriptase controls. Results are produced from two biological replicates, indicated by the '2'.

To gain a better estimation of where the 5' end of the *astmm2* was located, the same procedure that was used to estimate the 3' end was applied. The same cDNA library that was previously generated using primer, *astmm2*_R1, was used as a template for PCR. Different forward primers, moving progressively upstream (generating a PCR product of 250, 300 and 400 bp) and going beyond the putative promoter region were designed. Only one replicate for +TMA-grown cells was used in this analysis. All primers combinations resulted in the greater amplification of a product in +TMA-grown cells compared to that of the -TMA-grown cells (Figure 4.15), confirming the upregulation of *astmm2* in the presence of TMA. A small amount of product was retrieved from –TMA-grown cells that wasn't present in either the –RT controls or the no template control suggesting that a low basal level of transcription of the asRNA strand may occur. As a PCR product was amplified

using the forward primer, *astmm2*_F4, the putative promoter that was predicted computationally may not be the true transcriptional start site for this *astmm2*.

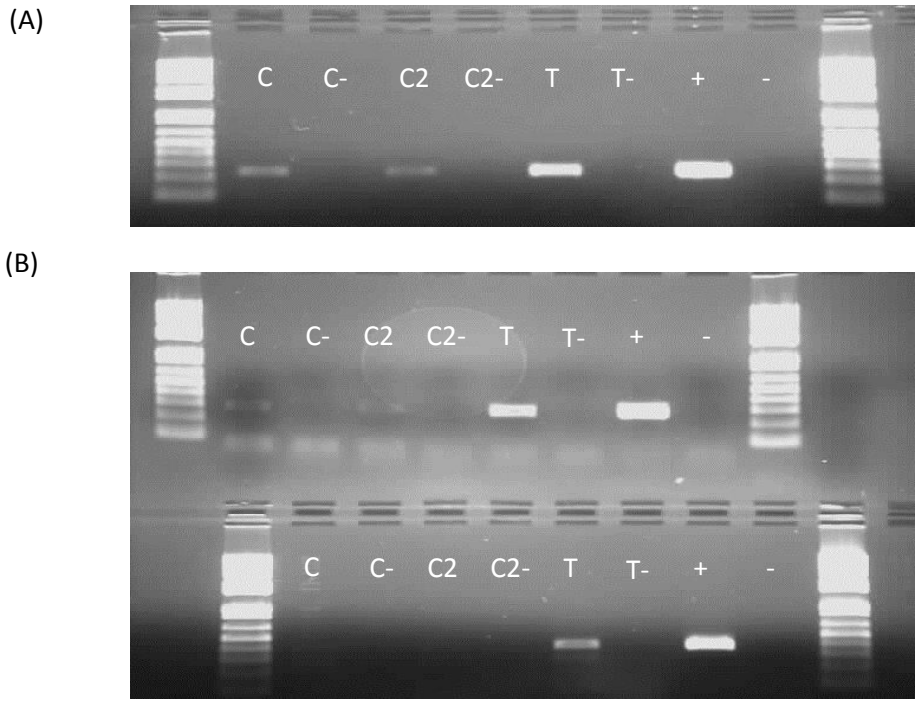

Figure 4.15. RT-PCR of the as*tmm2*. Amplification from cDNA libraries generated using the reverse primer, *astmm2*_R1 and the forward primer, *astmm2*_F2. (Middle gel) Amplification from cDNA libraries generated using the reverse primer *astmm2*_R1, and the forward primer, *astmm2*_F3 **(A)**. Amplification from cDNA libraries using the reverse primer, *astmm2*_R1 and the forward primer, *astmm2*_F4 **(B)**. Abbreviations: C, control; T, +TMA. Lane 8, positive control using template DNA. Lane 9, negative no template control. (-) symbol denotes minus (-) reverse transcriptase controls. Ladders are the same as in Figure 4.12. Results are from two biological replicates indicated by the '2'.

RNA extracted from cells grown under the conditions outlined in section 4.2.4 was screened for the presence of *astmm2*. This was achieved by generating a cDNA library using *astmm2*_R1. Amplification of the cDNA library was performed using the same reverse primer and either *astmm2*_F1 or *astmm2*_F2. The results presented in Figure 4.16 suggest that when *R. pomeroyi* was grown on TMA, TMAO or TMAO in the presence of DMS, there was upregulation of *astmm2*. The greatest amplification of *astmm2* was observed with RNA from TMA-grown

cultures. The RT-PCR results do not show a clear on/ off result, indicating that there may either be some other mechanism in place or that the balance between levels of sense strand and antisense strand results in translation of a functional Tmm.

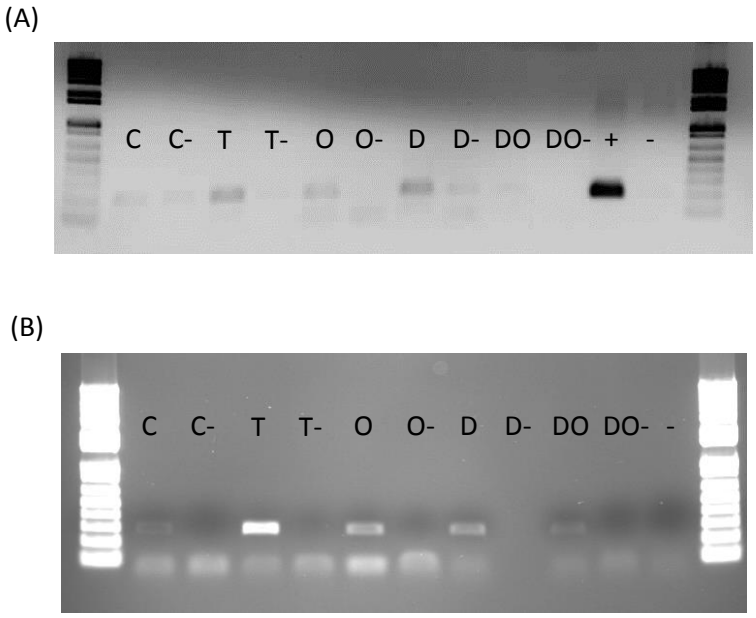

Figure 4.16. RT-PCR targeting *astmm2* using the primer sets *astmm2*_F1/R2 **(A)** or *astmm2*_F1/R2 **(B)**. Abbreviations: C, wild-type grown in glucose and NH_4; T, wild-type grown in glucose + TMA; O, wild-type grown in glucose + TMAO; D, wild-type grown in glucose + NH_4 + DMS; DO, wild-type grown in glucose + TMAO + DMS. – symbol denotes minus (–) RT controls.

4.2.9. Marker exchange mutagenesis of SPO1552, a periplasmic substrate binding protein from the HAAT family

SPO1552, annotated as a SBP from the HAAT family, is located adjacent to *tmm* in almost all MRC isolates. The same genetic arrangement is also found in a number of soil bacteria that possess *tmm* within their genomes, for example, a number of *Hyphomicrobium* spp. and *Aminobacter aminovorans* AM1 (Table 4.1). However, unlike the TMAO ABC transporter, this gene does not appear to be present in a number of marine bacteria, including members of the SAR11 clade, and it is

therefore unclear whether or not this gene has an essential role in the uptake of TMA.

Table 4.1. Comparative genomic analysis of TMA and TMAO catabolic and transport genes in a range of bacteria. +/- denotes presence/absence of genes in genomes.

Strain	Tmm	SPO1552-like	Tdm	TmoX
Ruegeria pomeroyi DSS-3	+	+	+	+
Roseovarius nubinhibens	+	+	+	+
Phaeobacter caeruleus	+	+	+	+
Roseobacter litoralis Och149	+	+	+	+
Roseobacter denitrificans Och114	+	+	+	+
Candidatus Pelagibacter ubique HTCC1062	+	-	+	+
Candidatus Pelagibacter sp. HTCC7211	+	-	+	+
Pelagibacteraceae sp. HIMB59	+	-	+	+
Paraccoccus sp. N5	+	+	+	-
Paracoccus sp. J4	+	+	+	-
Aminobacter aminovorans AM1	+	+	+	+

Abbreviations: Tmm, TMA monooxygenase; SPO1552-like, homologs of putative DMS transporter; Tdm, TMAO demethylase, TmoX, substrate binding protein specific for TMAO.

Again, marker exchange mutagenesis was performed in order to investigate whether this transporter has a role in TMA uptake in *R. pomeroyi*. The mutant, *ΔSpo1552::Gm* could still grow on all the MAs including TMA, TMAO, DMA, MMA as well as the quaternary amines, GBT, choline and carnitine. The results from this experiment reveal that this transporter is not essential for growth of *R.*

pomeroyi on MAs in *R. pomeroyi*, especially TMA or QAs. This is in line with the "patchy" distribution of this gene within TMA-utilising bacteria.

To determine if this transporter has a role in DMS metabolism, the mutant, *ΔSpo1552::Gm*, was then grown on glucose as a C source and TMA or TMAO as a sole N source in the presence of DMS. The experiment was also set up with wild-type cultures as a positive control. A clear reduction in the rate of DMS consumption could be observed for the mutant when grown on either TMA or TMAO as the sole N source, indicating that SPO1552 may encode a transporter that has a role in DMS uptake (Figure 4.17). Wild-type cells grown on TMA or TMAO completely degraded all DMS before 90 h. However, the mutant, *ΔSpo1552::Gm*, took 239 h to completely degrade all the DMS when grown on TMA and when grown on TMAO did not completely degrade all the DMS within the 239 h (Figure 4.17). The DNA sequence integrity of the mutant either side of the disrupted gene was checked by sequencing and no mutations had occurred, indicating that no possible effects of the mutagenesis were affecting flanking genes, *tmm* or *tmoR*.

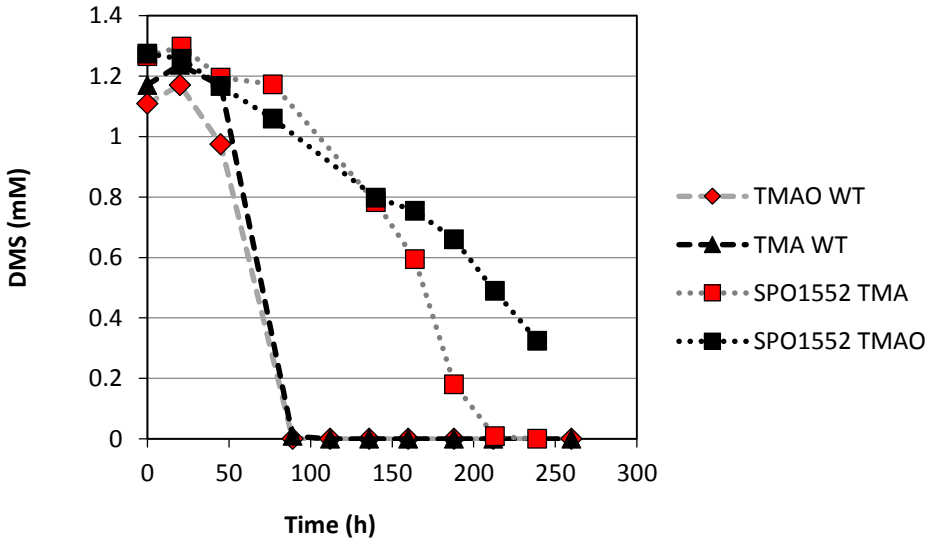

Figure 4.17. Oxidation of DMS during growth of *R. pomeroyi* wild-type and the mutant, *ΔSpo1552::Gm*, on TMA or TMAO (0.5 mM) as the sole N source. Cultures were grown in triplicate and error bars denote SD.

4.3. Discussion

4.3.1. Confirmation that *tmm* is essential for growth of *R. pomeroyi* on TMA

Results confirm that in *R. pomeroyi* DSS-3, Tmm is essential for growth on TMA. The TMA-TMAO pathway is the most dominant pathway (compared to the TMADH pathway, see section 1.6.2) in the marine environment (Chen et al., 2011) and may help to partially explain the detection of TMAO in the surface waters (Gibb and Hatton, 2004). However, in addition to the turnover of TMA, TMAO can enter the water column directly as a result of synthesis by larger eukaryotic marine biota (Treberg et al., 2006). The genome of *Methylophaga thiooxidans* DMS010 does not contain *tmm* but does contain a gene encoding the TMADH and it is known that this organism, or at least an isolate with >99% sequence identity (16S rRNA) can grow on TMA as a sole C and N source (Chapter 6). *Methylophaga* spp. do not form part of the dominant microbial community associated with marine surface waters (Janvier et al., 2003; Rusch et al., 2007), therefore although there may be other enzymes present in the marine environment that can degrade TMA, Tmm is likely to be the dominant enzyme governing this process.

4.3.2. Regulation of Tmm

The regulation of the Tmm is intriguing in the sense that DMS, a compound Tmm has a high affinity for, can also effect the transcription of *tmm*. The fact that DMS is only oxidised when *R. pomeroyi* is grown in the presence of MAs suggests that production of a functional Tmm is MA-dependent. Purified Tmm from SAR11 clade and MRC bacteria can oxidise DMS *in vitro* (Chen et al 2011), therefore it is unlikely that MA-dependent functionality of Tmm is controlled at the post-

translational level. SAR11 clade bacteria often use riboswitches to control the expression of certain enzymes (Tripp et al., 2009). Riboswitches are regions of the RNA transcript located in the 5' untranslated region of a transcript and are involved in regulating the translation of a given RNA transcript. This mechanism was proven to be important in the production of malate synthase, an enzyme linked to the glyoxylate cycle which is involved in central C metabolism, using a glycine-activated riboswitch (Tripp et al., 2009). In this model, a catabolite can interact with the RNA molecule and change the conformational secondary structure of the single-stranded RNA molecule, altering the accessibility of the ribosomal binding site (RBS). Further work has shown that in SAR11 clade bacteria, riboswitches are also involved in N regulation where a continual pool of RNA is produced but only a functional protein corresponding to the RNA transcript is synthesised under certain conditions (Smith et al., 2013). In this example, a putative ammonium exporter, AmtB, is found in the peptide pool during N-replete conditions but not under N-deplete conditions, whilst RNA transcripts of this gene are found in both conditions. However, the majority of the work presented in this chapter points towards a mechanism of post-transcriptional control regulated by the existence of asRNA. This mechanism is fundamentally different to the post-transcriptional regulation identified in SAR11 bacteria.

The role of asRNA in post-transcriptionally regulating gene expression has received a great deal of attention over the past years (Thomason and Storz, 2010; Georg and Hess, 2011). The rise of this field was aided by methods to accurately capture the transcriptional profiles of a given bacterium and to computationally predict regions where asRNA is likely to occur (Georg and Hess, 2011; Sesto et al., 2013). The identification of small RNA molecules and their potential biological functions has

now been experimentally proven in a number of bacterial isolates and at least 22% of the total number of genes in a given bacterium can have a complementary asRNA molecule, according to bioinformatics analyses (Thomason and Storz, 2010; Sesto et al., 2013). In *Synechocystis*, asRNA has a direct role on the longevity and ribosomal binding efficiency at the 5' untranslated region of the photosynthetic gene, *psbA2*, ultimately affecting the level of translation of *psbA* (Sakurai et al., 2012). As as*tmm1* is not upregulated to the same extent as as*tmm2*, the asRNA molecule associated with *tmm* may have a different role in stabilising the primary transcript. In *Prochlorococcus* sp. MED4, asRNA helps stabilise a primary transcript by reducing the level of 3' endonuclease activity associated with RNA degradation by blocking the RNase E recognition site on the single stranded RNA transcript (Stazic et al., 2011). This mode of action may be responsible for the observed phenotype in *R. pomeroyi* and the level of translation may result from the change in the number of asRNA molecules versus primary *tmm* transcripts present during growth.

4.4.3. Identification of a potential DMS transporter

The fact that a SBP is almost always found in association with Tmm within the genomes of a number of MRC isolates capable of TMA-dependent DMS oxidation suggested that this transporter may be involved in either TMA or DMS transport. The results shown here reveal that mutation of this transporter does not alter the ability of *R. pomeroyi* to utilise TMA although it cannot be ruled out that this transporter is a potential TMA transporter under *in situ* concentrations. However, for the mutant, the rate of DMS oxidation was significantly reduced compared to that of the wild-type, suggesting that impaired uptake of DMS into the cell may be

limiting this process. Mutation of *tmoX* (Chapter 3) also led to the reduction, but not complete blockage of TMAO degradation, indicating that TMAO could still be transported into the cell via another unspecified transport system. In these experiments in Chapter 3, although the number of cells remained low, TMAO degradation still occurred, leading to the gradual increase of growth of the TMAO transporter mutants. In the DMS oxidation experiments, the number of *ΔSpo1552::Gm* cells was substantially higher throughout the experiment than the number of *ΔtmoX::Gm* cells during its experiment (3.2.2.5). The higher number of *ΔSpo1552::Gm* results from the fact that DMS is not required for growth on glucose and NH_4^+ in *R. pomeroyi*. This higher number of *ΔSpo1552::Gm* cells in the DMS oxidation experiment may explain why the difference between DMS oxidation rates for the wild-type and *ΔSpo1552::Gm* is less than that observed for the TMAO transporter experiment. As this transporter is present in the genomes of MRC isolates, but not SAR11 clade bacteria, there is almost certainly another transporter involved in the uptake of TMA and potentially DMS.

4.3.4. Implications for DMS oxidation by TMA-utilising marine bacteria

Previous work has shown that DMS oxidation to DMSO can enhance chemoorganoheterotrophic growth in some marine bacteria (Boden et al., 2011a; Green et al., 2011). Unlike DMS dehydrogenase which can liberate two electrons through the oxidation of DMS to DMSO (McDevitt et al., 2002), Tmm does not result in any net gain of electrons or reducing equivalents. Indeed, Tmm actually uses a reducing equivalent, NADPH, and therefore is an energy consuming reaction. This begs the question ‘why do these bacteria possess an enzyme that shares a similar high affinity for two differing substrates?’ The FAD-binding site

of FMOs, has been likened to a 'cocked gun' often present in a reduced state within the cell awaiting a suitable substrate (Krueger and Williams, 2005). Mammalian FMOs produces both superoxide anion radicals and hydrogen peroxide through spontaneous NADPH oxidation in the absence of these substrates (Williams et al., 1985; Krueger and Williams, 2005). Indeed, in purified rabbit liver FMO, up to 41% of the total NADPH oxidised resulted in hydrogen peroxide production (Tynes et al., 1986). Co-oxidation of DMS by Tmm may therefore have a role in the prevention of free radical formation and subsequent oxidative stress when TMA stocks are depleted. Another explanation is that DMSO is potentially a more preferable antioxidant than DMS as it can accumulate to greater quantities within the cell (Simó et al. 2000). In a number of algal species, it has been observed that DMSO acts as a highly effective antioxidant (Lee and DeMora, 1999; Sunda et al., 2002; Riseman and DiTullio, 2004; Bucciarelli et al., 2013). Concentrations of particulate DMSO have been shown to be positively correlated with the dinoflagellates and prymesiophytes including the coccolithophore, *Emiliania huxleyi* (Simó et al., 1998; Lee and DeMora, 1999; Simó et al., 2000; Hatton and Wilson, 2007). The authors from these studies hypothesised that the primary source of DMSO production is through the oxidation of DMS with reactive oxygen species (ROS), however, at least for *E. huxleyi*, a *tmm*-homolog is present within its genome and may facilitate the production of DMSO.

Bacteria of the MRC are frequently associated with phytoplankton blooms and often represents a major proportion of the active microbial community involved in the turnover of algal-derived organic matter, including DMSP (González et al., 2000; Zubkov et al., 2001; Vila et al., 2004; Buchan et al., 2005; Alonso and Pernthaler, 2006). It is known that bacterial consumption of DMS leads to the

formation of DMSO during phytoplankton blooms and in productive oceanic regions (Hatton et al., 1998; Mikhail et al., 2004; Hatton and Wilson, 2007). Recent data from station L4 showed that during periods of high primary production, concentrations of TMA showed a transient increase (C. Cree, personal communications), suggesting that DMS and TMA coexist together in the surface seawater. This indicates that DMS and TMA coexist together in the surface seawater and suggests that TMA may well be present concurrently with DMS during periods of elevated primary production. It is therefore predicted that co-oxidation by TMA-utilising bacteria could be responsible for the observed conversion of DMS to DMSO in these productive surface waters and this hypothesis needs to be investigated further. The link between MAs and reduced sulfur compounds may also be important in the loss of DMS from coral beds, where stressed coral produce large amounts of DMSP in response to thermal stress (Raina et al., 2013). The microbial community associated with corals is often dominated by the MRC and this clade may present an efficient sink for DMS if MAs are present to induce Tmm (Lema et al., 2014).

Chapter 5

Trimethylamine and trimethylamine *N*-oxide are supplementary energy sources for *R. pomeroyi*

5.1. Introduction

Bacterioplankton in the Sargasso Sea have been shown to fully oxidise the methyl groups from a range of methylated compounds, including TMA and TMAO, to CO_2 (Sun et al., 2011). Using *C*. Pelagibacter ubique HTCC1062, a representative of the SAR11 clade, the same authors also showed that incubations with TMAO and MMA led to an increase in cellular ATP levels in C and energy starved cells (Sun et al., 2011). In addition, TMAO oxidation has been shown to increase both the growth rate and growth yield of the methylotrophic betaproteobacterium, *Methylophilus* sp. HTCC2181 when it was grown on methanol as a sole C and energy source (Halsey et al., 2012). In this study the authors confirmed that a greater proportion of the C from methanol was assimilated into biomass instead of dissimilated to generate reducing power as the oxidation of TMAO could help satisfy cellular energy budgets (Halsey et al., 2012).

The growth rate and growth yield of *R*. *pomeroyi* has been shown to be enhanced by the oxidation of thiosulfate when *R*. *pomeroyi* was grown on an organic C substrate (Moran et al., 2004). As *R*. *pomeroyi* cannot grow on TMA as a sole C and energy source, this bacterium is the ideal candidate to test the hypothesis that TMA and TMAO can also act as supplementary energy sources for marine non-methylotrophic bacteria capable of growing on MAs as a sole N source.

The aim of this Chapter was to confirm that TMA and TMAO are supplementary energy sources for *R*. *pomeroyi* and what the ecophysiological implications of TMA or TMAO metabolism are. The mutant strains generated in the previous two Chapters were used to confirm that all of the physiological phenotypes identified are down to metabolism of either TMA or TMAO. The work described in this

chapter also aimed to identify the pathway for energy production in *R. pomeroyi*, which is predicted to be the H_4F-linked oxidation pathway (see Chapter 1, section 1.9), by generating mutants targeting the gene (*fhs*) encoding formyl-H_4F synthetase (Fhs). In addition, experiments were designed to determine whether *R. pomeroyi* releases NH_4^+ during the catabolism of TMA or TMAO and if this NH_4^+ could be subsequently utilised by another bacterium.

5.2. Specific experimental design

5.2.1. Co-catabolism of TMA and TMAO with glucose and NH_4^+

For the wild-type, and the mutants, *Δtmm::Gm* and *Δtdm::Gm* (Chapters 4 and 3), starter cultures were incubated for 24 h with glucose (10mM) and NH_4^+ prior to inoculation (5 % v/v) into triplicate cultures with glucose (10 mM) and NH_4^+ plus or minus TMA or TMAO (5 mM). Growth and MA consumption were quantified throughout the experiment (see section 2.5.3).

5.2.2. Relationship between trimethylamine concentration, growth yield and growth rate in *R. pomeroyi*

As the enzyme system responsible for TMA catabolism is inducible, starter cultures were set up using wild-type cells grown on glucose and NH_4^+ as before but this time with TMA added (0.25 mM). This was to reduce any lag phase associated with the induction of the enzymes required for catabolism of TMA. Differing concentrations of TMA (0.5, 1, 2, 3 mM) were added to cultures in triplicate and the growth of the cultures was recorded.

5.2.3. Effect of MAs on the survival of *R. pomeroyi* during carbon starvation experiment and quantification of intracellular ATP

R. pomeroyi wild-type and the mutants *Δtmm::Gm* and *Δtdm::Gm*, were grown to mid-late exponential phase (OD_{540} ~1) prior to resuspension in fresh medium with no exogenous C source. Cell suspensions were aliquoted (0.5 ml) into 2 ml microcentrifuge tubes (adapted from Sun et al., 2011) and incubated overnight on a rotary shaker (140 rpm) at 30ºC. TMA or TMAO (1 mM) was added to cultures. After overnight incubations a further spike of TMA or TMAO (1 mM) was added to cultures and incubated for a further 2 h prior to harvesting via centrifugation (8,000 x g for 5 min) for quantification of cellular ATP (see Chapter 2.).

5.3. Results

5.3.1. TMA and TMAO are co-catabolised with an organic substrate

R. pomeroyi oxidised TMA and TMAO in the presence of both glucose and NH_4^+ (Figure 5.1A). The rate of TMA and TMAO oxidation was greatest through exponential growth but did continue throughout stationary phase when glucose was exhausted from the medium (data not shown). TMA oxidation by wild-type cells resulted in a greater OD_{540} (2.91 ± 0.05) (Figure 5.1a) compared to the mutant, *Δtmm::Gm* (OD_{540} =2.063 ± 0.06), which was unable to catabolise TMA (Chapter 3). TMAO oxidation in wild-type cells (Figure 5.1b) also led to a greater OD_{540} (2.46± 0.02) compared to the mutant, *Δtdm::Gm* (OD_{540} = 1.94± 0.07), which cannot oxidise TMAO (Chapter 3). TMA oxidation to TMAO could still function in the *Δtdm::Gm* mutant, resulting in the accumulation of extracellular TMAO in the medium (Figure 5.1c). Together, these results suggest that in *R. pomeroyi*, TMA

or TMAO oxidation may help stimulate its growth when grown on glucose. However, as OD_{540} is a crude measure of growth, further experiments were conducted in order to fully investigate the effect of TMA or TMAO oxidation on the growth of *R. pomeroyi*.

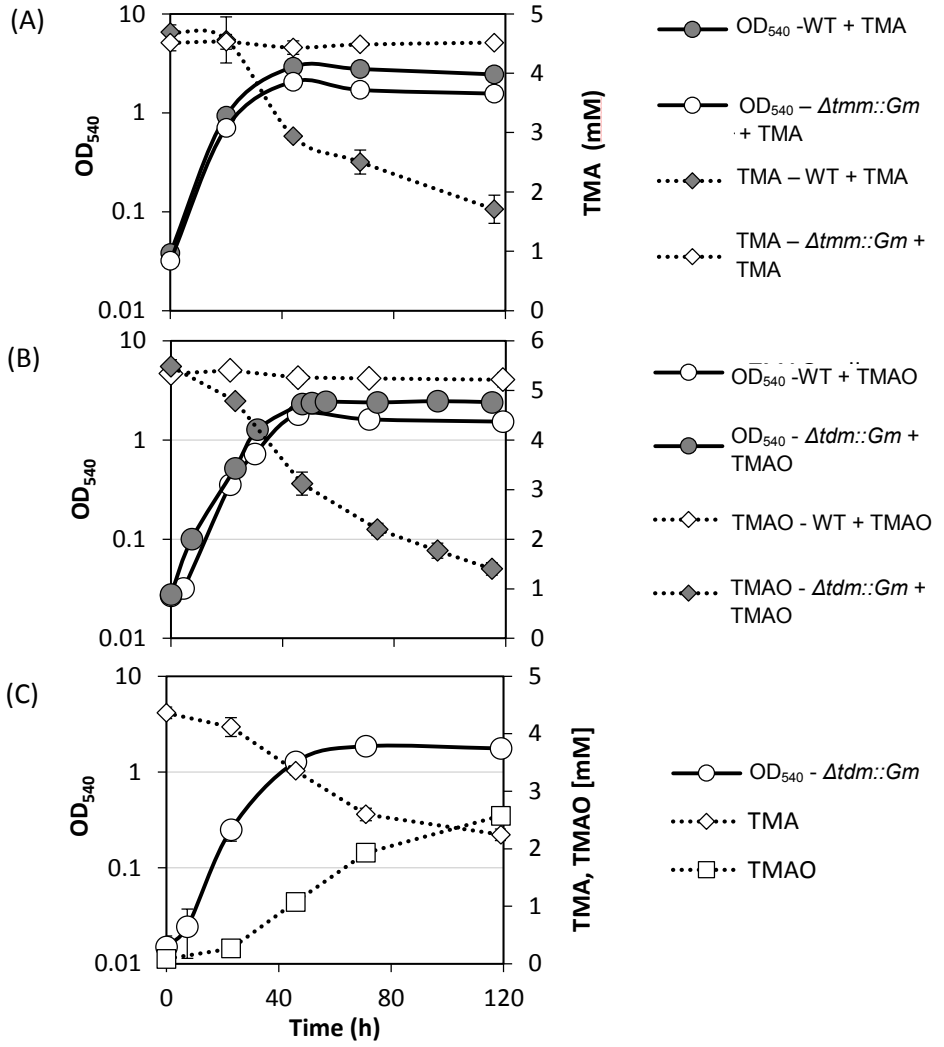

Figure 5.1. (A) Catabolism of TMA during growth of *R. pomeroyi* wild-type (grey circles) and the *Δtmm::Gm* mutant (white circles) on glucose and NH_4^+. TMA in the culture medium was quantified throughout growth for both wild-type (grey diamonds) and the mutant (white diamonds). **(B)** Catabolism of TMAO during growth of *R. pomeroyi* wild type (grey circles) and the *Δtdm::Gm* mutant (white circles) on glucose and NH_4^+. TMAO in the culture medium was quantified throughout growth for both wild type (grey diamonds) and the mutant (white diamonds). **(C)** Catabolism of TMA (white diamonds) and subsequent build-up of TMAO (white squares) during growth of the *Δtdm::Gm* mutant (white circles) on glucose and NH_4^+. Cultures were grown in triplicate and error bars denote SD.

5.3.2. Catabolism of TMA and TMAO results in higher growth yields of *R. pomeroyi* during chemoheterotrophic growth on glucose

An initial screen was conducted using a plate assay method whereby *R. pomeroyi* was grown on glucose-deplete MAMS plates with or without TMA (3 mM). Colonies grew larger in the presence of TMA, suggesting a greater proportion of the glucose was assimilated into biomass (Figure 5.2).

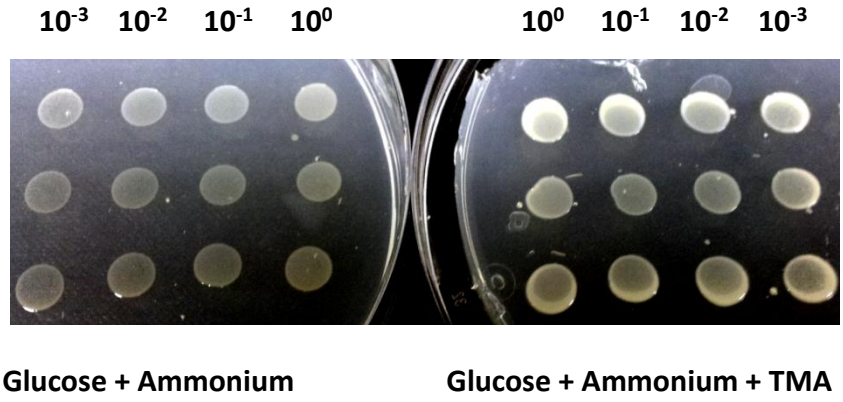

Figure 5.2 Growth of *R. pomeroyi* on glucose-deplete solid medium either plus (right-hand side) or minus (left-hand side) TMA (3 mM). 20 µl aliquots from a serial dilution (10^0 to 10^{-3} fold dilutions) were spotted onto plates and incubated for 10 days at room temperature. Colonies were more dense on plates containing TMA as a supplementary energy source.

To quantify the enhanced growth yield due to the addition of either TMA or TMAO, the dry weight (dw) of *R. pomeroyi* wild-type and the mutants was calibrated to the OD_{540}. Cultures were grown until late-exponential phase. There was no significant difference in the dw (mg l^{-1}) and OD_{540} for cultures grown on either glucose and NH_4^+ or glucose and NH_4^+ plus TMA. In both instances an OD_{540} =1 equated 254 mg dw ml^{-1} (Figure 5.3). *R. pomeroyi* was grown in batch culture under glucose-deplete conditions and either supplemented with or without TMA (5 mM) or TMAO (5 mM). Wild-type cells grown on glucose alone reached a final biomass of 504 ± 14.3 mg dw l^{-1} (Figure 5.4) and when supplemented with either TMA or

TMAO, a final biomass of 616 ± 8.9 mg dw l^{-1} (+22%) and 626 ± 12.6 mg dw l^{-1} (+24%), respectively, was achieved. The *Δtmm::Gm* mutant, which cannot catabolise TMA, had no increase in final biomass (519 ± 21.4 mg dw l^{-1}) compared to the glucose-only cultures (534 ± 14.3 mg dw l^{-1}). However, when *Δtmm::Gm* was supplemented with TMAO, the final biomass was 664 ± 13.3 mg dw l^{-1} (+24%) (Figure 5.4). Supplementing the *Δtdm::Gm* mutant with either TMA or TMAO did not result in any increase in final biomass (glucose =489 ± 14.5; +TMA = 453 ± 20.6; +TMAO = 487 ± 31.7 mg dry wt l^{-1}). When wild-type *R. pomeroyi* cells were grown in a glucose-limited chemostat (dilution rate = 0.05 h^{-1}), a 30.4% increase in growth yield was observed when supplemented with TMA (5 mM) whilst the growth yield of the mutant, *Δtmm::Gm,* did not change (Table 5.1).

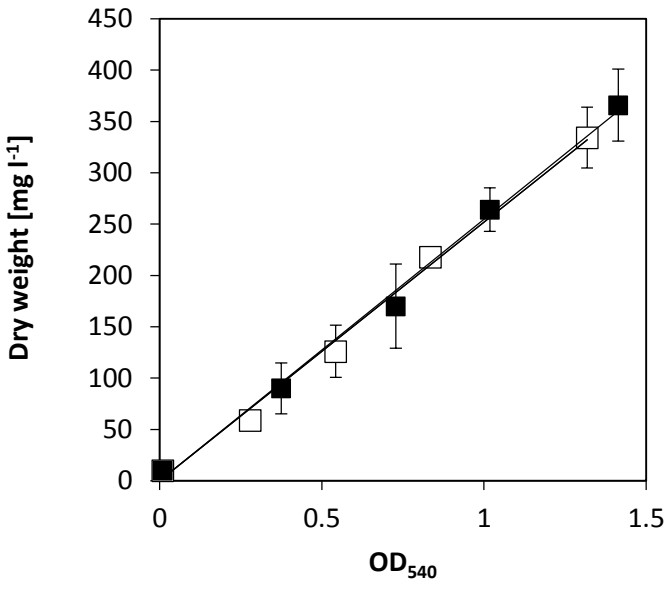

Figure 5.3. Dry weight of *R. pomeroyi* grown on glucose and NH_4^+ either plus (black squares) or minus (white squares) trimethylamine (TMA) plotted against OD_{540}. Cultures were collected on 0.22 μm filter pads and dried to a constant weight. Filters were washed with 10 ml dH_2O to remove any salts. Each point represents the mean of triplicate determinations and error bars denote SD.

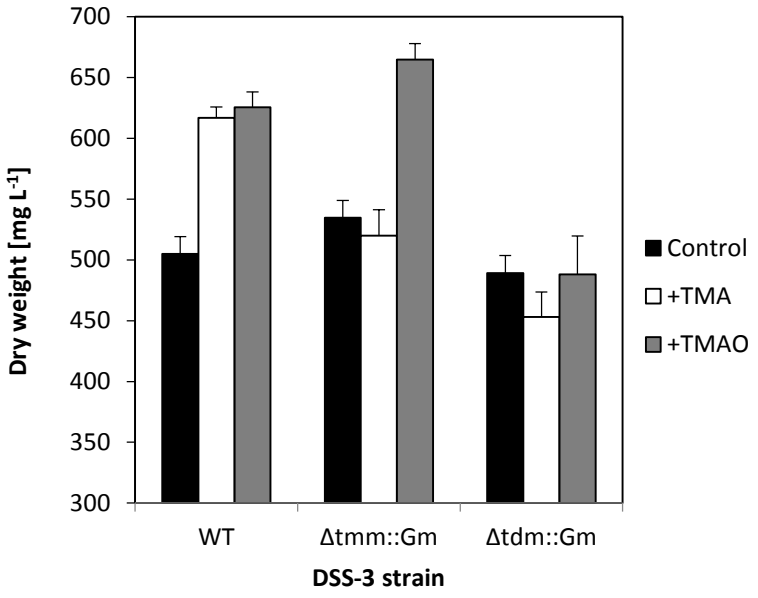

Figure 5.4 Final growth yields of *R*. *pomeroyi* wild-type and mutant strains, *Δtmm::Gm* and *Δtdm::Gm*, grown on glucose and NH_4^+ (black bars) and supplemented with either 5 mM TMA (white bars) or 5 mM TMAO (grey bars). Results presented are the mean of triplicate cultures and error bars denote SD.

Table 5.1. Growth yields of *R*. *pomeroyi* grown in continuous chemostat cultures.

Strain	g dry biomass per mol glucose	g dry biomass per mol carbon	Difference with TMA (%)	TMA conc. remaining (mM)
Wild-type				
-TMA	48.77	8.13	-	-
+TMA	63.61	10.60	30.4	2.2
Δtmm::Gm				
-TMA	48.42	8.07	-	-
+TMA	48.08	8.01	-	5

Abbreviations: *Δtmm::Gm,* wild-type with disrupted TMA monooxygenase

5.3.3. Response of glucose-grown *R. pomeroyi* cells to incremental increases in TMA

To determine whether TMA led to an increase in the growth rate as well as growth yield of *R. pomeroyi*, the bacterium was grown on incremental concentrations of TMA in the culture medium (0, 0.5, 1, 2, 3 mM). Unlike the previous experiments, the starter culture was grown in the presence of TMA to induce all the biochemical machinery required to fully catabolise TMA to CO_2 and NH_4^+ (see section 5.2.2). A positive correlation was observed between specific growth rate and the concentration of TMA, where the specific growth rate increased from 0.061 ± 0.002 (h^{-1}) for cells incubated with no TMA to 0.087 ± 0.003 (h^{-1}) for cells incubated with 3 mM TMA (Figure 5.5A). Likewise, the final growth yield increased from 484 ± 10.39 (no TMA) up to 600 ± 8.79 (3 mM TMA) (Figure 5.5B). Using intermediate concentrations of TMA (0.5-1 mM) resulted in an intermediate increase in growth rates and growth yields compared to glucose-only cultures. This experiment further confirms that TMA catabolism can partially fulfill the energetic demands of the cell allowing a greater proportion of glucose to be incorporated into biomass. Together, these data confirm that oxidation of MAs can enhance chemoorganoheterotrophic growth on glucose in *R. pomeroyi*.

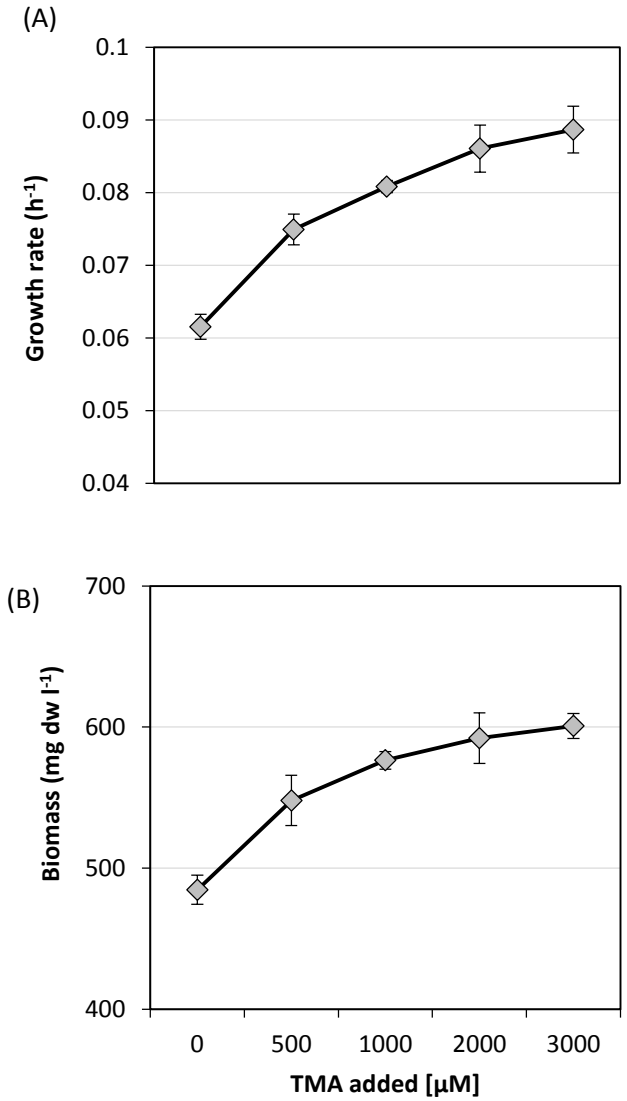

Figure 5.5. Comparison of the specific growth rates **(A)** and final growth yields **(B)** of the wild-type *R*. *pomeroyi* grown on glucose and NH_4^+ when supplemented with increasing concentrations of TMA, using a starting inoculum that was pre-incubated with TMA (24 h). Error bars denote SD. Results presented are the mean of triplicate cultures.

A synergistic effect in the enhancement of heterotrophic growth was also observed when *R*. *pomeroyi* was incubated with two exogenous energy sources (TMA + thiosulfate). During these incubations low concentrations of glucose (100 µM) were stochastically spiked (a total of four times) into the medium every 24-48 h (400 µM total C). Cells incubated without a supplementary energy source (TMA or thiosulfate) reached a final growth yield of 31.7 ± 1.5 mg dw l^{-1} (Figure 5.6). Cells

incubated with either TMA or thiosulfate alone reached a final growth yield of 42.2 ± 4.7 and 44.3 ± 5.4 mg dw ml^{-1}, respectively. Cells incubated with both TMA and thiosulfate reached a final growth yield of 70.8 ± 4.9 mg dw ml^{-1}, which equated to over a 2-fold increase in biomass.

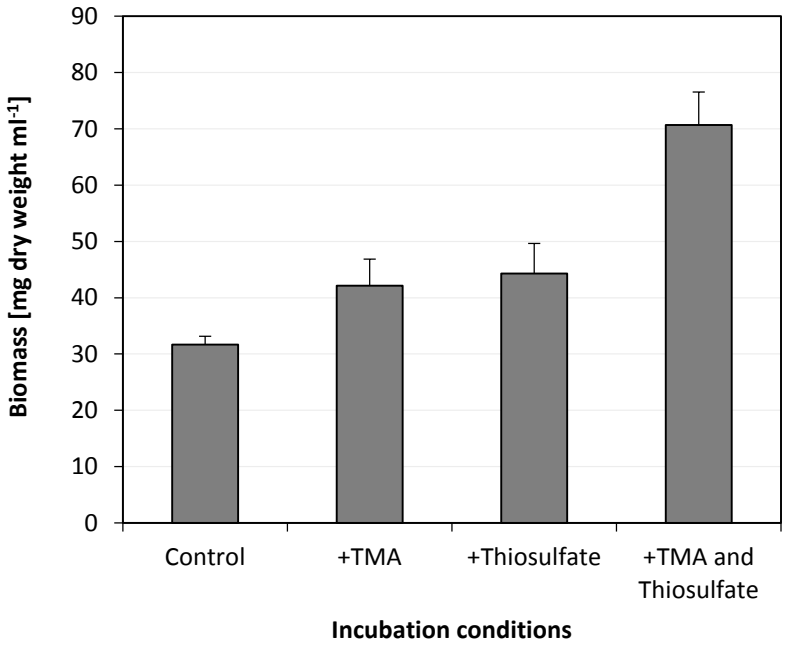

Figure 5.6. The final growth yield of *R. pomeroyi* after 7 days during which four separate additions of glucose (100 μM) were spiked into the medium every 24-48 h (400 μM C total). Cultures were incubated with TMA (2 mM) or thiosulfate (2 mM) or both and the same concentrations were added every 48 h. Error bars denote SD. Results presented are the mean of triplicate cultures.

5.3.4. The effects of TMA supplementation on a closely-related *Roseobacter* isolate, *Citreicella* sp. SE45

Citreicella sp. SE45, isolated from a US salt marsh (Gifford et al., 2013), is another member of the MRC and can also grow on TMA as a sole N source, but not as a sole C source (Chen 2012). Saltmarshes are typified by having high concentrations of MAs, including TMA, derived from the anaerobic degradation of compatible osmolytes such as GBT (King, 1984). Therefore, one would expect that *Citreicella* sp. SE45 should be able to take advantage of the presence of TMA in this environment. When this bacterium was grown using glucose-deplete MAMS medium, the addition of TMA led to an increase in final growth yield (Figure 5.7), thus demonstrating that the catabolism of TMA can also enhance chemoorganoheterotrophic growth of another closely related bacterium.

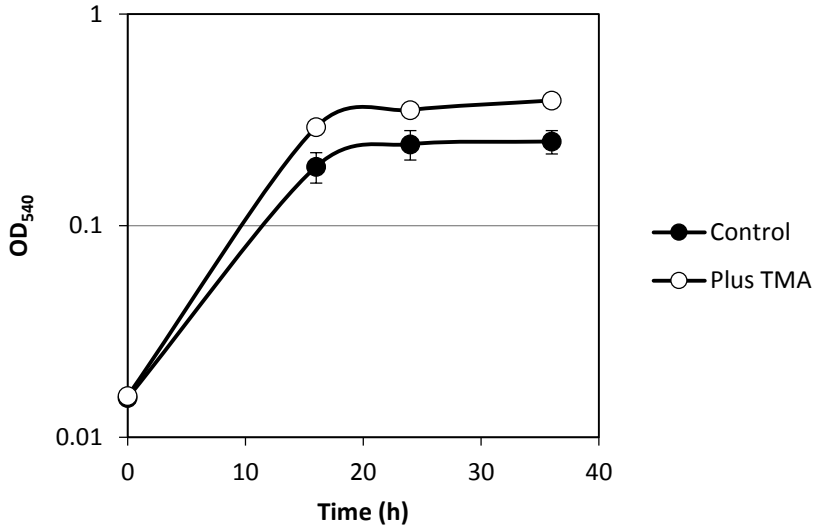

Figure 5.7. *Citreicella* sp. SE45 grown in glucose-deplete medium plus (white circles) or minus (back circles) TMA (3 mM). The presence of TMA resulted in an increase in final growth yield. Each point represents the mean of triplicate cultures and error bars denote SD.

5.3.5. Catabolism of TMA and TMAO results in ATP production which increases cell survival through periods of carbon starvation

R. pomeroyi was grown on TMA as a sole N source to induce the enzymes involved in MA catabolism, e.g. Tmm, Tdm and GmaS (Figure 5.12), prior to re-suspension in a fresh minimal medium with no C or energy source. Cells were either supplemented with TMA or TMAO or had no exogenous energy source (control). Both TMA and TMAO were rapidly catabolised over 8 days, although the rate of TMAO catabolism slowed during the final two days (Figure 5.8A). The rate of TMA and TMAO oxidation in this experiment was a lot higher than in the initial batch experiment when cells entered stationary phase. This may be due to the possible build-up of toxic metabolites or reduction in essential nutrients which may affect the rate of MA oxidation. At the start of energy starvation, the number of viable cells in all cultures was 4.0×10^9 cells ml^{-1} (Figure 5.8B). After 4 days, the number of viable cells incubated in the control cultures dropped to 7.4×10^8 cells ml^{-1}, whilst the cell numbers were 2.2×10^9 cells ml^{-1} in the presence of TMAO and 1.1×10^9 cells ml^{-1} in the presence of TMA, respectively. After 8 days, the number of viable cells from cultures with no exogenous C dropped to 2.9×10^7 cells ml^{-1} whilst +TMAO and +TMA cultures had 9.0×10^8 ml^{-1} and 7.5×10^8 cells ml^{-1}, respectively. In summary, the number of viable cells surviving periods of energy starvation was an order of magnitude greater when cells were incubated with either TMA or TMAO.

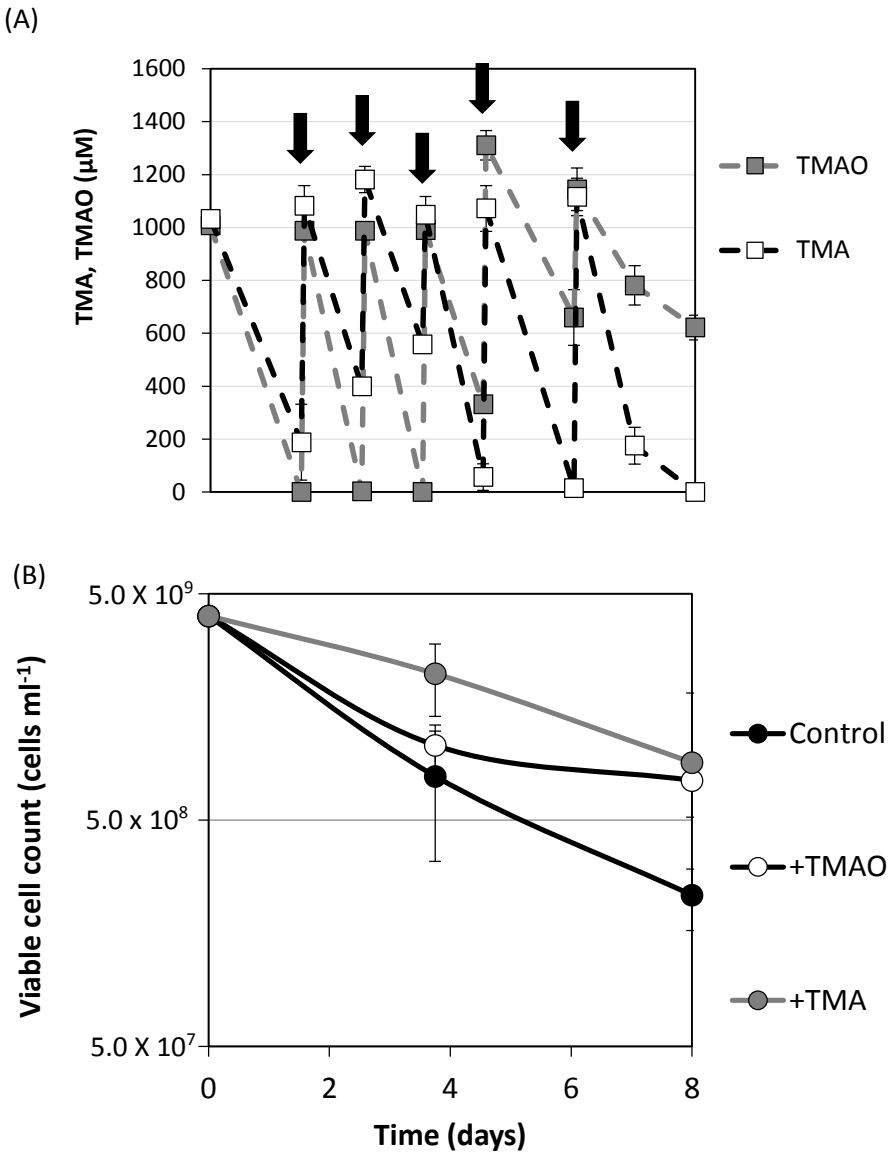

Figure 5.8. **(A)** Quantification of TMA (white squares) and TMAO (grey squares) during incubations with energy-starved *R*. *pomeroyi* cells. **(B)** Quantification of viable cells in C and energy-starved *R*. *pomeroyi* cultures incubated with either no exogenous C (black circles), TMA (white circles) or TMAO (grey circles). Error bars denote SD. Results presented are the mean of triplicate cultures. Arrows indicate additions of either TMA or TMAO.

To confirm that cells could indeed generate ATP from the oxidation of MAs, cells were energy- starved overnight prior to the addition of either TMA (1 mM) or TMAO (1 mM) and incubated for a further 2 h. Wild-type cells incubated with

either TMA or TMAO had 93.6 ± 4.2 and 92.1 ± 7.8 zeptomoles ATP cell^{-1}, respectively (Figure 5.9) whilst the intracellular concentration of ATP (see section 2.5.2) was lower for cells in the no substrate control (58.3 ± 9.7 zeptomoles ATP cell^{-1}). Incubating the mutant, *Δtmm::Gm*, with TMA resulted in no increase in intracellular ATP (54 ± 5.3 zeptomoles ATP cell^{-1}) compared to the no substrate control (52.2 ± 8.1 zeptomoles ATP cell^{-1}), whilst incubation with TMAO did result in an increase in intracellular ATP (80.7 ± 4.9 zeptomoles ATP cell^{-1}). As expected, incubation with TMA or TMAO did not result in an increase of intracellular ATP concentrations for the *Δtdm::Gm* mutant (control = 56.4 ± 3.4; TMA = 55.7 ± 2.1; TMAO = 56.1 ± 2.2 zeptomoles ATP cell^{-1}).

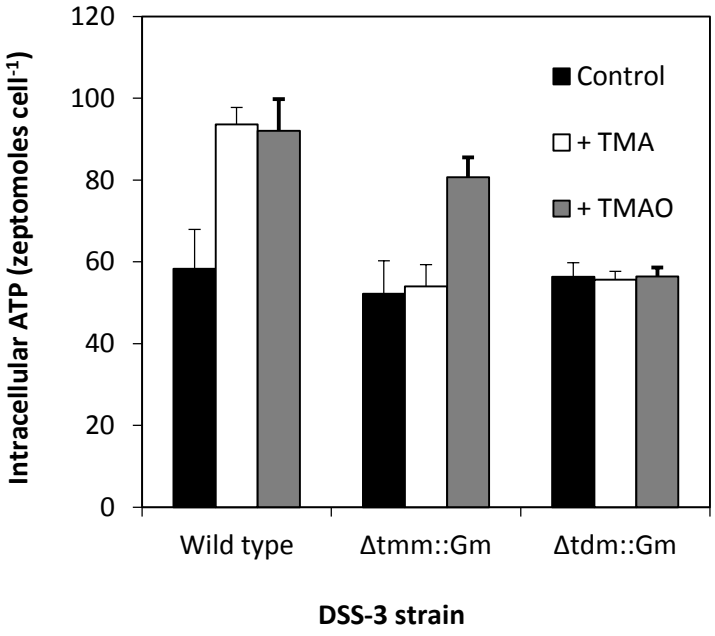

Figure 5.9. Quantification of intracellular ATP concentrations from *R. pomeroyi* cultures energy-starved for 18 h prior to incubation for a further 2 h with either 1 mM TMA (white bars), 1 mM TMAO (grey bars) or no exogenous C source (black bars). Error bars denote SD. Results presented are the mean of triplicate cultures.

5.3.6. The turnover of TMA and TMAO releases NH_4^+ which can cross-feed into another marine bacterium

As *R*. *pomeroyi* can metabolise MAs in order to produce reducing equivalents and ATP, it is hypothesised that the amine group would undergo remineralisation to NH_4^+. This NH_4^+ may subsequently be released from cells and could provide a source of N for other marine microorganisms (Figure. 5.10). To test this hypothesis, we designed a co-culture experiment with *R*. *pomeroyi* and the methylotrophic bacterium, *M*. *methanica* (Boden et al, 2011a). This bacterium can grow on methane or methanol as a sole C source, but cannot use TMA as either a C or N source.

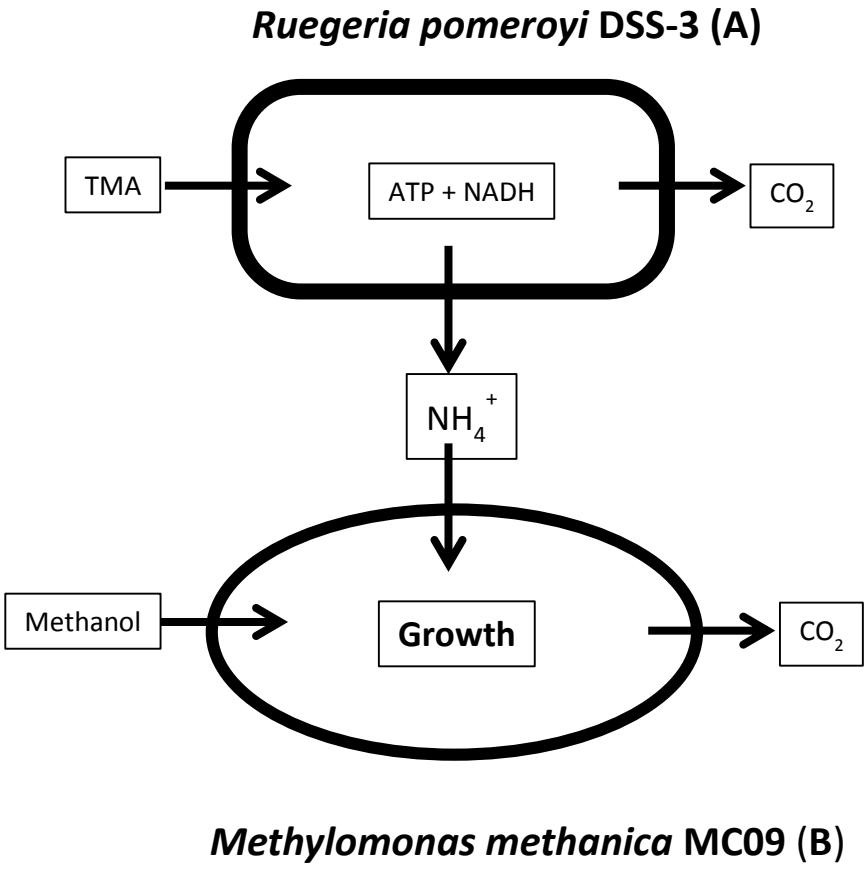

Figure 5.10. Schematic diagram of the flow of N in a co-culture system involving *R*. *pomeroyi* and *Methylomonas methanica* MC09. NH_4^+ liberated from the catabolism of TMA can be used by another bacterium to support its growth.

A C-starved and N-starved *R. pomeroyi* culture (~10^8 cells ml^{-1}) was inoculated with *M. methanica* (~10^7 cells ml^{-1}) and supplied methanol (1 mM) as the only C source in the system as methanol is only utilised by *M. methanica*. Cultures were either supplemented with NH_4Cl (1 mM) or TMA (1 mM) prior to incubation. Incubation of wild-type *R. pomeroyi* with methanol and TMA resulted in no growth whilst TMA was depleted from the medium (similar to section 5.3.5). Addition of NH_4Cl resulted in growth of *M. methanica* when incubated with either wild-type (3.9×10^8 cells ml^{-1}) or the *Δtmm::Gm* mutant (3.3×10^8 cells ml^{-1}) confirming that *R. pomeroyi* does not inhibit growth of *M. methanica* (Figure 5.11). Wild-type cells of *R. pomeroyi* depleted TMA from the medium, resulting in growth of *M. methanica* (2.6×10^8 cells ml^{-1}). However, no growth of *M. methanica* occurred (2.8×10^7 cells ml^{-1}) during incubations with the *Δtmm::Gm* mutant of *R. pomeroyi*, as a consequence of no TMA degradation during the 9 day incubation period (Figure 5.11). These data provide clear evidence that NH_4^+ released during the catabolism of TMA is cross-fed into another bacterium.

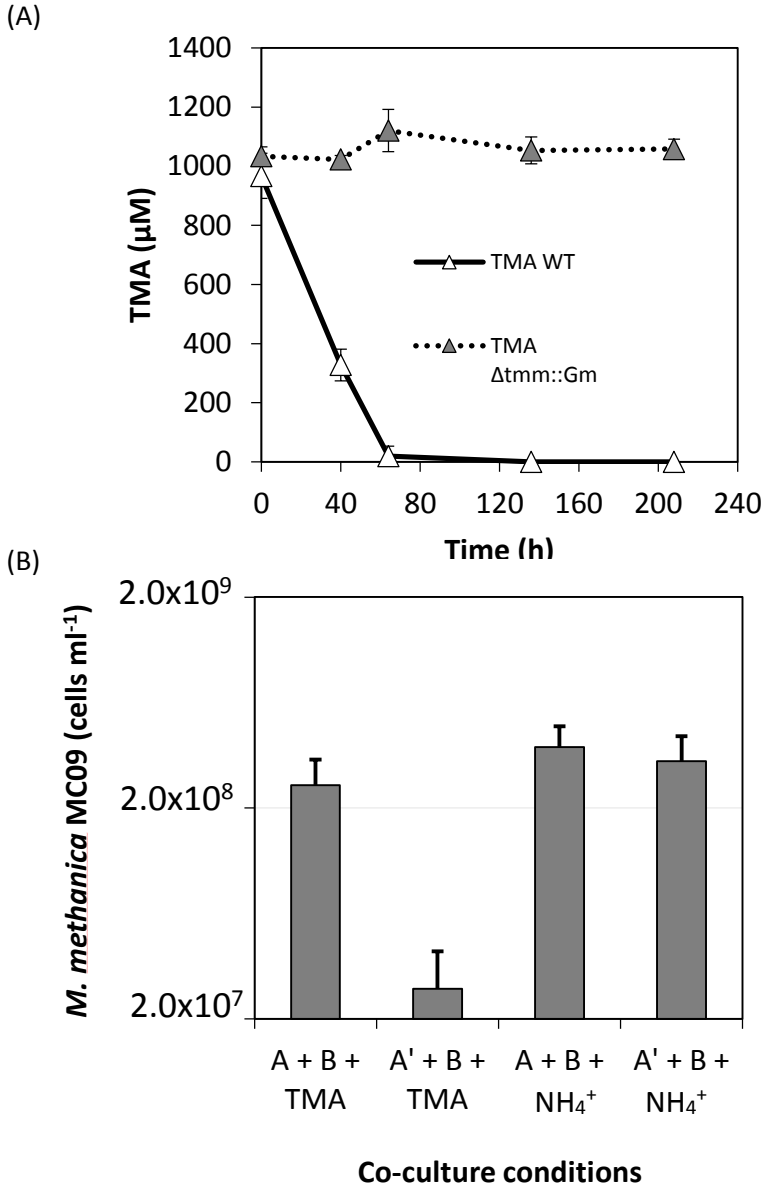

Figure 5.11. **(A)** The cell count of *Methylomonas methanica* MC09 after incubation for 9 days with either *R*. *pomeroyi* wild-type (A) or *Δtmm::Gm* mutant (A') and supplemented with either NH_4^+ (1 mM) or TMA (1 mM). **(B)** Quantification of TMA during incubation with wild-type (white triangles) or *Δtmm::Gm* mutant (grey triangles). Error bars denote SD. Results presented are the mean of triplicate cultures.

5.3.7 The role of the H_4F-linked pathway in TMA and TMAO oxidation to CO_2

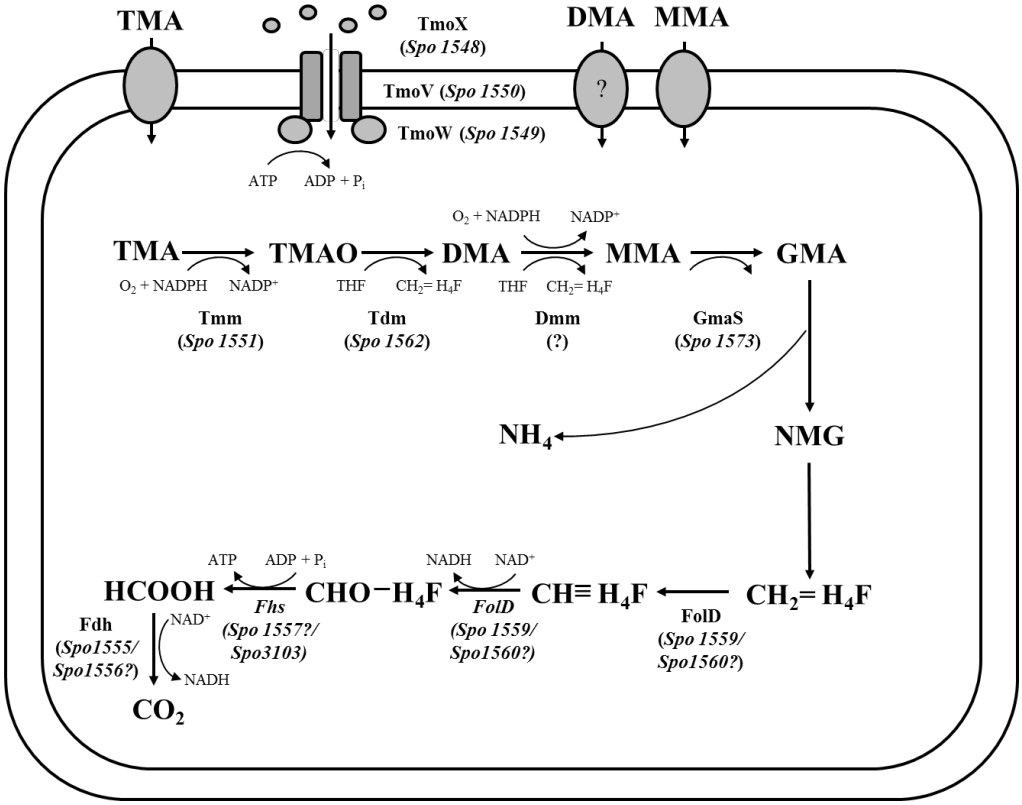

Figure 5.12. The proposed pathway of TMA metabolism in isolates related to the marine *Roseobacter* clade based on the model marine bacterium, *Ruegeria pomeroyi* DSS-3. Abbreviations; TMA, trimethylamine; TMAO, trimethylamine *N*-oxide; DMA, dimethylamine; MMA, monomethylamine; GMA, gamma-glutamylmethylamide; NMG, i-methylglumate; HCOOH, formate; CHO-H_4F, formyl-tetrahydrofolate; CHO=H_4F, methylene-tetrahydrofolate; CHOΞH_4F, methenyl-tetrahydrofolate; H_4F, tetrahydrofolate; CO_2, carbon dioxide.

As Tdm has a H_4F binding domain (Chapter 3), it is predicted that C1 oxidation is performed by the H_4F-linked pathway (Figure 5.12). The vast majority of marine bacteria capable of MA catabolism possess this pathway, including members of the MRC and SAR11 clade (Sun et al., 2011; Chen, 2012). To determine if the H_4F-linked pathway is involved in the catabolism of MAs, RNA was extracted from cultures grown on either glucose and NH_4^+ (control), glucose and TMA, glucose and TMAO, glucose and NH_4^+ plus DMS, and glucose and TMAO plus DMS (same

as in Chapter 4). RT-PCR was performed targeting *fhs* which encodes Fhs, the enzyme responsible for the conversion of Formyl-H_4F to formate (Marx et al., 2003b; Chen, 2012). The control culture and the culture grown in the presence of only DMS with no MAs, did not provide any evidence for the up-regulation of *fhs* (Figure 5.13). However, in the presence of either TMA or TMAO, amplification of *fhs* from cDNA was observed, suggesting that this gene may be involved in the oxidation of the methyl groups cleaved off during the catabolism of MAs. The 16S rRNA controls for these cultures are displayed in Chapter 4, section 4.2.4.

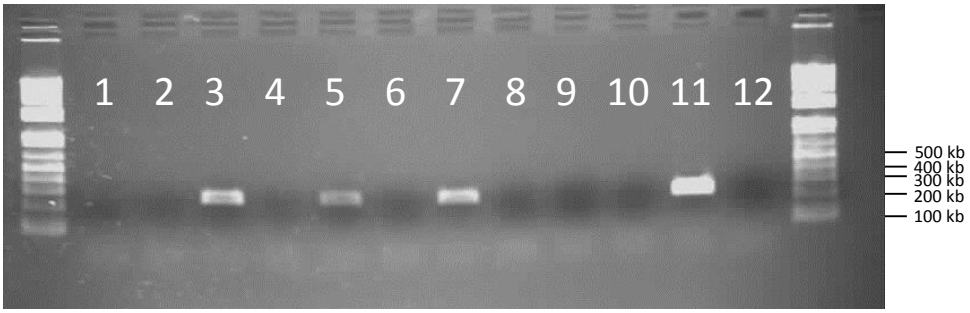

Figure 5.13. RT-PCR of the *fhs* genes in *R. pomeroyi* grown under different conditions. Lane 1, control; lane 2, control -RT; lane 3, TMA-grown; lane 4, TMA –RT; lane 5, TMAO-grown; lane 6 TMAO –RT; lane 7, TMAO + DMS-grown; lane 8 TMAO + DMS –RT; lane 9, NH_4^+ + DMS-grown, lane 10, NH_4^+ + DMS –RT, lane 11, DNA control, lane 12, no template control.

5.3.8. Mutagenesis of both copies of *fhs* in *R. pomeroyi*

Scrutinising the genome of *R. pomeroyi* revealed that this bacterium has two copies of *fhs* that share 100% identity at the amino acid level and differ by only five bases at the nucleotide level. *fhs-1* (SPO1557) is located within an operon containing the other genes required for H_4F-linked C1 oxidation (*folD*, *fdh*) (Figure 5.14). This operon is situated close to the genes involved in MA catabolism (*tmm*, *tdm*, *tmoX*). *fhs-2* (SPO3103) is located further upstream in the genome and has another copy of

folD downstream. Using *fhs* from *R. pomeroyi* as a query sequence to look at the genome-sequenced MRC isolates uploaded to the IMG/JGI database, it was determined that these two gene arrangements are frequently found within the MRC, often in isolation, i.e. only one copy is present within their genomes. This suggests that both forms may be functional in *R. pomeroyi*.

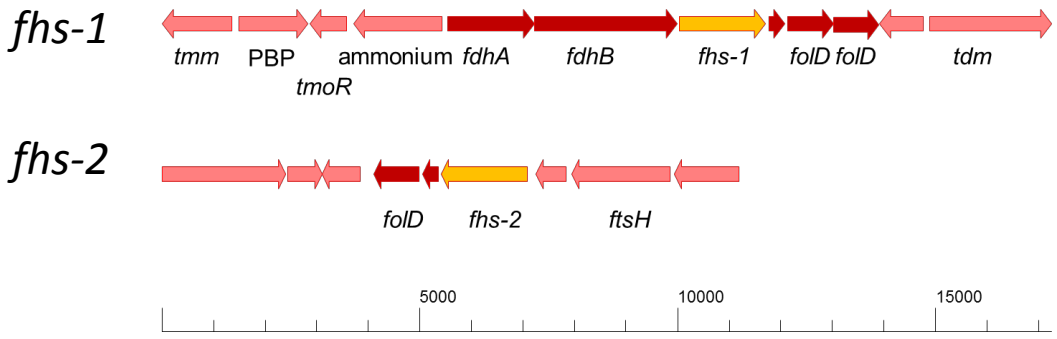

Figure 5.14. Gene neighbourhoods of each copy of *fhs*. Scale bar represents number of bases Abbreviations: *folD*, ; *tmm*, TMA monooxygenase; *tdm*, TMAO demethylase; *fhs*, formyl-H_4F synthetase, *tmoR*, regulator of *tmm*; ammonium, unspecified ammonium transporter; *ftsH*, ATP-dependent metalloprotease; *fhdA*, formate dehydrogenase *alpha* subunit; *fhdB*, formate dehydrogenase *beta* subunit, PBP, putative DMS/ TMA transporter.

To determine if *fhs* is involved in the oxidation of the methyl groups of MAs to CO_2, two mutant strains were constructed. The first was a single mutant targeting the *fhs-1*, generating the mutant, *Δfhs-1::Gm*. The second was a double mutant where the second copy was also mutated, generating the mutant, *Δfhs-1::GmΔfhs-2::Spc* (hereafter termed the *fhs* null mutant). To specify which genes were individually targeted for mutagenesis, PCR primers were designed which amplified regions external to *fhs-1* as this gene has a different upstream region compared to *fhs-2* (Figure 5.15). Once *fhs-1* was mutated, primers targeting the internal regions of the *fhs-2* were designed mutate the second copy.

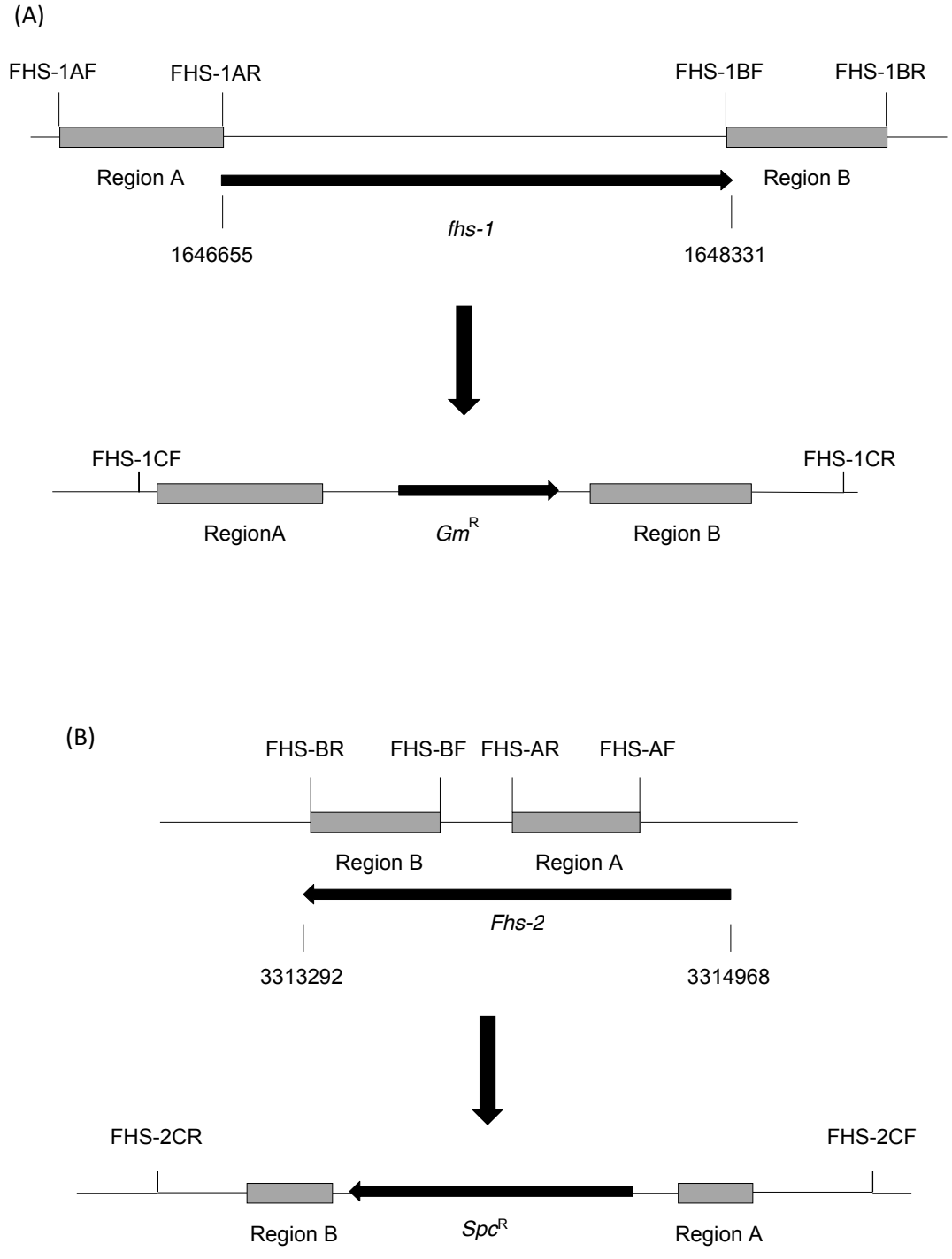

Figure 5.15. Genetic maps showing both copies of the *fhs* gene (A) *fhs-1*, (B) *fhs-2*, and the subsequent insertion of an antibiotic resistance marker used for the construction of gene knock-outs. Primers used for cloning are indicated in the figure. Abbreviations: *Gm*R, gentamicin; *Spc*R, spectinomycin. Numbers denote position of basepairs within the in the genome of *R*. *pomeroyi*.

To determine if the oxidation of TMA or TMAO was affected in these newly constructed mutant strains, the wild-type, *Δfhs-1::Gm* and the *fhs* null mutant were C-starved (see section 5.3.5.) and supplemented with TMAO (1 mM) or TMA (1 mM). The rate of TMA or TMAO depletion from the cultures was monitored. For the wild-type cells, C-starved and energy-starved cultures depleted ~1mM of TMAO every 24 h throughout the experiment (Figure 5.16A). The *fhs* null mutant, however, only degraded 0.4 mM during the entire experiment (Figure 5.16B). The *fhs* null mutant was complemented with its native *fhs*. *fhs* was amplified by PCR and cloned into the expression vector, pBBR1MSC-km, along with the putative promoter region upstream of the H_4F-linked oxidation operon (Figure 5.15) as previously described in section 3.2.2.5. Complementation with the native form of *fhs* (hereafter referred to as 'the complemented mutant') restored complete oxidation of TMAO. In the wild-type culture, the rate of TMA degradation was slightly slower (~442 μM d^{-1}) than TMAO degradation (~1158 μM d^{-1}). However in the *fhs* null mutant, TMA degradation was severely reduced (66 μM d^{-1}, between 23-96 h) and the build-up of TMAO in the culture medium was also detected (Figure 5.16C). As expected, complementation of the mutant with the native *fhs* restored the wild-type phenotype (Figure 5.16D). The single mutant, *Δfhs-1::Gm*, has a similar phenotype to the wild-type suggesting that the second copy is also functional (Figure 5.15B).

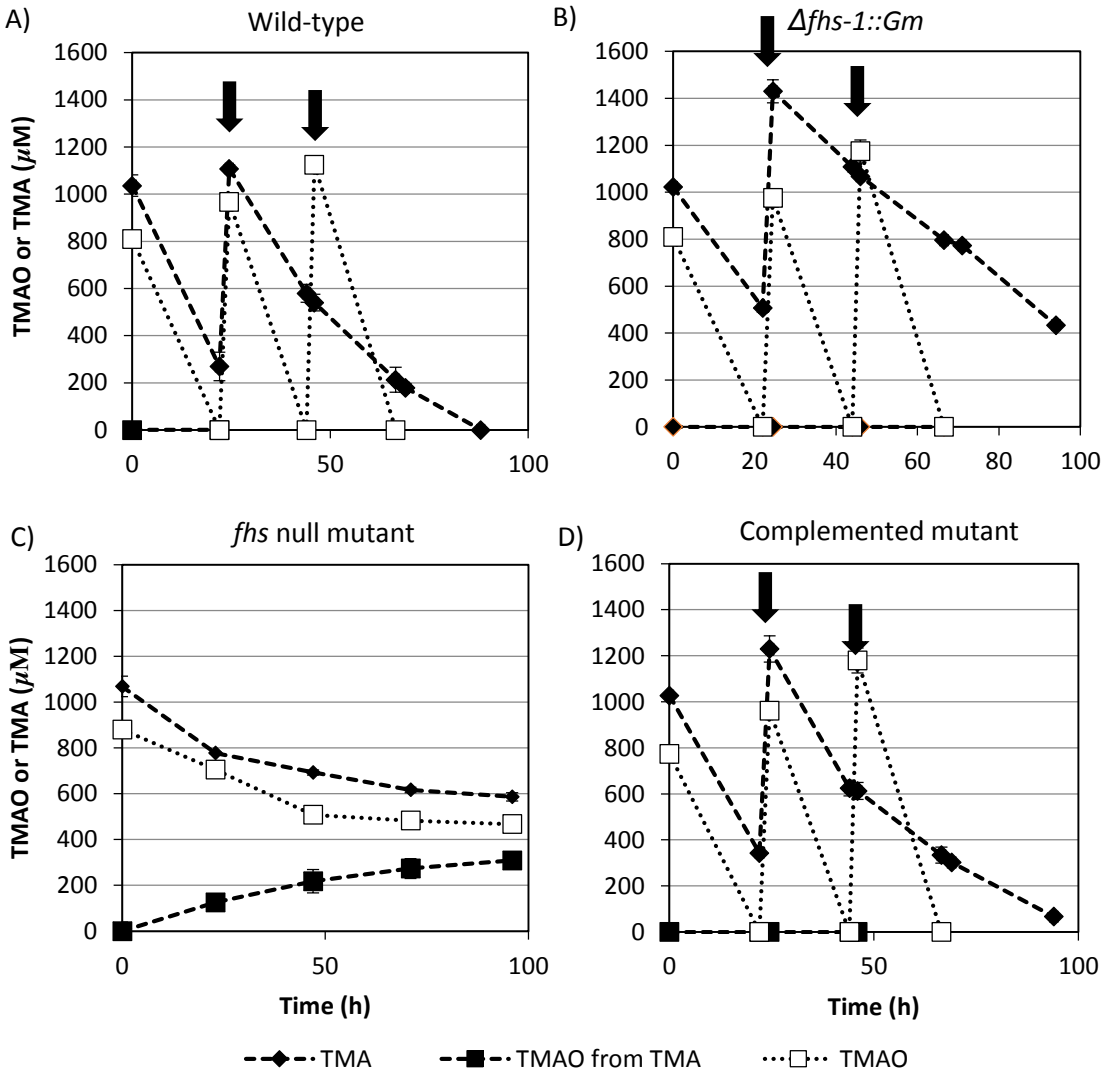

Figure 5.16. Quantification of either TMA (black diamonds) or TMAO (white squares) during incubations with C-starved and energy-starved *R*. *pomeroyi* wild-type **(A)**, *Δfhs-1::Gm* **(B)**, the *fhs* null mutant **(C)**, or the complemented mutant **(D)**. The build-up of TMAO (TMAO from TMA-black squares) in cultures in incubated with TMA was also quantified but it was only detected in the *fhs* null mutant cultures. All cultures were grown in triplicate and error bars denote SD. Arrows indicate additions of either TMA or TMAO.

5.4. Discussion

5.4.1. Ecological implications for the metabolism of MAs

Recent evidence has implicated marine heterotrophic bacteria in the cycling of these compounds (Chen et al., 2010b; Sun et al., 2011; Chen, 2012). The work in this Chapter has revealed that heterotrophic bacteria, unable to incorporate the C in MAs due to an incomplete set of genes and enzymes neccessary for incorporation of this C through the serine cycle, can still oxidise the methyl groups to CO_2 in order to generate both reducing equivalents and ATP. *R. pomeroyi* rapidly metabolised the TMA and TMAO whilst growing on an organic substrate, in this case a sugar, and also when it was both C and energy-starved. In fact, when *R. pomeroyi* was energy-starved, the rate of TMA or TMAO consumption increased, suggesting that the degradation of MAs may be primarily for energy rather than N. There are at least four major implications associated with these observations: 1) Catabolism of MAs can result in the more efficient conversion of organic substrates into biomass which provides an ecological advantage to heterotrophic bacteria capable of catabolising these compounds (Moran & Miller, 2007); 2) The turnover of MAs in the marine environment may be rapid during times of high primary productivity due to an influx of organic substrates from phytoplankton exudation and cell death which stimulates the activity of MRC bacteria (González et al., 2000; Zubkov et al., 2001; Buchan et al., 2005); 3) Marine heterotrophic bacteria are likely to be an efficient biological sink for MAs, reducing their flux into the atmosphere and lowering their climate-active effects; 4) The metabolism of MAs primarily as an energy source results in the remineralisation of organic N back to NH_4^+, which in turn can support the growth of other microbial communities in the marine environment.

Although the turnover of TMAO can stimulate ATP production in an isolate from the SAR11 clade, *C*. Pelagibacter ubique HTCC1062, no effect on the growth of this bacterium was identified (Sun, et al 2011). A similar study, conducted using the obligate methylotrophic bacterium, *Methylophilus* sp. HTCC2181, revealed that the turnover of TMAO resulted in ATP production, which in turn increased the bacterial growth efficiency of this bacterium (Halsey et al., 2012). The work in this Chapter is in agreement with these previous studies that show the turnover of TMA or TMAO can stimulate growth, however, based on the current literature, this is the first time that a positive effect on growth has been observed in a marine heterotrophic bacterium. As the turnover of MAs helps to maintain ATP concentrations during periods of organic C starvation, cells may be able to respond faster and more efficiently to fluxes of organic C. Indeed, *C*. Pelagibacter ubique HTCC1062 had higher rates of taurine uptake when cells were incubated through periods of C starvation in the light (Steindler, et al, 2011). This bacterium can generate ATP through a specialised light-driven proton pump (proteorhodopsin) and when incubated in the light, this mechanism has been shown to increase intracellular ATP levels in this bacterium (Steindler et al., 2011). Marine bacteria, in particular members of the SAR11 clade and MRC, devote a large amount of resources into the production of highly efficient ATP-driven ABC-cassette transport systems (Sowell et al, 2008, Sowell et al, 2011, Williams et al, 2012, Gifford et al, 2013). Therefore, the turnover of MAs to generate ATP may increase the ability of these two bacterial clades to scavenge nutrients from the surface waters. The ability to generate reducing equivalents and ATP from the oxidation of MAs may also help prevent the breakdown of intracellular C reserves which will help to maintain cell viability through periods of C starvation. This effect may be

taking place in *R*. *pomeroyi* (see section 5.3.5) where the number of viable cells remaining in the culture was an order of magnitude higher when incubated with either TMA or TMAO. The preservation of intracellular C reserves has been observed when *C*. Pelagibacter ubique HTCC1062 was incubated in the light (Gómez-Consarnau et al, 2010, Steindler et al 2011).

Thiosulfate oxidation is a widespread trait within the MRC (Newton et al, 2010) and it has been previously shown that thiosulfate oxidation can increase the efficiency by which both *C*. *thiooxidans* and *R*. *pomeroyi* utilised organic substrates again through the stimulation of ATP production (Moran et al, 2004, Sorokin et al, 2005). When *R*. *pomeroyi* was provided with two supplementary energy sources, TMA and thiosulfate, this bacterium co-catabolised these compounds which resulted in an even greater efficiency in organic substrate utilisation. In this scenario, the final biomass of *R*. *pomeroyi* was double that achieved when incubated with an organic substrate alone. Both TMA and thiosulfate are 'energy rich' in the sense that between 7-8 ATP molecules are generated from the oxidation of one TMA or thiosulfate molecule, assuming the reducing equivalents/ electrons generated are fed into the electron transport chain (Friedrich et al., 2000; Friedrich et al., 2001) (Figure 5.15). In contrast, carbon monoxide (CO) is a relatively 'energy poor' compound, only liberating two electrons and this metabolism does not appear to result in enhancement of growth of *R*. *pomeroyi* (Cunliffe 2012). However, in natural conditions, the liberation of just two electrons may provide enough benefit to warrant the catabolism of CO. The work presented in this Chapter complements a larger body of evidence which points towards the ecological success of certain heterotrophic bacterial groups culminating from their ability to generate cellular

energy from a wide range of sources (Eiler, 2006, Moran & Miller, 2007, Boden et al, 2011b, Green et al, 2011, Steindler et al, 2011, Sun et al, 2011).

5.4.2. Remineralisation of organic N into NH_4^+

One of the major findings from this Chapter is the fact that MAs may provide a source of inorganic N in the surface waters of the ocean in the form of NH_4^+. Although the source of MAs in marine surface waters remains unknown, it is likely to come from the breakdown of compatible osmolytes and lipid constituents, such as GBT and choline (King, 1984). Recent evidence has even shown the existence of an aerobic pathway for the production of TMA as a result of the enzymatic cleavage of carnitine (Zhu et al., 2014). Therefore, amines may represent a pool of N-rich organic compounds which are rapidly remineralised back into NH_4^+. Although there is very little empirical evidence to support this hypothesis, research conducted over two decades ago has shown that in the laboratory, phytoplankton and their exudates are rapidly remineralised by the bacterioplankton, liberating NH_4^+ (Garber et al, 1984). In the co-culture experiment (section 5.2.6.) the same process is taking place whereby TMA is turned over by a bacterium, primarily as a source of reducing equivalent and ATP, and the excess NH_4 is cross-fed into another bacterium to support its growth. This concept can be theoretically expanded to all N-rich compounds including the precursors of MAs, such as GBT, choline (see Chapter 7), and carnitine, as well as purine and pyrimidine compounds. This hypothesis holds only if bacterial cells use MAs primarily as an energy source and not as a N source. However, the work in this Chapter has clearly shown that the turnover of MAs can have multiple beneficial physiological effects, for example, maintaining cell viability through periods of C starvation, as well as increasing the

growth yield and growth rate of cells growing chemoorganotrophically. In marine surface waters, the abundance *Roseobacter* species is positively correlated with seasonal increases in primary production (Hahnke et al, 2013, González et al, 2000, Buchan et al, 2005, Gilbert et al., 2012; Taylor et al., 2014, Nelson et al, 2014) and it can therefore be hypothesised that the potential to remineralise MAs may be a property of the bacterioplankton associated with phytoplankton blooms.

5.4.3. The role of *fhs* in energy production

Many abundant marine bacteria, including representatives of the MRC and SAR11 clade, lack the genes required for C1 assimilation through either the RuMP pathway or serine cycle and are therefore not true methylotrophic organisms (Chistoserdova, 2011; Sun et al., 2011; Chen, 2012). In methylotrophs, the main route for C1 oxidation is via the H_4MPT pathway which is found in a number of marine *Methylophaga* species (Boden et al., 2011b). For bacteria possessing the H_4MPT pathway, the H_4F-linked pathway is primarily used for the assimilation (reductive direction) of C1 compounds (Chistoserdova, 2011). However as the majority of marine bacteria do not possess the H_4MPT pathway (Rusch et al., 2007; Sun et al., 2011; Chen, 2012), the main route for C1 oxidation is predicted to be via the H_4F-linked pathway, which is predicted to work in reverse (oxidative direction). Based on RT-PCR data (section 5.3.7), there was clear evidence that *fhs* is upregulated in the presence of MAs, but not in the presence of another methylated compound, DMS. This suggests that expression of this pathway is likely governed by the production of methylene-H_4F, one of its downstream metabolites or a change in reductant balance. As DMSO appears to be the end-point for DMS oxidation in *R. pomeroyi* (Chapter 4), the lack of upregulation of the genes required for C1 oxidation is expected. As *R. pomeroyi* has two identical copies (at the amino acid

level) of *fhs* both genes were simultaneously deleted from the wild-type genome. Analysis of this mutant showed clearly that both copies of *fhs* play a role in the oxidation of methyl groups generated during MA catabolism. When the first copy of *fhs* was deleted, the single *fhs* mutant had essentially the same phenotype as the wild-type, confirming that the second copy of *fhs* can fulfill the requirement for oxidation of C1 moieties. Also, when the *fhs* null mutant was complemented with its native form of *fhs*, the promoter from the start of the H_4F-linked operon was used to initiate transcription and subsequent expression of *fhs*. Therefore, this confirms that this operon, which is under the control of the promoter used for complementation, responds to MA metabolism. Further experimental work regarding the role of *fhs* in MA and QA catabolism is presented in Chapter 7.

Chapter 6

Isolation of TMA/TMAO-utilising bacteria and development of functional gene markers targeting Tdm

6.1. Introduction

Chen (2012) isolated a number of bacterial strains from the seawater that are related to the MRC using TMA as a sole N source. In this study, it became apparent that the community of MRC bacteria present in the seawater was diverse, therefore providing additional evidence that this clade is involved in the degradation of MAs in the marine environment. The same study also showed that a diverse consortium of non-methylotrophic bacteria were present in the seawater that could degrade TMA and MMA (Chen, 2012). Previous work has focused on the methylotrophic communities present in the seawater that are capable of utilising DMS, methanol or MMA as a sole C source (Neufeld et al., 2007; Schäfer, 2007; Neufeld et al., 2008). Although a number of studies have looked at the key players in DMSP degradation, the microorganisms that were isolated on this compound are not necessarily methylotrophs as they can utilise the propionate (three carbon, C3) side- chain for growth (González et al., 1999; González et al., 2003; Howard et al., 2008). The major conclusion from the data presented in these studies is that both the MRC and bacteria related to the *Gammaproteobacteria* are capable of utilising methylated compounds to fulfil their methylotrophic lifestyle or supplement their heterotrophic lifestyle.

Although it is now known that members of the SAR11 clade and MRC can utilise TMA as either a supplementary energy source or a N source (Sun et al., 2011, Chen, 2012, Chapter 5), at present, no study has investigated the methylotrophic community present in the seawater that can utilise TMA or TMAO as a sole C and energy source. Therefore, the aims of this Chapter were to expand the current knowledge regarding the microbial community present within the seawater that is

capable of utilising either TMAO or TMA as either a sole C, N and energy source, or just a sole N source.

6.2. Results

6.2.1. Isolation of MA-utilising strains

Using both seawater collected (10/2011 and 06/2012) from the L4 sampling station, Plymouth, UK and seawater collected (06/2013) from a saltmarsh pond, Stiffkey, Norfolk, UK, a number of enrichments were set up with TMAO (1 mM) as the sole C and N source. For enrichments using Stiffkey seawater, TMAO (0.5 mM) was only used as a sole N source and succinate (5 mM) was added to the medium. A seasalts minimal medium (Chen, 2012) was used and mixed with seawater in a 1: 1 ratio. A number of bacteria were isolated using solid agar with TMA or TMAO as either a sole C, N and energy source or TMAO as a sole N source. Using the 27F and 1492R primers targeting the bacterial 16S rRNA gene, a number of isolates retrieved from enrichment cultures were screened for phylogenetic identification. At the L4 sampling site, two strains related to the MRC were isolated, hereafter termed *Roseobacter* sp. TMAL401 and *Roseobacter* sp. TMAL402 as well as a number of *Methylophaga* isolates closely related to *Methylophaga thiooxidans* DMS010 (Figure 6.1). From the saltmarsh pond water, three more isolates related to the MRC were retrieved, strain SM003, SM006, SM010. MRC strain SM006 appears to belong in the genus, *Roseovarius*, however, it should be noted that the bootstrap values at the majority of nodes within the MRC cluster are very low. Therefore, the tree may not be an accurate representation of the individual species phylogeny. There is a low level of congruity between the multi-locus analysis conducted by Voget et al. (2014) (see introduction, Figure 1.12) and the 16S rRNA tree shown in Figure 6.1. For example, *Citreicella* sp. SE45 (subgroup 3) falls

within a cluster with a number of *Phaeobacter* and *Ruegeria* isolates (subgroup 1). It is therefore not possible to determine the exact phylogeny of the new isolates based solely on the 16S rRNA gene and a more detailed analysis is required using different functional markers.

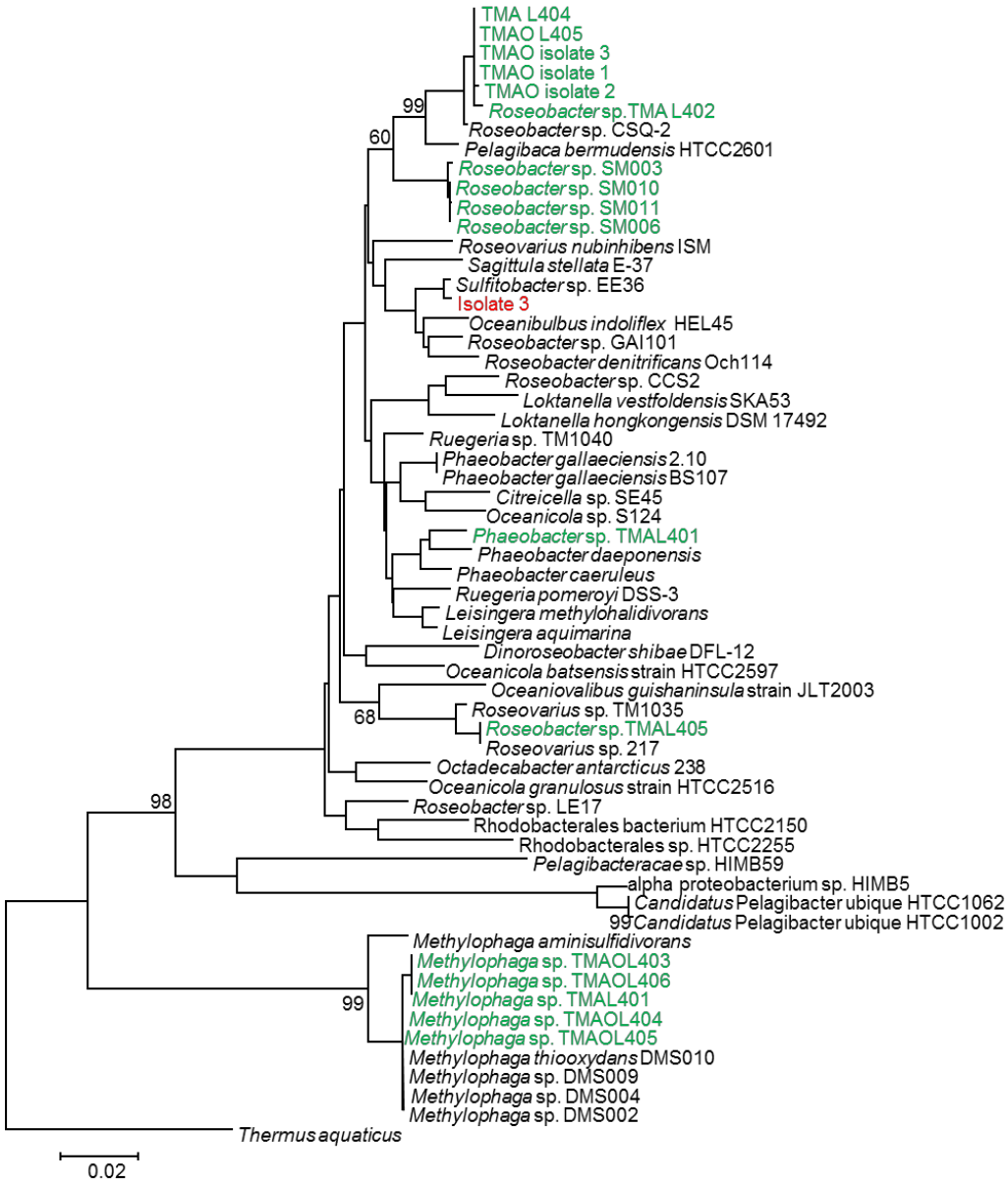

Figure 6.1. Phylogeny of the bacterial strains isolated using TMA or TMAO as a sole C, N and energy source. The tree was constructed using the neighbour-joining method and values at the major nodes represent confidence scores based on 500 replications. Approximately 1400 nucleotide positions were used in the alignment. The alignment and tree were constructed using MEGA 6.1. Evolutionary distances were calculated using the p-distance matrix. Strains in green represent isolates retrieved during this study that can grow on MAs as either a sole C, N and energy source or a N source. Isolate 3 (red) represent strains isolated from enrichment cultures that was unable to grow on MAs.

6.2.2. Phylogeny of the new isolates based on the functional marker, *gmaS*

To gain a better understanding of the phylogeny of the new TMA/TMAO-utilising isolates, degenerate primers targeting *gmaS* and *tmm* designed by Chen (2012) were employed. A number of new homologs were added to the GmaS alignment, initially conducted by Chen et al. (2011) and later by Chen (2012), to encompass all new marine microbial genomes of interest that have recently been sequenced. *gmaS* was present in the genomes of both the SAR116 clade representative, *Candidatus* Puniceispirillum marinum IMCC1322 and a representative from the (*Roseobacter* clade affiliated) RCA-sub group (Selje et al., 2004), *Planktomarina temperata* RCA23 (Figure 6.2.). Interestingly, the GmaS homologs from these two strains cluster together with GmaS homologs from the MRC suggesting horizontal gene transfer may have taken place. *M. thiooxidans* and *Methylophaga aminisulfidovorans* MP, which have MMADH for the degradation of MMA encoded by the *mau* operon (see section, 1.6.1), also have *gmaS* as well as the other genes required for MMA degradation through the GMA/ NMG pathway in their genomes (Figure 6.2). Based on the functional marker, *gmaS*, TMAL401 is again closely related to isolates from the *Phaeobacter* and *Leisingera* genera, strengthening the evidence that TMAL401 belongs in the genus, *Phaeobacter*. The GmaS homolog from strain SM006 is closely related to GmaS homologs from *Roseovarius* spp., whilst the remaining GmaS homologs from the other isolates cluster closely with *Ruegeria* spp. and *R. litoralis*. Again, because of the low bootstrap values observed it is hard to draw any firm conclusions about the precise phylogeny of these isolates, but a pattern of phylogeny is starting to emerge.

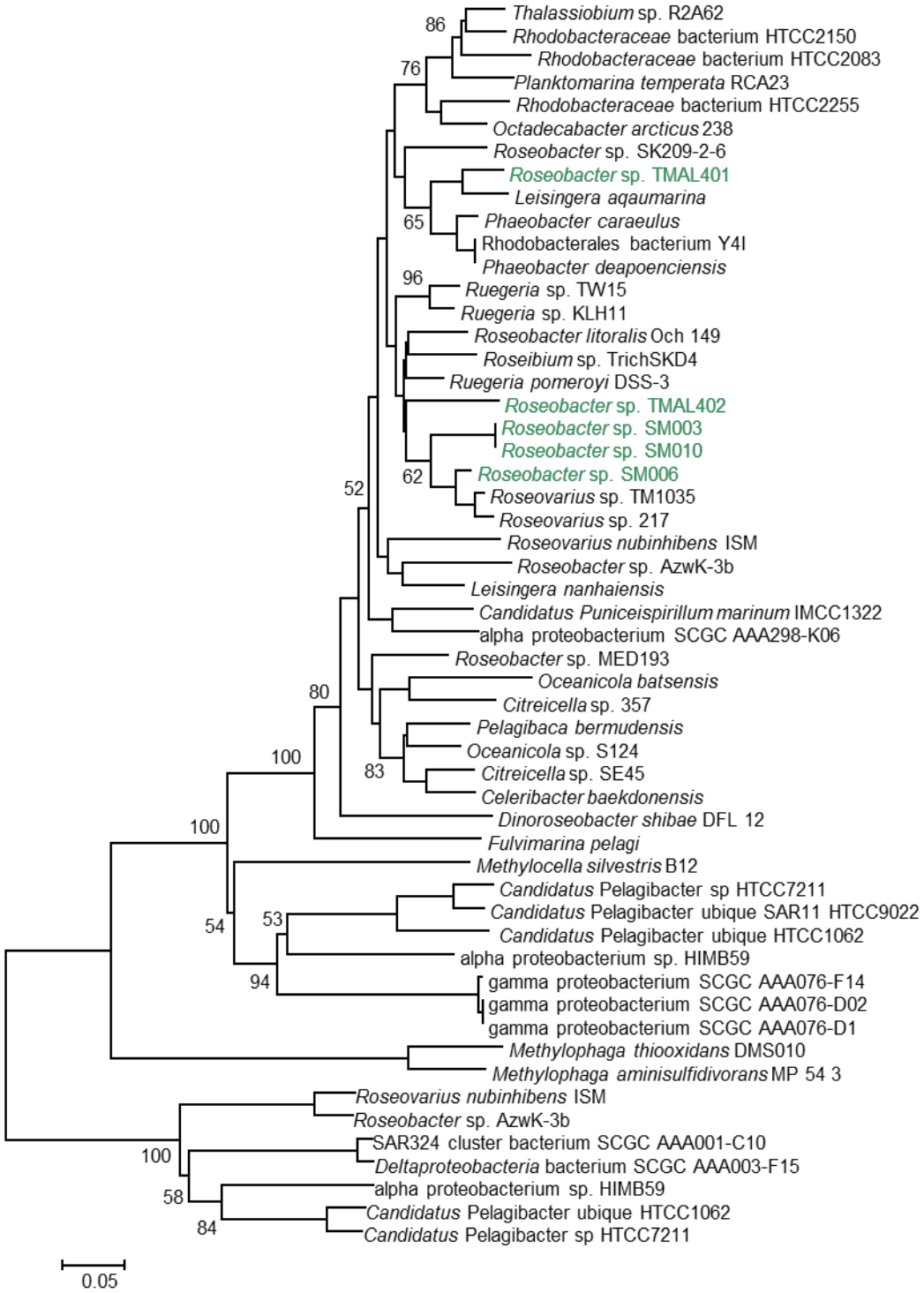

Figure 6.2. Phylogeny of the bacterial strains isolated on TMA as a sole C, N and energy source using the functional marker, *gmaS*. ~265 amino acids were used for the alignment. For more major nodes, bootstrap values >50% are shown (500 replicates). Evolutionary distances were calculated using the p-distance matrix The *gmaS*-like homolog was used as an outgroup. The tree was constructed using the neighbor-joining method in MEGA 6.1.

A number of *gmaS*-like homologs were found in several marine bacterial isolates including isolates from the SAR11 clade, the MRC and representatives from the *Deltaproteobacteria* and *Gammaproteobacteria*. These GmaS-like homologs form an outgroup with the experimentally validated GmaS homologs and therefore the function cannot be inferred and warrants further investigation (Figure 6.2). This *gmaS*-like gene is situated within a cluster that has three ORFs annotated as *mgsABC*-like genes and they are not mutually exclusive to the *bona fide gmaS/ mgsABC* cluster. However, in the majority of marine bacteria this cluster is mutually exclusive with the genes that encode DMA monooxygenase (Dmm) (data not shown) apart from the MRC isolate, *R. nubinhibens*, which has both copies. This different gene cluster may therefore represent an alternative route of the degradation of DMA, directly transforming it to NMG. In support of this prediction, bacterial genomes from the SAR11 clade do not contain the genes encoding Dmm but do possess this *gmaS/ mgsABC*- like gene cluster. This cluster is found in between *tdm* and the *bona fide gmaS/ mgsABC* cluster and is potentially co-transcribed in one single operon (Figure 6.3).

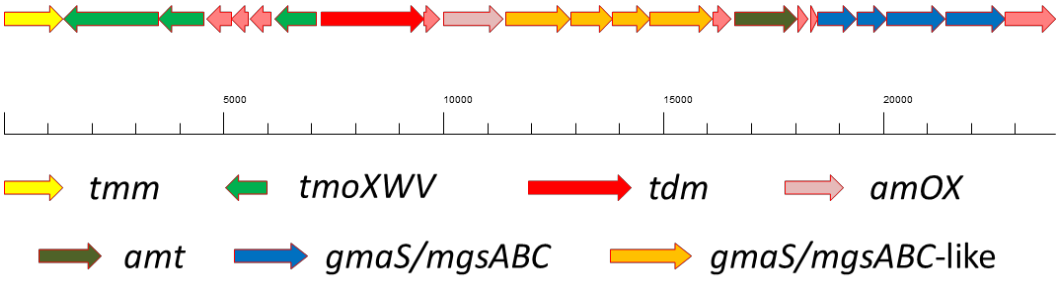

Figure 6.3. The genetic neighbourhood containing the genes required for the catabolism of MAs in *Candidatus* Pelagibacter ubique HTCC1062. The *gmaS*/*mgS*-like gene cluster is located between *tdm* and the *bona fide gmaS*/*mgS* gene cluster. Abbreviations: *tmm*, TMA monooxygenase; *tmoXWV*, TMAO transporter; *tdm*, TMAO demethylase; *amOX*, putative amine oxidase (Smith et al., 2013); *amt*, putative ammonium transporter; *gmaS*/*mgsABC*, *bona fide* gamma-glutamylmethylamide

synthetase/ *N*-methylglutamate synthase, *gmaS*/*mgsABC*-like, gamma-glutamylmethylamide synthetase-like/ *N*-methylglutamate synthase-like.

6.2.3. Phylogeny of the new isolates based on the functional marker, *tmm*

The phylogeny of *tmm* confirms that TMAL401 is closely related to *Phaeobacter* spp. whilst TMAL402 again clusters closely with *R*. *pomeroyi* (Figure 6.4). The Tmm homologs from strain SM003 and SM010 are also related closely to the Tmm from *R*. *pomeroyi* although less so than that of TMAL402. To gain a better understanding about the ecology of *tmm* in the marine environment, this primer set was also used to amplify *tmm* homologs from the Stiffkey saltmarsh. A total of ~90 clones were picked for further sequencing, using the M13F/R primers (see Chapter 2, section 2.4.7.). A number of clones related to different *tmm* homologs within the MRC were amplified confirming the hypothesis that the MRC is a diverse bacterial group within the saltmarsh microbial community. The majority of clones did not cluster closely with any known representatives of the MRC and formed distinct branches in the tree (Figure 6.4). This observation supports the notion that there appears to be a difference in the ecology of the uncultivated and cultivated microbial community and that the majority of strains are still uncultivable. Strains, SM003, SM006 and SM010 were all isolated from the saltmarsh during enrichment cultures with artificially high concentrations of TMAO and succinate whilst only one Tmm homolog, related to *Roseobacter* sp. SM006, was retrieved from *in situ* DNA samples. Therefore, it can be reasoned that the strains isolated during the enrichments are 'weeds' which are adapted to respond to the high transient fluxes of MAs. In addition, during the enrichments their rapid increase in abundance is not counteracted via top-down processes, such as predation or viral lysis, or at least it is not enough to offset their rapid increase in cell numbers.

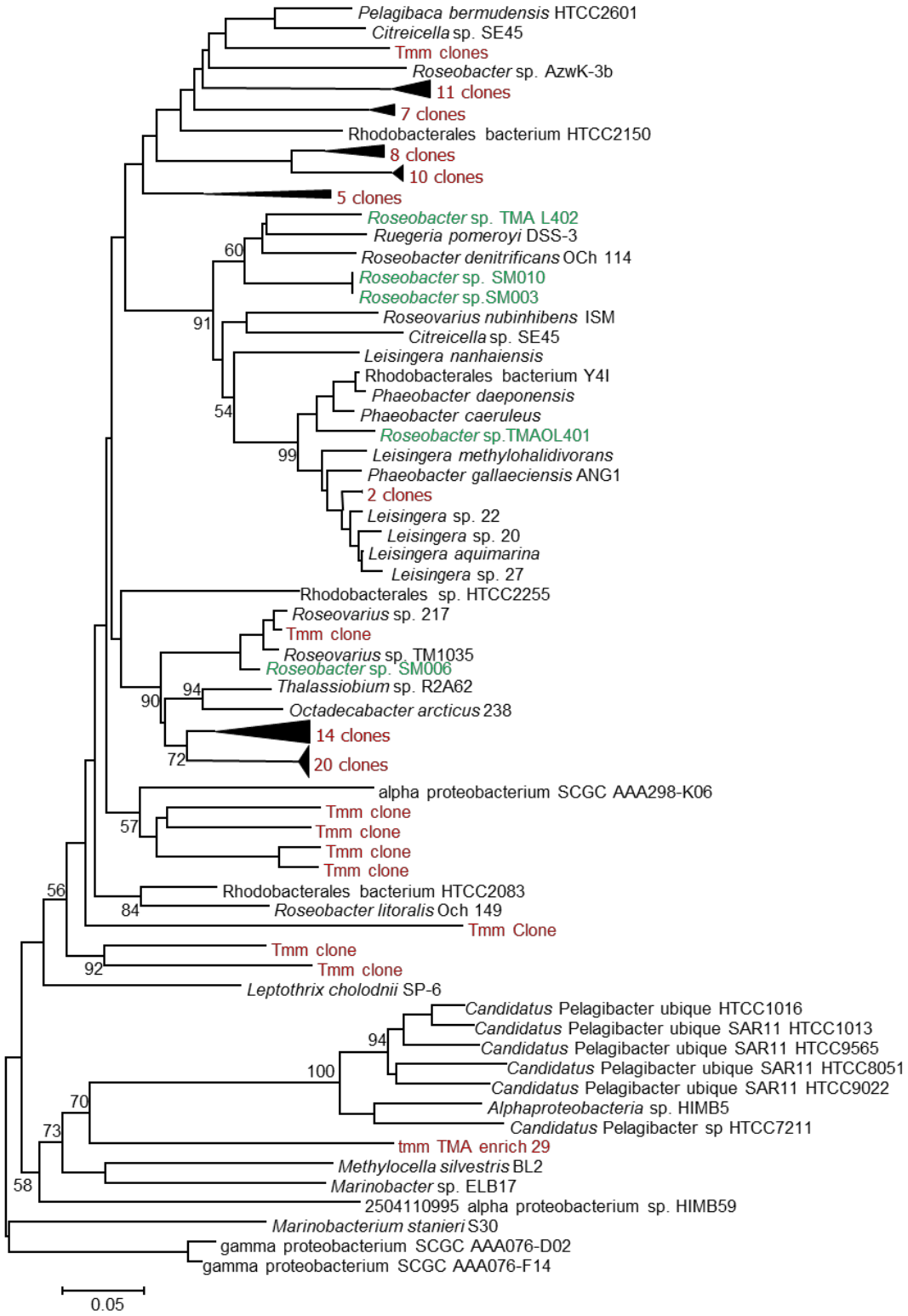

Figure 6.4. Phylogeny of Tmm including bacterial strains isolated on TMA or TMAO as a sole C, N and energy source. ~255 amino acids were used for the alignment. Bootstrap values >50% are shown (500 replicates). Tmm homologs related to *Gammaproteobacteria* were used as the outgroup. The tree was constructed using the neighbor-joining method in MEGA 6.1. Evolutionary distances were calculated using the p-distance matrix. Red equals sequences retrieved from clones amplified from the saltmarsh. Green equals Tmm sequences retrieved form isolates.

6.2.4. Development of a functional marker, *tdm*

As a number of marine bacteria possess *tdm*, but not *tmm*, it was necessary to design degenerate primers in order to develop a functional marker that can be used to assess the *in situ* bacterial community capable of degrading TMAO. A previous alignment of Tdm (Chapter 3) was scrutinised for regions of conservation, initially at the amino acid level, along the length of the gene. After conversion to a nucleotide sequence, primers were designed, based on these regions of conservation. Primer sets were designed that amplified a region ~400-500 bp in length so that they could ultimately be used in conjunction with high-throughput sequencing technologies. Where possible, regions with higher GC content and almost no redundancy were chosen to improve the chances of correct amplification (Figure 6.6), especially towards the 3' end of the primers. Sequences representing homologs found in bacteria related to the MRC, SAR11 clade and *Gammaproteobacteria* were used in the alignment.

(A)

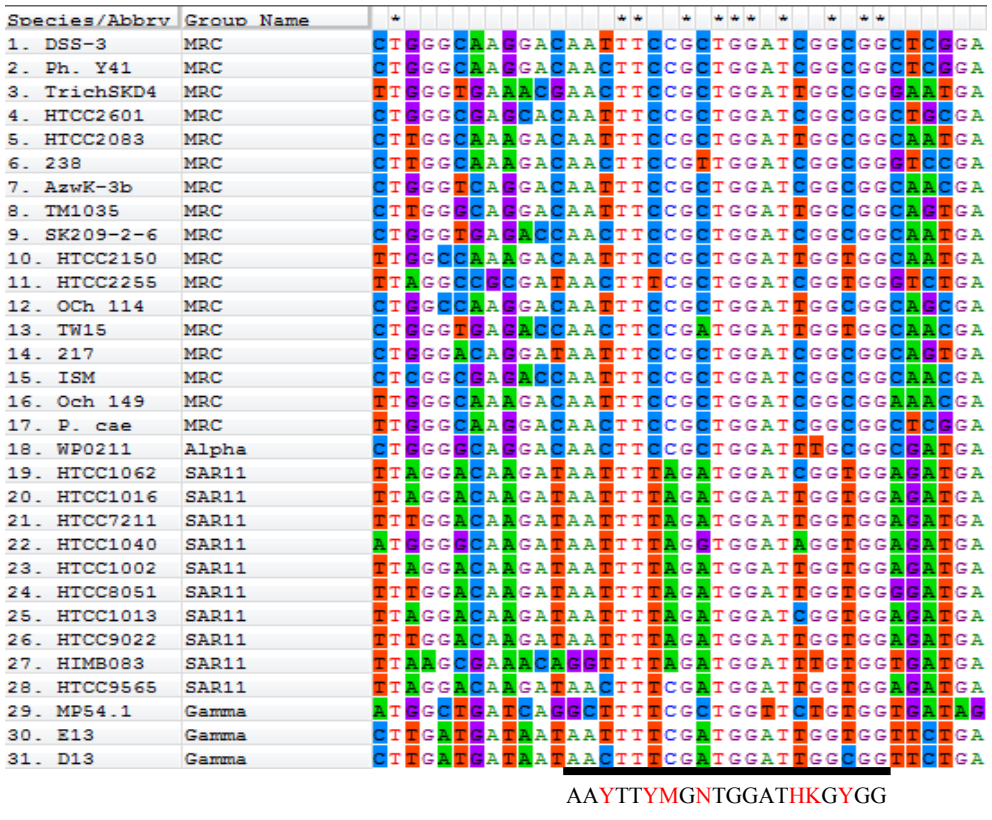

(B)

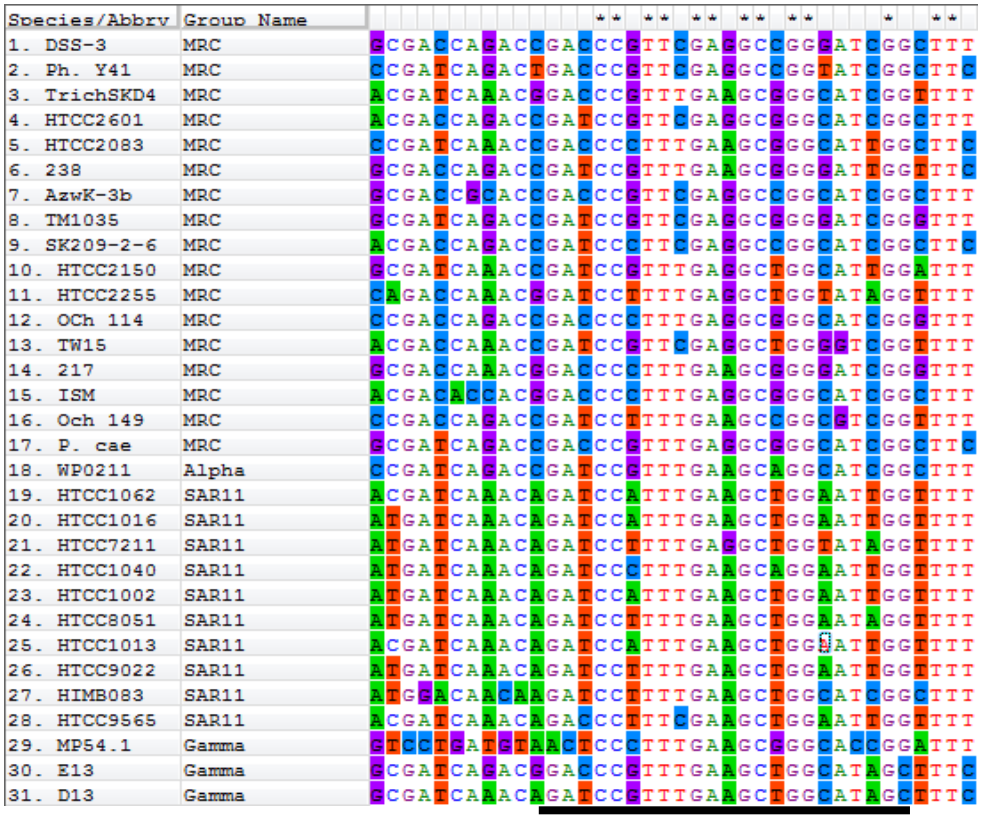

Figure 6.5. Alignment of marine Tdm homologs at the nucleotide level and design of the primers, Tdm_screen_1631F **(A)** and Tdm_screen_2082R **(B).** Red letters indicate where a degenerate base was included into the primer design. A total of 30 different Tdm homologs were used in the alignment including homologs form the MRC, SAR11 clade and representatives of the *Gammaproteobacteria*. Conserved sites were toggled at the 70% similarity level. The alignment was generated using MEGA 6.1. Species abbreviations; DSS-3, *R. pomeroyi*; Ph. Y41, *Phaeobacter* sp. Y41; TrichSDK4, *Roseibium* sp. TrichSDK4; HTCC2601, *Pelagibaca bermudensis* HTCC2601; HTCC2083, *Rhodobacteraceae* bacterium HTCC2083; 238, *Octadecabacter arcticus* 238; Azwk-3b; *Roseobacter* sp. Azwk-3b; TM1035, *Roseovarius* sp. TM1035; SK209-2-6, *Roseobacter* sp. SK209-2-6; HTCC2150, *Rhodobacteraceae* bacterium HTCC2150; HTCC2255, *Rhodobacteraceae* bacterium HTCC2255; Och 114, *Roseobacter denitrificans* Och114; TW15, *Ruegeria* sp. TW15; 217, *Roseovarius* sp. 217; ISM, *Roseovarius nubinhibens* ISM; Och 149, *Roseobacter litoralis* Och 149; *P. cae, Phaeobacter caeruleus*; WP2011, *Thalassospira profundimaris* WP0211; HTCC1062, *Candidatus* Pelagibacter ubique HTCC1062; HTCC1016, *Candidatus* Pelagibacter ubique HTCC1062; 7211, *Candidatus* Pelagibacter sp. HTCC7211; HTCC1040, *Candidatus* Pelagibacter sp. HTCC1040; HTCC1002, *Candidatus* Pelagibacter ubique HTCC1002; HTCC8051, *Candidatus* Pelagibacter sp. HTCC8051; HTCC1013, *Candidatus* Pelagibacter ubique HTCC1013; HTCC9022, *Candidatus* Pelagibacter ubique HTCC9022; HIMB083, *Candidatus* Pelagibacter sp. HIMB083; HTCC9565, *Candidatus* Pelagibacter sp. HTCC9565; MP54.1, *Methylophaga aminisulfidivorans* MP54.1; E13 Gammaproteobacterium SCGC AAA076-E13; D13, Gammaproteobacterium SCGC AAA076-E13.

To identify the optimum conditions required for the amplification of *tdm*, a range of different annealing temperatures were tested using *R*. *pomeroyi* DNA as the template (Figure 6.6). An annealing temperature of 53ºC gave the best tradeoff between yield and specificity. An elongation step (72ºC) of 25 s resulted in the amplification of larger undesired PCR products; however, these were significantly reduced by shortening the elongation time to 20 s (Figure 6.6). 35 cycles was sufficient to generate a strong PCR product. Next, a number of strains from the MRC were used as a template for PCR. Amplification of *tdm* from different strains proved successful, for example, TMAL401, TMAL402, SM030 and *Roseovarius* sp. TM1035 (Figure 6.7A). Finally, the primers were tested on saltmarsh seawater to determine if they could amplify *tdm* from natural bacterial communities. Again, amplification from the saltmarsh was successful indicating that these primers could be used to assess the *in situ* diversity of the bacterial TMAO-utilising community (Figure 6.7b).

(A)

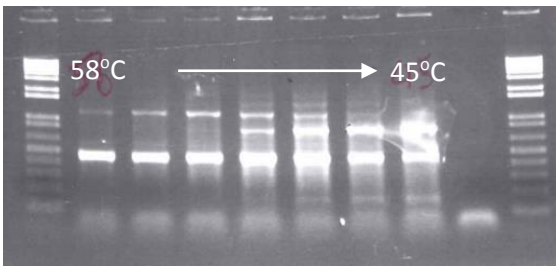

(B)

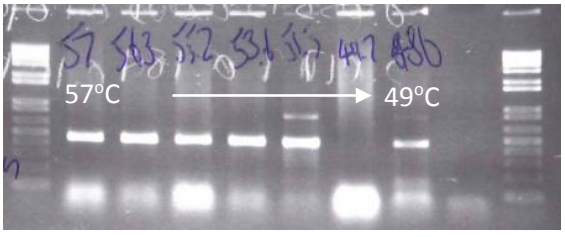

Figure 6.6. PCR amplification of *tdm* from *R*. *pomeroyi* using a range of different annealing temperatures (58-45ºC) with an elongation step of 25 s **(upper panel)** or using an elongation step of 20 s **(lower panel)**, using the primers Tdm_screen_F1/R1.

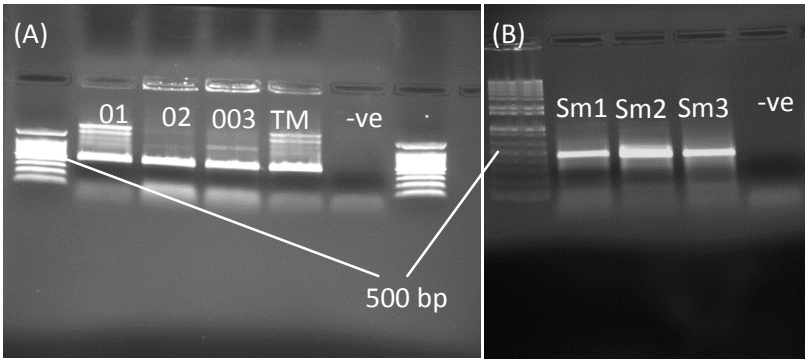

Figure 6.7. Amplification of *tdm* from strains isolated from TMA or TMAO enrichments. *Roseovarius* sp. TM1035 was also used as a template for PCR **(A)**. Amplification of *tdm* from Stiffkey saltmarsh seawater **(B)**. Abbreviations: 01, *Roseobacter* sp. TMAL401; 02, *Roseobacter* sp. TMAL402; 003, *Roseobacter* sp. SM003; TM, *Roseovarius* sp. TM1035; Sm1, saltmarsh seawater sample one; Sm2, saltmarsh seawater sample two; Sm3, saltmarsh seawater sample three; -ve, negative control.

6.2.5. Phylogeny of the isolates based on the functional marker, *tdm*

Using the new functional marker, *tdm*, the phylogeny of the new isolates was investigated. The Tdm homolog from strain SM006 was again closely related to *Roseovarius* spp. (Figure 6.8). Tdm of TMAL401 was again closely related to *Phaeobacter* spp. Tdm homologs from TMAL402 and strain SM003 and SM010 were again most closely related to the Tdm homolog from *R. pomeroyi*. Based on the short sequence used for the phylogeny (~150 aa in length) strain SM003 and SM010 were indistinguishable. Interestingly, TMAL402, which is most closely related to *R. pomeroyi* based on Tmm and Tdm phylogenetic analysis, can grow on TMA as a sole C source (methylotrophy) which is in contrast to *R. pomeroyi* itself. However, using the conventional 16S rRNA gene marker, TMAL402 and *R. pomeroyi* appeared to be more distantly related (Figure 6.1)

DNA extracted from the salt marsh that was used for generating the *tmm* clone library was again used as a template for the amplification of *tdm* sequences. A total

of ~50 clones were picked for further sequencing, again using the M13F/R primers (see Chapter 2, section 2.4.7). Approximately one in five sequences retrieved were incorrect, amplifying an ATPase-type subunit of a transport gene and these were accordingly binned from further analyses. The majority of sequences retrieved from the saltmarsh did not cluster closely with those from cultivated isolates (Figure 6.8). Similar results were observed when using the functional marker, *tmm* for assessing *tmm*-containing microorganisms from this salt marsh (Figure 6.4). This further suggests that there is a difference between the *in situ* MRC community and the one retrieved during conventional enrichment and isolation methods.

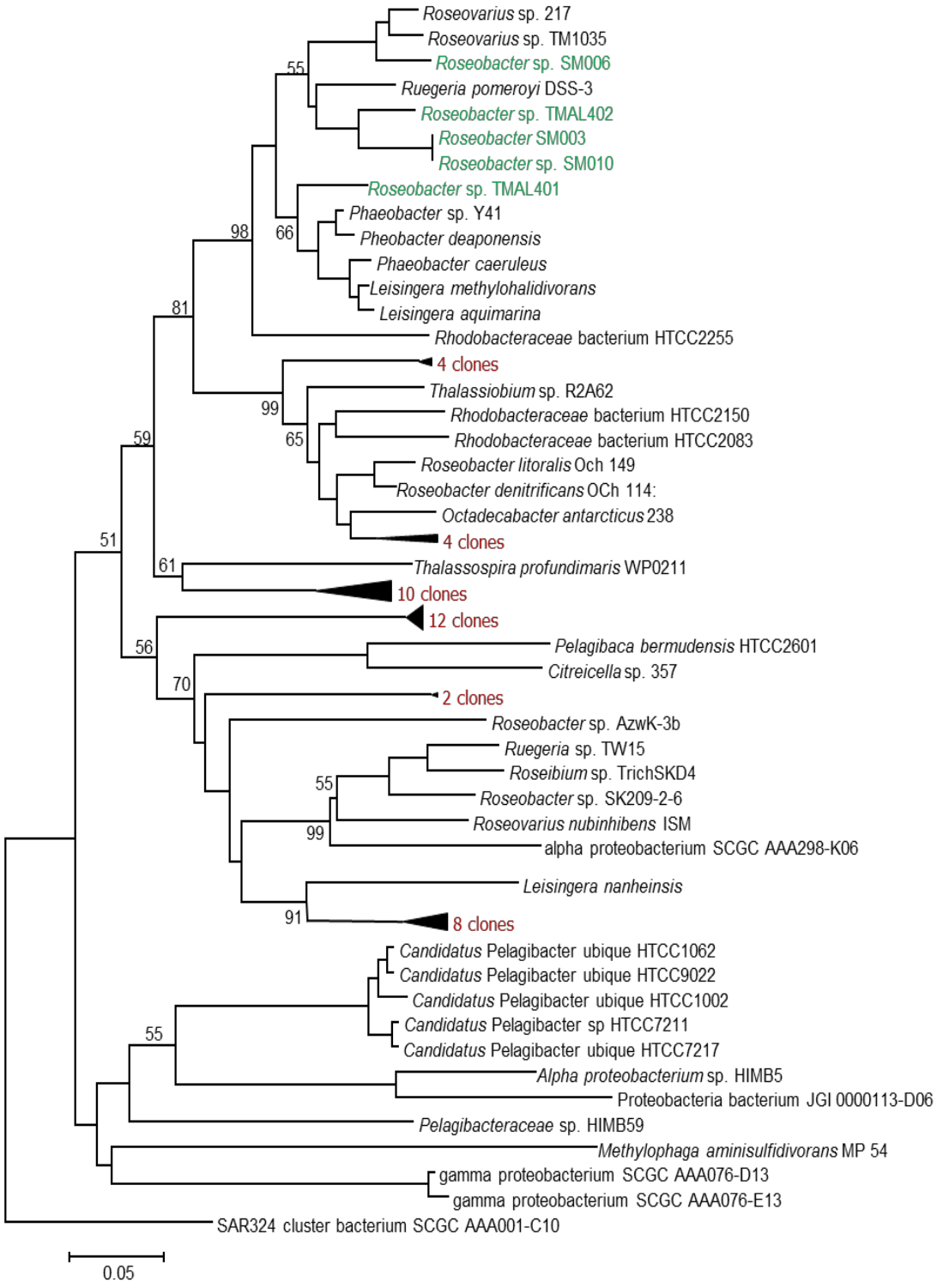

Figure 6.8. Phylogeny of marine Tdm homologs including the bacterial strains isolated using TMA or TMAO as a sole C, N and energy source. Tdm from SAR324 SCGC AAA01-C10, related to the *Deltaproteobacteria* was used to form the outgroup. ~155 amino acids were used for the alignment. Bootstrap values >50% are shown (500 replicates). The tree was constructed using the neighbour-joining method in MEGA 6.1 and evolutionary distances were calculated using the p-distance matrix. Red equals sequences retrieved from clones amplified from the saltmarsh. Green equals Tmm sequences retrieved form isolates.

Eight clones were related to the sub-cluster that contains the TMAO-only utilising bacteria (do not possess *tmm*) and may provide evidence that a sub-community is present in the seawater than specialises in TMAO-catabolism only. However, this hypothesis is tentative as *R. nubinhibens* and *Leisingera nanhaiensis* are also within this sub-cluster and both possess a *tmm* within their genomes. The Tdm homolog from *Thalassospira profundimaris*, a non-MRC isolate of the *Alphaproteobacteria* (Liu et al., 2007), appears to cluster with Tdm homologs from the MRC, suggesting a possible case for horizontal gene transfer. 10 clones retrieved from the Stiffkey saltmarsh showed highest similarity to the Tdm from *T. profundimaris*. However, as these Tdm sequences are not identical to that of *T. profundimaris* and fall within the MRC cluster, these clones may represent a novel Tdm group of MRC bacteria.

6.3.6. Growth characterisation of the MA-utilising *Roseobacter* isolates

The newly isolated strains were further tested for their growth on MAs. All strains could use MMA, DMA, TMAO or TMA (1 mM) as a sole N source alongside either succinate (5 mM) or glucose (5 mM) as a sole C source. Strain TMAL401, TMAL402 and SM006 could also grow using TMA (3 mM) or TMAO (3 mM) as a sole C and N source and are *bona fide* methylotrophs (Table 6.1). All strains could also use CAR, GBT, CHO as a sole C and N source. Growth on DSMP, methanol or other osmolytes, such as taurine or creatine as a sole C and energy source was not determined. TMAL401 was highly motile which is in agreement with the observation that *Phaeobacter* spp. are motile in order to help attachment to surfaces and entry into host systems (Porsby et al., 2008; Thole et al., 2012).

Table 6.1. Growth characterisation of the MRC isolates using different growth substrates.

Growth substrate	TMAL401	TMAL402	SM003	SM006	SM010
MMA N*	+	+	+	+	+
DMA N*	+	+	+	+	+
TMAO N*	+	+	+	+	+
TMA N*	+	+	+	+	+
MMA C^	+	+	-	+	-
DMA C^	+	+	-	+	-
TMAO C^	+	+	-	+	-
TMA C^	+	+	-	+	-
GBT	+	+	+	+	+
Choline	+	+	+	+	+
Carnitine	+	+	+	+	+
Glucose	+	+	+	+	+
Succinate	+	+	+	+	+

*Using MAs as a sole N source and succinate or glucose as the C source; ^ using MAs as a sole C source. +/- indicate a clear increase in OD_{540} compared to no carbon controls.

The strains, TMAL401 and TMAL402, were grown on TMA (3 mM) or TMAO (3 mM) as a sole C and N source, however, TMAL402 appeared to be inhibited by this concentration of TMAO. The same phenomenon was also observed when *R. pomeroyi* was grown on TMAO as a sole N source either when the starting concentration was too high (>0.5 mM) or the number of cells in the starting inoculum was too low (data not shown). Turnover of TMA and TMAO occurred within 24 hours and both strains reached an OD_{540} ~0.25 (Figure 6.9). TMAL401,

which appeared to be closely related to *Phaeobacter* spp. showed a reduction in OD_{540} during its stationary phase of growth. *Phaeobacter* spp. are well known for their production of secondary metabolites (Thole et al., 2012; Prado et al., 2009) and this strain (TMAL401) appeared to also release a secondary metabolite which resulted in a colour change of the culture medium. Upon addition of another 3 mM TMAO or TMA, cultures showed further growth and reached an OD_{540} ~0.5 and 0.6 for TMAL401 and TMAL402, respectively. After this second spike of MA, cultures rapidly removed TMA (3-3.5 mM <10 h) and TMAO (~2 mM < 10 h) from the culture medium Again, growth seized when cultures depleted all TMA or TMAO confirming that their growth is limited by MAs. TMAL401 again appeared to die off quicker than TMAL402 during this second phase of stationary growth.

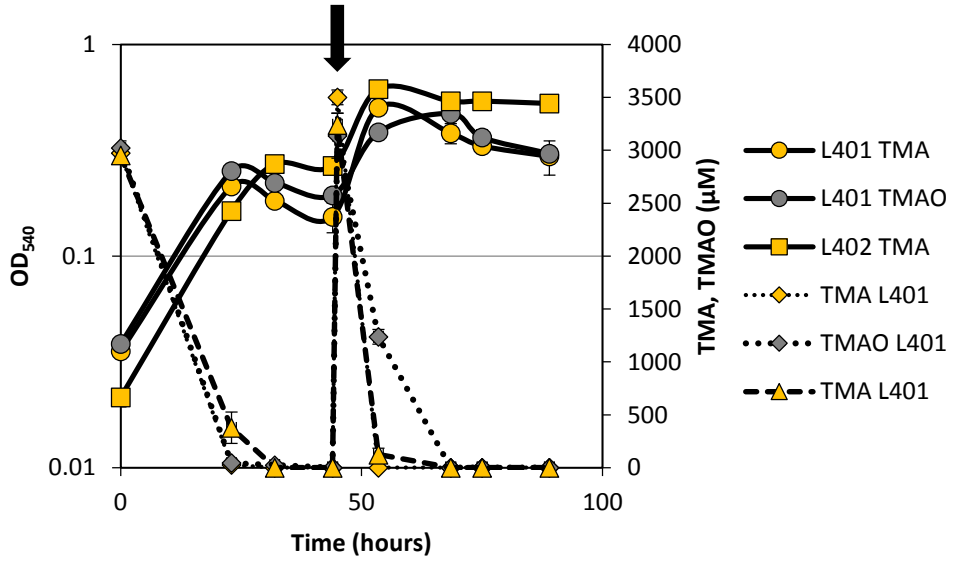

Figure 6.9. Growth of TMAL401 (circles) and TMAL402 (squares) supplemented with 3 mM TMA (yellow) or 3 mM TMAO (grey) as a sole C and energy source. Both TMA and TMAO were quantified throughout the experiment (diamonds). Cultures were grown in triplicate. Error bars denote SD. Arrow indicates the addition of TMA or TMAO.

6.4. Discussion

The data presented in this Chapter supports previous work showing that in coastal marine seawaters, representatives of the MRC, *Methylophaga* spp. are responsible for the turnover of TMA and TMAO, a class of labile low molecular weight compounds, similar to methanol, MMA and DMSP (González et al., 2000; Neufeld et al., 2007; Schäfer, 2007; Neufeld et al., 2008; Chen, 2012). *Methylophaga* spp. and other uncultured members of *Gammaproteobacteria* appear to respond to the addition of artificially high concentrations of methylated compounds, such as methanol or MMA, when these compounds represent the only source of C and energy (Neufeld et al., 2007; Schäfer, 2007; Neufeld et al., 2008). However, there is little evidence to suggest that when methylated compounds (MMA or TMA) are supplemented to seawater in conjunction with organic C sources, *Methylophaga* spp. are able to compete against heterotrophic bacteria, namely representatives from the MRC (Chen, 2012). *Methylophaga* spp. were only isolated from cultures using TMA or TMAO as a sole C, N and energy, which stimulated the growth of the methylotrophic MA-utilising microbial community (section 6.2.1). Although *Methylophaga* is a major microbial player in the turnover of methylated compounds within the Stiffkey saltmarsh when these compounds presented the only source of C and energy (Pratcher, Muhs & Schäfer, unpublished data), using TMAO as a sole N source failed to stimulate the growth of these organisms in enrichment cultures and were therefore not isolated from the saltmarsh environment in this study (Figure 6.1).

Interestingly, *Methylophaga* spp., closely related (>99% identity, 16S rRNA) to *M. thiooxidans* were isolated (*Methylophaga* sp. TMAOL401, TMAL404) from

TMAO-enriched cultures despite the fact *tdm* is not present in the genome of *M. thiooxidans*. *tdm* is present in the genome of other *Methylophaga* species, e.g. *M. aminisulfidivorans*; therefore it is possible that the strain isolated in this study may not be identical to *M. thiooxidans*, representing a different 'ecotype' which contains *tdm*. Unfortunately, the newly designed primer set were not tried on *Methylophaga* DNA as these strains were lost during the period of study. Closely related strains of the cyanobacterium, *Prochlorococcus*, are found in the marine environment, where a high-light ecotype and a low-light ecotype are separated in the water column and have divergent genome characteristics despite having <3% difference in their 16S rRNA DNA sequence (Rocap et al., 2003). Although these 'ecotypes' would be classified as a single species based on their 16S rRNA sequence similarity (Hagström et al., 2002), they have different physiological optima which is the result of a small, but changeable 'auxiliary' genome, supplementary to the core genome of *Prochlorococcus*, allowing for the rapid adaptation to changing environmental parameters (niche differentiation) (Rocap et al., 2003). A similar observation for a 'core' and 'auxiliary' genome has been used to explain the number of closely related strains related to the SAR11 clade (*Pelagibacteraceae*) that are found in the surface seawater (Grote et al., 2012). Therefore, the same evolutionary processes may be occurring in *Methylophaga* spp. that are undergoing niche diversification. Alternatively, *Methylophaga* may reduce TMAO back to TMA, using one of the DMSO/ TMAO reductases, which is then sequentially demethylated through TMADH, DMADH and MMADH or GmaSMgsABC, MgdABCD (Boden et al., 2011b; Chistoserdova, 2011). Another possibility is that TMAO-demethylating bacteria may release DMA or MMA into the enrichment culture, making them available as a growth substrate for *Methylophaga*. In Chapter 5, it was observed that

R. *pomeroyi* can turnover TMA and TMAO when no other C and energy source is available. In these experiments, DMA and MMA could sometimes be detected, especially towards the end of the growth experiments (data not shown). This suggests that these DMA and MMA can potentially be released during the catabolism of their precursors, TMA or TMAO.

Chapter 7

Quaternary amine metabolism by members of the marine *Roseobacter* clade

7.1. Introduction

In the marine environment, choline has been detected at low mM concentrations and bacteria in these environments have been shown to actively take up choline from the seawater (Roulier et al., 1990; Kiene, 1998). To date, no comprehensive study regarding the microbial-mediated cycling of choline in the marine environment exists. In estuarine waters, choline can be converted intracellularly to GBT where it can be further oxidised to CO_2 or accumulated as an osmolyte (Kiene, 1998). Bacterioplankton in the Sargasso Sea, specifically isolates related to the SAR11 clade, oxidation of the methyl groups of GBT to CO_2 leads to an increase in intracellular ATP (Sun et al., 2011). In addition, *C*. Pelagibacter ubique HTCC1062, can grow on GBT as a sole C and energy source (Carini et al., 2013). The major route for the conversion of choline to GBT is through the *betIAB* operon which has been characterised in *Escherichia coli* and also confirmed in the symbiotic bacterium, *Sinorhizobium meliloti* (see Chapter 1, section 1.6.6). The fate of GBT in these two bacteria is very different. In *E*. *coli* GBT is accumulated as an osmolyte, whilst in *S*. *meliloti*, it can be metabolised as a source of C and energy (Landfald and Strøm, 1986; Barra et al., 2006). There are two alternative pathways for the degradation of GBT, however only one has been fully characterised. This fully characterised pathway was identified in *Pseudomonas aeruginosa* and uses a GBT and dimethylglycine (DMG) demethylase that are each encoded by two separate two gene clusters, *gbcAB* and *dmgAB* (Wargo et al., 2008). In *P*. *aeruginosa*, the final demethylation step is performed by a multimeric sarcosine oxidase encoded by the four genes, *soxABDG* (Wargo et al., 2008). The genes, *gbcAB*, required for the first two steps in this pathway were not identified in

genomes of SAR11 representatives, however, a putative GBT methyltransferase related to the one identified in *S*. *meliloti* was identified (Sun et al., 2011).

In Chapter 3, it became apparent that *R*. *pomeroyi* could grow on choline, GBT and carnitine as a sole N source. In addition, the isolates, TMAL401, TMAL402, SM003, SM006 and SM010 (Chapter 6) retrieved from both station L4, off the coast of Plymouth and the salt marsh in Stiffkey, Norfolk, could also use these compounds as a sole C, N and energy source (Chapter 6). Therefore, the aims of this Chapter were to: 1) Determine the genetic and enzymatic pathways responsible for the catabolism of choline using the model organism, *R*. *pomeroyi*. 2) Screen a range of marine bacteria for the presence of these genes in order to gain a better understanding about the cycling of choline in the oceans' surface waters.

7.2 Results

7.2.5. Growth on choline and GBT can liberate NH_4^+

In Chapter 5, it was demonstrated that the turnover of methylated compounds to reducing equivalents and ATP can result in the remineralisation of organic N in the form of NH_4^+ (Chapter 5, section 5.3.6). For all marine heterotrophs growing solely on amines as a C source, QAs are N-rich compounds as the C: N ratio is 5:1 and at least 50% of the C is predicted to be dissimilated to CO_2. The hypothesis tested was that growth on choline as a C, N and energy source would result in the release of NH_4^+ whilst growth on GBT or choline as a sole N source only would not. To achieve this, *R*. *pomeroyi* was supplemented with 10 mM glucose to make N the limiting nutrient in the system. When glucose was supplemented into the medium, the C: N ratio was raised (17: 1) above normal cell stoichiometry (6:1), therefore

no NH_4^+ was detected in the culture medium despite depletion of choline or GBT (Figure 7.12A). As expected, growth on 5 mM choline or GBT as a sole C and N source resulted in the buildup of NH_4^+ (>2 mM) in the culture medium (Figure 7.12B). Together, this confirms that when N is not the limiting nutrient, remineralisation of organic N in the form of NH_4^+ can occur through the degradation of QAs.

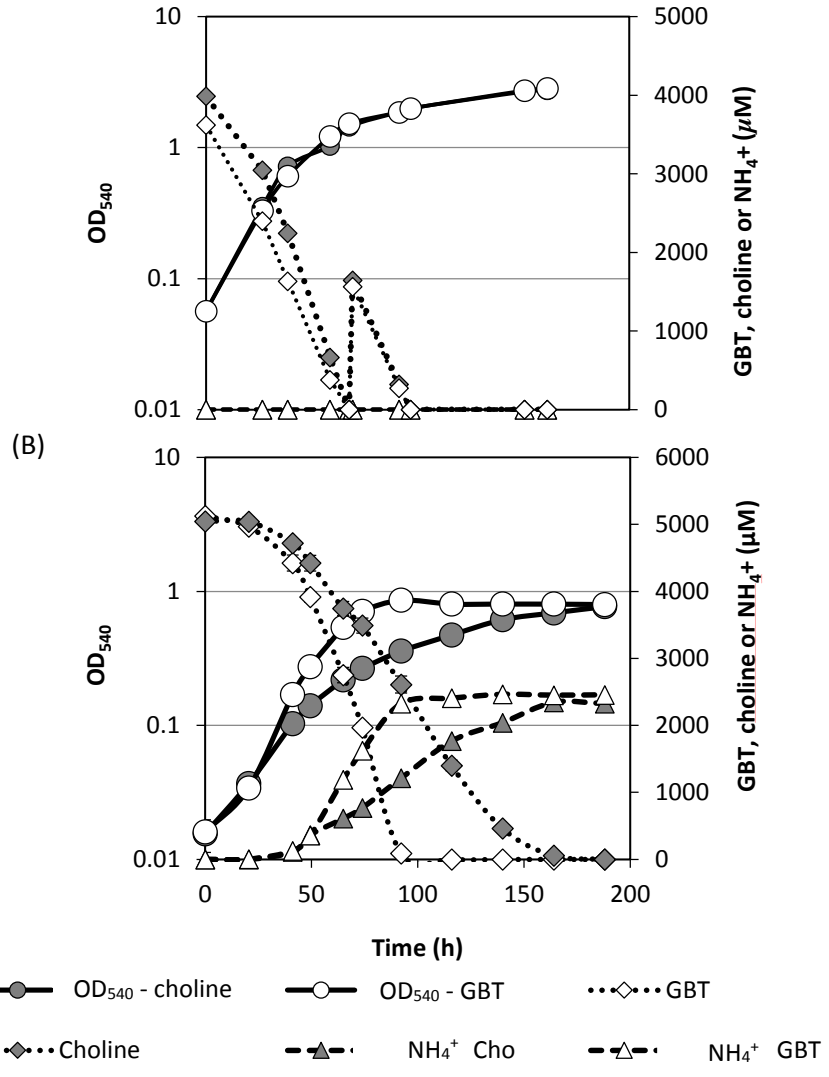

Figure 7.12. Growth of *R. pomeroyi* on choline (grey circles) or GBT (white circles) as a sole C and N source **(A)** or on choline or GBT as a sole N source with glucose (10 mM) added to the medium **(B)**. Choline (grey diamonds) and GBT (white diamonds) were quantified throughout the experiment. NH_4^+ was also quantified during the experiment in

either GBT- (white triangles) or choline-grown cultures (grey triangles). Cultures were grown in triplicate and error bars denote SD.

7.2.1. Choline catabolism to glycine betaine (GBT) requires two genes encoded by *betA* and *betB*

Figure 7.1 shows the proposed pathway for the catabolism of choline and its metabolites in *R. pomeroyi*. Using *S. meliloti* as the query genome, genes encoding enzymes for the conversion of choline to GBT by BetA (*betA*), BetB (*betB*) and the regulator (*betI*) were identified in *R. pomeroyi*. The ORF, SPO1088, corresponded to *betA* (identity 68.9%) and approximately 6 kb upstream were two ORFs annotated as genes encoding the *betI* and the gene encoding BetC (*betC*) (identity; 74.8%) (Figure 7.4). *betB* was located elsewhere in the genome, SPO0084 (69.5%).

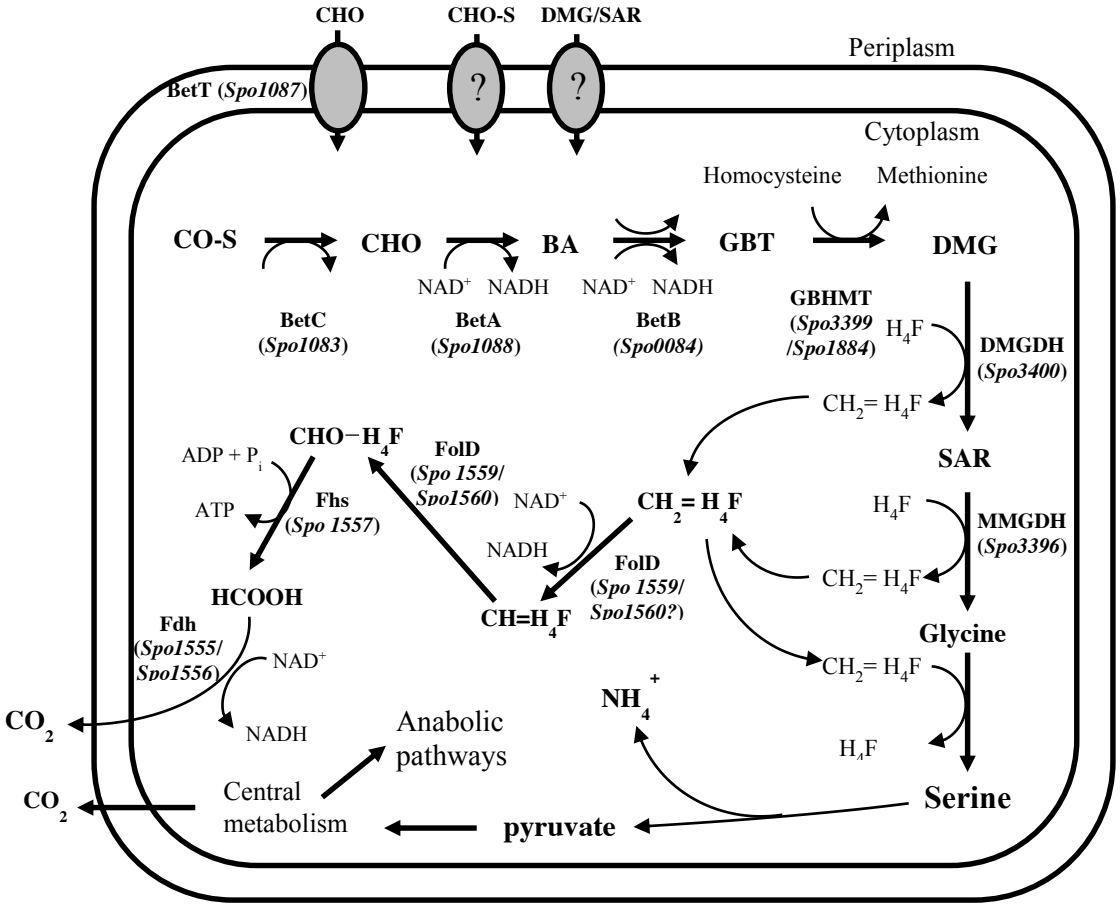

Figure 7.1 The proposed pathway of choline and choline O-sulfate catabolism in the model marine bacterium, *Ruegeria pomeroyi* DSS-3. Abbreviations; CHO, choline; GBT, glycine betaine; DMG, dimethylglycine; SAR, sarcosine; HCOOH, formate; CHO-H_4F, formyl-tetrahydrofolate; CH_2=H_4F, methylene-tetrahydrofolate; CHOΞH_4F, methenyl-tetrahydrofolate; H_4F, tetrahydrofolate; BetA, choline dehydrogenase; BetB, betaine aldehyde dehydrogenase; BetC, choline sulftase; BetT, betaine-choline-carnitine permease; BHMT, glycine betaine homocysteine methyltransferase; DMGDH, dimethylglycine dehydrogenase; MMGDH, sarcosine dehydrogenase; CO-S, choline O-sulfate; BA, betaine aldehyde; CO_2, carbon dioxide.

To confirm that the predicted *bet* genes are essential for growth on choline in *R. pomeroyi*, genetic mutants, *ΔbetA::Gm*, *ΔbetB::Gm* and also *ΔbetC::Gm* were constructed again using the marine model bacterium, *R. pomeroyi*. Although a mutant of *betC* was generated, the substrate for this enzyme (choline O-sulfate) could not be obtained before thesis completion. The mutants were constructed as previously described in Chapter 3 (Figure 7.2) and disruption of the genes was confirmed by PCR and sequencing (Figure 7.3).

(A)

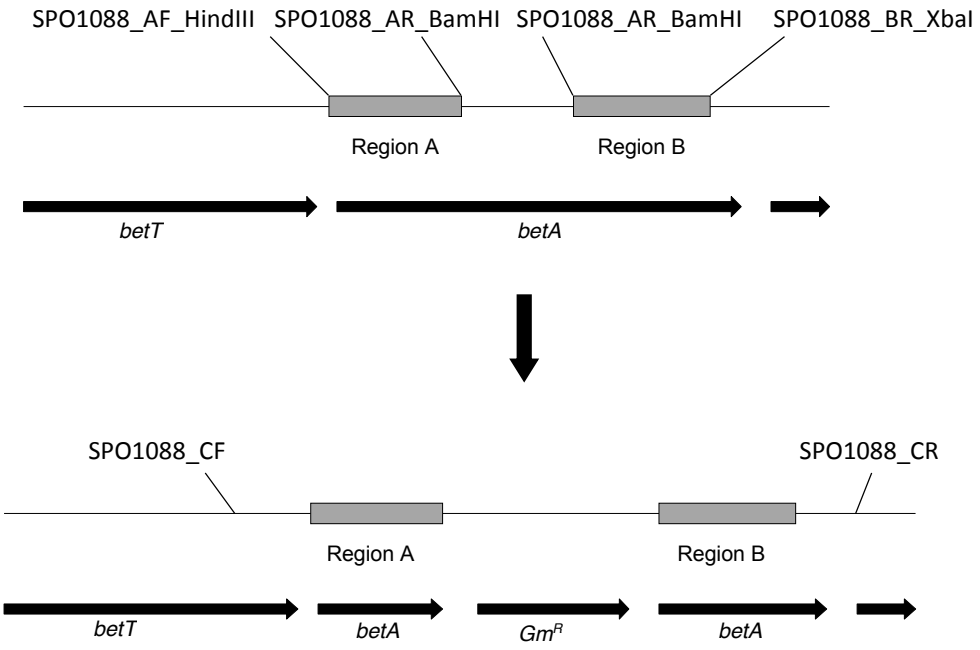

(B)

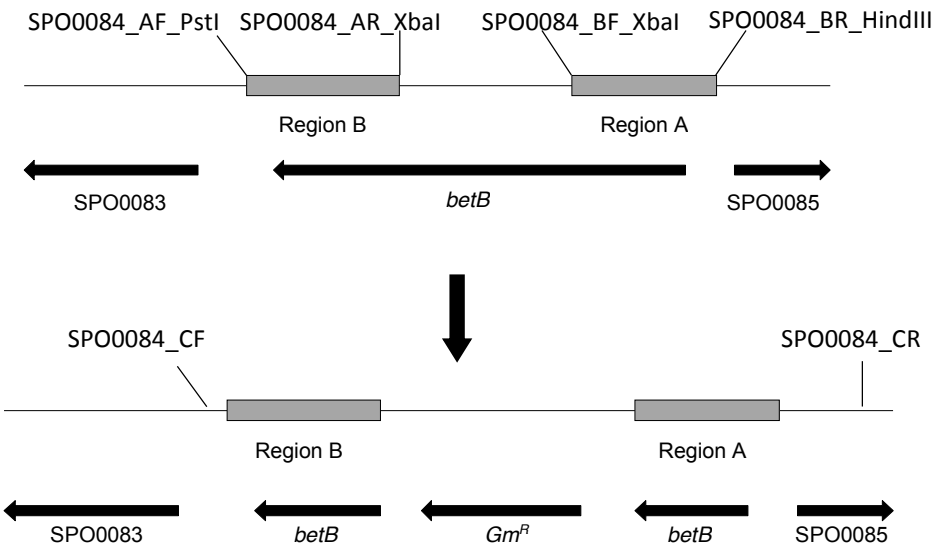

Figure. 7.2 (A) Genetic map outlining mutagenesis of *betA* showing the primers and restriction sites used to complete the construct. **(B)** Genetic map outlining mutagenesis of *betB* showing the primers and restriction sites used to complete the construct. Abbreviations: Gm^R, gentamicin resistance cassette; *betT*, choline permease, *betA*, choline dehydrogenase; *betB*,betaine aldehyde dehydrogenase.

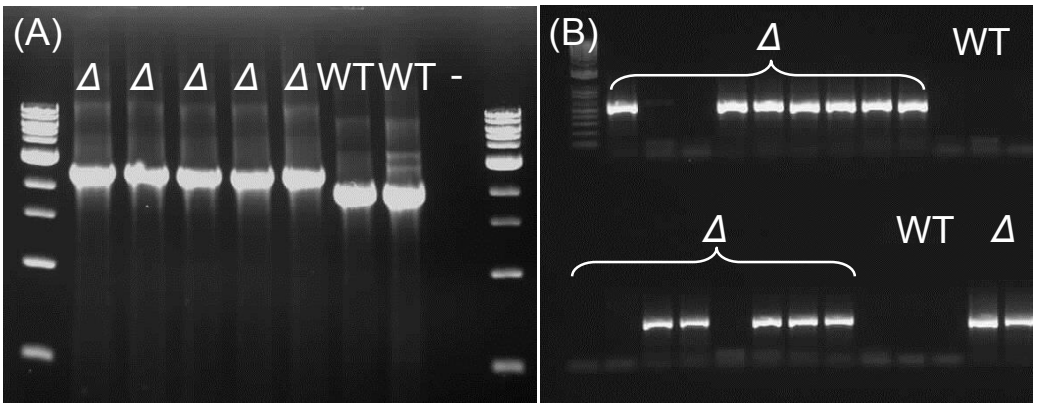

Figure. 7.3 PCR confirmation of the double cross-over mutant, *ΔbetA::Gm* **(A)** using the primers SPO1088_CF/CR and the mutant, ***ΔbetB::Gm***, using the primers SPO0084_CF/CR in conjunction with Gent_F/R **(B)**.

Wild-type *R. pomeroyi* grew well on choline (μ = 0.0731 ± 0.003 h^{-1}) and GBT (μ = 0.0860 ± 0.001 h^{-1}) and a total of 5 mM GBT or choline was completely removed from the culture medium after 72 and 95 h, respectively (Figure 7.4A). For the

mutant strains, *ΔbetA::Gm*, *ΔbetB::Gm*, growth on GBT was not affected whilst growth on choline was either fully or partially inhibited, respectively. The *ΔbetA::Gm* mutant failed to grow on choline as a sole C source and no depletion of choline from the medium was observed (Figure 7.4B). The *ΔbetB::Gm* mutant could still grow on choline as a sole C and energy source (Figure 7.4C), however the growth rate (μ = 0.0467 ± 0.008 h^{-1}) was reduced compared to that of the wild-type. During growth experiments on choline with *ΔbetB::Gm*, a transient build-up of betaine aldehyde was detected in the culture medium that was not detected in the wild-type cultures (data not shown). *R*. *pomeroyi* has a number of genes that may encode a similar aldehyde dehydrogenase and it is likely that one of these similar enzymes was able to perform the same function as BetB, albeit at a reduced efficiency.

Wild-type *ΔbetA::Gm*

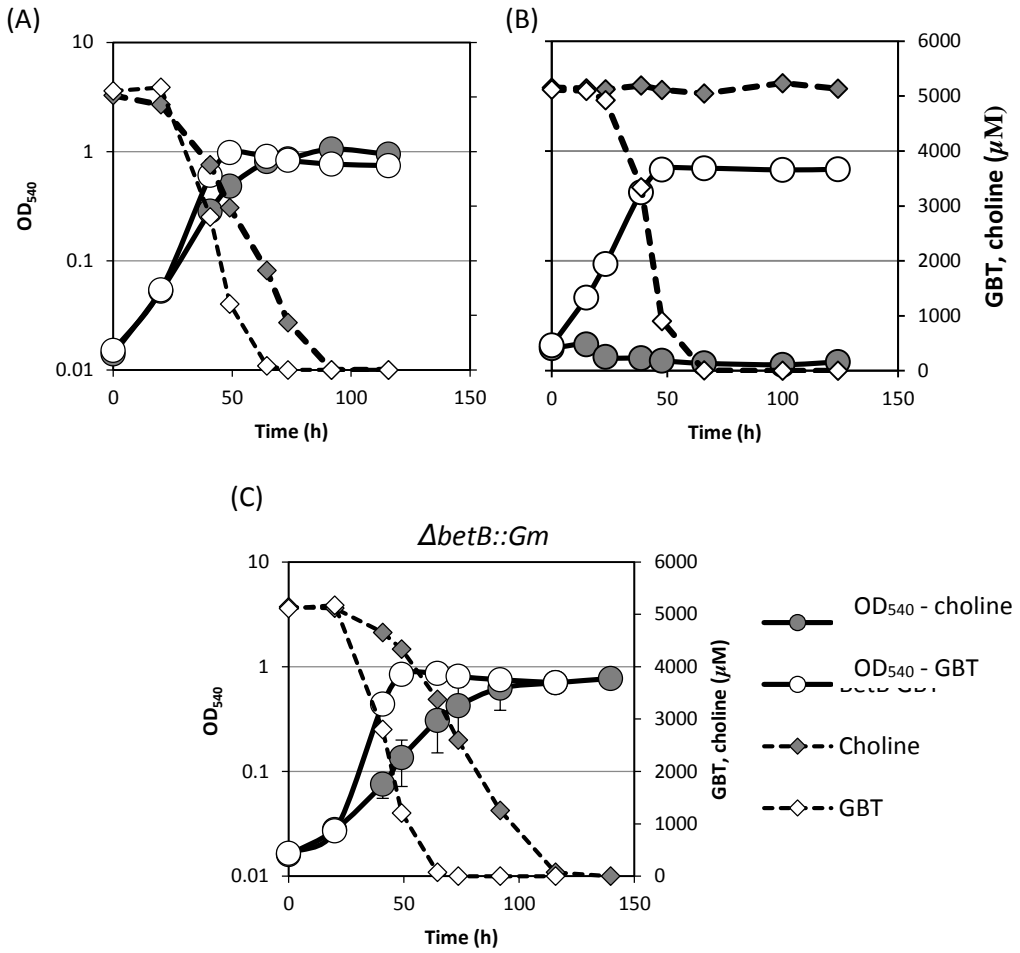

Figure 7.4. Growth of *Ruegeria pomeroyi* on either choline (grey circles) or GBT (white circles) as the sole C source using either the **(a)** Wild-type **(b)** the *ΔbetA::Gm* mutant or **(c)** the *ΔbetB::Gm* mutant. Cultures were grown in triplicate and error bars denote SD. Choline (grey diamonds) and GBT (white diamonds) concentrations were determined throughout the experiment.

7.2.2. The bet operon is widely distributed in the MRC of the *Alphaproteobacteria* and in *Vibrio* spp. of the *Gammaproteobacteria*

To better understand the potential importance of choline metabolism in the MRC, the genomes of various isolates from the MRC were screened for the presence of the *betABC* genes. 51/52 isolates of the MRC bacteria screened had the *betA* in their genomes whilst 49/52 had *betC* and 37/42 had *betB* (Table 7.1). It is interesting that not all strains possess *betB* as this gene was clearly involved, but not essential for

growth on choline in *R. pomeroyi* (Section 7.2.1). In the majority of isolates from the MRC, the *betIABC* genes are found in a single operon, for example in the isolates, *Roseobacter* sp, Azwk-3b and *Sagittula stellata* E-37 (Figure 7.5). Using BetA from *R. pomeroyi* as the query sequence, a BLASTp database was generated using the JGI-IMG database (Chapter 3). It was discovered that *betIAB*, but not *betC*, is also present in many isolates from the *Gammaproteobacteria*, particularly marine *Vibrio* strains (Figure 7.5A).

14 MRC isolates were screened for their ability to grow on choline and GBT as a sole C and energy source (Table 7.1) as well as the newly isolated TMAO/TMAO-utilising strains (Chapter 6). Growth on choline and GBT as a sole C source directly correlated with the presence of the *bet* genes in their genomes. *Dinoroseobacter shibae* DFL12 was the only bacterium of the MRC that does not possess any of the *bet* genes and failed to grow on choline or GBT. The capability to use either choline of GBT is more widespread within the MRC investigated than the ability to utilise MAs, such as TMA. This may reflect the fact that choline and GBT may be more abundant in the particular niches that these MRC isolates occupy.

Table 7.1 Comparative genomic analysis of genes involved in the catabolism of choline and downstream metabolites, GBT, DMG and sarcosine and growth on choline and GBT in genome-sequenced isolates of the MRC.

Strain	BetA	BetB	BetC	BetT	ChoX	F II	F I	Mmgdh	Dmgdh	SoxABDG	DMGDH II	DgcAB	GbcA	GbcB	CHO	GBT
Citreicella sp.SE45	+	+			+					+	+		+	+	+	+
Citreicella sp. 357	+	+			+					+	+		+	+	NT	NT
Dinoroseobacter shibae DFL12						+	+			+					-	-
Leisingera aquimarina DSM 24565	+	+	+	+		+	+	+	+				+	+	+	+
Leisingera nanhaiensis NH52F	+		+			+	+	+	+						+	+
Loktanella hongkongensis DSM 17492	+		+		+		+			+					NT	NT
Loktanella sp. SE 62	+	+			+		+						+	+	NT	NT
Loktanella vestfoldensis DSM16212	+	+	+		+	+	+		+						NT	NT
Loktanella vestfoldensis SKA53	+	+	+		+	+	+	+	+	+					NT	NT
Maritimibacter alkaliphilus HTCC2654	+	+	+		+		+	+					+	+	NT	NT
Oceanibulbus indolifex HEL45	+	+	+		+		+	+	+						NT	NT
Oceanicola batensis HTCC2597	+	+	+				+								NT	NT
Oceanicola granulosus HTCC2516	+	+	+		+		+			+			+	+	NT	NT

Oceanicola sp. S124	+	+	+		+		+	+					+	+	NT	NT
Octadecabacter arcticus 238	+		+		+	+	+	+	+						NT	NT
Octadecabacter antarcticus 307	+		+		+	+	+	+	+						NT	NT
Pelagibacter bermudensis HTCC2601	+	+	+		+		+			+	+		+	+	NT	NT
Phaeobacter arcticus DSM 23566	+	+	+	+		+	+	+	+				+	+	NT	NT
Phaeobacter caeruleus	+	+	+	+		+	+	+	+				+	+	NT	NT
Phaeobacter daeponensis TF-218	+	+	+	+		+	+	+	+				+	+	NT	NT
Phaeobacter gallaeciensis ANG1	+	+	+	+		+	+	+	+				+	+	NT	NT
Phaeobacter gallaeciensis DSM17395	+	+	+	+			+	+	+				+	+	+	+
Phaeobacter gallaeciensis 2.10	+	+	+	+			+	+	+				+	+	+	+
Phaeobacter inhibens T5	+	+	+	+			+	+	+				+	+	NT	NT
Phaeobacter sp. Y41	+		+	+		+	+	+	+				+	+	NT	NT
Rhodobacteraceae bacterium KLH11	+		+			+	+	+	+						NT	NT
Rhodobacteraceae bacterium HTCC2083	+	+	+			+	+	+	+						NT	NT
Rhodobacteraceae bacterium HTCC2150	+		+			+	+	+	+						NT	NT

Rhodobacteraceae bacterium HTCC2255	+	+	+			+	+	+	+						NT	NT
Roseobacter denitrificans Och 114	+	+	+			+	+	+	+	+					NT	NT
Roseobacter litoralis Och 149	+	+	+			+	+	+	+						+	+
Roseobacter sp. AawK-3b	+	+	+		+	+	+	+	+						NT	NT
Roseobacter sp. CCS2	+		+		+	+	+	+	+						NT	NT
Roseobacter sp. GAI101	+		+		+	+	+	+	+						NT	NT
Roseobacter sp. LE17	+	+			+	+	+	+	+						NT	NT
Roseobacter sp. MED193	+	+	+	+		+	+	+	+						+	+
Roseobacter sp. R2A57	+		+	+		+	+	+	+						NT	NT
Roseobacter sp. SK209-2-6	+	+	+	+			+	+	+				+	+	+	+
Roseovarius nubinhibens ISM	+		+			+	+	+	+						+	+
Roseovarius sp. TM1035	+		+		+	+	+	+	+						+	+
Roseovarius sp. 217	+		+		+	+	+	+	+						+	+
Ruegeria lacuscaerulensis ITI-1157	+	+	+			+	+	+	+						NT	NT
Ruegeria pomeroyi DSS-3	+	+	+	+		+	+	+	+						+	+

Ruegeria sp. TM1040	+	+	+	+			+			+			+	+	NT	NT
Ruegeria sp. TrichCH4B	+	+	+	+			+			+			+	+	NT	NT
Ruegeria sp. TW15	+	+	+			+	+	+	+						NT	NT
Ruegeria sp. R11	+	+	+	+			+	+	+						NT	NT
Sagittula stellata E-37	+				+	+	+	+	+				+	+	+	+
Sulfitobacter sp. EE-36	+	+	+	+	+		+								NT	NT
Sulfitobacter NAS-14.1	+	+	+	+	+		+								NT	NT
Thalassiobium sp. R2A62	+	+	+			+	+	+	+						NT	NT
Wenxinia marina DSM24838	+	+	+		+		+								NT	NT

Abbreviations: BetA, choline dehydrogenase; BetB, betaine aldehyde dehydrogenase; BetC, choline sulfatase; BetT, BCCT-type choline permease; ChoX, choline substrate binding protein; FII, betaine homocysteine methyltransferase form II; FI, betaine homocysteine methyltransferase form 1; Mmgdh, sarcosine dehydrogenase; Dmg dehydrogenase; soxABDG, multimeric sarcosine oxidase; Dmgdh II, dimethylglycine dehydrogenase homolog; DgcAB, dimethylglycine demethylase; GbcA, GBT demethylase alpha subunit; GbcB, GBT demethylase, beta subunit. +/- indicates presence of absence of genes in microbial genomes or testing positive or negative for growth based on OD_{540}.

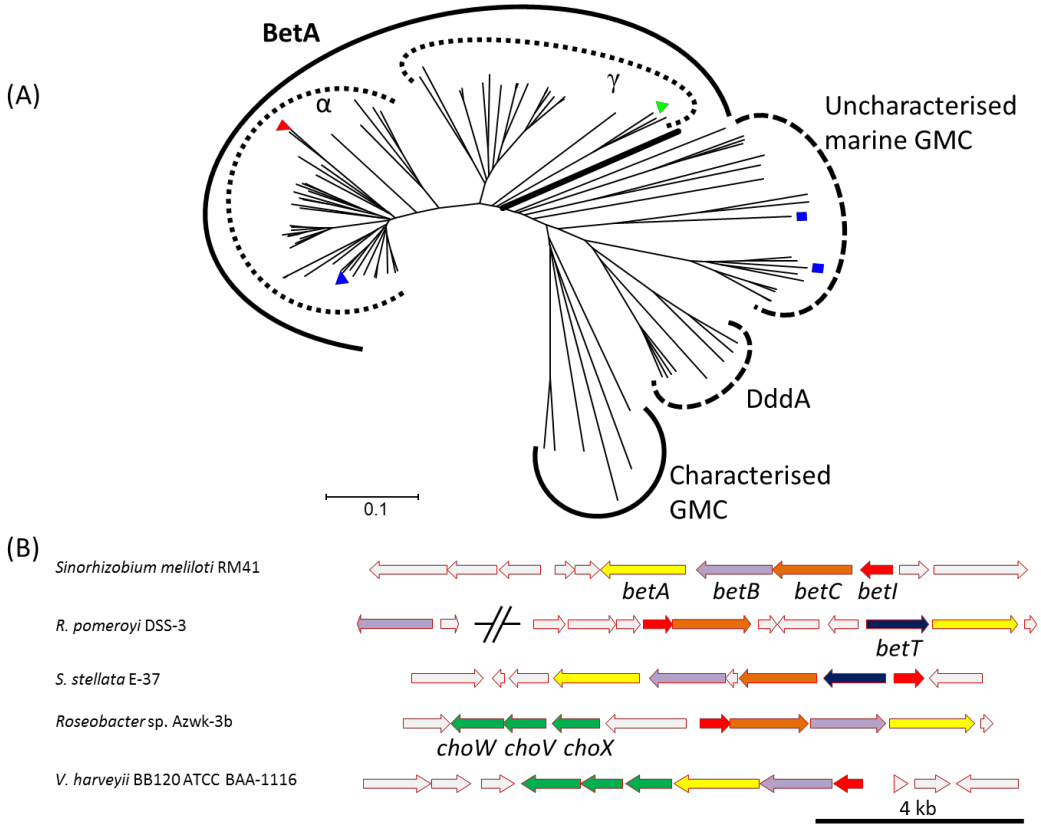

Figure 7.5. Phylogenetic analysis of choline dehydrogenase (BetA) using the neighbour-joining method **(A)**. Values at nodes represent bootstrap values from 500 replications. The tree was constructed using MEGA 5.2 (Tamura et al., 2011). Evolutionary distances were calculated using the p-distance matrix. The out group was formed using the *bona fide* DddA sequence from a number of MRC isolates. **(b)** Genetic neighbourhoods of *bet* genes in representative marine bacterial isolates and the soil bacterium, *S. meliloti*. Abbreviations; *α*, *Alphaproteobacteria*; *γ*, *Gammaproteobacteria*; dddA, 3-hydroxypropionate dehydrogenase; GMC, glucose-methanol-choline dehydrogenase; BetA, choline dehydrogenase; *choX*, substrate binding protein of choline ABC transporter; *choV*, ATP-binding domain of choline ABC transporter; *choW*, transmembrane permease of choline ABC transporter; *betI*, regulator of *bet* operon; *betT*, choline permease, *betA*, choline dehydrogenase; *betB*, betaine aldehyde dehydrogenase; *betC*, choline sulfatase.

7.2.3. BetT is required for rapid growth on choline in *R. pomeroyi*

In *R. pomeroyi*, directly upstream of *betA* is *betT* (SPO1087), annotated as a BCCT-type transporter (Figure7.5b). A homolog similar to SPO1087 is known to be responsible for the uptake of extracellular choline in *E. coli* (Lamark et al., 1991). Interestingly, not all the isolates from the MRC have BetT (Table 7.1). Instead some MRC bacteria (e.g. *Roseovarius* sp. 217, *Octadecabacter arcticus* 238) have three ORFs, immediately upstream of the *betIABC* genes which are annotated as genes encoding three subunits of an ABC-type choline transporter (ChoXWV) (Chen et al., 2010). Phylogenetic analysis of the putative ChoX from MRC bacteria (Figure 7.6) revealed a close relationship with the ChoX from *S. meliloti* (Chen et al., 2010), suggesting that this gene is likely involved in choline metabolism. All isolates from the MRC (apart from *Sulfitobacter* spp.) either have the BetT-type or the ChoX-type choline transporter (Table 7.1). The presence of the BetT-type transporter is associated with MRC subclades one and two as defined by Newton et al. (2010) (see Chapter 1, section 1.10) whilst the ABC-type choline transporter, ChoXWV, is associated with MRC subclades three and four and *Vibrio* spp. (Figure 7.5b). It should be noted that neither the BetT-type or ChoXWV-type transporters were present in some MRC isolates which do possess the *betABC* genes in their genomes (e.g. *Leisingera aquimarina*), suggesting the existence of another as yet unidentified choline transporter.

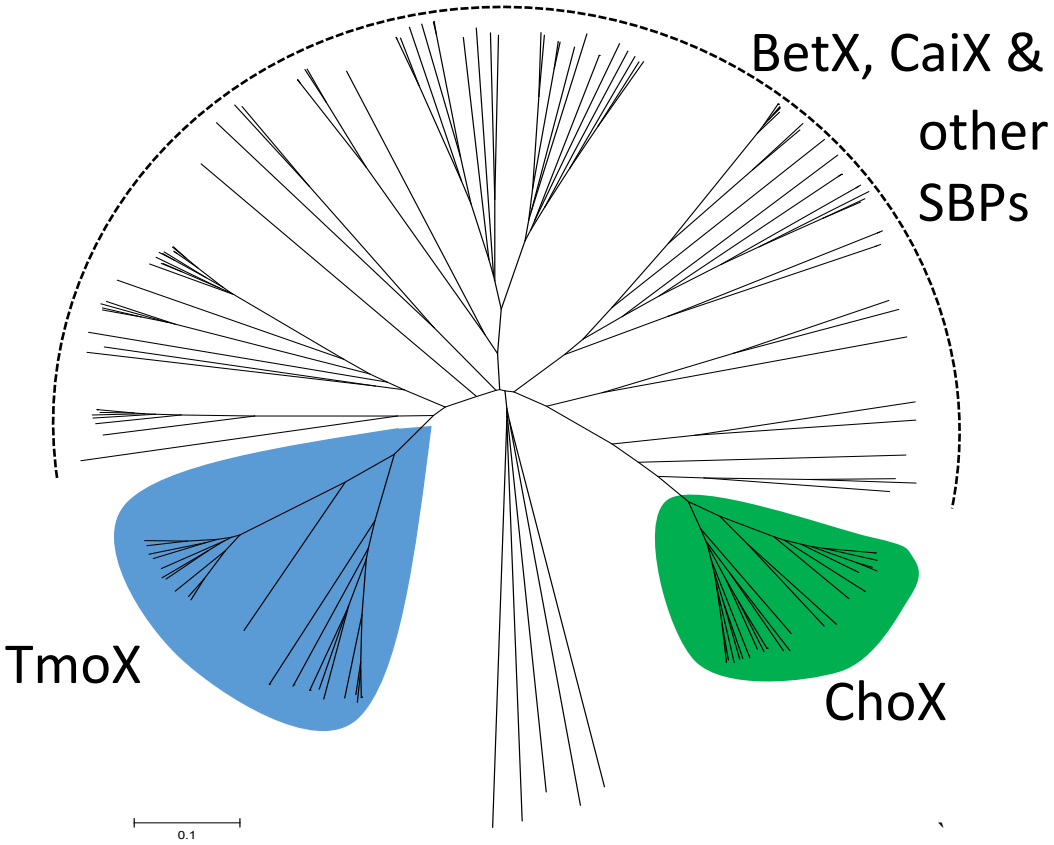

Figure 7.6. Phylogenetic analysis of the SBP (ChoX) using the neighbour-joining method. The tree was constructed using MEGA 5.2 (Tamura et al., 2011). The out group was formed using SBPs from cluster F based on the phylogenetic classification conducted by (Berntsson et al., 2010). Evolutionary distances were calculated using the p-distance matrix. The tree is similar to the one previously shown in Chapter 3, section 3.2.2.2. Abbreviations: ChoX, SBP specific for choline; TmoX, SBP specific for TMAO; BetX, specific for GBT; CaiX, SBP specific for carnitine.

To investigate the role of *betT* in choline metabolism in *R. pomeroyi*, the mutant *ΔbetT::Gm* was constructed. Confirmation of a double crossover event (homologous recombination) was confirmed where insertion of the gentamicin resistance cassette resulted in a greater sized PCR product amplified using the primers, SPO1087_CF/CR, compared to the wild-type with the native *betT* (Figure 7.7). The mutant could still grow on choline as its sole C source and energy, however the growth rate (μ = 0.0121 ± 0.002 h^{-1}) was reduced compared to that of the wild-type (μ = 0.0731 ± 0.003 h^{-1}) (Figure 7.8). Consequentially, the rate of choline depletion from the culture medium was significantly reduced compared to that of the wild-type (section 7.2.1). The fact that the *ΔbetT::Gm* mutant could still

grow on choline confirms that the downstream gene, *betA*, was still expressing a functional BetA in this mutant. Therefore, inactivation of *betT* does any not cause polar effect on downstream gene expression.

(A)

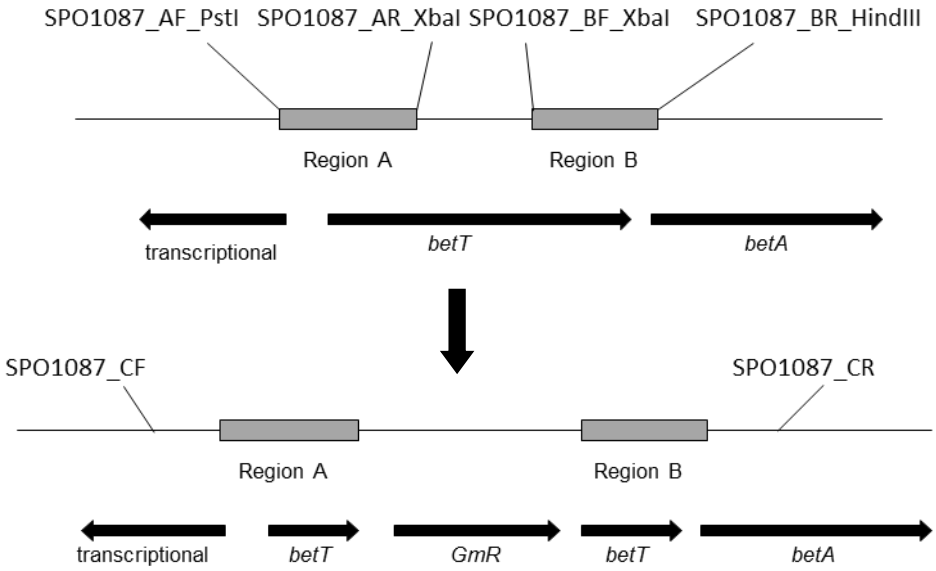

(B)

Figure 7.7. (A) Genetic map outlining mutagenesis of *betT* showing the primers and restriction sites used. **(B)** Confirmation of the double crossover mutant, *ΔbetT::Gm*, by PCR using the primers Spo1087_CF and Spo1087_CR. Lanes 1-4 are *ΔbetT::Gm*, lanes 5,6 are wild-type, lane 7 is a no template control. Abbreviations: transcriptional, unknown transcriptional regulator.

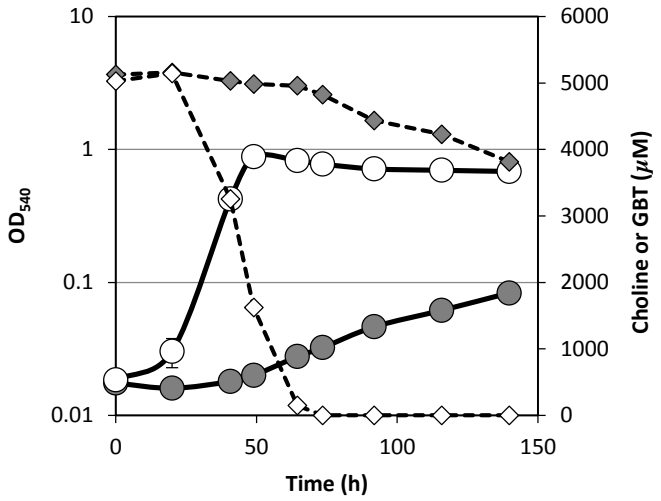

Figure 7.8. Growth of the mutant, *ΔbetT::Gm*, on either choline (grey circles) or GBT (white circles) as the sole C source. Choline (grey diamonds) and choline (white diamonds) were quantified throughout the experiment. Cultures were grown in triplicate and error bars denote SD.

7.2.4. GBT catabolism in the MRC

Two distinct classes of enzymes are involved in aerobic GBT catabolism to dimethylglycine (DMG) in bacteria. One is a GBT demethylase (GbcAB) encoded by *gbcAB* in *P. aeruginosa* (Wargo et al., 2008) and the other is a GBT homocysteine methyltransferase (BHMT) found in *S. meliloti* (Barra et al., 2006). Using the BHMT gene (SMc04325) from *S. meliloti* as a query, a homolog in *R. pomeroyi*, SPO1884 was identified (identity 57%). This gene is present in 50/52 isolates from the MRC (Table 1), hereafter called BHMT Form I. A second homolog was also found in *R. pomeroyi*, albeit with lower homology to the BHMT in *S. meliloti*, SPO3398 (identity 27%), hereafter called BHMT Form II. Form II was less prevalent among the MRC isolates, present in only 32/52 genomes. *Citreicella* sp. SE45 and *Citreicella* sp. 357 do not possess either form of BHMT, but they do have genes that share homolog (see below for details) with *gbcAB* (Wargo et al, 2009). Phylogenetic analysis revealed that BHMT form II is more

closely related to the eukaryotic BHMTs and SAR11 homologs (Sun et al., 2011), whilst form I is closely related to the experimentally-validated BHMT from *S. meliloti* (Figure 7.9).

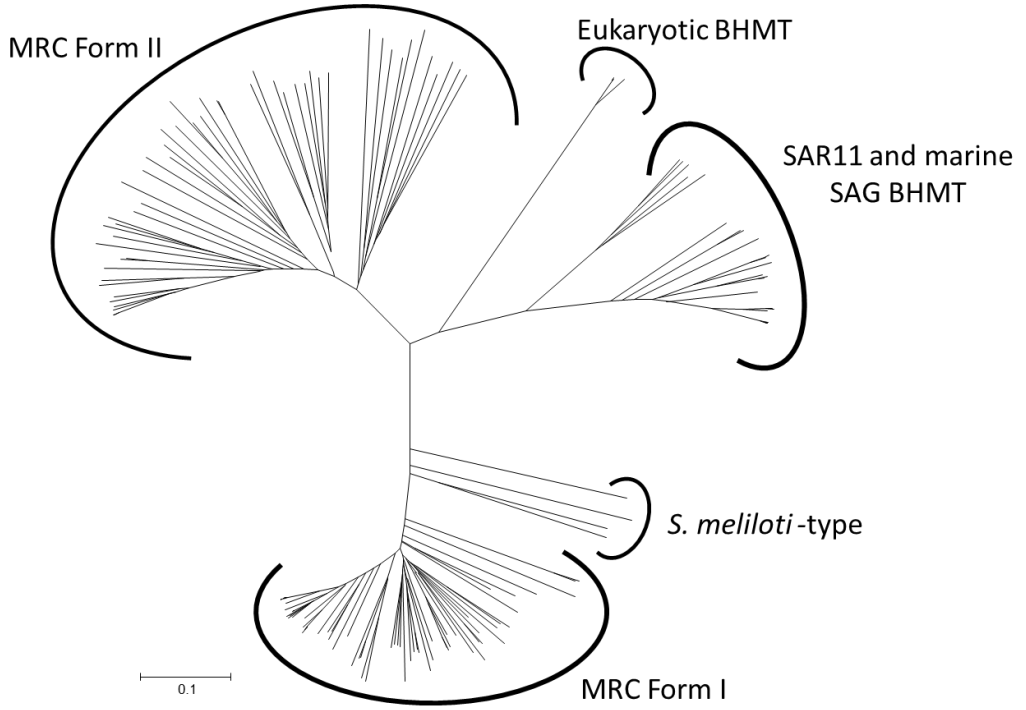

Figure 7.9. Phylogenetic analysis of the putative glycine betaine homocysteine methyltransferase (BHMT) identified within the genomes of marine bacteria. Evolutionary distances were calculated using the p-distance matrix using amino acid sequences. Eukaryotic BHMT and BHMT from *S. meliloti* were included as reference sequences. A number of other closely related homologs were also included. The tree was constructed in MEGA 5.2 (Tamura et al., 2011) using the neighbour-joining method. Values at the modes represent bootstrap values from 500 replications.

BHMT form II is located within a cluster containing genes encoding for an alcohol dehydrogenase (SPO3399), an AraC-type regulator (SPO3397), two aminomethyltransferases (SPO3400, SPO3396), and three smaller genes encoding a LysE transporter (SPO3402), a DNA binding protein (XRE-type repressor, SPO3403) and a hypothetical protein (SPO3401). This genetic arrangement is shown in Figure 7.10. The two aminomethyltransferases have low homolog to the mitochondrial sarcosine and DMG dehydrogenases found in mammalian cells and it is therefore predicted that these two ORFs (SPO3400, SPO3396) may encode enzymes for the simultaneous demethylation of DMG and sarcosine forming glycine (Figure 7.1). The two aminomethyltransferases are found in the majority of MRC genomes and are often found in the same gene arrangement as found in *R. pomeroyi*. However, in some strains, BHMT form II and also the AraC-type regulator are absent from the genomes, suggesting that form II of the BHMT may not be essential for the catabolism of GBT. This may be explained by the fact that all but two MRC isolates have the BHMT I which has a greater similarity to the *bona fide* BHMT from *S. melilloti*.

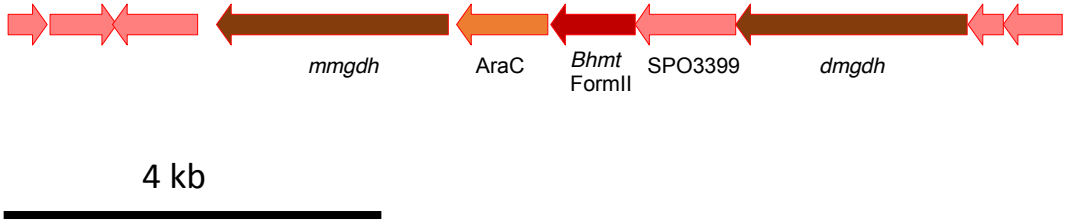

Figure 7.10. Genetic neighbourhood of BHMT form II. Abbreviations: mmgdh, sarcosine dehydrogenase; AraC, transcriptional regulator AraC-type; Bhmt Form II, GBT methyltransferase, SPO3399, alcohol dehydrogenase; dmgdh, dimethylglycine dehydrogenase. Scale bar denotes length in kbps.

Two ORFs annotated as genes encoding a sarcosine dehydrogenase and a DMG dehydrogenase were also found in the genomes of SAR11 clade bacteria (Sun et al., 2011). These share approximately 40-45% sequence identity and 37-39% at the amino acid level, respectively to the homologs in *R*. *pomeroyi*. Besides using a monomeric sarcosine dehydrogenase, bacteria can also demethylate sarcosine by using a multimeric sarcosine oxidase which is made up of four sub units, alpha (SoxA), beta (SoxB), gamma (SoxG) and delta (SoxD). *R*. *pomeroyi* has three *soxABGD* gene clusters predicted to encode the multimeric sarcosine oxidase, however one of these clusters encodes the enzymes involved in the metabolism of MMA (Latypova et al., 2010; Chen, 2012). The other two share reasonable homology (SoxB, 57% identity) with the *bona fide* sarcosine oxidase from *Corynebacterium* (Chlumsky et al., 1995). *soxABDG* is also found within the genomes of SAR11 strains (Sun et al, 2011), therefore it cannot be ruled out that there is some redundancy in this pathway, however this has to be confirmed experimentally.

Citreicella sp. SE45, which can still grow on choline and GBT despite lacking BHMT, does have two ORFS (CSE45_5278, CSE45_5279) which share modest homology with *gbcA* (identity 48.98%) and *gbcB* (identity 47.58%). *Citreicella* sp. SE45 also lacks homologs for either the sarcosine or DMG dehydrogenases found in other MRC isolates. However, adjacent to *gbcAB*, there are ORFS annotated as genes encoding the four subunits of the multimeric sarcosine oxidase (*soxABDG*) (Figure 7.11). In this region a DMG dehydrogenase, different to the DMG dehydrogenase in other MRC isolates, is also present. *gbaAB* were also found in a number of other MRC isolates and apart from *Phaeobacter* strains, were usually found in isolates lacking form II (Table 7.1).

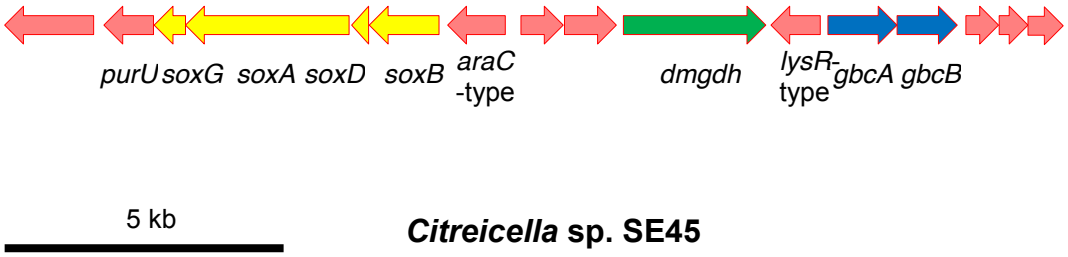

Figure 7.11. Genetic neighbourhood of the putative genes involved in GBT metabolism in *Citreicella* sp. SE45. Abbreviations: *purU*, formate-tetrahydrofolate deformylase; *soxG*, sarcosine oxidase gamma subunit; *soxA*, sarcosine oxidase alpha subunit; *soxD*, sarconsine oxidase delta subunit; *soxB*, sarcosine oxidase beta subunit, *dmgdh*, dimethylglycine dehydrogenase; *gbcA*, GBT methyltransferase alpha subunit; *gbcB*, GBT methyltransferase beta subunit.

7.2.6. The role of Fhs in methyl group oxidation of MAs and QAs

The two aminomethyltransferases, predicted to be involved in the sequential demethylation of DMG and sarcosine have H_4F binding domains, similar to that of the recently identified Tdm (Chapter 3). Therefore, the sarcosine and DMG dehydrogenases are likely to be involved in the conjugation of H_4F and formaldehyde released during the demethylation of DMG and sarcosine, producing methylene-H_4F. To determine the role of *fhs*, the gene that encodes formyl-H_4F synthetase (Fhs) in the oxidation of methyl groups during growth on choline, the *fhs* null mutant that was previously generated in Chapter 5 was further characterised. Compared with the growth rate of the wild-type (μ = 0.073 ± 0.003 h^{-1}), the *fhs* null mutant had a significantly reduced growth rate (μ = 0.033 ±.008 h^{-1}) and final growth yield (*fhs* null mutant OD_{540} = 0.27, wild-type OD_{540} = 1.17) when grown on choline as a sole C source (Figure 7.13A). In the *fhs* null mutant cultures, the initial rate of choline depletion was slower than that of the wild-type, however complete degradation of choline still occurred. During the experiment, in *fhs* null mutant cultures, there was a gradual build-up of the metabolite, GBT

(Figure 7.13B). However in the wild-type cultures, only a transient spike in GBT was observed. The complemented *fhs* mutant had a partially restored growth rate (μ= 0.050 ± 0.002 h^{-1}) and final growth yield (OD_{540} = 0.84) (Figure 7.13A), due to the restored ability to utilise GBT (Figure 7.13B).

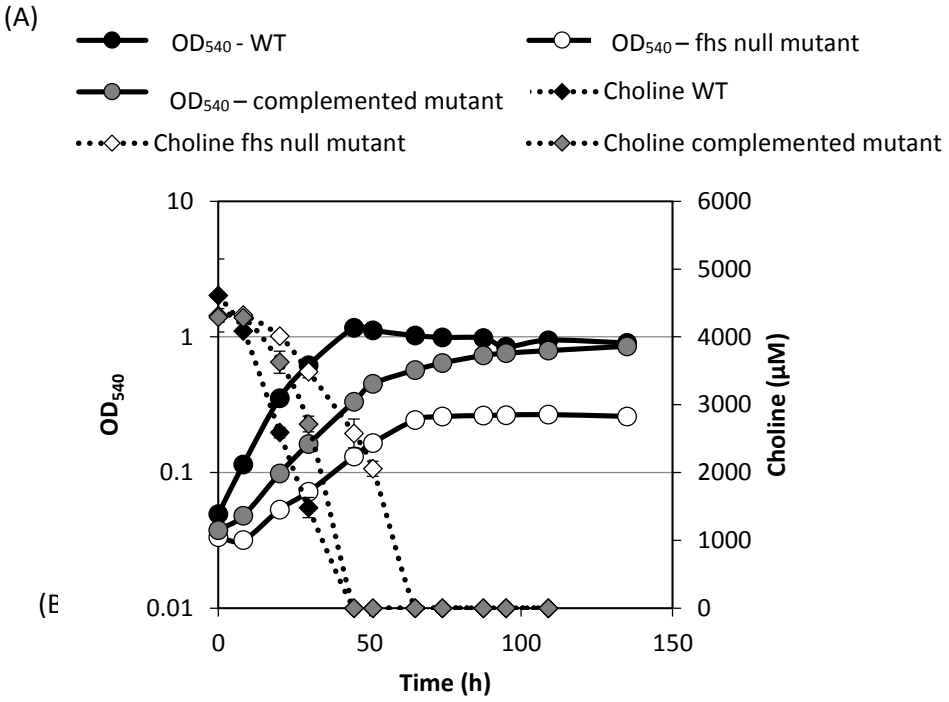

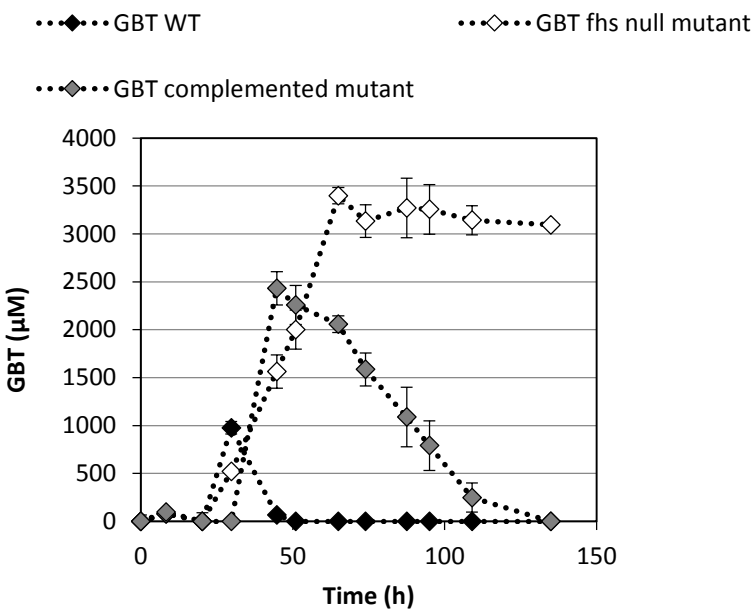

Figure 7.13. Growth (circles) of the *R*. *pomeroyi* wild-type (black), *fhs* null mutant (white), and complemented mutant (grey) on choline (5mM) (diamonds) as a sole C, N and energy source **(A)**. GBT (diamonds) in the culture medium was quantified throughout growth **(B)**. Cultures were grown in triplicate and error bars denote SD.

To determine whether the *fhs* mutation affected growth on the downstream methylated-metabolites of choline catabolism, the wild-type, the *fhs* null mutant and the complemented mutant were grown on either glycine, sarcosine, DMG or GBT as a sole C and energy source. For wild-type cells, the final OD_{540} of the cultures showed a positive correlation with increasing number of methyl groups, with growth on glycine resulting in the lowest OD_{540} and growth on GBT resulting in the greatest (Figure 7.14A). In the *fhs* null mutant, the same response was observed for both sarcosine and DMG, where DMG resulted in the greatest OD_{540}, however the null mutant failed to grow on GBT (Figure 7.14B). Growth on GBT, however, could be restored by complementing the mutant with the native *fhs* of *R*. *pomeroyi* (Figure 7.14C).

(A) (B)

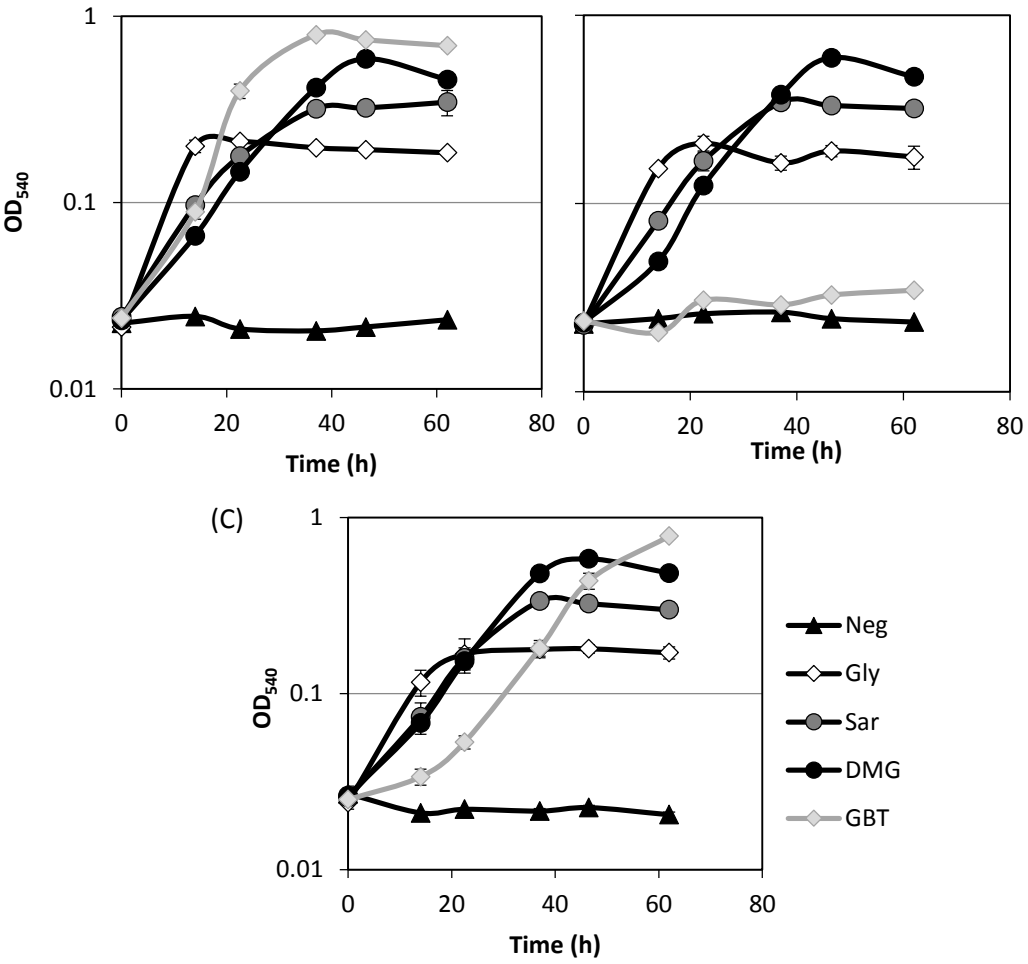

Figure 7.14. Growth (circles) of *R*. *pomeroyi* wild-type **(A)**, the *fhs* null mutant **(B)**, and the complemented mutant **(C)** on glycine (gly), sarcosine (Sar), dimethylglycine (DMG), glycine betaine (GBT) or choline (CHO) as the sole C source. Cultures were grown in triplicate and error bars denote SD.

Although the *fhs* null mutant could not grow on GBT as a sole C source, it could still grow on GBT and TMA as an N source. This suggests that when *R*. *pomeroyi* was grown in the presence of another C and energy source, the sequential demethylation steps were still occurring, liberating the N in these compounds which can then be assimilated into biomass (Figure 7.15A). However in the *fhs* null mutant, the growth rate on GBT and TMA as a N source was reduced compared to that of the wild type. In the complemented mutant, the wild-type growth rate was again partially restored (Figure 7.15A). For the *fhs* null mutant, growth on NH_4^+ as a N source appeared to be unaffected, indicating that reduced growth GBT or TMA

may have resulted from an impaired ability to oxidise the methyl groups in these compounds. Growth on MMA, which only has one methyl group, was also less affected (Figure 7.15B) strengthening the hypothesis that a functional Fhs is essential for proper catabolism of MAs and QAs.

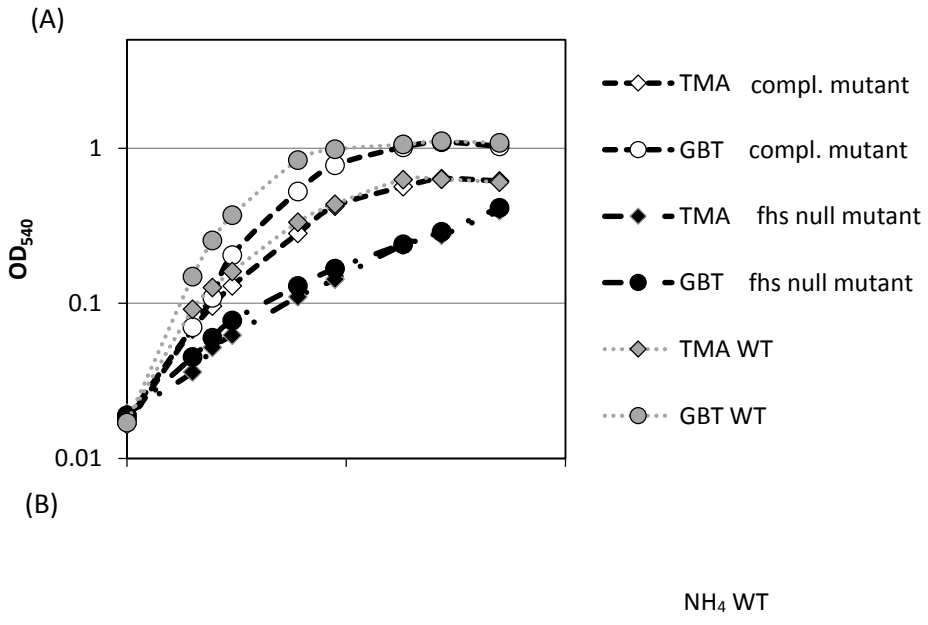

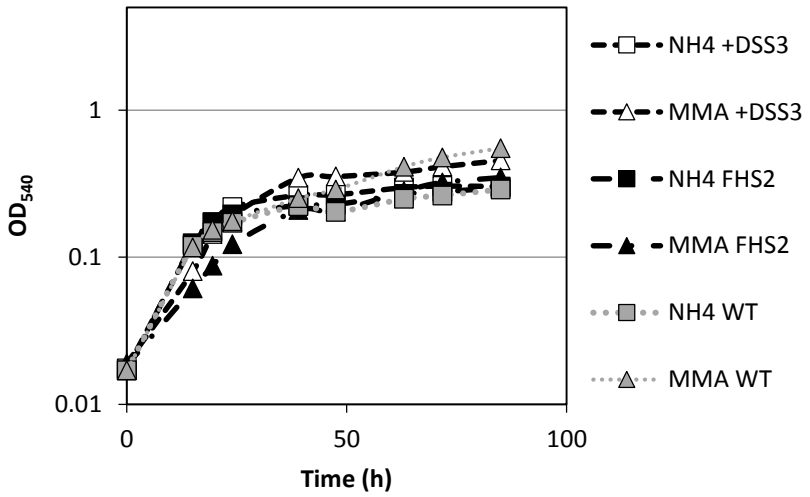

Figure 7.15. Growth (circles) of *R. pomeroyi* wild-type, the *fhs* null mutant, and the complemented mutant on NH_4^+ or MMA **(A)**, or TMA or GBT **(B)** as a sole N source with glucose as the sole C source. Cultures were grown in triplicate. Error bars denote SD.

During GBT demethylation, homocysteine accepts the methyl group from GBT, generating methionine as a product. In turn, methionine can be further recycled back to homocysteine by transferring the methyl group back to an acceptor, likely to be H_4F. Therefore, if H_4F is not being fully recycled in the *fhs* mutant, due to a blockage the H_4F-linked pathway, the conversion of methionine back to homocysteine may limit the amount of homocysteine available for accepting the methyl group from GBT. However, as the null mutant can still grow on GBT as a N source, this is unlikely to be the reason for the impaired ability to grow on GBT as a sole C source. To confirm that homocysteine recycling, ultimately governed by a lack of free H_4F, is not the reason for the impairment of GBT catabolism, the *fhs* null mutant was grown on homocysteine, homocysteine and GBT, glucose and GBT or on GBT alone. *R. pomeroyi* can grow on homocysteine, therefore making interpretation of the results difficult. In spite of this, there did not appear to be any difference in growth yield between homocysteine-grown and homocysteine and GBT-grown cultures (Figure 7.16A). To further confirm if the recycling of H_4F had

any effect on GBT catabolism, the *fhs* null mutant was grown on glucose, GBT and H_4F to see if this restored GBT consumption rates seen in the wild-type. GBT consumption rates were compared against wild-type cultures. Again no difference in the consumption rate was observed in the null mutant cultures grown with or without the addition of H_4F (Figure 7.16B). The wild-type culture showed a much greater rate of GBT consumption.

(A)

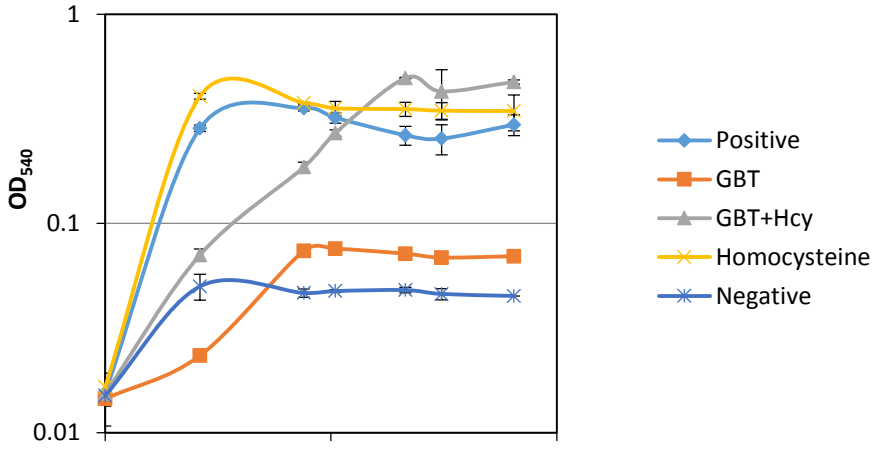

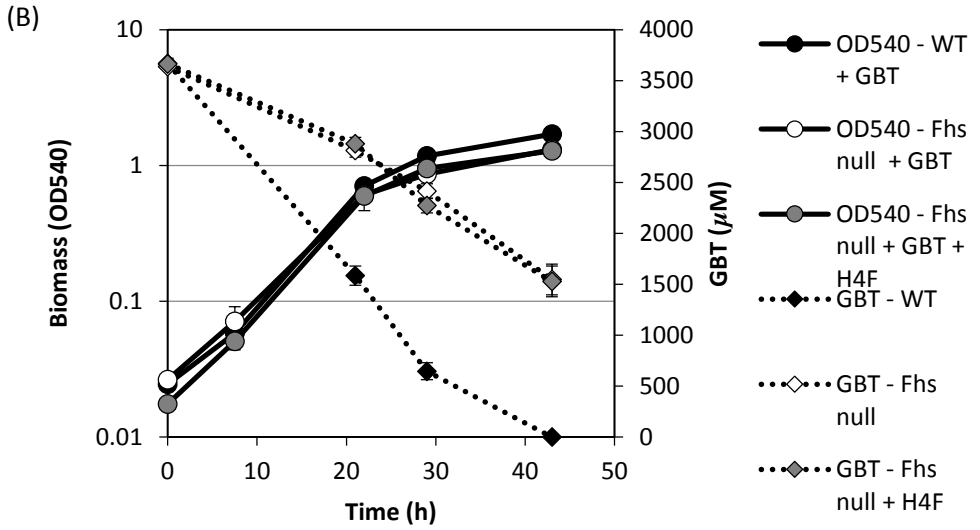

Figure 7.16. **(A)** Growth of the *R*. *pomeroyi fhs* null mutant on either GBT (red squares), GBT + homocysteine (green triangles), homocysteine only (purple crosses) or glucose and GBT (blue triangles). A negative control with no exogenous C source was also set up (blue cross-hairs). **(B)** *R*. *pomeroyi* wild-type (Black circles) or *fhs* null mutant grown on glucose + GBT (white circles) or glucose + GBT + H_4F (grey circles). The concentration of GBT in the culture medium was determined throughout the experiment. Wild-type cells depleted GBT the fastest (black triangles). There was no difference in the rate of GBT depletion for the *fhs* null mutant cultures grown without (white triangles) or with H_4F (grey triangles). All cultures were grown in triplicate and error bars denote SD.

As growth on choline is halted in the *fhs* null mutant when choline (6 mM) was completely removed from the medium, it can be hypothesised that cells may be limited by reducing equivalents and ATP. To confirm that the cells are limited for reducing equivalents, the *fhs* null mutant was again grown on choline with or without the addition of formate. Formate should partially help restore the wild-type phenotype as the conversion of formate to CO_2 by formate dehydrogenase generates one NADH molecule (Chistoserdova et al., 2004). Cultures grown in the presence of choline only reached a final OD_{540} ~0.27 (Figure 7.17A). Supplementation with formate (13 mM total) resulted in greater growth (OD_{540} ~ 0.50), especially when

formate was added after all the choline was depleted from the culture medium (Figure 7.17A). Consequently, the concentration of GBT in cultures supplemented with formate was lower than cultures grown on choline alone (Figure 5.17B). The addition of more choline (4 mM) also resulted in the continuation of growth after cultures had reached stationary phase. A third addition of choline (3 mM) again results in the continuation of growth in cells that has reached stationary phase for a second time (Figure 5.17A). Together, these data show that in *R*. *pomeroyi*, the reducing equivalents as well as the ATP generated through oxidation of the C1 groups is essential for growth on GBT.

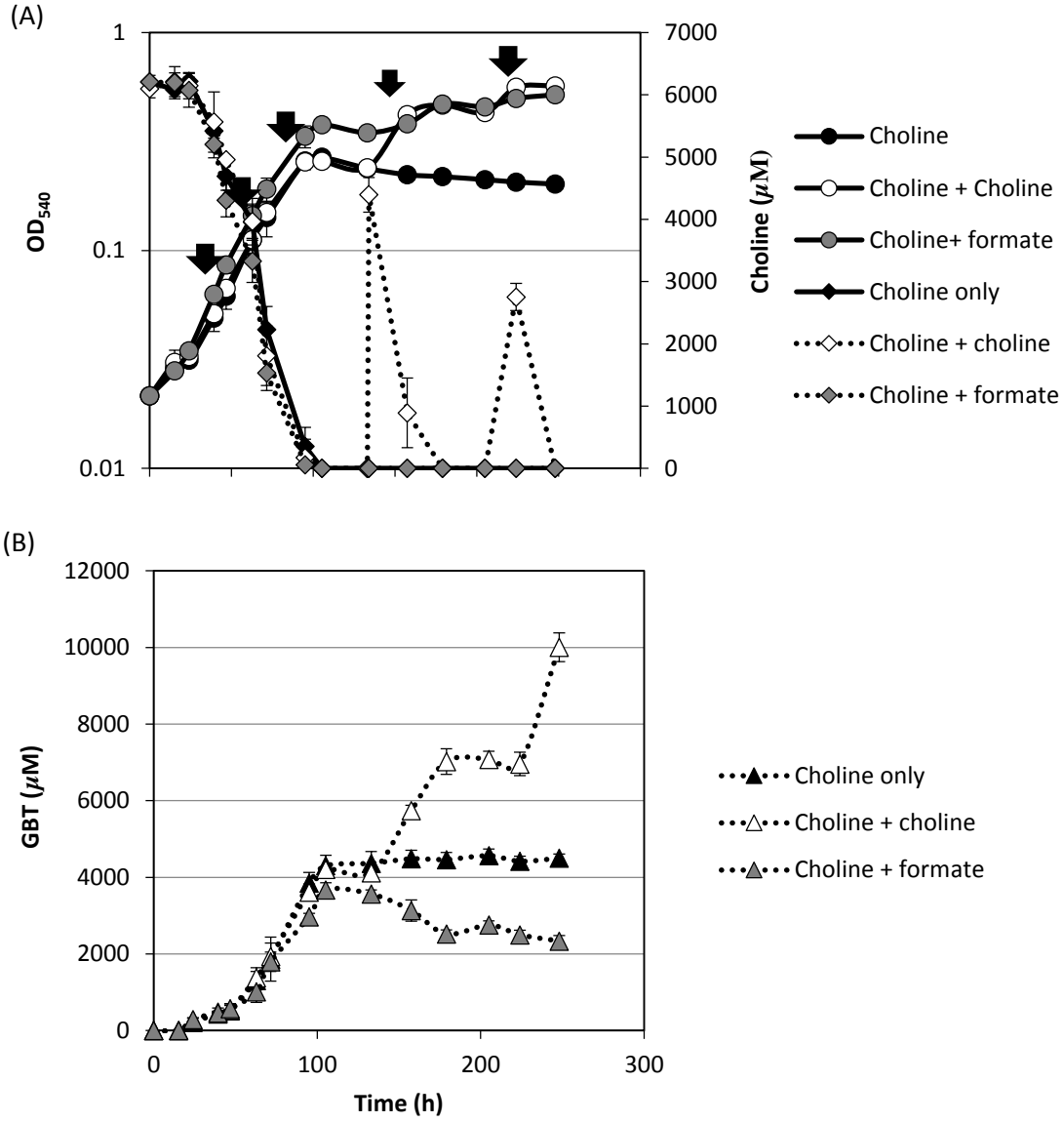

Figure 7.17. (A) Growth of the *fhs* null mutant (circles) on choline supplemented with either formate or additional choline. Choline was quantified throughout the experiment. Arrows denote additions of formate (13 mM total). The first three additions were with 1mM formate, the latter two with 5mM. **(B)** Quantification of GBT in the culture medium during the experiment. All cultures were grown in triplicate and error bars denote SD.

7.3. Discussion

7.3.1. The occurrence of the *bet* operon in marine bacteria

Bacteria from the MRC are frequently associated with marine eukaryotic biota, such as microalgae, epiphytic plants, coral mucus, turbot larva rearings, seahorse mucus as well as a number of different molluscs (Buchan et al., 2005; Seyedsayamdost et al., 2011; Thole et al., 2012; Lema et al., 2014). It is therefore of interest that almost all of the MRC isolates screened have the genetic capability to degrade choline which serves as a C, N and energy source for these bacteria. As choline is ubiquitous within eukaryotic cells (Ikawa and Taylor, 1973), the widespread occurrence of *bet* genes within the MRC suggests that choline may represent a significant nutrient source for these bacteria and may provide an ecological advantage when living in close association with eukaryotic organisms. *P*. *aeruginosa*, can make use of the lipid, phosphatidylcholine, utilising not only the phosphorylcholine head group, but also the glycerol and fatty acid side chains associated with the lipid (Sun et al., 2014). The ability for *P*. *aeruginosa* to utilise phosphatidylcholine, which forms 80% of the lipids found in lung surfactant, is a key mechanism behind their ability to reach high cell densities within the lung (Bernhard et al., 1997; Bernhard et al., 2001). Therefore, further research should focus on whether or not MRC bacteria and *Vibrio* spp. can directly access the phospholipid, phosphatidylcholine, which is abundant in the membranes of marine eukaryotes (Ikawa and Taylor, 1973).

The fact that the *betIAB* cluster is also found within isolates related to *Vibrio* strengthens the hypothesis that choline may play a role in the pathogenicity and/ or mutualistic relationship of these bacteria. In *P*. *aeruginosa*, choline and its catabolites are a regulator of virulence factors (Wargo et al., 2009; Fitzsimmons et al., 2012). Further investigation is required to determine if this is the case in *Vibrio* spp. or MRC isolates that are known to possess haemolytic or proteolytic activities

towards a range of different hosts and their associated pathogens (Hjelm et al., 2004; Seyedsayamdost et al., 2011; Riclea et al., 2012; Thole et al., 2012). The fact that MRC isolates but not *Vibrio* spp. possess *betC*, which is essential for the transformation of choline O-sulfate to choline (Østerås et al., 1998), supports the notion that choline O-sulfate is more commonly associated with marine eukaryotic flora (Hanson et al., 1991; Murakeözy et al., 2003) and not fauna.

7.3.2. Identification of BetT in *R. pomeroyi*

The BetT found in the genomes of MRC bacteria appears different to the previous BetT proteins characterised from either *E. coli* or *P. syringae* in the fact that those BetT proteins are over 100 amino acids longer in length. The difference may be due to presence of a long tail (C-terminus) associated with these previously characterised BetT proteins. The elongated C-terminus is believed to have a role in responding to changes in osmolarity helping to transport choline into the cell during salt-stress (osmoregulation) (Chen and Beattie, 2008). Therefore, the BetT in MRC bacteria may not respond to osmotic challenges and may simply have a primary role in the rapid uptake of choline for nutrient acquisition. The *ΔbetT::Gm* mutant showed no change in growth on GBT suggesting that there is an independent transporter responsible for the uptake of this compound. Compared to some osmolyte ABC-type transporters, BCCT-type transporters are characterised by having a narrow substrate range (Choquet et al., 2005; Chen and Beattie, 2008) and it is therefore not surprising that only the growth of *R. pomeroyi* on choline was affected. Furthermore, a number of possible ORFs (SPO2441, SPO1131, SPOA0231) that encode for SBPs associated with a glycine/ proline betaine transport system (based on annotation) are present within the genomes of *R. pomeroyi* and other MRC isolates and are the likely candidates for GBT

metabolism. These ORFS are similar to the ChoX (Chen et al., 2010a) and TmoX found in marine bacteria (section 7.2.3. and Chapter 3).

7.3.3. GBT catabolism in marine bacteria

Bacteria related to the SAR11 clade can also catabolise GBT and a number of homologs related to BHMT (Figure 7.4A) as well as DMG and sarcosine dehydrogenases, have been identified that may be responsible for carrying out this process (Sun et al., 2011). These dehydrogenases do show homology to the genes identified in MRC bacteria. We found no evidence that the SAR11 clade can catabolise choline as neither the *betIABC* operon, *betT* or *choX* were identified in their genomes. The occurrence of GBT in the marine environment is generally thought to be more widespread than that of choline due to the fact choline is rapidly transformed to GBT to aid with osmoprotection (Gauthier and Le Rudulier, 1990; Ghoul et al., 1990). In addition, all the choline-specific BCCT-type transporters that have been identified were found in bacteria that have a close association with either a plant or animal host (Andresen et al., 1988; Fan et al., 2003; Chen and Beattie, 2008). SAR11 clade bacteria are free-living, oligotrophic bacteria that usually show an inverse correlation of abundance (relative and absolute) with eukaryotic microalgae and do not form close associations with eukaryotic flora (Morris et al., 2002; Giovannoni et al., 2005; Gilbert et al., 2012; Rinta-Kanto et al., 2012; Luo et al., 2013; Taylor et al., 2014). In coastal waters, numbers of SAR11 cells tend to peak during months where primary production by eukaryotic microalgae is low and lower when blooms of these organism occur, a phenomenon that is often reversed by MRC cells (González et al., 2000; Eilers et al., 2001; Zubkov et al., 2001; Polz et al., 2006; Rink et al., 2007; Gilbert et al., 2012; Taylor et al., 2014). As SAR11 bacteria have stream-lined genomes (Giovannoni et al., 2005), they may have lost

the genes required for choline metabolism as this compound may not be associated with their ecological niche.

7.3.4. The role of Fhs in choline metabolism

The data presented in this Chapter complements the data shown in Chapter 5 that revealed when *fhs* is disrupted in *R. pomeroyi*, the turnover of TMA and TMAO in C-starved cells is impaired. However, the experiments in this Chapter or Chapter 5 do not clarify whether or not complete oxidation to CO_2 has been terminated. *R. pomeroyi* does possess the genes required for C1 oxidation through the glutathione-linked (GSH) C1 oxidation pathway which has been shown to alleviate stress caused by formaldehyde toxicity (Harms et al., 1996; Marx et al., 2003a; Martinez-Gomez et al., 2013). The GSH-linked pathway usually requires the enzyme, formaldehyde-activating enzyme (Fae), to facilitate the conjugation of formaldehyde to GSH or the alternative cofactor, H_4MPT (increasing the rate of conjugation by up to 10-fold) (Goenrich et al., 2002; Chen, 2012). Unlike the majority of non-marine representative methylotrophs, isolates from the MRC, including *R. pomeroyi*, lack *fae*, therefore it is unclear whether or not the GSH-linked pathway can deal with any potential build-up of formaldehyde during the catabolism of MAs or QAs in the *fhs* null mutant. In *Methylobacterium extorquens* PA1, formaldehyde leakage via the GMA/NMG pathway during growth on MMA was observed (Nayak and Marx, 2014). Therefore, in the *fhs* null mutant, formaldehyde leakage, due to a lack of free H_4F, may present a problem for the cell and may explain the slower growth rates observed for the *fhs* null mutant when growing on either GBT or TMA as a sole N source. In reality a combination of impaired reducing power generation and free H_4F is the likely explanation behind the phenotypes observed in the *fhs* null mutant. The role of *fhs* and therefore the

H_4F-linked C1 oxidation pathway in the catabolism of methylated compounds, such as MAs and QAs, is clearly essential for the proper physiological functioning of *R. pomeroyi*.

Chapter 8

Summary and Future perspectives

8.1. Chapter 3 – TMAO metabolism

This chapter aimed to identify the key gene involved in the demethylation of TMAO to DMA using *R. pomeroyi* as the model bacterium. In achieving this, an ABC-type transporter specific for TMAO was also identified and found to be highly expressed within the ocean's surface waters, based on the re-analysis of a number of metatranscriptomic and metaproteomic datasets. This work has highlighted how low throughput targeted research can complement high-throughput omics studies to help improve our understanding of how the world's oceans function. Development of a reproducible method for mutagenesis was essential in driving the remainder of the project forward. A number of subsequent mutant strains were generated using this method to help answer similar questions regarding the fundamental metabolism of *R. pomeroyi*. The method of using MMA as a selection source to remove background *E. coli* was simple, but proved very effective and greatly improved the success rate of conjugation.

One major question that was not answered in this chapter is 'What is the specificity and affinity of the TmoX towards TMAO and related compounds?' Several experiments could be performed to address this question, but the most appropriate one would be to utilise the methods developed by Hermann et al. (2013) to determine the K_D of the SBP. This would confirm whether or not TmoX has any affinity towards TMA, as the data presented in Chapter 3 are not conclusive. Compared with isolates from the MRC, bacteria from the SAR11 clade generally have fewer SBPs within their streamlined genomes. It is therefore essential that these binding-affinity assays are conducted using purified TmoX from bacteria related to both the SAR11 clade and MRC to investigate whether their respective TmoX homologs share a similar substrate specificity profiles.

8.2. Chapter 4 – Regulation of Tmm

Chapter 4 focused on determining the regulatory mechanisms governing the expression of Tmm in *R*. *pomeroyi*. There is sufficient evidence presented in this Chapter to conclude that a post-transcriptional mechanism controlling expression of Tmm is taking place in *R*. *pomeroyi*. Preliminary data has revealed a potential role for asRNA in regulating the expression of Tmm and further research is required to determine the precise role this RNA molecule is playing. MA-dependent DMS oxidation as a metabolic trait can be expanded to other members of the MRC (Lidbury and Muhs, unpublished data). One key investigation is to determine the precise length and proposed mode of action for this asRNA molecule, *astmm2*. Once this has been achieved, either a 'knock down' or a 'knock up' strain of *R*. *pomeroyi* for *astmm2* can be generated to confirm the mode of action of this molecule.

8.3. Chapter 5 -TMA/ TMAO as an energy source

The work presented in this Chapter clearly demonstrated the physiological benefit of oxidising TMA or TMAO in order to generate reducing equivalents and ATP. The idea that marine heterotrophic bacteria use a range of compounds to generate energy is not necessarily new, but to the best of my knowledge, this is the first time the effect of two energy sources (TMA and thiosulfate) supplemented to a bacterium in parallel, has been investigated. The results from this experiment clearly indicate that metabolising two energy sources simultaneously provides an even greater enhancement in the bacterial growth efficiency of *R*. *pomeroyi*. This chapter also confirmed a 'proof of concept' that rapid turnover of MAs can result in the remineralisation of NH_4^+ which can then be cross-fed into another bacterium. As it is unclear what limits heterotrophic bacterial growth in marine systems, one

can only speculate on whether or not this process happens *in situ*. Regardless, this Chapter has demonstrated that N-rich compounds are continuously oxidised, independently of growth, and are therefore a likely source of NH_4^+.

Chapter 4 also investigated the role of the H_4F-linked pathway in the oxidation of TMA. Although it is clear that this pathway is required for the 'proper' functioning of *R. pomeroyi*, the results do not clarify whether or not this pathway is essential for the complete oxidation of TMA through to CO_2. For example, as the *fhs* null mutant can still grow on TMA as a sole nitrogen source, it is unclear whether or not there is either a build up of one of the intermediates in the H_4F-linked pathway or whether it can use the GSH-linked pathway to convert formaldehyde to CO_2. Combining heavy isotope, ^{13}C-TMA, with mass flux analysis would enable a better understanding of the metabolism of both the wild-type and *fhs* null mutant.

8.4. Chapter 6 – Isolation of methylotrophic TMA/ TMAO-utilising bacteria

The isolation of methylotrophic bacteria related to the MRC in conjunction with environmental screening of the saltmarsh expands our knowledge on the potential TMA and TMAO utilising bacteria in the marine environment. The development of primers targeting *tdm* using a variety of known Tdm sequences should allow for a more detailed assessment of the ecology of this functional group. It is still unclear whether or not these primers are effective at amplifying *tdm* from SAR11 clade bacteria as there was no SAR11 DNA to test during this research. Seawater collected from the open-ocean gyres or from station L4 during the winter time would be an ideal sample source to confirm whether these primers are truly capable of amplifying *tdm* from a diverse range of marine bacteria, including the SAR11

clade. If this is the case, this primer set can be employed to determine the ecology of the TMAO-utilising community over a seasonal cycle at the station L4. A number of studies have already shown that during the spring, the MRC become the dominant clade whilst during the winter, the SAR11 clade is numerically dominant (Gilbert et al., 2012; Taylor et al., 2014). This primer set could therefore be utilised to investigate whether it is the TMAO-utilising proportion of the MRC (roughly 15/40 sequenced isolates) that become dominant during the spring blooms. This data may provide some insightful information regarding the importance of MAs during a bloom event. Re-isolation of the *Methylophaga* strains is necessary to determine whether or not these isolates use Tdm to grow methylotrophically on TMAO. Furthermore, confirming the function of the *gmaS*/*mgsABC*-like gene cluster, using the *R*. *nubinhibens* will help shed light on the occurrence of this gene within the genomes of a number of phylogenetically divergent marine bacteria.

8.5. Chapter 7 – Choline metabolism in marine bacteria

Chapter 7 has revealed the widespread occurrence of the genes required for choline metabolism within the MRC and the genus, *Vibrio*. Using *R*. *pomeroyi* as the model bacterium, mutagenesis confirmed the pathway for the conversion of choline to GBT via the *bet* operon originally characterised in *E*. *coli*. These genes can now be used as functional markers to assess the ecology of these bacteria and may be used in conjunction with ^{14}C-radiolabelled or ^{13}C-stable isotope probing experiments to gain a better insight into the major choline-utilisers present in the marine environment. The cycling of choline is probably very rapid and tightly coupled to eukaryotic cells where concentrations and residence times in the water column are predicted to be low and short-lived, respectively. Results presented in this Chapter also showed that Fhs is vital in C1 oxidation by providing a source of reducing

equivalent to the cell. For the *fhs* null mutant, growth on GBT is completely inhibited when this compound is the only source of reducing equivalents and ATP. Therefore, the data confirmed that the H_4F-linked oxidation pathway is essential in maintaining normal physiological functioning within the cell during C1 metabolism.

Some of the genes and enzymes in the pathway of GBT catabolism have not been experimentally confirmed. Specifically, the genes and enzymes responsible for the second and third steps of GBT demethylation still need characterisation. In *R. pomeroyi* and other isolates related to the MRC, both a putative monomeric sarcosine dehydrogenase and a multimeric sarcosine oxidase are present. Interestingly, this redundancy may be similar to that of a number of methylotrophs which have the MMA dehydrogenase (MMADH) encoded by the *mauAB* as well as the genes required for the glutamate-dependent pathway (GMA/NMG). Also, *Citreicella* sp. SE45 does not have any of the genes found in other isolates related to the MRC, but does contain the *gbcAB* cluster which encodes for a different GBT methyltransferase as well as a different DMG dehydrogenase and the *soxABDG* cluster. It is therefore important to investigate how GBT is catabolised in this bacterium and what potential ecological differences arise from possessing a different mechanism for GBT catabolism

8.6. General conclusions

In summary, the data presented in this thesis demonstrates the ability of marine heterotrophic bacteria to utilise MAs and QAs as a source of nutrients. A number of key genes and enzymes essential for the catabolism of these compounds have been identified and shown to be abundant in ecologically important marine bacteria. A number of questions regarding the oxidation of methyl groups of MAs and QAs

remain unanswered and provides an avenue for further research. In addition, the role that asRNA molecules may play in the regulation of gene expression in *R. pomeroyi* warrants further investigation.

References

Aktas, M., Jost, K.A., Fritz, C., and Narberhaus, F. (2011) Choline uptake in *Agrobacterium tumefaciens* by the high-Affinity ChoXWV transporter. *J Bacteriol* **193**: 5119-5129.

Albers, S.V., Elferink, M.G., Charlebois, R.L., Sensen, C.W., Driessen, A.J., and Konings, W.N. (1999) Glucose transport in the extremely thermoacidophilic *Sulfolobus solfataricus* involves a high-affinity membrane-integrated binding protein. *J Bacteriol* **181**: 4285-4291.

Alberta, J.A., and Dawson, J.H. (1987) Purification to homogeneity and initial physical characterisation of secondary amine monooxygenase. *J Biol Chem* **262**: 11857-11863.

Alonso, C., and Pernthaler, J. (2006) *Roseobacter* and SAR11 dominate microbial glucose uptake in coastal North Sea waters. *Environ Microbiol* **8**: 2022-2030.

Andresen, P.A., Kaasen, I., Styrvold, O.B., Boulnois, G., and Strom, A.R. (1988) Molecular cloning, physical mapping and expression of the bet genes governing the osmoregulatory choline-glycine betaine pathway of *Escherichia coli*. *J Gen Microbiol* **134**: 1737-1746.

Anthony, C. (1982) *The biochemistry of methylotrophs*. London, UK: Academic Press.

Arata, H., Shimizu, M., and Takamiya, K. (1992) Purification and properties of Trimethylamine *N*-Oxide reductase from aerobic photosynthetic bacterium *Roseobacter denitrificans*. *J Biochem* **112**: 470-475.

Azam, F., Fenchel, T., Field, J.G., Gray, J.S., Meyer-Reil, L.A., and F, T. (1983) The ecological role of water-column microbes in the sea. *Mar Ecol Prog Ser* **10**: 257-263.

Azam, F., and Malfatti, F. (2007) Microbial structuring of marine ecosystems. *Nat Rev Microbiol* **5**: 782-791.

Barra, L., Fontenelle, C., Ermel, G., Trautwetter, A., Walker, G.C., and Blanco, C. (2006) Interrelations between glycine betaine catabolism and methionine biosynthesis in *Sinorhizobium meliloti* strain 102F34. *J Bacteriol* **188**: 7195-7204.

Barrett, E.L., and Kwan, H.S. (1985) Bacterial reduction of trimethylamine *N*-oxide. *Annu Rev Microbiol* **39**: 131-149.

Bernhard, W., Wang, J.Y., Tschernig, T., Tümmler, B., Hedrich, H.J., and von der Hardt, H. (1997) Lung surfactant in a cystic fibrosis animal model: increased alveolar phospholipid pool size without altered composition and surface tension function in *cftrm1HGU*/*m1HGU* mice. *Thorax* **52**: 723-730.

Bernhard, W., Hoffmann, S., Dombrowsky, H., Rau, G.A., Kamlage, A., Kappler, M. et al. (2001) Phosphatidylcholine molecular species in lung surfactant. *Am J Resp Cell Mol* **25**: 725-731.

Berntsson, R.P.A., Smits, S.H.J., Schmitt, L., Slotboom, D.-J., and Poolman, B. (2010) A structural classification of substrate-binding proteins. *FEBS Letters* **584**: 2606-2617.

Bibby, T.S., Gorbunov, M.Y., Wyman, K.W., and Falkowski, P.G. (2008) Photosynthetic community responses to upwelling in mesoscale eddies in the subtropical North Atlantic and Pacific Oceans. *Deep Sea Res Part II* **55**: 1310-1320.

Biers, E.J., Wang, K., Pennington, C., Belas, R., Chen, F., and Moran, M.A. (2008) Occurrence and expression of gene transfer agent genes in marine bacterioplankton. *Appl Envir Microbiol* **74**: 2933-2939.

Blunden, G., and Gordon, S., M. (1986) Betaines and their sulphonio analogues inmarine algae. *Prog Physiol Res* **4**: 39-80.

Boch, J., Kempf, B., and Bremer, E. (1994) Osmoregulation in *Bacillus subtilis*: synthesis of the osmoprotectant glycine betaine from exogenously provided choline. *J Bacteriol* **176**: 5364-5371.

Boden, R., Murrell, J.C., and Schäfer, H. (2011a) Dimethylsulfide is an energy source for the heterotrophic marine bacterium *Sagittula stellata*. *FEMS Microbiol Lett* **322**: 188-193.

Boden, R., Ferriera, S., Johnson, J., Kelly, D.P., Murrell, J.C., and Schäfer, H. (2011b) Draft genome sequence of the chemolithoheterotrophic, halophilic methylotroph *Methylophaga thiooxydans* DMS010. *J Bacteriol* **193**: 3154-3155.

Boden, R., Cunliffe, M., Scanlan, J., Moussard, H., Kits, K.D., Klotz, M.G. et al. (2011c) Complete genome sequence of the aerobic marine methanotroph *Methylomonas methanica* MC09. *J Bacteriol* **193**: 7001-7002.

Buc, J., Santini, C.-L., Giordani, R., Czjzek, M., Wu, L.-F., and Giordano, G. (1999) Enzymatic and physiological properties of the tungsten-substituted molybdenum TMAO reductase from *Escherichia coli*. *Mol Microbiol* **32**: 159-168.

Bucciarelli, E., Céline Ridame, C., Sunda, W.G., Dimier-Hugueney, C., Cheize, M., and Belviso, S. (2013) Increased intracellular concentrations of DMSP and DMSO in iron-limited oceanic phytoplankton *Thalassiosira oceanica* and *Trichodesmium erythraeum*. *Assoc Limnol Oceanogr* **58**: 1667-1679.

Buchan, A., González, J.M., and Moran, M.A. (2005) Overview of the Marine Roseobacter lineage. *Appl Environ Microbiol* **71**: 5665-5677.

Calderón, S.M., Poor, N.D., and Campbell, S.W. (2007) Estimation of the particle and gas scavenging contributions to wet deposition of organic nitrogen. *Atmos Environ* **41**: 4281-4290.

Campbell, L., Liu, H., Nolla, H.A., and Vaulot, D. (1997) Annual variability of phytoplankton and bacteria in the subtropical North Pacific Ocean at Station ALOHA during the 1991–1994 ENSO event. *Deep Sea Res Pt I* **44**: 167-192.

Capone, D.G., and Carpenter, E.J. (1982) Nitrogen fixation in the marine environment. *Science* **217**: 1140-1142.

Capone, D.G., Bronk, D.A., Mulholland, M.R., and Carpenter, E.J. (eds) (2008) *Nitrogen in the Marine Environment*, 2nd edn. Amsterdam, the Netherland: Elsevier.

Carini, P., Steindler, L., Beszteri, S., and Giovannoni, S.J. (2013) Nutrient requirements for growth of the extreme oligotroph '*Candidatus* Pelagibacter ubique' HTCC1062 on a defined medium. *ISME J* **7**: 592-602.

Carpenter, L.J., Archer, S.D., and Beale, R. (2012) Ocean-atmosphere trace gas exchange. *Chem Soc Rev* **41**: 6473-6506.

Catalfomo, P., Block, J., H., Constantine, G., H., and Kirk, P., W. (1973) Choline sulfate (ester) in marine higher fungi. *Mar Chem* **1**: 157-162.

Chandler, S.R. (1983) The utilisation of methylamine nitrogen by the methanotrophic bacterium Pseudomonad P. PhD thesis. University of Reading, UK.

Charlson, R.J., Lovelock, J.E., Andreae, M.O., and Warren, S.G. (1987) Oceanic phytoplankton, atmospheric sulphur, cloud albedo and climate. *Nature* **326**: 655-661.

Chen, C., Malek, A.A., Wargo, M.J., Hogan, D.A., and Beattie, G.A. (2010a) The ATP-binding cassette transporter Cbc (choline/betaine/carnitine) recruits multiple substrate-binding proteins with strong specificity for distinct quaternary ammonium compounds. *Mol Microbiol* **75**: 29-45.

Chen, C., and Beattie, G.A. (2008) *Pseudomonas syringae* BetT is a low-affinity choline transporter that is responsible for superior osmoprotection by choline over glycine betaine. *J Bacteriol* **190**: 2717-2725.

Chen, Y. (2012) Comparative genomics of methylated amine utilisation by marine *Roseobacter* clade bacteria and development of functional gene markers (*tmm*, *gmaS*). *Environ Microbiol* **14**: 2308-2322.

Chen, Y., McAleer, K.L., and Murrell, J.C. (2010b) Monomethylamine as a nitrogen source for a nonmethylotrophic bacterium, *Agrobacterium tumefaciens*. *Appl Environ Microbiol* **76**: 4102-4104.

Chen, Y., Patel, N.A., Crombie, A., Scrivens, J.H., and Murrell, J.C. (2011) Bacterial flavin-containing monooxygenase is trimethylamine monooxygenase. *Proc Nat Acad Sci USA* **108**: 17791-17796.

Chistoserdova, L. (2011) Modularity of methylotrophy, revisited. *Environ Microbiol* **13**: 2603-2622.

Chistoserdova, L., Kalyuzhnaya, M.G., and Lidstrom, M.E. (2009) The expanding world of methylotrophic metabolism. *Annu Rev Microbiol* **63**: 477-499.

Chistoserdova, L., Laukel, M., Portais, J.-C., Vorholt, J.A., and Lidstrom, M.E. (2004) Multiple formate dehydrogenase enzymes in the facultative methylotroph *Methylobacterium extorquens* AM1 are dispensable for growth on methanol. *J Bacteriol* **186**: 22-28.

Chlumsky, L.J., Zhang, L., Jorns, M.S. (1995) Sequence analysis of sarcosine oxidase and nearby genes reveals homologies with key enzymes of folate one-carbon metabolism. *J Biol Chem* **270** (31): 18252-18259.

Choquet, G., Jehan, N., Pissavin, C., Blanco, C., and Jebbar, M. (2005) OusB, a broad-specificity abc-type transporter from *Erwinia chrysanthemi*, mediates uptake of glycine betaine and choline with a high affinity. *Appl Environ Microbiol* **71**: 3389-3398.

Cunliffe, M. (2011) Correlating carbon monoxide oxidation with *cox* genes in the abundant marine *Roseobacter* Clade. *ISME J* **5**: 685-691.

Cunliffe, M. (2012) Physiological and metabolic effects of carbon monoxide oxidation in the model marine bacterioplankton *Ruegeria pomeroyi* DSS-3. *Appl Environ Microbiol*. **79** (2): 738-740.

Curson, A.R.J., Todd, J.D., Sullivan, M.J., and Johnston, A.W.B. (2011) Catabolism of dimethylsulphoniopropionate: microorganisms, enzymes and genes. *Nat Rev Micro* **9**: 849-859.

Davidson, A.L., and Chen, J. (2004) ATP-binding cassette transporters in bacteria. *Annual Review of Biochemistry* **73**: 241-268.

Davidson, V.L. (2004) Electron transfer in quinoproteins. *Arch Biochem Biophys* **428**: 32-40.

Dennis, J.J., and Zylstra, G.J. (1998) Plasposons: modular Self-cloning minitransposon derivatives for rapid genetic analysis of gram-negative bacterial genomes. *Appl Environ Microbiol* **64**: 2710-2715.

DuRand, M.D., Olson, R.J., and Chisholm, S.W. (2001) Phytoplankton population dynamics at the Bermuda Atlantic Time-series station in the Sargasso Sea. *Deep Sea Res Part II* **48**: 1983-2003.

Eilers, H., Pernthaler, J., Peplies, J., Glöckner, F.O., Gerdts, G., and Amann, R. (2001) Isolation of Novel Pelagic Bacteria from the German Bight and Their Seasonal Contributions to Surface Picoplankton. *Appl Environ Microbiol* **67**: 5134-5142.

Elser, J.J., Sterner, R.W., Gorokhova, E., Fagan, W.F., Markow, T.A., Cotner, J.B. et al. (2000) Biological stoichiometry from genes to ecosystems. *Ecology Letters* **3**: 540-550.

Facchini, M.C., Decesari, S., Rinaldi, M., Carbone, C., Finessi, E., Mircea, M. et al. (2008) Important source of marine secondary organic aerosol from biogenic amines. *Environ Sci Technol* **42**: 9116-9121.

Falkowski, P.G., Barber, R.T., and Smetacek, V. (1998) Biogeochemical controls and feedbacks on ocean primary production. *Science* **281**: 200-206.

Fan, X., Pericone, C.D., Lysenko, E., Goldfine, H., and Weiser, J.N. (2003) Multiple mechanisms for choline transport and utilisation in *Haemophilus influenzae*. *Mol Microbiol* **50**: 537-548.

Field, C.B., Behrenfeld, M.J., Randerson, J.T., and Falkowski, P. (1998) Primary production of the biosphere: integrating terrestrial and oceanic components. *Science* **281**: 237-240.

Fitzsimmons, L.F., Hampel, K.J., and Wargo, M.J. (2012) Cellular choline and glycine betaine pools impact osmoprotection and phospholipase c production in *Pseudomonas aeruginosa*. *J Bacteriol* **194**: 4718-4726.

Fitzsimons, M.F., Kahni-danon, B., and Dawitt, M. (2001) Distributions and adsorption of the methylamines in the inter-tidal sediments of an East Anglian estuary. *Environ Exp Bot* **46**: 225-236.

Fraaije, M.W., Kamerbeek, N.M., van Berkel, W.J.H., and Janssen, D.B. (2002) Identification of a Baeyer–Villiger monooxygenase sequence motif. *FEBS Letters* **518**: 43-47.

Friedrich, C.G., Rother, D., Bardischewsky, F., Quentmeier, A., and Fischer, J. (2001) Oxidation of reduced inorganic sulfur compounds by bacteria: Emergence of a common mechanism? *Appl Environ Microbiol* **67**: 2873-2882.

Friedrich, C.G., Quentmeier, A., Bardischewsky, F., Rother, D., Kraft, R., Kostka, S., and Prinz, H. (2000) Novel genes coding for lithotrophic sulfur oxidation of *Paracoccus pantotrophus* GB17. *J Bacteriol* **182**: 4677-4687.

Fu, X.-Y., Xue, C.-H., Miao, B.-C., Liang, J.-N., Li, Z.-J., and Cui, F.-x. (2006) Purification and characterisation of trimethylamine-*N*-oxide demethylase from jumbo squid (*Dosidicus gigas*). *J Agr Food Chem* **54**: 968-972.

Garber, J.H. (1984) Laboratory study of nitrogen and phosphorus remineralization during the decomposition of coastal plankton and seston. *Estuar Coast Shelf Sci* **18**: 685-702.

Gauthier, M.J., and Le Rudulier, D. (1990) Survival in seawater of *Escherichia coli* cells grown in marine sediments containing glycine betaine. *Appl Environ Microbiol* **56**: 2915-2918.

Ge, X., Wexler, A.S., and Clegg, S.L. (2011) Atmospheric amines – Part I. A review. *Atmos Environ* **45**: 524-546.

Georg, J., and Hess, W.R. (2011) cis-Antisense RNA, another level of gene regulation in bacteria. *Microbiol Mol Biol Rev* **75**: 286-300.

Ghoul, M., Bernard, T., and Cormier, M. (1990) Evidence that *Escherichia coli* accumulates glycine betaine from marine sediments. *Appl Environ Microbiol* **56**: 551-554.

Gibb, S.W., and Hatton, A.D. (2004) The occurrence and distribution of trimethylamine *N*-oxide in Antarctic coastal waters. *Mar Chem* **91**: 65-75.

Gibb, S.W., Mantoura, R.F.C., Liss, P.S., and Barlow, R.G. (1999) Distributions and biogeochemistries of methylamines and ammonium in the Arabian Sea. *Deep Sea Res Pt II* **46**: 593-615.

Giebel, H.-A., Brinkhoff, T., Zwisler, W., Selje, N., and Simon, M. (2009) Distribution of *Roseobacter* RCA and SAR11 lineages and distinct bacterial communities from the subtropics to the Southern Ocean. *Environ Microbiol* **11**: 2164-2178.

Giebel, H.-A., Kalhoefer, D., Lemke, A., Thole, S., Gahl-Janssen, R., Simon, M., and Brinkhoff, T. (2011) Distribution of *Roseobacter* RCA and SAR11 lineages in the North Sea and characteristics of an abundant RCA isolate. *ISME J* **5**: 8-19.

Gifford, S.M., Sharma, S., Booth, M., and Moran, M.A. (2013) Expression patterns reveal niche diversification in a marine microbial assemblage. *ISME J* **7**: 281-298.

Gilbert, B., McDonald, I.R., Finch, R., Stafford, G.P., Nielsen, A.K., and Murrell, J.C. (2000) Molecular analysis of the pmo (particulate methane monooxygenase) operons from two type II methanotrophs. *Appl Environ Microbiol* **66**: 966-975.

Gilbert, J.A., Steele, J.A., Caporaso, J.G., Steinbruck, L., Reeder, J., Temperton, B. et al. (2012) Defining seasonal marine microbial community dynamics. *ISME J* **6**: 298-308.

Giovannoni, S.J., and Vergin, K.L. (2012) Seasonality in ocean microbial communities. *Science* **335**: 671-676.

Giovannoni, S.J., Thrash, C.J., and Temperton, B. (2014) Implications of streamlining theory for microbial ecology. *ISME J* **8**: 1553-1565.

Giovannoni, S.J., Tripp, H.J., Givan, S., Podar, M., Vergin, K.L., Baptista, D. et al. (2005) Genome streamlining in a cosmopolitan oceanic bacterium. *Science* **309**: 1242-1245.

Goenrich, M., Bartoschek, S., Hagemeier, C.H., Griesinger, C., and Vorholt, J.A. (2002) A Glutathione-dependent formaldehyde-activating enzyme (Gfa) from *Paracoccus denitrificans* detected and purified via two-dimensional proton exchange NMR Spectroscopy. *J Biol Chem* **277**: 3069-3072.

Gon, S., Giudici-Orticoni, M.-T., Méjean, V., and Iobbi-Nivol, C. (2001) Electron transfer and binding of the c-type cytochrome torc to the trimethylamine *N*-oxide reductase in *Escherichia coli*. *J Biol Chem* **276**: 11545-11551.

González, J.M., Kiene, R.P., and Moran, M.A. (1999) Transformation of sulfur compounds by an abundant lineage of marine bacteria in the α-subclass of the class *Proteobacteria*. *Appl Environ Microbiol* **65**: 3810-3819.

González, J.M., Simó, R., Massana, R., Covert, J.S., Casamayor, E.O., Pedrós-Alió, C., and Moran, M.A. (2000) Bacterial community structure associated with a dimethylsulfoniopropionate-producing North Atlantic algal bloom. *Appl Environ Microbiol* **66**: 4237-4246.

González, J.M., Covert, J.S., Whitman, W.B., Henriksen, J.R., Mayer, F., Scharf, B. et al. (2003) *Silicibacter pomeroyi* sp. nov. and *Roseovarius nubinhibens* sp. nov., dimethylsulfoniopropionate-demethylating bacteria from marine environments. *Int J Syst Evol Micro* **53**: 1261-1269.

Graham, J.E., and Wilkinson, B.J. (1992) *Staphylococcus aureus* osmoregulation: roles for choline, glycine betaine, proline, and taurine. *J Bacteriol* **174**: 2711-2716.

Green, D.H., Shenoy, D.M., Hart, M.C., and Hatton, A.D. (2011) Coupling of dimethylsulfide oxidation to biomass production by a marine flavobacterium. *Appl Environ Microbiol* **77**: 3137-3140.

Green, R.T., Todd, J.D., and Johnston, A.W.B. (2013) Manganese uptake in marine bacteria; the novel MntX transporter is widespread in Roseobacters, Vibrios, Alteromonadales and the SAR11 and SAR116 clades. *ISME J* **7**: 581-591.

Grote, J., Thrash, J.C., Huggett, M.J., Landry, Z.C., Carini, P., Giovannoni, S.J., and Rappé, M.S. (2012) Streamlining and core genome conservation among highly divergent members of the SAR11 Clade. *mBio* **3**.

Hagström, Å., Pommier, T., Rohwer, F., Simu, K., Stolte, W., Svensson, D., and Zweifel, U.L. (2002) Use of 16S Ribosomal DNA for delineation of marine bacterioplankton species. *Appl Environ Microbiol* **68**: 3628-3633.

Hahnke, S., Brock, N.L., Zell, C., Simon, M., Dickschat, J.S., and Brinkhoff, T. (2013) Physiological diversity of *Roseobacter* clade bacteria co-occurring during a phytoplankton bloom in the North Sea. *Syst Appl Microbiol* **36** (1): 39-48.

Halsey, K.H., Carter, A.E., and Giovannoni, S.J. (2012) Synergistic metabolism of a broad range of C1 compounds in the marine methylotrophic bacterium HTCC2181. *Environ Microbiol* **14**: 630-640.

Hanson, A.D., Rathinasabapathi, B., Chamberlin, B., and Gage, D.A. (1991) comparative physiological evidence that β-alanine betaine and choline-O-sulfate act as compatible osmolytes in halophytic *Limonium* species. *Plant Physiol* **97**: 1199-1205.

Harms, N., Ras, J., Reijnders, W.N., van Spanning, R.J., and Stouthamer, A.H. (1996) S-formylglutathione hydrolase of *Paracoccus denitrificans* is homologous to human esterase D: a universal pathway for formaldehyde detoxification? *J Bacteriol* **178**: 6296-6299.

Hatton, A., and Wilson, S. (2007) Particulate dimethylsulphoxide and dimethylsulphoniopropionate in phytoplankton cultures and Scottish coastal waters. *Aquat Sci* **69**: 330-340.

Hatton, A., Shenoy, D., Hart, M., Mogg, A., and Green, D. (2012) Metabolism of DMSP, DMS and DMSO by the cultivable bacterial community associated with the DMSP-producing dinoflagellate *Scrippsiella trochoidea*. *Biogeochemistry* **110**: 131-146.

Hatton, A.D., Turner, S.M., Malin, G., and Liss, P.S. (1998) Dimethylsulphoxide and other biogenic sulphur compounds in the Galapagos Plume. *Deep Sea Res Pt II* **45**: 1043-1053.

Herrmann, C.K., Bukata, L., Melli, L., Marchesini, M.I., Caramelo, J.J., and Comerci, D.J. (2013) Identification and characterisation of a high-affinity choline uptake system of *Brucella abortus*. *J Bacteriol* **195**: 493-501.

Hjelm, M., Riaza, A., Formoso, F., Melchiorsen, J., and Gram, L. (2004) Seasonal incidence of autochthonous antagonistic *Roseobacter* spp. and *Vibrionaceae* strains in a Turbot larva (*Scophthalmus maximus*) rearing system. *Appl Environ Microbiol* **70**: 7288-7294.

Holland, H.D., Lazar, B., and McCaffrey, M. (1986) Evolution of the atmosphere and oceans. *Nature* **320**: 27-33.

Horn, C., Sohn-Bösser, L., Breed, J., Welte, W., Schmitt, L., and Bremer, E. (2006) Molecular determinants for substrate specificity of the ligand-binding protein OpuAC from *Bacillus subtilis* for the compatible solutes glycine betaine and proline betaine. *J Mol Biol* **357**: 592-606.

Howard, E.C., Sun, S., Biers, E.J., and Moran, M.A. (2008) Abundant and diverse bacteria involved in DMSP degradation in marine surface waters. *Environ Microbiol* **10**: 2397-2410.

Hunt, D.E., Lin, Y., Church, M.J., Karl, D.M., Tringe, S.G., Izzo, L.K., and Johnson, Z.I. (2013) Relationship between abundance and specific activity of bacterioplankton in open ocean surface waters. *Appl Environ Microbiol* **79**: 177-184.

Ikawa, M., and Taylor, R., F., (1973) Choline and related substances in Algae. In *Marine Pharmacognosy: Action of Marine Biotoxins at the cellular level*. Martin, D., and Padilla, G., M. (eds). New York: Academic Press INC., pp. 203-236.

Janvier, M., Regnault, B., and Grimont, P. (2003) Development and use of fluorescent 16S rRNA-targeted probes for the specific detection of *Methylophaga* species by *in situ* hybridisation in marine sediments. *Res Microbiol* **154**: 483-490.

Kanagawa, T., Dazai, M., and Fukuoka, S. (1982) Degradation of O,O-dimethyl phosphorodithioate by *Thiobacillus thioparus* TK-1 and *Pseudomonas* AK-2. *Arg Biol Chem Toyko* **46**: 2571-2578.

Kiene, R.P. (1998) Uptake of choline and its conversion to glycine betaine by bacteria in estuarine waters. *Appl Environ Microbiol* **64**: 1045-1051.

Kimura, M., Seki, N., and Kimura, I. (2000) Purification and characterisation of trimethylamine-*N*-oxide demethylase from Walleye Pollack muscle. *Fisheries Sci* **66**: 967-973.

King, G.M. (1984) Metabolism of trimethylamine, choline, and glycine betaine by sulfate-reducing and methanogenic bacteria in marine sediments. *Appl Environ Microbiol* **48**: 719-725.

King, G.M., Klug, M.J., and Lovley, D.R. (1983) Metabolism of acetate, methanol, and methylated amines in intertidal sediments of Lowes Cove, Maine. *Appl Environ Microbiol* **45**: 1848-1853.

Kirkwood, M., Le Brun, N.E., Todd, J.D., and Johnston, A.W.B. (2010) The dddP gene of *Roseovarius nubinhibens* encodes a novel lyase that cleaves dimethylsulfoniopropionate into acrylate plus dimethylsulfide. *Microbiology* **156**: 1900-1906.

Kovach, M.E., Elzer, P.H., Steven Hill, D., Robertson, G.T., Farris, M.A., Roop Ii, R.M., and Peterson, K.M. (1995) Four new derivatives of the broad-host-range

cloning vector pBBR1MCS, carrying different antibiotic-resistance cassettes. *Gene* **166**: 175-176.

Krueger, S.K., and Williams, D.E. (2005) Mammalian flavin-containing monooxygenases: structure/ function, genetic polymorphisms and role in drug metabolism. *Pharmacol Therapeut* **106**: 357-387.

Kustka, A., Sañudo-Wilhelmy, S., Carpenter, E.J., Capone, D.G., and Raven, J.A. (2003) A revised estimate of the iron use efficiency of nitrogen fixation, with special reference to the marine cyanobacterium *Trichodesmium* spp. (cyanophyta). *J Phycol* **39**: 12-25.

Lamark, T., Røkenes, T.P., McDougall, J., and Strøm, A.R. (1996) The complex bet promoters of *Escherichia coli*: regulation by oxygen (ArcA), choline (BetI), and osmotic stress. *J Bacteriol* **178**: 1655-1662.

Lamark, T., Kaasen, I., Eshoo, M.W., Falkenberg, P., McDougall, J., and Strøm, A.R. (1991) DNA sequence and analysis of the *bet* genes encoding the osmoregulatory choline—glycine betaine pathway of *Escherichia coli*. *Mol Microbiol* **5**: 1049-1064.

Landfald, B., and Strøm, A.R. (1986) Choline-glycine betaine pathway confers a high level of osmotic tolerance in *Escherichia coli*. *J Bacteriol* **165**: 849-855.

Large, P.J. (1971) Non-oxidative demethylation of trimethylamine *N*-oxide by *Pseudomonas aminovorans*. *FEBS Lett* **18**: 297-300.

Latypova, E., Yang, S., Wang, Y.-S., Wang, T., Chavkin, T.A., Hackett, M. et al. (2010) Genetics of the glutamate-mediated methylamine utilisation pathway in the facultative methylotrophic beta-proteobacterium *Methyloversatilis universalis* FAM5. *Mol Microbiol* **75**: 426-439.

Lee, P.A., and DeMora, S.J., (1999) Intracellular dimethylsulfoxide (DMSO) in unicellular marine algae: Speculations on its origin and possible biological role. *J Phycol* **35**: 8-18.

Lema, K.A., Bourne, D.G., and Willis, B.L. (2014) Onset and establishment of diazotrophs and other bacterial associates in the early life history stages of the coral *Acropora millepora*. *Molecular Ecology* **23** (19): 4682-4695.

Liu, C., Wu, Y., Li, L., Ma, Y., and Shao, Z. (2007) *Thalassospira xiamenensis* sp. nov. and *Thalassospira profundimaris* sp. nov. *Int J Syst Evol Micro* **57**: 316-320.

Luo, H., Csűros, M., Hughes, A.L., and Moran, M.A. (2013) Evolution of divergent life history strategies in marine *Alphaproteobacteria*. *mBio* **4**.

Maizel, J.V., Benson, A.A., and Tolbert, N.E. (1956) Identification of phosphoryl choline as an important constituent of plant sap. *Plant Physiol* **31**: 407-408.

Malmstrom, R.R., Kiene, R.P., and Kirchman, D.L. (2004) Identification and enumeration of bacteria assimilating dimethylsulfoniopropionate (DMSP) in the North Atlantic and Gulf of Mexico. *Limnol Oceanogr* **49**: 597-606.

Martinez-Gomez, N.C., Nguyen, S., and Lidstrom, M.E. (2013) Elucidation of the role of the methylene-tetrahydromethanopterin dehydrogenase MtdA in the tetrahydromethanopterin-dependent oxidation pathway in *Methylobacterium extorquens* AM1. *J Bacteriol* **195**: 2359-2367.

Marx, C.J., and Lidstrom, M.E. (2004) Development of an insertional expression vector system for *Methylobacterium extorquens* AM1 and generation of null mutants lacking *mtdA* and/or *fch*. *Microbiology* **150**: 9-19.

Marx, C.J., Chistoserdova, L., and Lidstrom, M.E. (2003a) Formaldehyde-detoxifying role of the tetrahydromethanopterin-linked pathway in *Methylobacterium extorquens* AM1. *J Bacteriol* **185**: 7160-7168.

Marx, C.J., Laukel, M., Vorholt, J.A., and Lidstrom, M.E. (2003b) Purification of the formate-tetrahydrofolate ligase from *Methylobacterium extorquens* AM1 and demonstration of its requirement for methylotrophic growth. *J Bacteriol* **185**: 7169-7175.

McDevitt, C.A., Hugenholtz, P., Hanson, G.R., and McEwan, A.G. (2002) Molecular analysis of dimethyl sulphide dehydrogenase from *Rhodovulum sulfidophilum*: its place in the dimethylsulphoxide reductase family of microbial molybdopterin-containing enzymes. *Mol Microbiol* **44**: 1575-1587.

Meskys, R., Harris, R.J., Casaite, V., Basran, J., and Scrutton, N.S. (2001) Organisation of the genes involved in dimethylglycine and sarcosine degradation in *Arthrobacter* spp. *Eur J Biochem* **268**: 3390-3398.

Mikhail, Z., J, L.L., Rudolf, A., and P, K.R. (2004) Temporal patterns of biological dimethylsulfide (DMS) consumption during laboratory-induced phytoplankton bloom cycles. *Mar Ecol Prog Ser (Halstenbek)* **271**: 77-86.

Miller, J. H. (ed.). 1972. *Experiments in molecular genetics*. 352-355. Cold Spring Harbor Laboratory, Cold Spring Harbor, N.Y.

Miller, T.R., and Belas, R. (2004) Dimethylsulfoniopropionate metabolism by *Pfiesteria*-associated *Roseobacter* spp. *Appl Environ Microbiol* **70**: 3383-3391.

Mitch, W., A., Sharp, J., O., Trussell, R., Rhodes., Valentine, R., L., Alvarez-Cohen, L., and Sedlak, D., L. (2003) *N*-Nitrosodimethylamine (NDMA) as a drinking water contaminant: A review. *Environ Eng Sci* **20**: 389-404.

Mitchell, S.C., and Smith, R.L. (2001) Trimethylaminuria: The fish malodor syndrome. *Drug Metab Dispos* **29**: 517-521.

Moran, M.A., and Miller, W.L. (2007) Resourceful heterotrophs make the most of light in the coastal ocean. *Nat Rev Micro* **5**: 792-800.

Moran, M.A., Buchan, A., Gonzalez, J.M., Heidelberg, J.F., Whitman, W.B., Kiene, R.P. et al. (2004) Genome sequence of *Silicibacter pomeroyi* reveals adaptations to the marine environment. *Nature* **432**: 910-913.

Morris, R.M., Rappe, M.S., Connon, S.A., Vergin, K.L., Siebold, W.A., Carlson, C.A., and Giovannoni, S.J. (2002) SAR11 clade dominates ocean surface bacterioplankton communities. *Nature* **420**: 806-810.

Murakeözy, É.P., Nagy, Z., Duhazé, C., Bouchereau, A., and Tuba, Z. (2003) Seasonal changes in the levels of compatible osmolytes in three halophytic species of inland saline vegetation in Hungary. *J Plant Physiol* **160**: 395-401.

Muyzer, G., de Waal, E.C., and Uitterlinden, A.G. (1993) Profiling of complex microbial populations by denaturing gradient gel electrophoresis analysis of polymerase chain reaction-amplified genes coding for 16S rRNA. *Appl Environ Microbiol* **59**: 695-700.

Myers, P., and Zatman, L. (1971) The metabolism of trimethylamine *N*-oxide by *Bacillus* PM6. *Biochem J* **121**: 10P.

Müller, C., Iinuma, Y., Karstensen, J., van Pinxteren, D., Lehmann, S., Gnauk, T., and Herrmann, H. (2009) Seasonal variation of aliphatic amines in marine sub-micrometer particles at the Cape Verde islands. *Atmos Chem Phys* **9**: 9587-9597.

Nagy, P.L., Marolewski, A., Benkovic, S.J., and Zalkin, H. (1995) Formyltetrahydrofolate hydrolase, a regulatory enzyme that functions to balance pools of tetrahydrofolate and one-carbon tetrahydrofolate adducts in *Escherichia coli*. *J Bacteriol* **177**: 1292-1298.

Nau-Wagner, G., Boch, J., Le Good, J.A., and Bremer, E. (1999) High-Affinity Transport of choline-O-sulfate and its ese as a compatible solute in *Bacillus subtilis*. *Appl Environ Microbiol* **65**: 560-568.

Nayak, D.D., and Marx, C.J. (2014) Methylamine Utilization via the N-Methylglutamate pathway in *Methylobacterium extorquens* PA1 involves a novel flow of carbon through c1 assimilation and dissimilation pathways. *J Bacteriol* **196**: 4130-4139.

Nelson, C.E., Carlson, C.A., Ewart, C.S., and Halewood, E.R. (2014) Community differentiation and population enrichment of Sargasso Sea bacterioplankton in the euphotic zone of a mesoscale mode-water eddy. *Environ Microbiol* **16**: 871-887.

Neufeld, J.D., Boden, R., Moussard, H., Schäfer, H., and Murrell, J.C. (2008) Substrate-specific clades of active marine methylotrophs associated with a phytoplankton bloom in a temperate coastal environment. *Appl Environ Microbiol* **74**: 7321-7328.

Neufeld, J.D., Schafer, H., Cox, M.J., Boden, R., McDonald, I.R., and Murrell, J.C. (2007) Stable-isotope probing implicates *Methylophaga* spp. and novel

Gammaproteobacteria in marine methanol and methylamine metabolism. *ISME J* **1**: 480-491.

Newton, R.J., Griffin, L.E., Bowles, K.M., Meile, C., Gifford, S., Givens, C.E. et al. (2010) Genome characteristics of a generalist marine bacterial lineage. *ISME J* **4**: 784-798.

Oremland, R.S., and Polcin, S. (1982) Methanogenesis and sulfate reduction: competitive and noncompetitive substrates in estuarine sediments. *Appl Environ Microbiol* **44**: 1270-1276.

Østerås, M., Boncompagni, E., Vincent, N., Poggi, M.-C., and Le Rudulier, D. (1998) Presence of a gene encoding choline sulfatase in *Sinorhizobium meliloti* bet operon: Choline-O-sulfate is metabolized into glycine betaine. *Proc Nat Acad Sci USA* **95**: 11394-11399.

Ottesen, E.A., Marin, R., III, Preston, C.M., Young, C.R., Ryan, J.P., Scholin, C.A., and DeLong, E.F. (2011) Metatranscriptomic analysis of autonomously collected and preserved marine bacterioplankton. *ISME J* **5**: 1881-1895.

Ottesen, E.A., Young, C.R., Eppley, J.M., Ryan, J.P., Chavez, F.P., Scholin, C.A., and DeLong, E.F. (2013) Pattern and synchrony of gene expression among sympatric marine microbial populations. *Proc Nat Acad Sci USA*.

Otto, A., Stoltz, M., Sailer, H.-P., and Brandsch, R. (1996) Biogenesis of the covalently flavinylated mitochondrial enzyme dimethylglycine dehydrogenase. *J Biol Chem* **271**: 9823-9829.

Parkin, K.L., and Hultin, H.O. (1986) Characterisation of trimethylamine *N*-Oxide (TMAO) demethylase activity from fish muscle microsomes. *J Biochem* **100**: 77-86.

Partensky, F., Hess, W.R., and Vaulot, D. (1999) *Prochlorococcus*, a marine photosynthetic prokaryote of global significance. *Microbiol Mol Biol Rev* **63**: 106-127.

Place Jr, P.F., Ziemba, L.D., and Griffin, R.J. (2010) Observations of nucleation-mode particle events and size distributions at a rural New England site. *Atmos Environ* **44**: 88-94.

Polovina, J.J., Howell, E.A., and Abecassis, M. (2008) Ocean's least productive waters are expanding. *Geophys Res Lett* **35**.

Polz, M.F., Hunt, D.E., Preheim, S.P., and Weinreich, D.M. (2006) Patterns and mechanisms of genetic and phenotypic differentiation in marine microbes. *Philos T Roy Soc B* **361**: 2009-2021.

Porsby, C.H., Nielsen, K.F., and Gram, L. (2008) *Phaeobacter* and *Ruegeria* species of the *Roseobacter* clade colonize separate niches in a Danish Turbot

(*Scophthalmus maximus*)-rearing farm and antagonise *Vibrio anguillarum* under different growth conditions. *Appl Environ Microbiol* **74**: 7356-7364.

Prado, S., Montes, J., Romalde, J., L., and Barja, J., L. (2009) Inhibitory activity of *Phaeobacter* strains against aquaculture pathogenic bacteria. *Int Microbiol* **12**: 107-114.

Raina, J.-B., Tapiolas, D.M., Foret, S., Lutz, A., Abrego, D., Ceh, J. et al. (2013) DMSP biosynthesis by an animal and its role in coral thermal stress response. *Nature* **502**: 677-680.

Raymond, J.A., and Plopper, G.E. (2002) A bacterial TMAO transporter. *Comp Biochem Phys B* **133**: 29-34.

Rebouche, C.J. (1992) Carnitine function and requirements during the life cycle. *FASEB J* **6**: 3379-3386.

Reese, M.G. (2001) Application of a time-delay neural network to promoter annotation in the Drosophila melanogaster genome. *Comput Chem* **26**: 51-56.

Riclea, R., Gleitzmann, J., Bruns, H., Junker, C., Schulz, B., and Dickschat, J.S. (2012) Algicidal lactones from the marine Roseobacter clade bacterium *Ruegeria pomeroyi*. *Beilstein J Org Chem* **8**: 941-950.

Riding, R. (1992) The algal breath of life. *Nature* **359**: 13-14.

Rink, B., Seeberger, S., Martens, T., Duerselen, C.D., Simon, M., and Brinkhoff, T. (2007) Effects of phytoplankton bloom in a coastal ecosystem on the composition of bacterial communities. *Aquat Microb Ecol* **48**: 47-60.

Rinta-Kanto, J.M., Sun, S., Sharma, S., Kiene, R.P., and Moran, M.A. (2012) Bacterial community transcription patterns during a marine phytoplankton bloom. *Environ Microbiol* **14**: 228-239.

Riseman, S.F., and DiTullio, G.R. (2004) Particulate dimethylsulfoniopropionate and dimethylsulfoxide in relation to iron availability and algal community structure in the Peru Upwelling System. *Can J Fish Aquat Sci* **61**: 721-735.

Rocap, G., Larimer, F.W., Lamerdin, J., Malfatti, S., Chain, P., Ahlgren, N.A. et al. (2003) Genome divergence in two *Prochlorococcus* ecotypes reflects oceanic niche differentiation. *Nature* **424**: 1042-1047.

Roulier, M.A., Palenik, B., and Morel, F.M.M. (1990) A method for the measurement of choline and hydrogen peroxide in seawater. *Mar Chem***30**: 409-421.

Rusch, D.B., Halpern, A.L., Sutton, G., Heidelberg, K.B., Williamson, S., Yooseph, S. et al. (2007) The *Sorcerer II* Global Ocean Sampling expedition: Northwest Atlantic through Eastern Tropical Pacific. *PLoS Biol* **5**: e77.

Ryther, J.H., and Dunstan, W.M. (1971) Nitrogen, phosphorus, and eutrophication in the coastal marine environment. *Science* **171**: 1008-1013.

Sakurai, I., Stazic, D., Eisenhut, M., Vuorio, E., Steglich, C., Hess, W.R., and Aro, E.-M. (2012) Positive regulation of *psbA* gene expression by cis-encoded antisense RNAs in *Synechocystis* sp. PCC 6803. *Plant Physiol* **160**: 1000-1010.

Sambrook, J., Russell, D., and Irwin, N. (2001) *Molecular cloning: a laboratory manual*. New York, Cold Spring Harbor Laboratory Press.

Schäfer, H. (2007) Isolation of *Methylophaga* spp. from marine dimethylsulfide-degrading enrichment cultures and identification of polypeptides induced during growth on dimethylsulfide. *Appl Environ Microbiol* **73**: 2580-2591.

Schäfer, H., McDonald, I.R., Nightingale, P.D., and Murrell, J.C. (2005) Evidence for the presence of a CmuA methyltransferase pathway in novel marine methyl halide-oxidizing bacteria. *Environ Microbiol* **7**: 839-852.

Sebastian, M., and Ammerman, J.W. (2009) The alkaline phosphatase PhoX is more widely distributed in marine bacteria than the classical PhoA. *ISME J* **3**: 563-572.

Sebastian, M., and Ammerman, J.W. (2011) Role of the phosphatase PhoX in the phosphorus metabolism of the marine bacterium *Ruegeria pomeroyi* DSS-3. *Environ Microbiol Reports* **3**: 535-542.

Selje, N., Simon, M., and Brinkhoff, T. (2004) A newly discovered *Roseobacter* cluster in temperate and polar oceans. *Nature* **427**: 445-448.

Sesto, N., Wurtzel, O., Archambaud, C., Sorek, R., and Cossart, P. (2013) The excludon: a new concept in bacterial antisense RNA-mediated gene regulation. *Nat Rev Micro* **11**: 75-82.

Seyedsayamdost, M.R., Case, R.J., Kolter, R., and Clardy, J. (2011) The Jekyll-and-Hyde chemistry of *Phaeobacter gallaeciensis*. *Nat Chem* **3**: 331-335.

Sheik, C.S., Jain, S., and Dick, G.J. (2013) Metabolic flexibility of enigmatic SAR324 revealed through metagenomics and metatranscriptomics. *Environ Microbiol*: **16** (1): 304-317.

Shiba, T. (1991) *Roseobacter litoralis* gen. nov., sp. nov., and *Roseobacter denitrificans* sp. nov., aerobic pink-pigmented bacteria which contain bacteriochlorophyll a. *Syst Appl Microbiol* **14**: 140-145.

Silvestro, A., Pommier, J., Pascal, M.-C., and Giordano, G. (1989) The inducible trimethylamine *N*-oxide reductase of *Escherichia coli* K12: its localisation and inducers. *BBA-Protein Struct M* **999**: 208-216.

Simo, R., Hatton, A., Malin, G., and Liss, P. (1998) Particulate dimethyl sulphoxide in seawater: production by microplankton. *Mar Ecol Prog Ser* **167**: 291-296.

Simó, R., Pedrós-Alió, C., Malin, G., and Grimalt, J.O. (2000) Biological turnover of DMS, DMSP and DMSO in contrasting open-sea waters. *Mar Ecol Prog Ser* **203**: 1-11.

Smith, D.P., Thrash, J.C., Nicora, C.D., Lipton, M.S., Burnum-Johnson, K.E., Carini, P. et al. (2013) Proteomic and transcriptomic analyses of "*Candidatus* Pelagibacter ubique" describe the first pii-independent response to nitrogen limitation in a free-living alphaproteobacterium. *mBio* **4**.

Smith, L.T., Pocard, J.A., Bernard, T., and Le Rudulier, D. (1988) Osmotic control of glycine betaine biosynthesis and degradation in *Rhizobium meliloti*. *J Bacteriol* **170**: 3142-3149.

Sorokin, D.Y., Tourova, T.P., and Muyzer, G. (2005) *Citreicella thiooxidans* gen. nov., sp. nov., a novel lithoheterotrophic sulfur-oxidizing bacterium from the Black Sea. *Syst Appl Microbiol* **28**: 679-687.

Sorooshian, A., Padró, L.T., Nenes, A., Feingold, G., McComiskey, A., Hersey, S.P. et al. (2009) On the link between ocean biota emissions, aerosol, and maritime clouds: Airborne, ground, and satellite measurements off the coast of California. *Global Biogeochem Cyc* **23**: GB4007.

Sowell, S.M., Abraham, P.E., Shah, M., Verberkmoes, N.C., Smith, D.P., Barofsky, D.F., and Giovannoni, S.J. (2011) Environmental proteomics of microbial plankton in a highly productive coastal upwelling system. *ISME J* **5**: 856-865.

Sowell, S.M., Wilhelm, L.J., Norbeck, A.D., Lipton, M.S., Nicora, C.D., Barofsky, D.F. et al. (2008) Transport functions dominate the SAR11 metaproteome at low-nutrient extremes in the Sargasso Sea. *ISME J* **3**: 93-105.

Stazic, D., Lindell, D., and Steglich, C. (2011) Antisense RNA protects mRNA from RNase E degradation by RNA–RNA duplex formation during phage infection. *Nucleic Acids Res* **39**: 4890-4899.

Steenkamp, D.J., and Husain, M. (1982) The effect of tetrahydrofolate on the reduction of electron transfer flavoprotein by sarcosine and dimethylglycine dehydrogenases. *The Biochem J* **203**: 707-715.

Simon, R., Priefer, U.B., Puhler, A., (1983) A broad host range mobilization system for in vivo genetic engineering: Transposon mutagenesis in Gram-negative bacteria, Biotechnology **1**: 784–791.

Steindler, L., Schwalbach, M.S., Smith, D.P., Chan, F., and Giovannoni, S.J. (2011) Energy starved *Candidatus* Pelagibacter Ubique substitutes light-mediated ATP production for endogenous carbon respiration. *PLoS ONE* **6**: e19725.

Studer, A., McAnulla, C., Büchele, R., Leisinger, T., and Vuilleumier, S. (2002) Chloromethane-induced genes define a third C1 utilisation pathway in *Methylobacterium chloromethanicum* CM4. *J Bacteriol* **184**: 3476-3484.

Styrvold, O.B., Falkenberg, P., Landfald, B., Eshoo, M.W., Bjørnsen, T., and Strøm, A.R. (1986) Selection, mapping, and characterization of osmoregulatory mutants of *Escherichia coli* blocked in the choline-glycine betaine pathway. *J Bacteriol* **165**: 856-863.

Sun, J., Steindler, L., Thrash, J.C., Halsey, K.H., Smith, D.P., Carter, A.E. et al. (2011) One carbon metabolism in SAR11 pelagic marine bacteria. *PLoS ONE* **6**: e23973.

Sun, L., Curson, A.J., Todd, J., and Johnston, A.B. (2012) Diversity of DMSP transport in marine bacteria, revealed by genetic analyses. *Biogeochem* **110**: 121-130.

Sun, Z., Kang, Y., Norris, M.H., Troyer, R.M., Son, M.S., Schweizer, H.P. et al. (2014) Blocking phosphatidylcholine utilisation in *Pseudomonas aeruginosa*, via mutagenesis of fatty acid, glycerol and choline degradation pathways, confirms the importance of this nutrient source *in vivo*. *PLoS ONE* **9**: e103778.

Sunda, W., Kieber, D.J., Kiene, R.P., and Huntsman, S. (2002) An antioxidant function for DMSP and DMS in marine algae. *Nature* **418**: 317-320.

Suttle, C.A. (2007) Marine viruses - major players in the global ecosystem. *Nat Rev Micro* **5**: 801-812.

Swan, B.K., Martinez-Garcia, M., Preston, C.M., Sczyrba, A., Woyke, T., Lamy, D. et al. (2011) Potential for chemolithoautotrophy among ubiquitous bacteria lineages in the dark ocean. *Science* **333**: 1296-1300.

Swan, B.K., Tupper, B., Sczyrba, A., Lauro, F.M., Martinez-Garcia, M., González, J.M. et al. (2013) Prevalent genome streamlining and latitudinal divergence of planktonic bacteria in the surface ocean. *Proc Nat Acad Sci USA* **110**: 11463-11468.

Tamura, K., Peterson, D., Peterson, N., Stecher, G., Nei, M., and Kumar, S. (2011) MEGA5: Molecular evolutionary genetics analysis using maximum likelihood, evolutionary distance, and maximum parsimony methods. *Mol Biol Evol* **28** (10): 2731-2739.

Tanaka, N., Kusakabe, Y., Ito, K., Yoshimoto, T., and Nakamura, K.T. (2003) Crystal structure of glutathione-independent formaldehyde dehydrogenase. *Chem Biol Interact* **143–144**: 211-218.

Taylor, J.D., Cottingham, S.D., Billinge, J., and Cunliffe, M. (2014) Seasonal microbial community dynamics correlate with phytoplankton-derived polysaccharides in surface coastal waters. *ISME J* **8**: 245-248.

Thole, S., Kalhoefer, D., Voget, S., Berger, M., Engelhardt, T., Liesegang, H. et al. (2012) *Phaeobacter gallaeciensis* genomes from globally opposite locations reveal high similarity of adaptation to surface life. *ISME J* **6**: 2229-2244.

Thomas, G.H. (2010) Homes for the orphans: utilisation of multiple substrate-binding proteins by ABC transporters. *Mol Microbiol* **75**: 6-9.

Thomas, W.H. (1970) On nitrogen deficiency in tropical Pacific oceanic phytoplankton: photosynthetic parameters in poor and rich water. *Limnol Oceanogr* **15**: 380-385.

Thomason, M.K., and Storz, G. (2010) Bacterial antisense RNAs: How many are there, and what are they doing? *Annu Rev Gen* **44**: 167-188.

Todd, J.D., Kirkwood, M., Newton-Payne, S., and Johnston, A.W.B. (2012) DddW, a third DMSP lyase in a model *Roseobacter* marine bacterium, *Ruegeria pomeroyi* DSS-3. *ISME J* **6**: 223-226.

Treberg, J.R., Speers-Roesch, B., Piermarini, P.M., Ip, Y.K., Ballantyne, J.S., and Driedzic, W.R. (2006) The accumulation of methylamine counteracting solutes in elasmobranchs with differing levels of urea: a comparison of marine and freshwater species. *J Exp Biol* **209**: 860-870.

Tripp, H.J., Schwalbach, M.S., Meyer, M.M., Kitner, J.B., Breaker, R.R., and Giovannoni, S.J. (2009) Unique glycine-activated riboswitch linked to glycine–serine auxotrophy in SAR11. *Environ Microbiol* **11**: 230-238.

Tynes, R.E., Sabourin, P.J., Hodgson, E., and Philpot, R.M. (1986) Formation of hydrogen peroxide and N-hydroxylated amines catalysed by pulmonary flavin-containing monooxygenases in the presence of primary alkylamines. *Arch Biochem Biophys* **251**: 654-664.

Van Neste, A., Duce, R.A., and Lee, C. (1987) Methylamines in the marine atmosphere. *Geophys Res Lett* **14**: 711-714.

Vergin, K. L., Done, B., Carlson, C.A., Giovannoni, S.J. (2013) Spatiotemporal distributions of rare bacterioplankton populations indicate adaptive strategies in the oligotrophic ocean. *Aquat Microb Ecol* **71**: 1-13.

Vieira, J., & Messing, J. (1982). The pUC plasmids, an M13mp7-derived system for insertion mutagenesis and sequencing with synthetic universal primers. *Gene* **19** (3): 259-268.

Vila, M., Simó, R., Kiene, R.P., Pinhassi, J., González, J.M., Moran, M.A., and Pedrós-Alió, C. (2004) Use of microautoradiography combined with fluorescence *in situ* hybridisation to determine dimethylsulfoniopropionate incorporation by marine bacterioplankton taxa. *Appl Environ Microbiol* **70**: 4648-4657.

Voget, S., Wemheuer, B., Brinkhoff, T., Vollmers, J., Dietrich, S., Giebel, H.-A. et al. (2014) Adaptation of an abundant *Roseobacter* RCA organism to pelagic systems revealed by genomic and transcriptomic analyses. *ISME J* **9** (2): 371-84.

Vollmer, W., and Tomasz, A. (2001) Identification of the teichoic acid phosphorylcholine esterase in *Streptococcus pneumoniae*. *Mol Microbiol* **39**: 1610-1622.

Wagner-Dobler, I., Ballhausen, B., Berger, M., Brinkhoff, T., Buchholz, I., Bunk, B. et al. (2009) The complete genome sequence of the algal symbiont *Dinoroseobacter shibae*: a hitchhiker's guide to life in the sea. *ISME J* **4**: 61-77.

Wargo, M.J., Szwergold, B.S., and Hogan, D.A. (2008) Identification of two gene clusters and a transcriptional regulator required for *Pseudomonas aeruginosa* glycine betaine catabolism. *J Bacteriol* **190**: 2690-2699.

Wargo, M.J., Ho, T.C., Gross, M.J., Whittaker, L.A., and Hogan, D.A. (2009) GbdR regulates *Pseudomonas aeruginosa plcH* and *pchP* transcription in response to choline catabolites. *Infect Immun* **77**: 1103-1111.

Weisburg, W.G., Barns, S.M., Pelletier, D.A., and Lane, D.J. (1991) 16S ribosomal DNA amplification for phylogenetic study. *J Bacteriol* **173**: 697-703.

Wessel, M., Klüsener, S., Gödeke, J., Fritz, C., Hacker, S., and Narberhaus, F. (2006) Virulence of *Agrobacterium tumefaciens* requires phosphatidylcholine in the bacterial membrane. *Mol Microbiol* **62**: 906-915.

Williams, D.E., Hale, S.E., Muerhoff, A.S., and Masters, B.S. (1985) Rabbit lung flavin-containing monooxygenase: Purification, characterisation, and induction during pregnancy. *Mol Pharmacol* **28**: 381-390.

Williams, T.J., Long, E., Evans, F., DeMaere, M.Z., Lauro, F.M., Raftery, M.J. et al. (2012) A metaproteomic assessment of winter and summer bacterioplankton from Antarctic Peninsula coastal surface waters. *ISME J* **6**: 1883-1900.

Wu, J., Sunda, W., Boyle, E.A., and Karl, D.M. (2000) Phosphate Depletion in the Western North Atlantic Ocean. *Science* **289**: 759-762.

Young, J., and Holland, I.B. (1999) ABC transporters: bacterial exporters-revisited five years on. *BBA - Biomembranes* **1461**: 177-200.

Zehr, J., P., and Kudela, R., M. (2011) Nitrogen cycle of the open ocean: From genes to ecosystems. *Ann Rev Mar Sci* **3**: 197-225

Zhu, Y., Jameson, E., Crosatti, M., Schäfer, H., Rajakumar, K., Bugg, T.D.H., and Chen, Y. (2014) Carnitine metabolism to trimethylamine by an unusual Rieske-type oxygenase from human microbiota. *Proc Nat Acad Sci USA* **111**: 4268-4273.

Ziegler, C., Bremer, E., and Krämer, R. (2010) The BCCT family of carriers: From physiology to crystal structure. *Mol Microbiol* **78**: 13-34.

Zubkov, M.V., Fuchs, B.M., Archer, S.D., Kiene, R.P., Amann, R., and Burkill, P.H. (2001) Linking the composition of bacterioplankton to rapid turnover of

dissolved dimethylsulphoniopropionate in an algal bloom in the North Sea. *Environ Microbiol* **3**: 304-311.